ENIGMA

Welcome
to the 8th and final ENIGMA network meeting!

A special welcome to the last two young researchers to join the network, Thomas Bretz and Daniela Dorner.

Thanks to the local organizers of the Metsähovi team (Merja, Anne, Ilona, Elina, and Talviki).

Regards to everybody from Luisa Ostorero

ENIGMA

Special thanks also to Alan Marscher, who exceeded the promised number of visits (!)

Among the former young researchers, Dina and Mirko left astronomy and couldn't come.
Former YR Krzysztof and Jose are in other jobs and couldn't attend.
Glad to see former YR Stefano.
Manolis, Lars, and Uwe are still in science but didn't respond

Status of ENIGMA

- 15 / 12 young researchers hired
- 8 / 8 network meetings organized
- 2 / 2 schools held
- 3rd year report accepted
- 28 (???) papers written
- 8 campaigns finished
- 1 set of proceedings missing
- 14000 hits (webpage) [improving]

ENIGMA

Comments on the Programme:

YR/Team leaders – today:
-YR/brief on my side/won't miss coffee
-TL: Finances, Reports

Final report:
Needs to be prepared in October.
Information to TL, to be completed by teams

Proceedings:
collection of contributions
Written contributions to be used in final reports

Higher Order Time Series analysis of AGN light curves

Dimitrios Emmanoulopoulos

8th ENIGMA meeting, 6-8 September 2006, Espoo Finland

Landessternwarte Heidelberg

ENIGMA

Overview

- What we mean with "Higher Order Time Series analysis (HOTSA)"
- The dynamical system of Mkn 421
- TS and dimensionality
- Method of Surrogates
- Conclusions

HOTSA

Linear Gaussian Systems

$$\left.\begin{array}{l}\mathcal{L}x_1(t) = y_1(t) \\ \mathcal{L}x_2(t) = y_2(t)\end{array}\right\} \Rightarrow \mathcal{L}\left[\lambda_1 x_1(t) + \lambda_2 x_2(t)\right] =$$

$$\lambda_1 \mathcal{L}x_1(t) + \lambda_2 \mathcal{L}x_2(t) =$$

$$\lambda_1 y_1(t) + \lambda_2 y_2(t)$$

$$\boxed{x_t = Ax_{t-1} + Be_t + C}$$

HOTSA

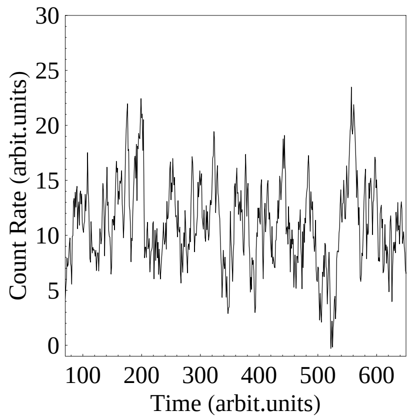

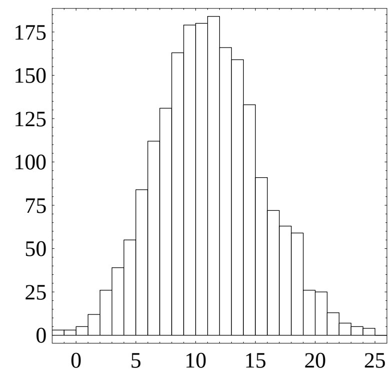

HOTSA

1^{st} and 2^{nd} statistical moments are sufficient to characterize the system.

SF: $S_x(\tau) = \frac{1}{N(\tau)} \sum \left[x(t+\tau) - x(t)\right]^2$

ACF: $ACF(\tau) = \frac{E[(x(t)-\mu)(x(t+\tau)-\mu)]}{\sigma^2}$

HOTSA

Non-Linear Systems

$$x_t = Ax_{t-1}^{1/3} + Bx_{t-1}^{1/2} + e_t + C$$

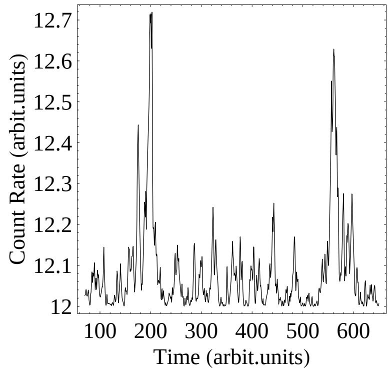

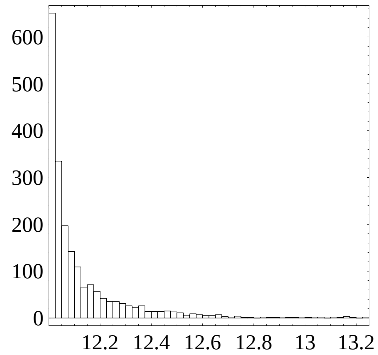

HOTSA

The SFs

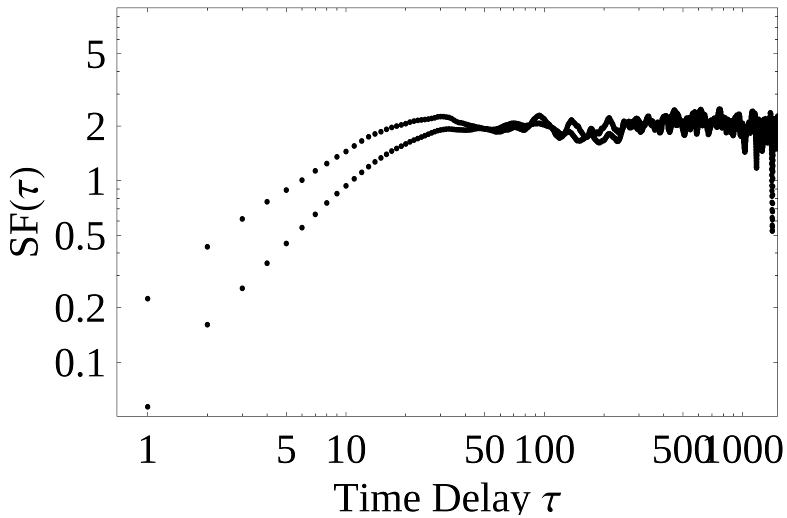

HOTSA

Which one is which?

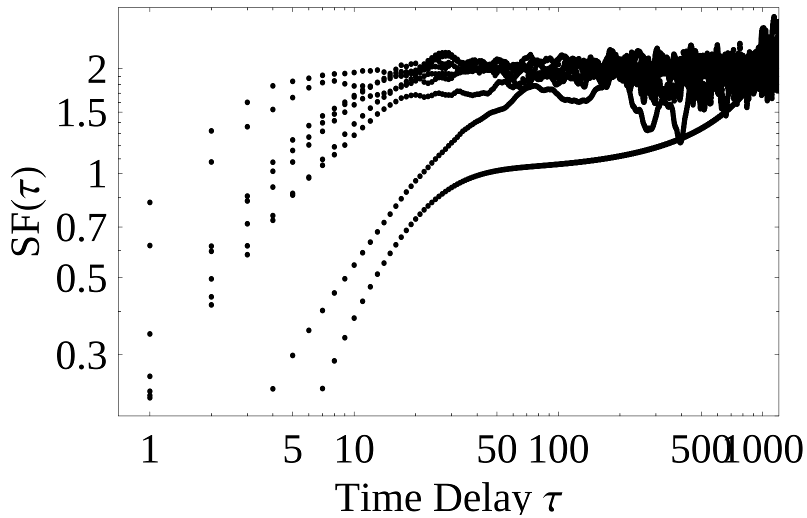

HOTSA

Which one is which?

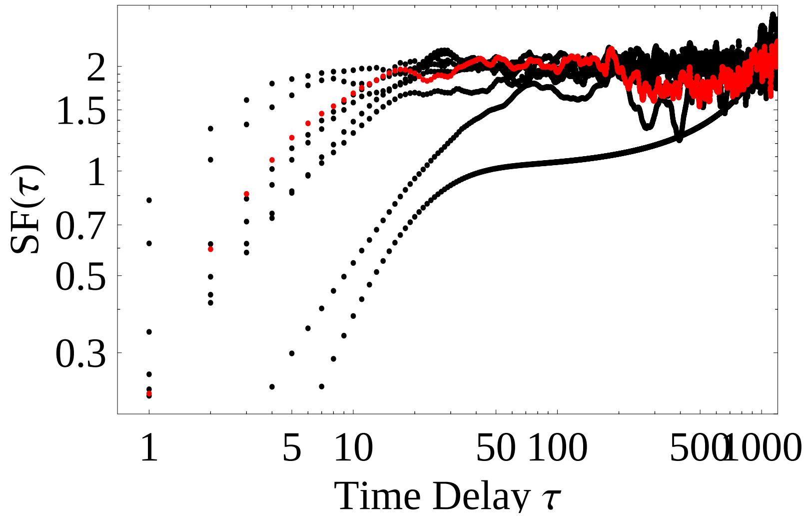

HOTSA

AGN light curves exhibit non-linear behavior.

(Leighly et al. 1997, Green et al. 1999)

Nonlinear tests

- The distribution of increments $\Delta x(t) = x(t+1) - x(t) \longrightarrow$ "Intermittency" (e.g. Subba Rao, Priestley Lessi, 1997, Guégan, 1994).
- Specification of the correlation dimension $C_m(r)$ (Grassberger, Phys.Rev.Lett. 1983,Theiler, Phys. Rev. A 1987) $\longrightarrow$ "Method of surrogates" (Theiler et al., Physica D 1992)

HOTSA

Distribution of increments $\Delta x(t) = x(t+1) - x(t)$

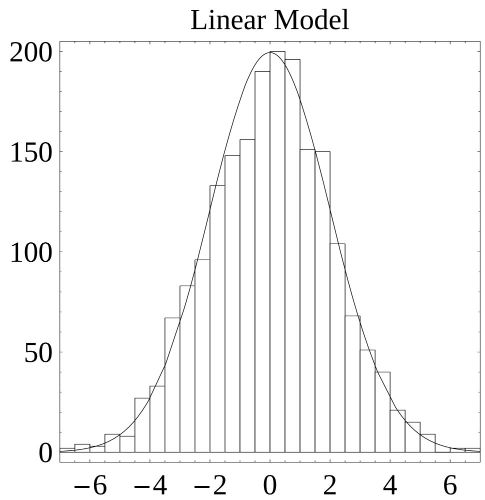

HOTSA

Distribution of increments $\Delta x(t) = x(t+1) - x(t)$

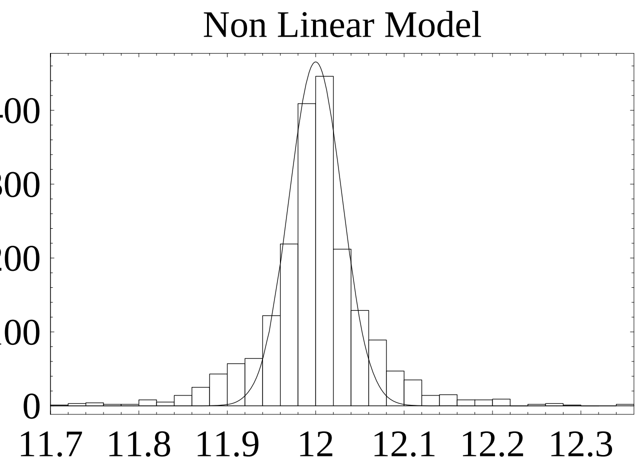

HOTSA

Distribution of increments $\Delta x(t) = x(t+1) - x(t)$

Exponential tails $\longrightarrow$ Larger probability to have "Burst events".

With Gaussian linear statistics

- We loose valuable information included in the data.
- We conclude to false/fake time scales.
- We do not consider the (dynamical) noise component which is inherent in the source (e.g. Lawrence et al. 1987, McHardy 1987,Vio et al. 2005)

The dynamical system of Mkn 421

For Mrk 421

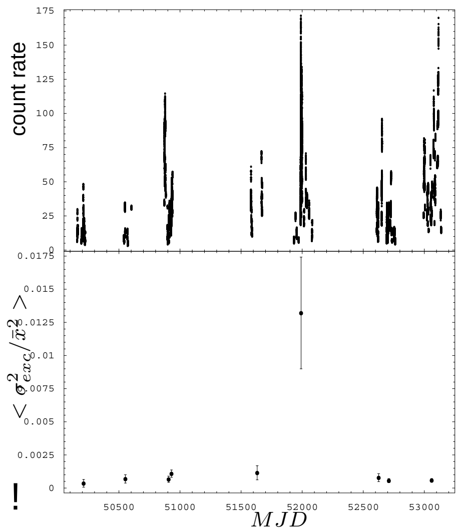

Non Stationarity !

The dynamical system of Mkn 421

For Mrk 421

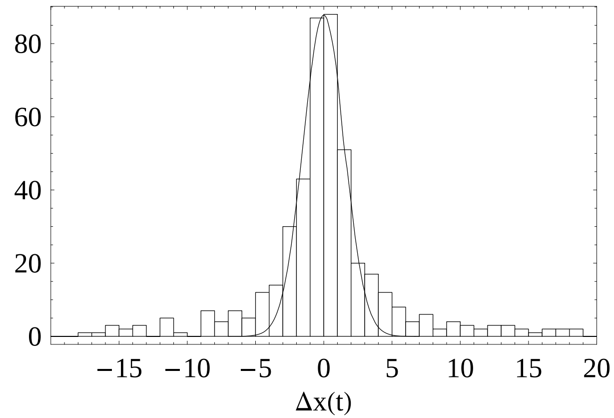

Existence of intermittent events!

The dynamical system of Mkn 421

The long term LC is the outcome of a nonlinear dynamical physical system.

The dynamical system of Mkn 421

The long term LC is the outcome of a nonlinear dynamical physical system.

What about shorter periods?Is there any trace of nonlinearity?

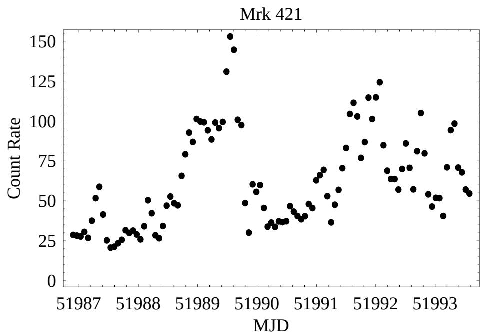

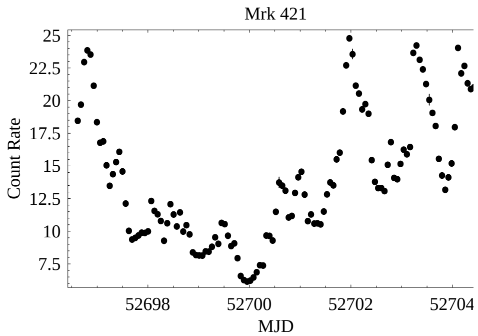

Dimensions in TS

- Capacity dimension (fractal dimension) D_0
- Information dimension D_1
- Correlation dimension D_2
- Pointwise dimension $D_{\mathrm{p},j}$
- Generalised dimension D_{q}
- Lyapunov dimension D_{L}

Dimensions in TS

Henon Map

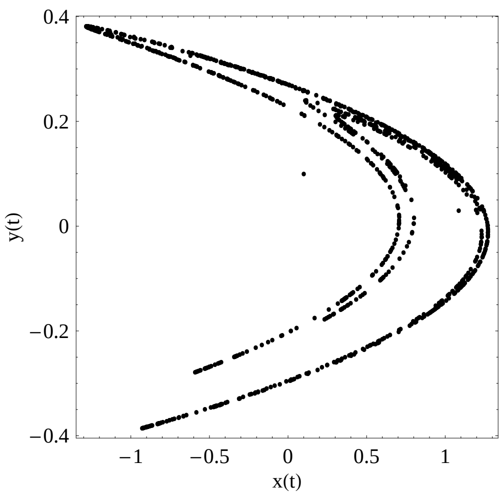

Dimensions in TS

Henon Map with delayed variables (2D, τ=1)

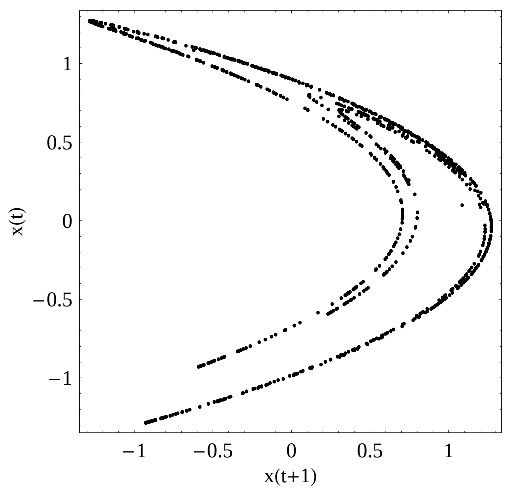

Dimensions in TS

Henon Map with delayed variables (2D, τ=3)

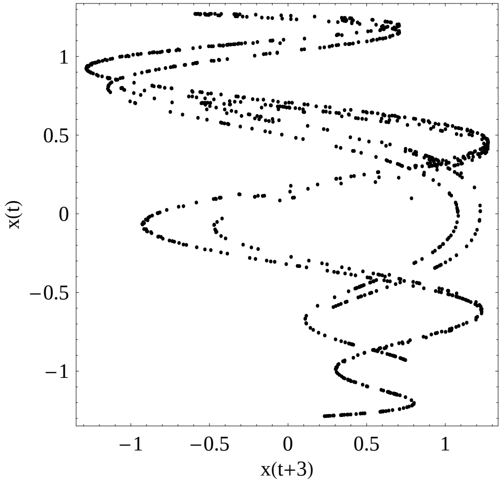

Dimensions in TS

Henon Map with delayed variables (3D, τ=1)

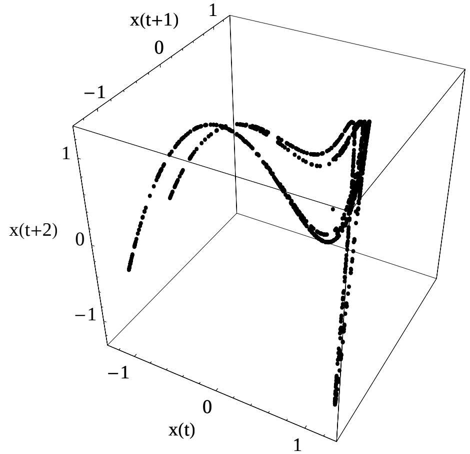

Dimensions in TS

We form hyperspheres around the points and we check for the existence of other points inside them.
The mean probability is

$$C_m(r) = \frac{\sum_{i=1}^{T} \sum_{j=1, i \neq j}^{T} H(r - ||\vec{x_i} - \vec{x_j}||)}{(T-1)T}$$

with
$\vec{x_i} = (x_i, x_{i+\tau}, \cdots, x_{i+(m-1)\tau})$ and $T = N - (m-1)\tau$

Dimensions in TS

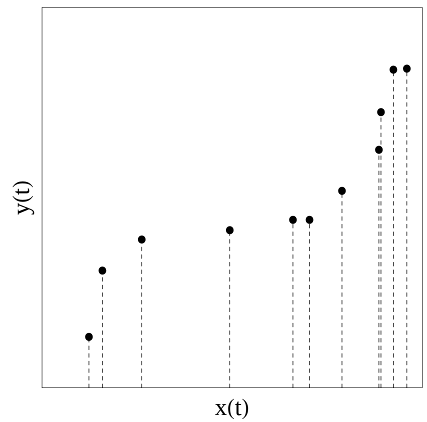

Dimensions in TS

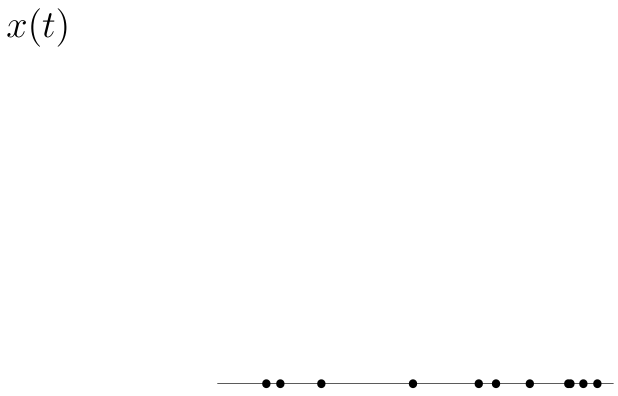

Dimensions in TS

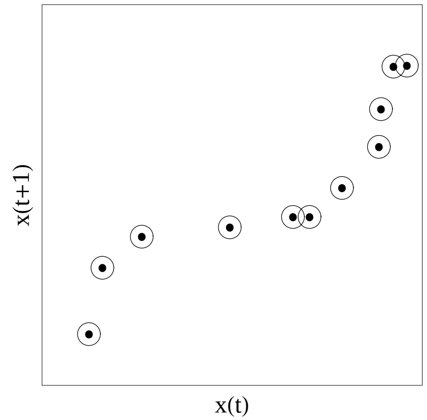

Dimensions in TS

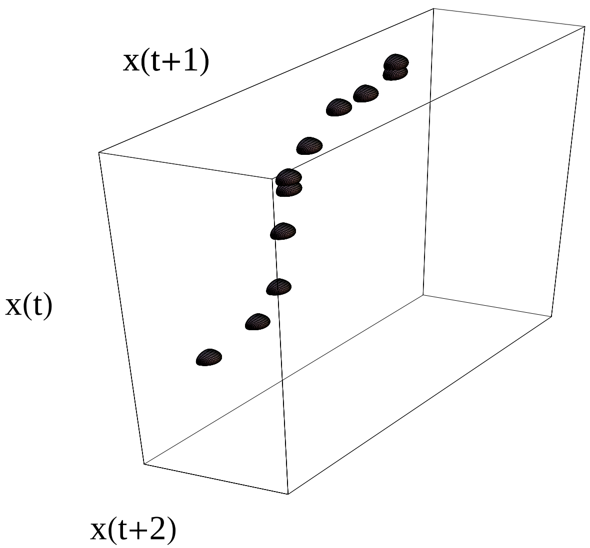

Dimensions in TS

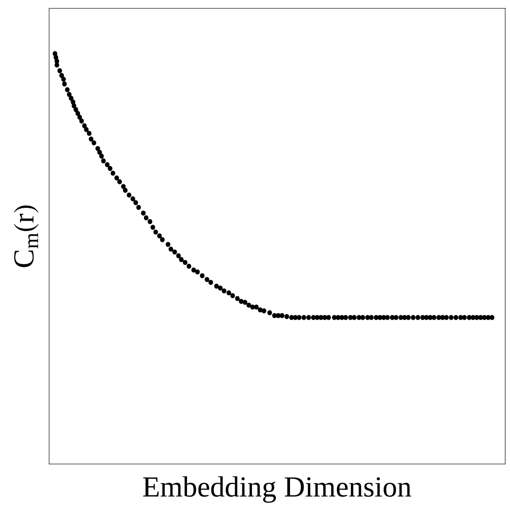

Method of surrogates

For Mrk 421 the Method of surrogates:

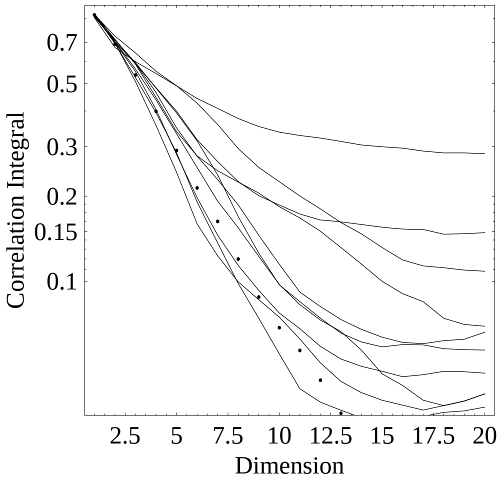

Method of surrogates

For Mrk 421 the Method of surrogates:

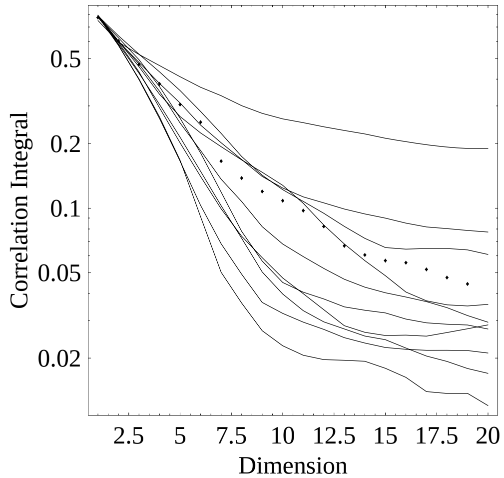

Method of surrogates

- More data !!!
- The light curves have a lot of dynamical noise.

Non linearity in small time scales can not be ruled out.

Conclusions

- Higher statistical orders are necessary for the full description of the system.

Conclusions

- Higher statistical orders are necessary for the full description of the system.
- Measurements errors and data gaps should always be included in every analysis method.

Conclusions

- Higher statistical orders are necessary for the full description of the system.
- Measurements errors and data gaps should always be included in every analysis method.
- Extended statistical studies of large data sets can reveal possible dynamical states of the source.

Conclusions

- Higher statistical orders are necessary for the full description of the system.
- Measurements errors and data gaps should always be included in every analysis method.
- Extended statistical studies of large data sets can reveal possible dynamical states of the source.
- The main purpose of the TS analysis is the prediction.

Last Conclusion

Thanks a lot!!!

The OJ 287 polarization monitoring programme: current status

Jochen Heidt (LSW), Kari Nilsson (Turku)
& the ENIGMA-team

in support of
the OJ2005-2008 campaign

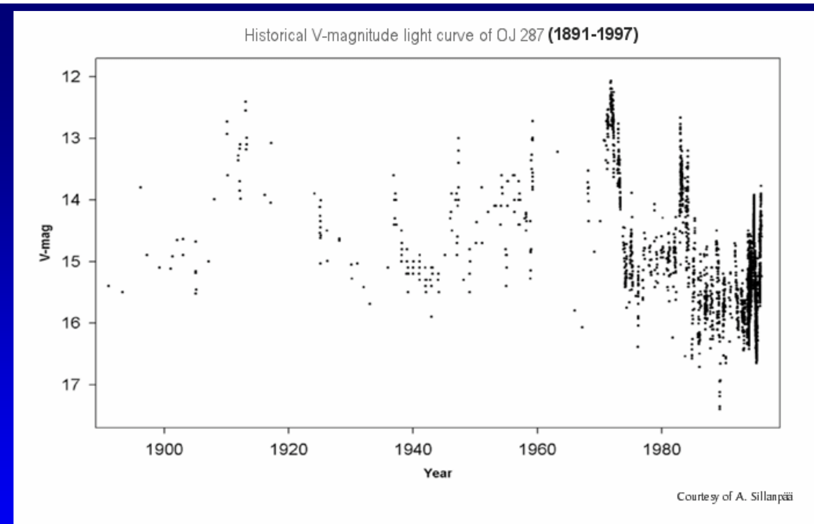

Periodic outbursts on timescales of about 12 years:

Binary BH in center of OJ 287, flares are caused by secondary hitting the accretion disk of the primary (Sillanpää et al. 1988)

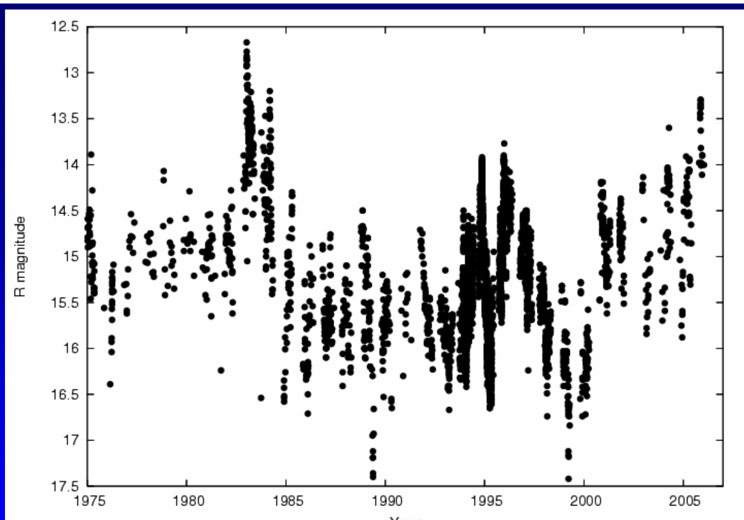

OJ-94 project: monitor the expected outburst in 1994

➔Somewhat unexpected: double-peaked outburst (as in 1982/1983)

➔New (refined) models - QUITE A LOT!!!!!

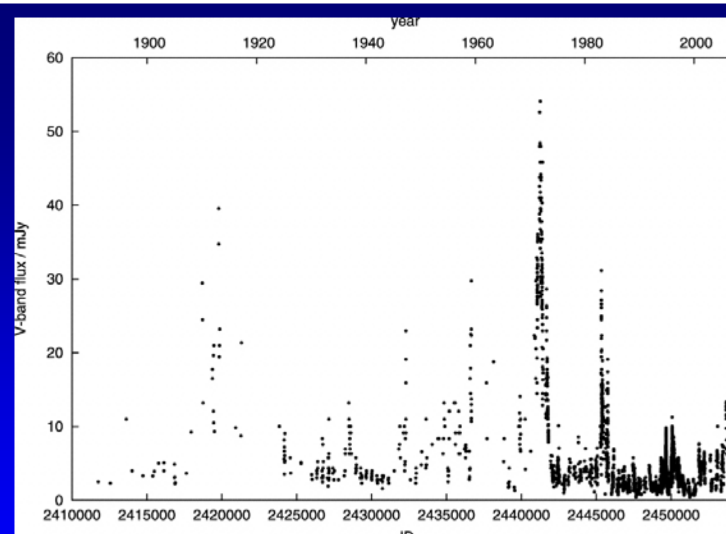

From Valtonen et al. 2006: even more models…not all mentioned here…

Models fall in 3 categories:

A: One BH with precessing jet and massive companion (Katz, 1997) or a binary BH system, each BH has a precessing jet (Villata et al. 1998)

B: Binary BH in the center, secondary BH in highly eccentric orbit, hits the accretion disk of the primary twice per revolution (Lehto & Valtonen, 1996, Sundelius et al. 1997, Pietilä et al. 1998, Valtonen et al. 2006a,b)

C: Binary BH in center, secondary BH in strictly periodic orbit, hits the accretion disk of the primary BH once per revolution (Valtaoja et al. 2000)

Category A:

Katz 1997: One massive BH with precessing jet due to massive companion disturbing the accretion disk of the primary (in analogy to SS 433 and Her X-1)

Expected: Poli ↑, PA → or change

Problem: No prediction for further outbursts ➔➔ Can not be tested

Villata et al. (1998): Binary BH system, each BH has a precessing jet

Expected: Poli ↑, PA → or change

➔Problem: makes predictions (July 2006, July 2007) but very hard (almost impossible) to test due to observability

Common problem: One naively would expect flare also in radio, not seen and not discussed!

Category B:

Binary BH in the center, secondary BH in highly eccentric orbit, hits the accretion disk of the primary twice per revolution causing two outbursts.

Expected: Poli ↓, PA → during both outbursts (unless accretion disk is magnetized), all models in category B can in principle be tested

Lehto & Valtonen, 1996: Prediction - Feb.-May 2006, Sept. 2007

Sundelius et al. 1997: Tidal influence of secondary BH on accretion disk shifts outbursts progessively towards earlier times.
Big point: Possibly observed indeed in Nov. 2005 by Valtonen et al. 2006a. Prediction for 2nd burst: Sept. 10, 2006 (Valtonen et al. 2006a)!

Pietilä et al. 1998: Explores parameter space of the Lehto & Valtonen (1996) model ➔ Dates of outbursts can change considerably

Valtonen et al. 2006b: More (too many) details on their 1996 model

Finally: No disk-jet interaction due to enhanced accretion flow in jet?

Category C:

Valtaoja et al. 2000: Binary BH in center, secondary BH in strictly periodic orbit, hits the accretion disk of the primary BH once per revolution (first outburst), increased accretion flow to center and finally jet ➔ ignites shock in jet (second outburst)

Expected: Poli ↓, PA → (first outburst)
Poli ↑, PA → or change (second outburst)

Prediction for 1st outburst: 2006, September 25 ± 2 weeks

Problem: Timing for secondary outburst difficult to predict, possibly autumn 2007, but how to detect the right one???

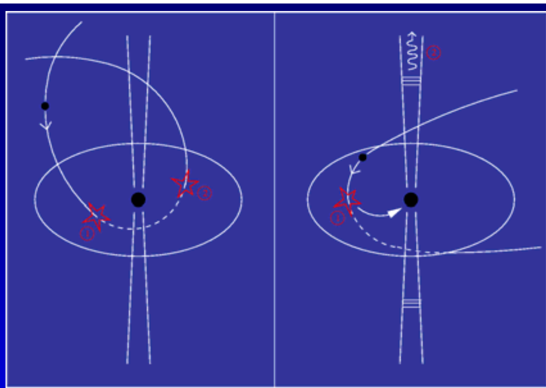

Lehto & Valtonen 1996:

I : March-May 2006, Poli ↓, PA→
II: September 2007, Poli ↓, PA→

Valtaoja et al 2000:

September 25, 2006, Poli ↓, PA→
Autumn 2007, Poli ↑, PA→ or change

Sundelius et al. 2007, Valtonen et al. 2006a:

I: November 2005, Poli ↓, PA→
II: September, 10 2006, Poli ↓, PA→

Current status of the polarization monitoring:

Running time: Jan 2006 – May 2008 with Calar Alto 2.2m and La Palma KVA telescopes.

So far: 30/50 data points from Calar Alto (1 measurement every 3rd night whenever CAFOS is mounted and Fabry-Perot not in use at AM < 2) until mid-June

63 data points from KVA until mid-May (HA limit ± 3hrs)

Sampling pretty inhomogeneous due to bad weather on both observatories in Jan/Feb (5 data points). Poor data in the critical Nov/Feb. 2005 period

Results always displayed almost in realtime at:
http://users.utu.fi/~kani

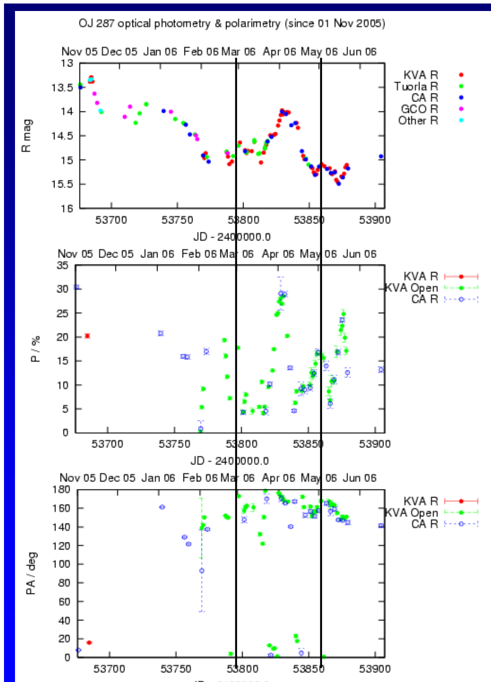

• Last update: June, 17!

• Outburst detected in period as expected for the Lehto & Valtonen 1996 model (black lines), but 1 mag outburst + increase of polarization by 30º ➔ synchrotron ,NOT LV

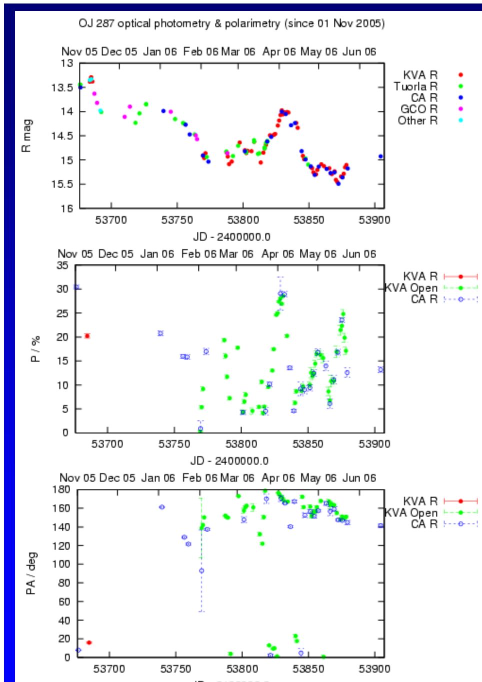

• Last update: June, 17!

• Outburst detected in period as expected for the Lehto & Valtonen 1996 model (black lines), but 1 mag outburst + increase of polarization by 30º ➔ synchrotron ,NOT LV

• Polarization behaviour in November in principle as expected for the Sundelius 1997 + Valtonen et al. 2006a models (polarization went down while flux increased although polarization is still higher than on average), BUT

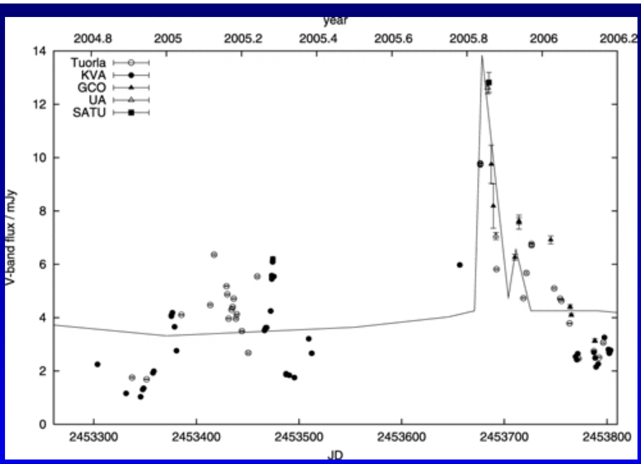

But: Proove of the Sundelius 1997 model is based on a poorly sampled flare in November 2005!

In fact: November flare is much broader an shows significant substructure (S. Ciprini, priv.com.)

Outlook

Yes, our long-term monitoring program already has provided great results, but it will be very hard to distinguish any properties expected from the models from the ones OJ 287 shows frequently (it is a crazy source)

Observations will resume soon (September 20) but autumn 2006 will not (dis)proove any model.

The 2007/2008 season will hopefully help us ➔ Especially the Valtaoja et al. 2000 model may be tested then (in case an outburst happens in September 2006 followed by another one in autumn 2007 showing polarization properties expected by that model (and if we can convince people that the flares are not just due to “standard“ OJ 287 jet processes)

Finally: 2 observatories are probably not sufficient, probably the Landessternwarte Heidelberg 70cm telescope will add further data to this project in the near future!

GPS studies during ENIGMA era

Ilona Torniainen
Metsähovi Radio Observatory
Helsinki University of Technology

M. Tornikoski, M. Aller, H. Aller, M. Mingaliev

GPS sources

- Gigahertz-peaked spectrum sources
  - Small, luminous, low variability?
  - Young, frustrated, recurrent??

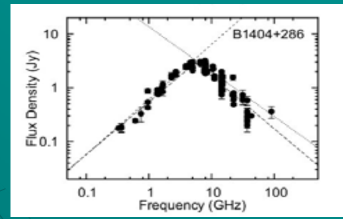

- Both galaxy and quasar type sources
  - Often considered different populations with only similar radio spectrum

GPS studies during ENIGMA project

- Original idea:
  - All-sky surveys done at ~low frequencies, sources peaking at high freq. easily ignored
  - Evidence for sources with high-peaking spectra (eg. Edge et al, 1996, 1998)
  - These high-peaking sources could affect the Planck foreground
  - HOW MANY HIGH-PEAKING SOURCES ARE THERE??

First sample

- Are there any high-peaking GPS sources in the Metsähovi monitoring sample?
- All possible radio data collected also for the GPS sources from the literature
- Sample included 44 previously identified inverted-spectrum sources and 16 candidates
  - Mostly quasar-type objects

First sample: results

- No new GPS sources among the candidates!
- 5 genuine GPS sources among the previously identified GPS sources
- Prominent variability in the previously identified GPS sources
- Many sources with temporarily inverted spectra

Ilona Torniainen
Metsähovi Radio Observatory
Finland

First sample: results

- Genuine GPS sources:
  5 sources
  - Low variability
  - Constant shape and peak in the spectrum
- Flat-spectrum sources:
  29 sources
  - High variability
  - Bright at high frequencies

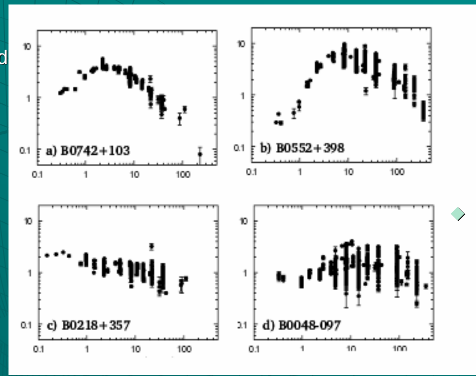

- Variable inverted-spectrum sources:
  12 sources
  - High variability
  - Shape and peak of the spectrum not constant
- Flat-spectrum sources with inverted spectra during flares:
  12 sources
  - Very high variability
  - Bright at high frequencies

Ilona Torniainen
Metsähovi Radio Observatory
Finland

Second sample

- Will the galaxy samples turn out to be as contaminated as the first sample??
- ~All bright galaxy-type GPS sources from the literature: 96 sources
- All possible radio data from the literature, observations

Ilona Torniainen
Metsähovi Radio Observatory
Finland

Second sample: results

- GPS: 29 sources

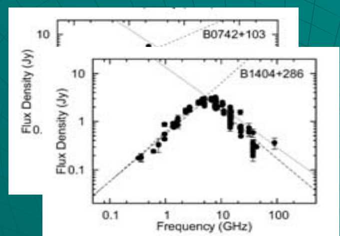

- Not enough data for GPS classification: 28

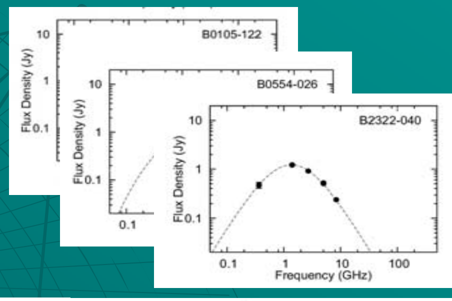

- Other kinds of sources: 39

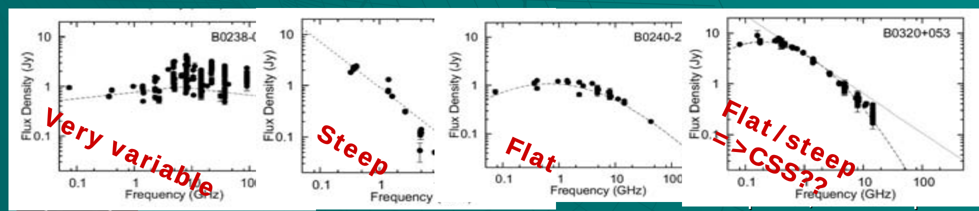

Summary

- Many of the GPS sources have been classified without sufficient monitoring
  - ⇒Unreliable or false identifications!!
- Identification of GPS galaxies seems more proper compared to GPS quasars
  - Note! Bias:
    - Quasars selected from well monitored samples
      => more variability
    - Galaxies just picked up from literature
      => many sources with just a few data points
      => some added only recently to our monitoring prog.
      => no reliable estimates on long-term behaviour

Ilona Torniainen
Metsähovi Radio Observatory
Finland

8th ENIGMA meeting
Sep 5-9, 2006 Espoo

The need for monitoring

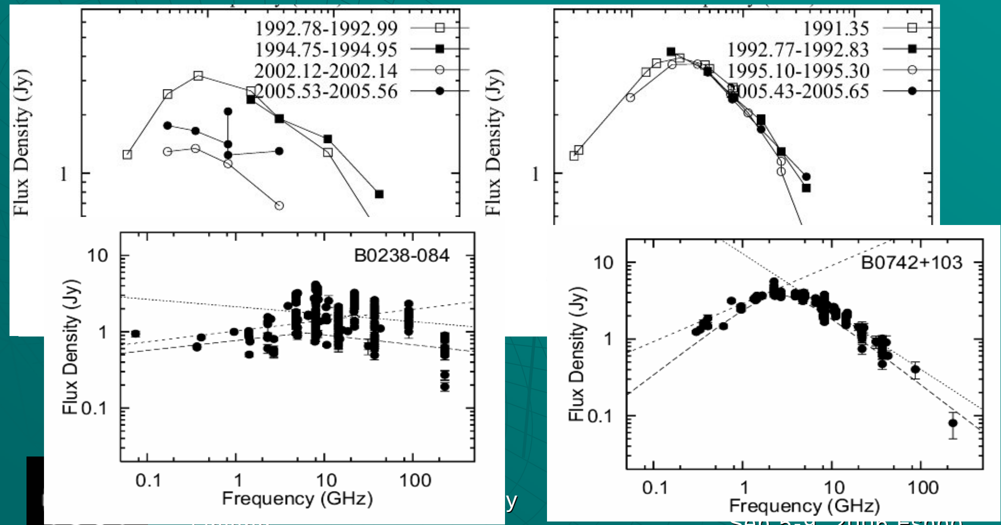

Finland
Sep 5-9, 2006 Espoo

GPS sources and Planck foreground science?

- AGNs v.0.0
  - "Normal" and flat-spectrum AGNs
- AGNs v.0.1
  - v.0.0 + "traditional" GPS sources
- AGNs v.0.2
  - v.0.1 + high-peaking GPS sources
- AGNs v.1.0
  - v.0.2 + sources with inverted spectrum during flares

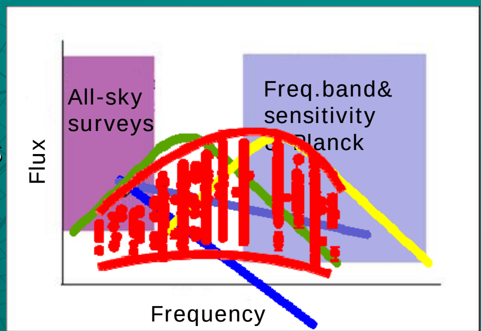

=> Complicated situation

Ilona Torniainen
Metsähovi Radio Observatory
Finland

8th ENIGMA meeting
Sep 5-9, 2006 Espoo

Future

- The monitoring continues
- Self-organized neural maps on GPS sources:
  - 209 sources from literature
  - Both gal and qso
  - All possible parameters
  - => To cluster the similar sources

Ilona Torniainen
Metsähovi Radio Observatory
Finland

8th ENIGMA meeting
Sep 5-9, 2006 Espoo

Variability time scales from long term monitoring

Talvikki Hovatta
Metsähovi Radio Observatory
Helsinki University of Technology

Merja Tornikoski, Markku Lainela, Esko Valtaoja, Margo Aller, Hugh Aller, Elina Nieppola, Ilona Torniainen

The 8th ENIGMA meeting
September 6-8, 2006
Espoo, Finland

Overview

- Introduction
- Data and Methods
- Observational time scales
- Considerations
- Intrinsic time scales
- Future

Introduction

- Variability studies of a large sample of sources
  - Time scale analysis
    - Differences between classes
    - Differences between frequencies
  - Comparing different methods
  - Comparing results with earlier paper by Lainela & Valtaoja (1993, ApJ, 416, 485)

The Data

- 80 sources from the Metsähovi monitoring sample
  - HPQ, LPQ and BLO sources and Radio Galaxies
- Data at 4.8, 8, 14.5, 22, 37, 90 and 230 GHz
  - data from Metsähovi at 22, 37 and 90 GHz
    - some have been monitored for over 25 years
  - 4.8, 8 and 14.5 GHz from the UMRAO
  - 90 and 230 GHz monitoring data from the SEST
  - 90 and 230GHz published data from IRAM

Methods

- The Structure Function
  - Smaller variations and the structure of the flux curve
- Discrete correlation function
  - Autocorrelation
- Lomb-Scargle periodogram
  - Peak-to-peak time scales

Average time scales

Frequency	SF	DCF	Periodogram
4.8 GHz	5.2*	6.6 (5.1**)	8.7 (7.5)
8 GHz	5.6	9.4 (7.1)	9.7 (9.0)
14.5 GHz	4.3	8.1 (6.6)	8.5 (8.0)
22 GHz	4.1	5.6 (4.4)	6.6 (5.5)
37 GHz	2.6	5.1 (4.1)	7.0 (6.2)
90 GHz	2.0	3.8 (3.5)	4.9 (3.7)

* All time scales are in years
** For DCF and Periodogram analysis also the time scale with no lower limit estimates (T/2) are shown

Talvikki Hovatta
Metsähovi Radio Observatory
The 8th ENIGMA meeting
September 6, 2006

Distributions of SF time scales

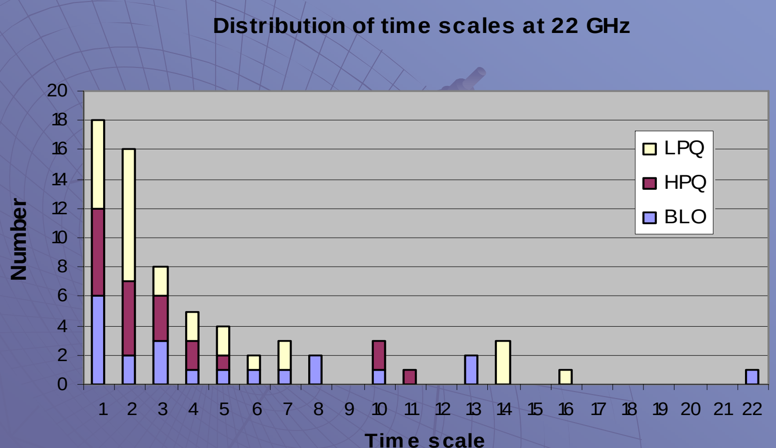

Talvikki Hovatta
Metsähovi Radio Observatory
The 8th ENIGMA meeting
September 6, 2006

Distributions of SF time scales

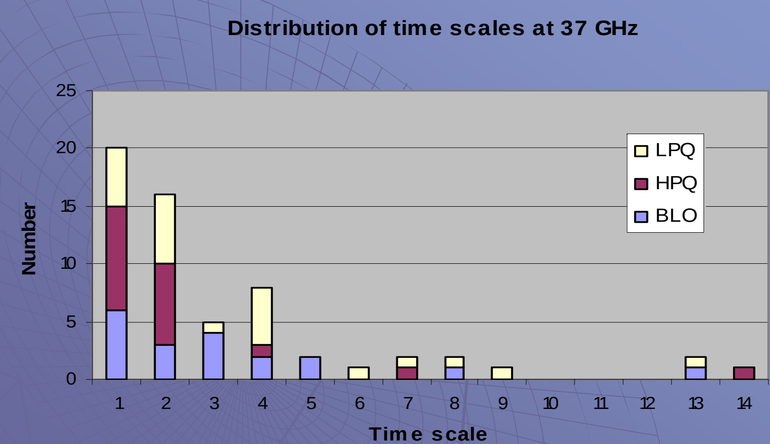

Talvikki Hovatta
Metsähovi Radio Observatory
The 8th ENIGMA meeting
September 6, 2006

Example 1156+295 (4C 29.45)

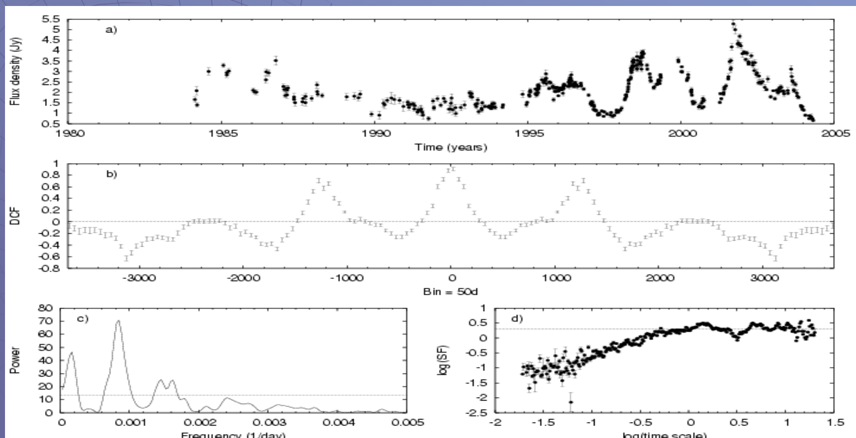

Example 1156+295 (4C 29.45)

- Time scales from DCF and Periodogram are very similar
  - 3.29 years from periodogram
  - 3.49 years from DCF
- Shorter time scale of 1.2 years from the SF
  - Much shorter compared to time scale of 6.8 years from Lainela & Valtaoja 1993

Comparison of SF time scales with earlier analysis

- 42 sources
- L&V found significant differences between classes
  - LPQs and HPQs differed from each other
- Averages have changed
  - 22 GHz: 2.6 years -> 4.8 years
  - 37 GHz: 2.3 years -> 2.6 years
- Number of lower limit estimates has decreased from 32 to 10

Considerations

- Harmonic T/n time scales from periodogram analysis
  - Real time scales shifted in time
- Baseline effects
- Gaps in the data
- Faint sources

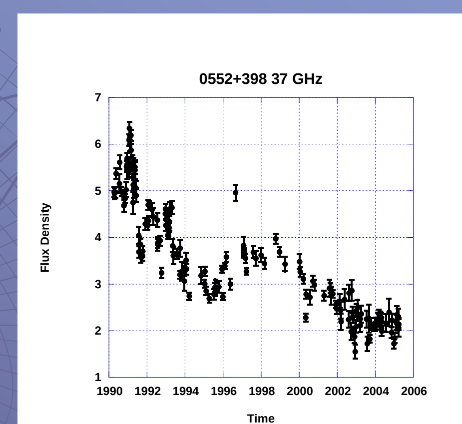

Summary of the Results

- Peak-to-peak flare time scales are long with average closer to 7 years
- Short term variations can be also seen
- More than one method is needed to reveal all of them

Summary of the results

- Higher frequencies ≥22 differed from lower ones significantly for all methods.
- Set of Kruskal-Wallis analysis for all methods did not reveal any significant differences between classes for most of the frequencies

Averages after z-correction

Freq	BLO	BLO intrinsic	HPQ	HPQ intrinsic	LPQ	LPQ intrinsic
4.8	9.58	7.08	7.34	4.02	9.15	4.49
8	9.38	6.84	9.52	5.07	9.76	4.94
14.5	7.83	6.13	8.59	4.73	8.87	4.26
22	6.50	5.02	6.39	3.36	6.87	3.18
37	7.03	5.50	6.74	3.57	7.28	3.55
90	4.90	2.89	5.10	2.94	4.58	2.62

Differences between the classes

- Intrinsic time scales from periodogram analysis revealed significant difference between BLOs and quasars.
- In SF and DCF analyses none of the classes differed clearly from others.

In Preparation

- Correction for Doppler-boosting
  - Doppler boosting factors from Lähteenmäki et al. 1999 (ApJ, 521, 493)
  - Correlation between corrected luminosity and time scales

Future

- Results will be published in Hovatta et al. later this year
- Nieppola et al. with more detailed analysis of BL Lacertae objects
  - Flares and time scales
- Wavelet analysis for the same sample
- Flare analysis for all well monitored flares

Long Term Radio Monitoring -- Why Do We Need It?

M. Tornikoski, A. Lähteenmäki [1)]
E. Valtaoja [2)]
T. Hovatta, E. Nieppola,
I. Torniainen, M. Kotiranta [1)]

[1)] Metsähovi Radio Observatory, Finland
[2)] Tuorla Observatory, Finland

Observations of various source samples

- Many on-going projects, also very large samples.
  - Typically, spectral indices & variability.
  - The Metsähovi group:
    Can we / the Planck satellite / other (sub)mm telescopes detect sources that have been *assumed* to be faint at higher frequencies?
    - GPS sources and candidates (talk by Torniainen et al.)
    - the complete BLO sample (talk by Nieppola et al.)
  - Often only few observing epochs
    (especially for the larger samples
    or when telescope time is very limited).

Observations of various source samples

- Many on-going projects, also very large samples.
  - Typically, spectral indices & variability.
  - The Metsähovi group:
    Can we / the Planck satellite / other (sub)mm telescopes detect sources that have been *assumed* to be faint at higher frequencies?
    - GPS sources and candidates (talk by Torniainen et al.)
    - the complete BLO sample (talk by Nieppola et al.)
  - Often only few observing epochs
    (especially for the larger samples
    or when telescope time is very limited).

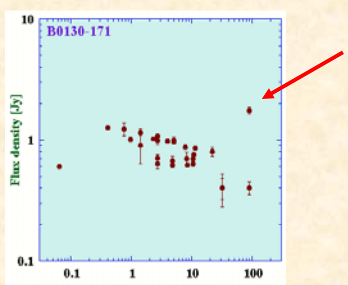

Merja Tornikoski
Metsähovi Radio Observatory

Some multifrequency data

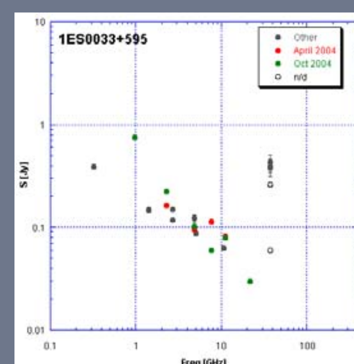

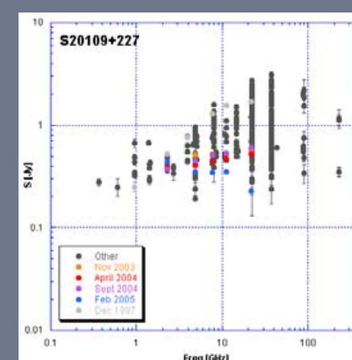

… multifrequency data

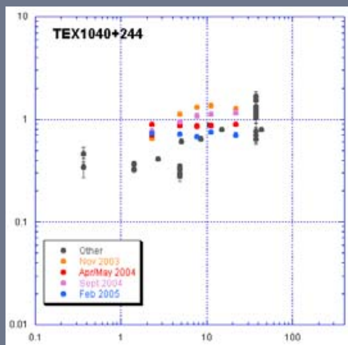

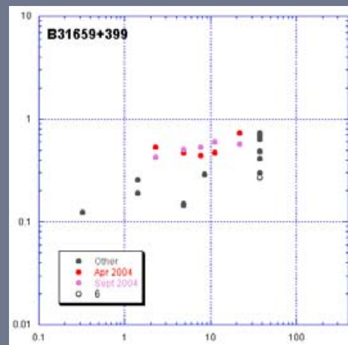

3 – 4 years of data.

How much do we know now?

Merja Tornikoski
Metsähovi Radio Observatory

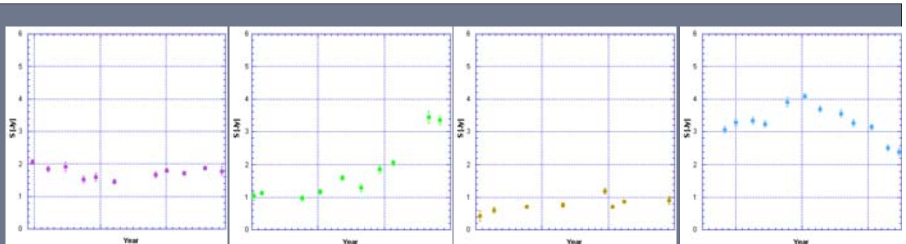

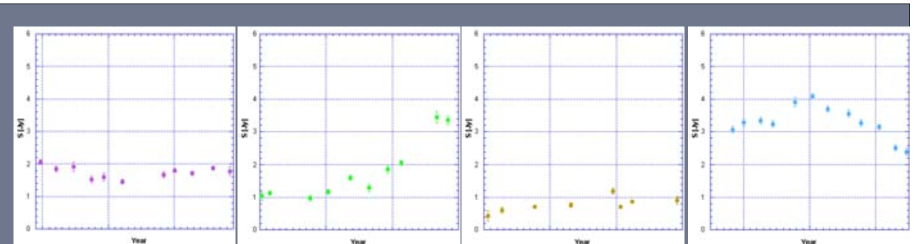

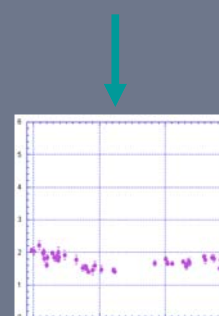

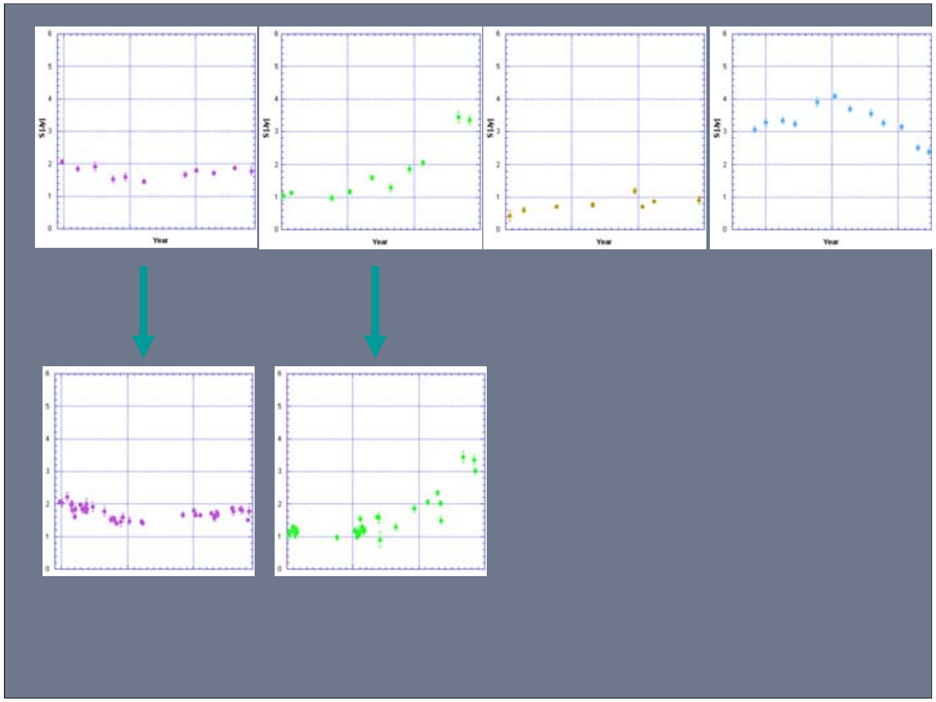

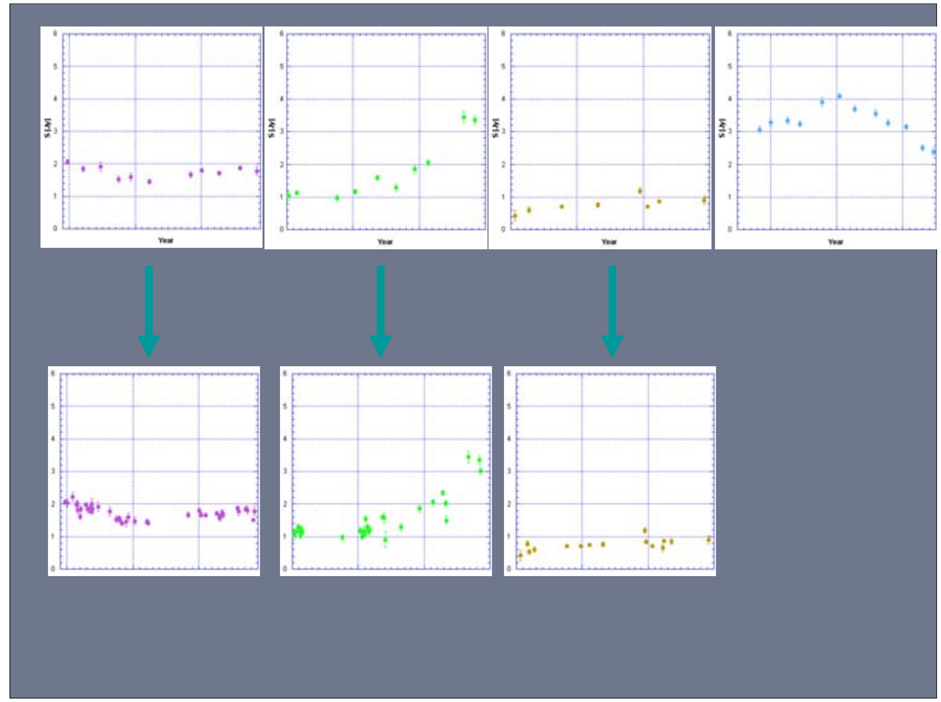

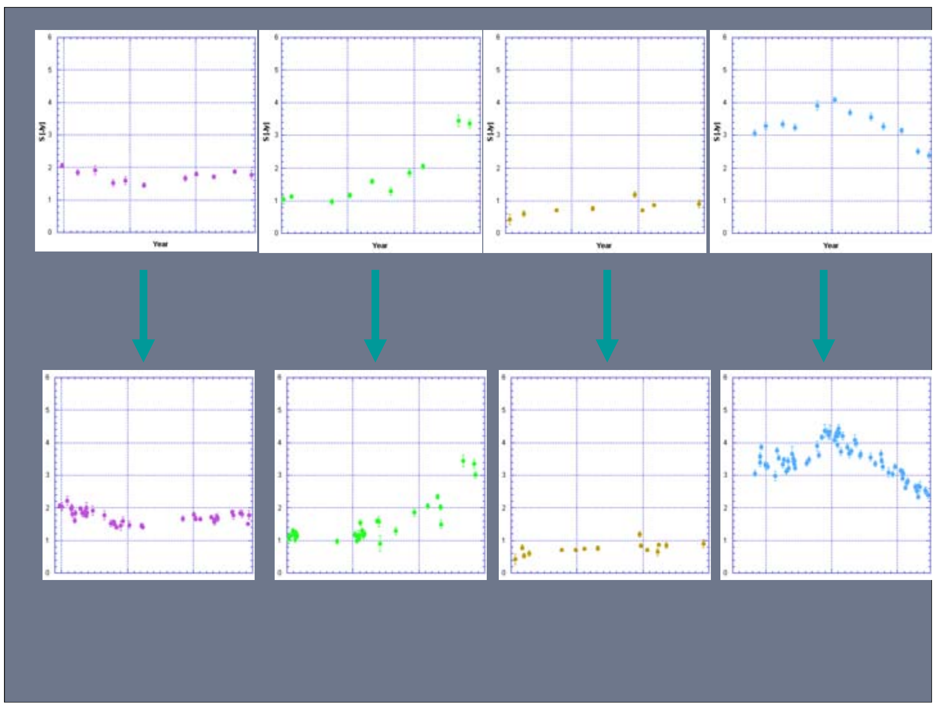

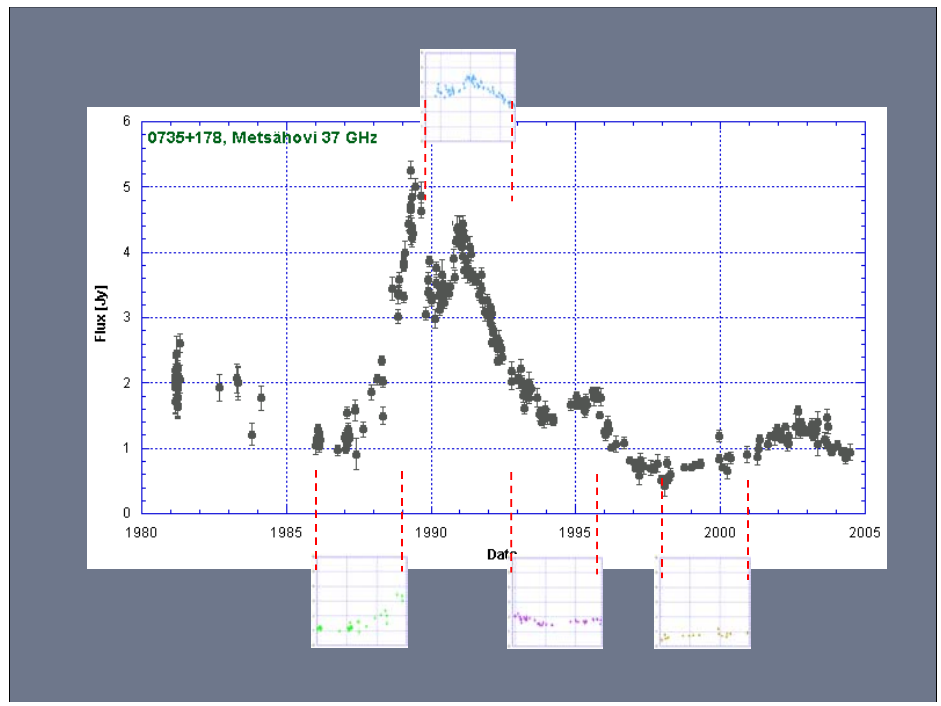
0735+178, Metsähovi 37 GHz
Flux [Jy]
Date
0
1
2
3
4
5
6
1980
1985
1990
1995
2000
2005

Three (five, ten, ...?) years of observations are <u>not enough</u> for determing a "typical behaviour" of an AGN!

<u>Long timescales</u> are more important than dense sampling!

More examples:

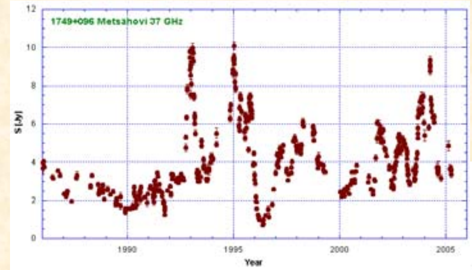

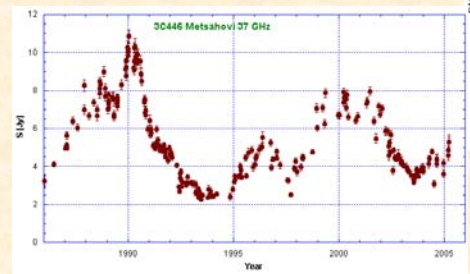

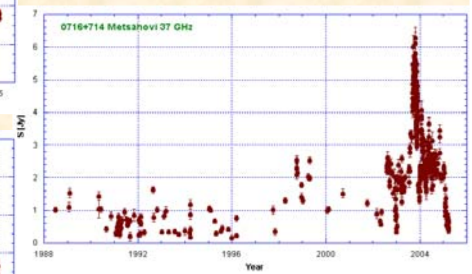

Some statistics

How much time (nr. of data points or a random observing epoch) does a source spend in an **1)** active **2)** intermediate **3)** quiescent state?

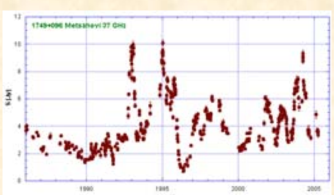

1)

2)

3)

Some statistics

How much time (nr. of data points or a random observing epoch) does a source spend in an **1)** active **2)** intermediate **3)** quiescent state?

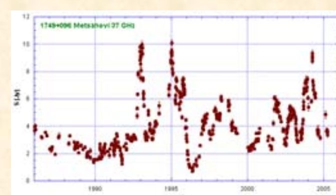

1)

2)

3)

For all the 80 best-monitored sources at 37 GHz:
1) 11%
2) 38%
3) 51%

9 times out of 10 we are likely to see the source in a quiescent or an intermediate state!

What does this mean?

- No idea about the "real" activity behaviour
  - Incorrect conclusions about variability, continuum spectra, detectability, effects on the CMB foregrounds, ...
  - Misinterpretations about source types, subtypes, ...
  - Exclusion of interesting objects!
- Multifrequency (radio) observing campaigns are bound to fail (or, at least "fail").
- Incorrect theoretical interpretations?

Extensive analysis of 25 years of multifrequency data
or
How to predict activity behaviour in AGNs?

- Typical flare timescales
  - From visual inspection, flare statistics, general activity statistics (quiescent/active/im.states), mathematical analysis (SF, DCF, periodograms...), flare decomposition & analysis.
  - For various source types, subtypes, individual sources...
  - Timescales vs. luminosities etc.
  - Note: 25 yrs of data very different from 10 yrs of data!

... 25 years of multifrequency data

- Typical flare structures
  - Very different shapes, durations, rise & decay times, duty cycles.
  - "Flare taxonomy": simple vs. multipart, rapid vs. slow, various rise&fall times and shapes – decomposing the flares.
  - $t_{var} \rightarrow T_{b,obs} \rightarrow D$
  - Connections with other frequency bands & VLBI.
- Typical flare amplitudes
  - Absolute, relative, vs. the frequency band.
  - Compare with predictions from the shock models.

… 25 years of multifrequency data

- How do we recognise a starting flare?
  - Not all flux increase results in a flare!
  - Timescale analysis & flare taxonomy & support observations: educated guesses.
  - Also: self-organised maps etc. advanced analysis methods.

    → "Flare Prediction Testbed"
- Have been focusing on observational aspects (esp. CMB foregrounds):

  "what are we likely to see in a given source at a given time?",

  moving towards the theory:

  the radio shock models, blazar sequence scenario, ...
- Several papers in preparation by the Metsähovi-Tuorla radio team.

S5 0716+71

Variability across the electromagnetic spectrum during 2003-2004

Luisa Ostorero
(Landessternwarte Heidelberg, Germany)

on behalf of the S5 0716+71 ENIGMA-WEBT collaboration

Outline

0716+714 long-term variability during 2003-2004

- Optical and near-infrared light curves
- Colour variations
- Comparison with the historical brightness trend

0716+714 short-term variability:

simultaneous X-ray and optical observations in April 2004

- X-ray variability
- A correlated optical/UV/X-ray flare
- Intra-day SED evolution

Summary

0716+714 long-term variability during 2003-2004

2003-2004 optical-NIR light curves

Status of the analysis of optical and near-infrared data collected during the extended campaign:

~17000 data from 32 observatories over a period of ~10 months (October 2003 – July 2004)

* photometry :	completed
* Calibration run with 3 stars (3,5,6):	completed
* color analysis:	work in progress

2003-2004 optical-NIR light curves

Lulin
Yunnan
Sampurnand
Hanle
Mt. Abu
Mt. Maidanak
Abastumani
SAI Crimean
Crimean
Jakokoski
Canakkale
Nyrola
Tuorla
MonteBoo
Catania
Campo Imperatore
Perugia
Heidelberg
Trebur
TIRGO
Torino
Hoher List
Sabadell
Calar Alto
NOT
KVA
WHT
Bell
St. Louis
WIYN
Coyote Hill
Univ. Victoria

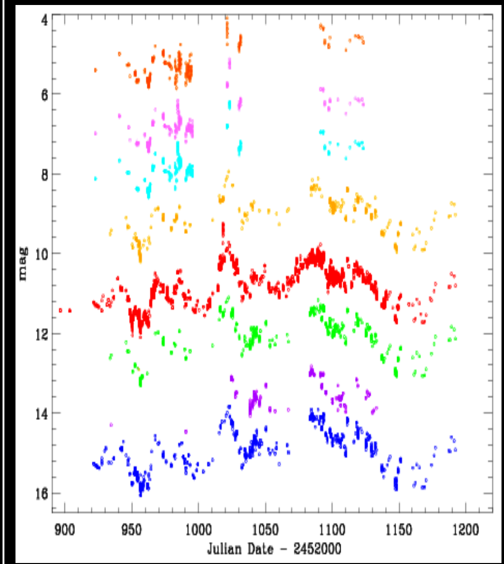

Ostorero et al., in prep.

outbursts ~ simultaneous at optical and NIR frequencies

long-term variations of comparable amplitude in all the bands

best sampling: B, R

2003-2004 colour variations

- Big spread in colour indices in the total color data set
  - ⇒ work in progress to reduce inter-instrumental colour offsets
- Selected the best B-R long-term da ta set:
  - Mt. Maidanak Obs. (Uzbekistan)
  - main light curve features: well sampled (coloured points)
- Computed colour indices by coupling data taken within Δt_{max}=5 min

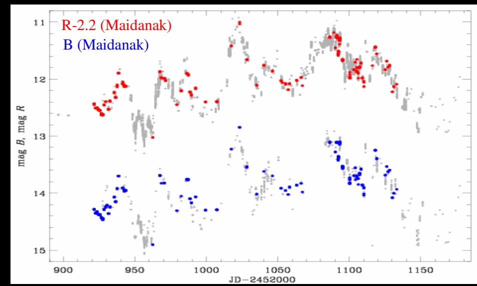

2003-2004 colour variations

- Big spread in colour indices in the total color data set
  - ⇒ work in progress to reduce inter-instrumental colour offsets
- Selected the best B-R long-term da ta set:
  - Mt. Maidanak Obs. (Uzbekistan)
  - main light curve features: well sampled (coloured points)
- Computed colour indices by coupling data taken within Δt_{max}=5 min

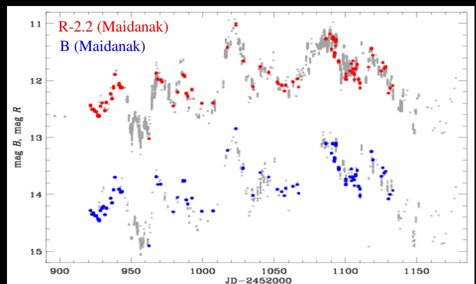

- No correlation between colur and brightness!

Pearson correlation coefficient
r_P=0.067
$P(r>r_P)$=19.3 %

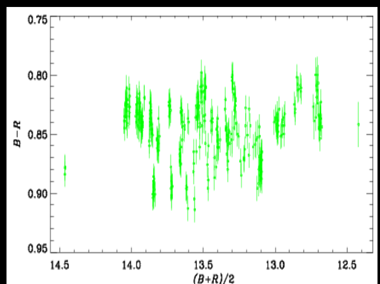

2003-2004 colour variations

- Big spread in colour indices in the total color data set
  - ⇒ work in progress to reduce inter-instrumental colour offsets
- Selected the best B-R long-term da ta set:
  - Mt. Maidanak Obs. (Uzbekistan)
  - main light curve features: well sampled (coloured points)
- Computed colour indices by coupling data taken within Δt_{max}=5 min

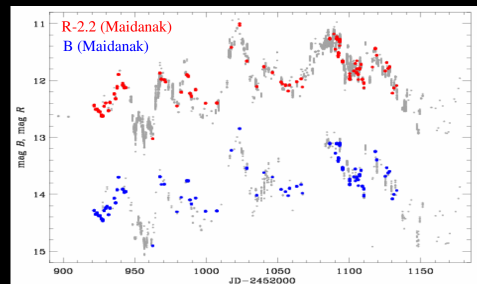

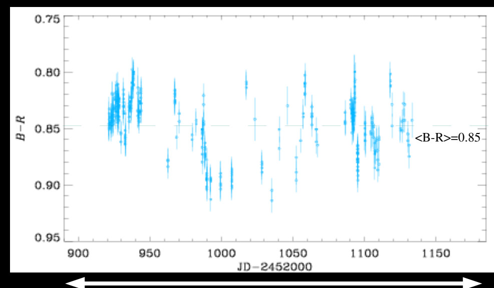

~ 10 months

2003-2004 colour variations

- Big spread in colour indices in the total color data set
  - ⇒ work in progress to reduce inter-instrumental colour offsets
- Selected the best B-R long-term da ta set:
  - Mt. Maidanak Obs. (Uzbekistan)
  - main light curve features: well sampled (coloured points)
- Computed colour indices by coupling data taken within Δt_{max}=5 min
- Possible association of flux bursts and colour index variations (*flatter-when-brighter*) (agreement with Ghisellini et al. 1997)

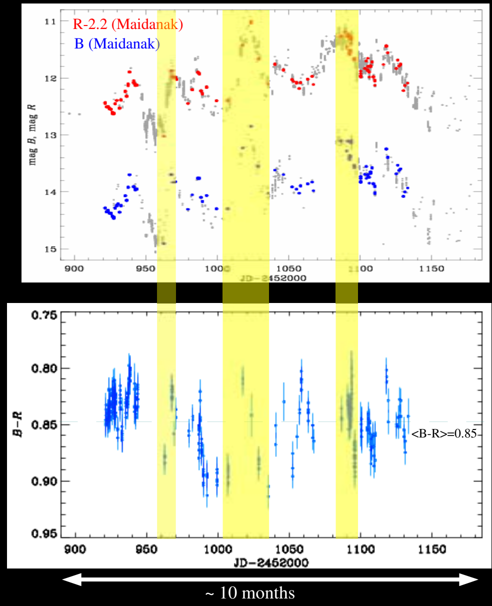

2003-2004 colour variations

- Big spread in colour indices in the total color data set
  - ⇒ work in progress to reduce inter-instrumental colour offsets
- Selected the best B-R long-term da ta set:
  - Mt. Maidanak Obs. (Uzbekistan)
  - main light curve features: well sampled (coloured points)
- Computed colour indices by coupling data taken within Δt_{max}=5 min
- Possible association of flux bursts and colour index variations (*flatter-when-brighter*) (agreement with Ghisellini et al. 1997)
- Color variations comparable for bursts of different amplitude >1 mag ~ 0.5 mag

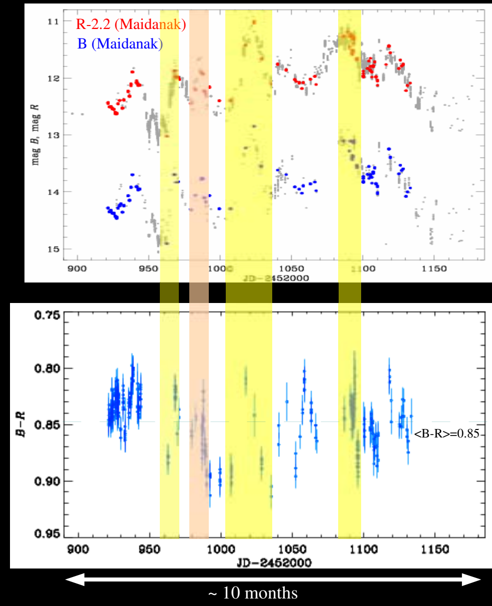

2003-2004 colour variations

- Big spread in colour indices in the total color data set
  - ⇒ work in progress to reduce inter-instrumental colour offsets
- Selected the best B-R long-term da ta set:
  - Mt. Maidanak Obs. (Uzbekistan)
  - main light curve features: well sampled (coloured points)
- Computed colour indices by coupling data taken within Δt_{max}=5 min
- Possible association of flux bursts and colour index variations (*flatter-when-brighter*) (agreement with Ghisellini et al. 1997)
- Color variations comparable for bursts of different amplitude >1 mag ~ 0.5 mag

...but also : comparable colour variations without any apparent flux burst!

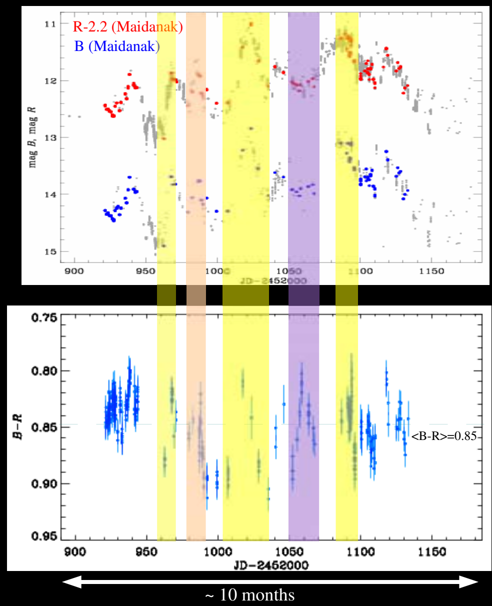

... Work in progress...

2003-2004 optical R-band light curve

Lulin
Yunnan
Sampurnand
Hanle
Mt. Maidanak
Abastumani
SAI Crimean
Crimean
Jakokoski
Canakkale
Nyrola
Tuorla
MonteBoo
Perugia
Heidelberg
Trebur
Torino
Hoher List
Calar Alto
KVA
WHT
Bell
St. Louis
WIYN
Coyote Hill
Univ. Victoria

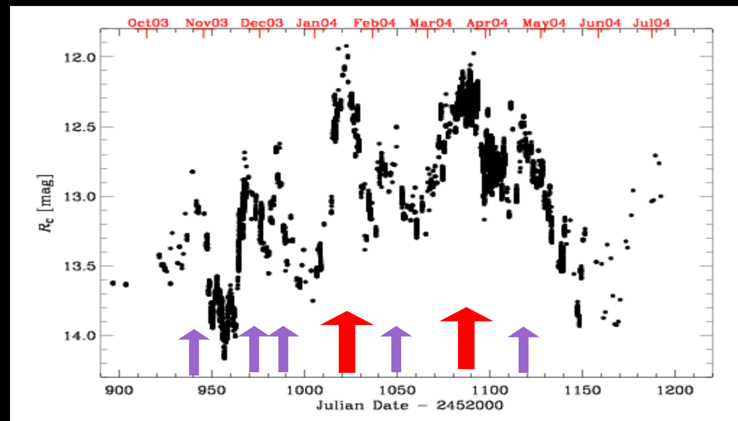

- Several outbursts lasting ~ 2-6 weeks
- 2 biggest outbursts: Jan 2004, Mar-Apr 2004 (~70 days apart)

How does this light curve compare to the historical behaviour?

1953-2003 optical B-band light curve: historical trend

B-band historical light curve (1953-2003)

from Nesci et al. 2005

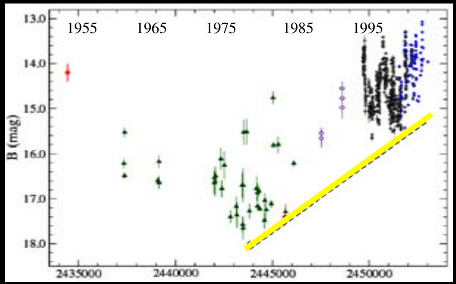

◆◆◆ 1953-1985: Archival plates (Nesci et al. 2005)
◆ 1994-2001: CCD monitoring (Raiteri et al. 2003)
◆ 2001-2003: CCD monitoring (Nesci et al. 2005)
long-term trend proposed by Nesci et al. (2005)

Nesci et al. (2005): investigation of the optical long-term (~50 years) behaviour of S5 0716+71 by means of archival plate data:

- source active in the past, but much fainter on average
- possible long-term brightening of ~ 0.11 mag/yr from 1975-80 to the present high state

1953-2003 optical B-band light curve: historical trend

B-band historical light curve (1953-2003)

from Nesci et al. 2005

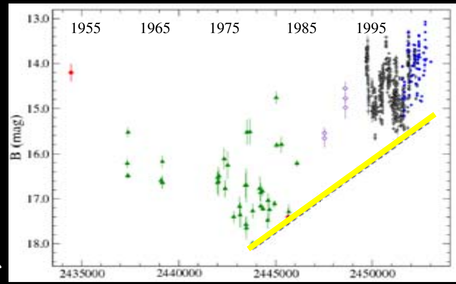

◆◆◆ 1953-1985: Archival plates (Nesci et al. 2005)
◆ 1994-2001: CCD monitoring (Raiteri et al. 2003)
◆ 2001-2003: CCD monitoring (Nesci et al. 2005)
long-term trend proposed by Nesci et al. (2005)

Nesci et al. (2005): investigation of the optical long-term (~50 years) behaviour of S5 0716+71 by means of archival plate data:

- source active in the past, but much fainter on average
- possible long-term brightening of ~ 0.11 mag/yr from 1975-80 to the present high state

Bach et al. (2005): analysis of VLBI monitoring data of 1992-2001
⇒ decrease of β_{app} of the jet components with time

➢ Scenario proposed by Nesci et al. (2005):
- slowly precessing jet, approaching the l.o.s.
$\theta = 5^{\circ} \rightarrow 0.7^{\circ}$; $\delta = 15 \rightarrow 22$; Γ=12-15
- prediction: optical dimming phase during the next ~10 years

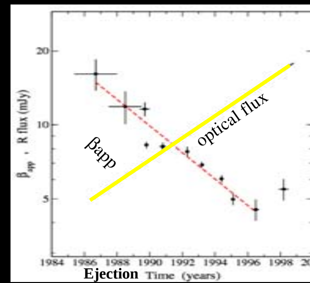

from Nesci et al. 2005

2003-2004 optical B-band light curve and historical trend

B-band historical light curve (1953-2003)

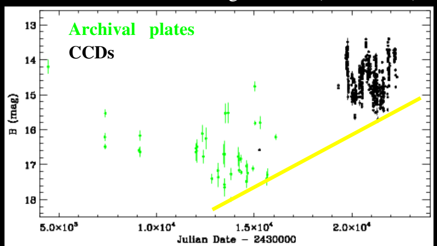

long-term trend proposed by Nesci et al. (2005)
◆ 1953-1985: Archival plates (Nesci et al. 2005)
◆ 1994-2001: CCD monitoring (Raiteri et al. 2003)

2003-2004 optical B-band light curve and historical trend

B-band historical light curve (1953-2003)

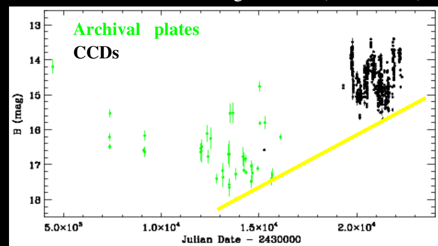

long-term trend proposed by Nesci et al. (2005)
◆ 1953-1985: Archival plates (Nesci et al. 2005)
◆ 1994-2001: CCD monitoring (Raiteri et al. 2003)

B-band historical light curve (1953-2004)

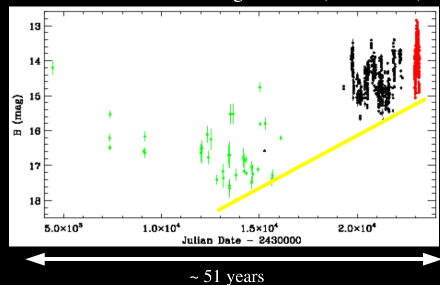

◆ 2003-2004: ENIGMA-WEBT campaign (Ostorero et al., in prep.)

two historical outburts, in agreement with the historical trend

➢ did we catch the more aligned jet state?

2003-2004 optical R-band light curve and historical trend

R-band light curve 1996-2003

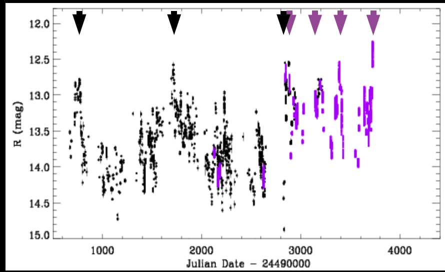

◆ Raiteri et al. (2003)
◆ Nesci et al. (2005); Montagni et al. (2006)

Variability time scales

1995-2002 : ~ 3.3 yr oscillating trend (Raiteri et al. 2003)
2002-2003 : ~1 yr outburst frequency (Nesci et al. 2005)
(3.3 yr - trend disproved)

2003-2004 optical R-band light curve and historical trend

R-band light curve 1996-2003

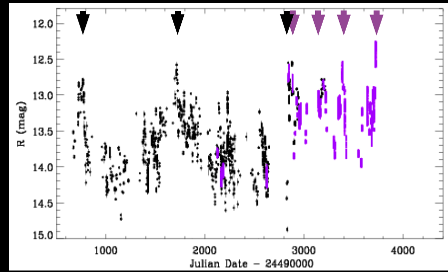

◆ Raiteri et al. (2003)
◆ Nesci et al. (2005); Montagni et al. (2006)

Variability time scales

1995-2002 : ~ 3.3 yr oscillating trend (Raiteri et al. 2003)
2002-2003 : ~1 yr outburst frequency (Nesci et al. 2005)
(3.3 yr - trend disproved)

R-band light curve 1996-2004

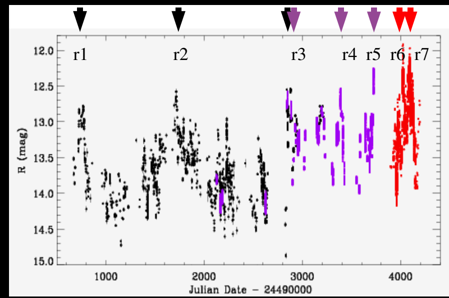

◆ 2003-2004: ENIGMA-WEBT campaign

Two outbursts: r6 and r7
- r6 (Jan 2004) : ~ 320 days after r5 (March 2003)
- r7 (Mar-Apr 2004): 70 days after r6

Possible trend of increasing frequency and brightness of the major outbursts

➢ agreement with the increase of the Doppler factor δ due to the alignment of a precessing jet with the l.o.s.

$$F \propto \delta^3(t)\cdot F' \qquad \frac{dF}{dt} \propto \delta^4(t)\left(\frac{dF'}{dt'}\right)$$

0716+714 short-term variability:

simultaneous X-ray and optical observations in April 2004

XMM and INTEGRAL ToO observation of April 2004

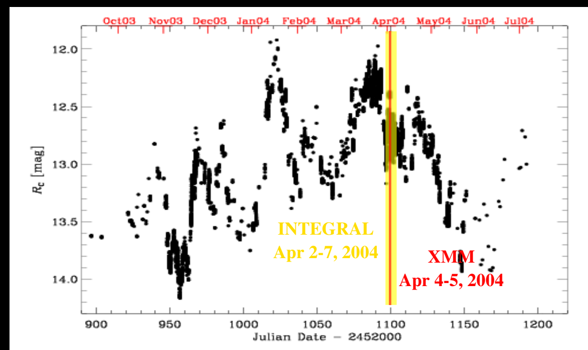

March-April 2004 optical outburst ⇒ trigger of a combined XMM and INTEGRAL ToO observation
[Proposals'P.I.s: G. Tagliaferri (XMM); E. Pian (INTEGRAL)]

Results: Pian, Foschini, Beckmann, et al. 2005 (INTEGRAL) A&A, 429, 427
Foschini, Tagliaferri, Pian, et al. 2006 (XMM) A&A, in press; astro-ph/0604600
Ferrero, Wagner, Emmanoulopoulos, & Ostorero 2006 (XMM) A&A, in press; astro-ph/0607023

XMM observation: X-ray spectrum

59 ks observation
PN + MOS data analysis in 0.5-10.0 keV

- broken and double power-law with Galactic absorption:
  - better and simpler parametrization of the data
  - easy interpretation in terms of synchrotron (softer, steeper) and inverse-Compton (harder, flatter) components
- concavity of the spectrum: evident (S5 0716+71: IBL)

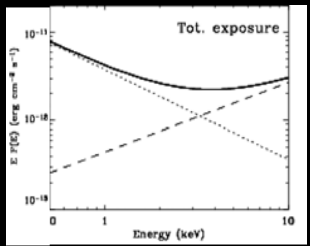

ex. PN data – fit values

Γ_1	E_{break} [keV]	Γ_2	$F_{2\text{-}10\ keV}$ $[10^{-12}erg/cm^2/s]$
	BROKEN P.L.		
2.83±0.01	1.91(+0.1;-0.08)	2.06 (+0.05, -0.06)	3.83(+0.11;-0.10)
	DOUBLE P.L. (see fig.)		
3.01±0.05		1.22 (+0.15, -0.02)	3.95(+0.45;-1.16)

from Ferrero et al. 2006

XMM observation: X-ray flux variability

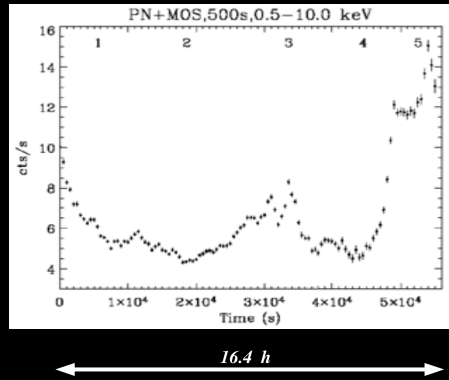

Combined PN+MOS light curve: 0.5-10 keV

Length: 59 ks
Bin size: 500 s

- FVA = 37±2%
- No characteristic variability time scales
- PDS slope: 2.64±0.36 ⇒ red noise process
- Shortest time-scale (before noise): 2.5 ks

[$R < 0.7\delta/(1+z)$ l.h. ~ $25\cdot10^{-6}\delta/(1+z)$ pc ~ few 100 μpc]

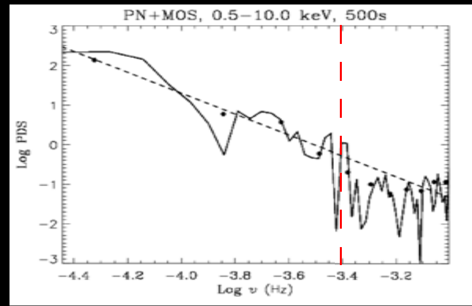

from Ferrero et al. 2006

XMM observation: X-ray flux variability

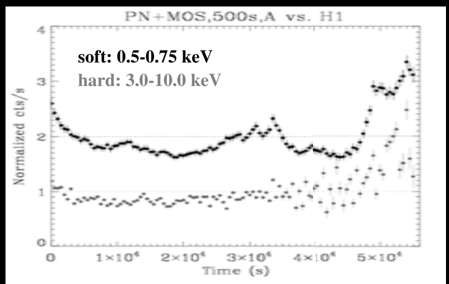

from Ferrero et al. 2006

Combined PN+MOS soft and hard light curves

Fractional variability amplitude:
soft band: FVA = 40±3%
hard band: FVA = 27±1%

- more variability in the soft band

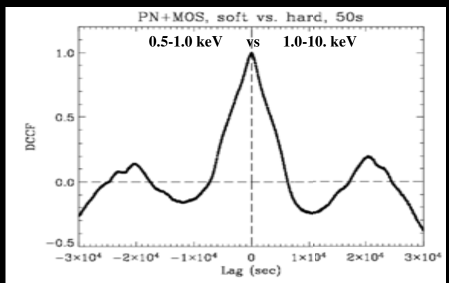

Discrete correlation function: soft vs hard

Bin size = 50 s
DCF peak position: τ_{peak}
(errors on τ_{peak}: simulations; 1000 runs)
negative lags = soft lag

- $\tau_{peak} = -50^{+125}_{-75}\,s$ ⇨ lags ≥ 100 s not present!

XMM observation: X-ray spectral variability

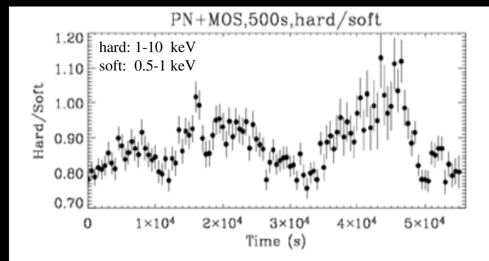

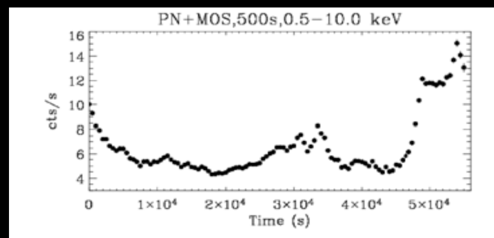

Hardness-ratio vs count-rate light curves
(soft: 0.5-1 keV; hard:1-10 keV)

- anticorrelation bw HR and flux: *softer-when-brighter* behaviour (opposite to the trend usually observed in HBL)
- need of investigating the role of the synchrotron and IC components, possibly time-dependent

from Ferrero et al. 2006

XMM observation: time-resolved X-ray spectral analysis

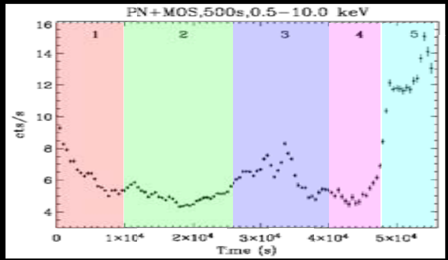

from Ferrero et al. 2006

Time-resolved spectral analysis

- light curve divided in 5 time intervals: compromise between high time resolution and good photon statistics
- spectral analysis with double power-law model repeated for each time interval

XMM observation: time-resolved X-ray spectral analysis interval 1

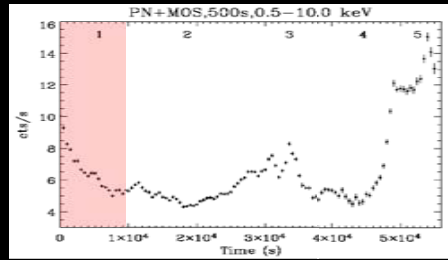

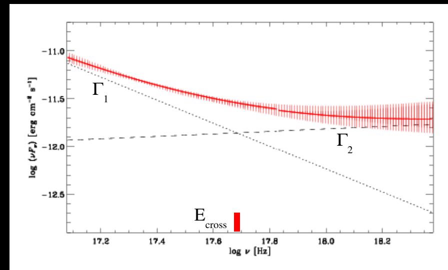

Γ_1 = 3.20

Γ_2 = 1.87

E_{cross} = 2.01 keV

Sinchr. % = 58

from Ferrero et al. 2006

XMM observation: time-resolved X-ray spectral analysis interval 2

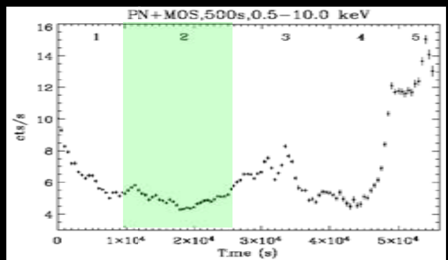

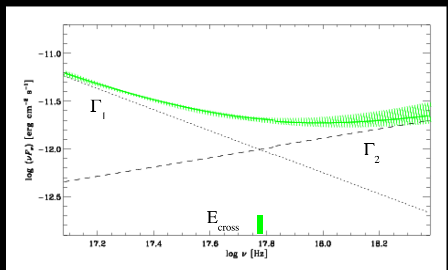

Γ_1 = 3.10

Γ_2 = 1.50

E_{cross} = 2.46 keV

Sinchr. % = 62

from Ferrero et al. 2006

XMM observation: time-resolved X-ray spectral analysis interval 3

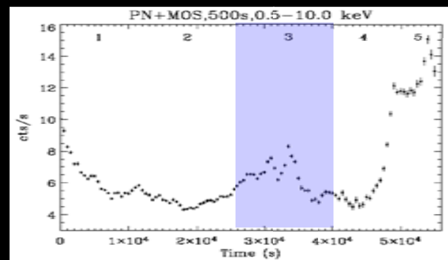

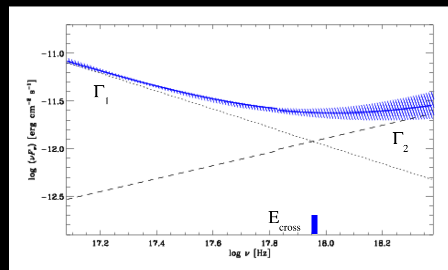

Γ_1 = 2.95

Γ_2 = 1.30

E_{cross} = 3.74 keV

Sinchr. % = 72

from Ferrero et al. 2006

XMM observation: time-resolved X-ray spectral analysis interval 4

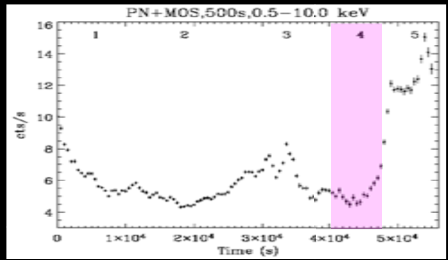

Γ_1 = 3.16

Γ_2 = 1.68

E_{cross} = 1.52 keV

Sinchr. % = 46

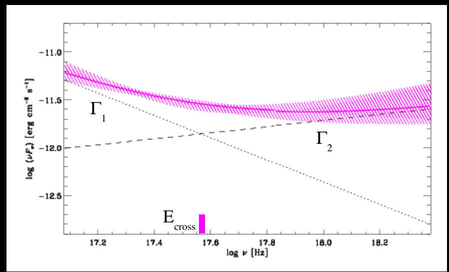

from Ferrero et al. 2006

XMM observation: time-resolved X-ray spectral analysis interval 5

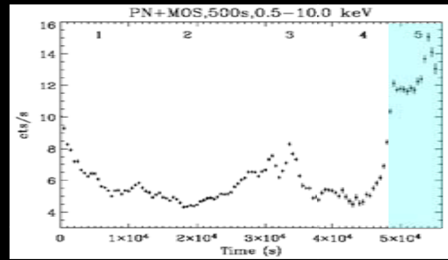

Γ_1 = 2.95

Γ_2 = 1.87

E_{cross} = 5.34 keV

Sinchr. % = 78

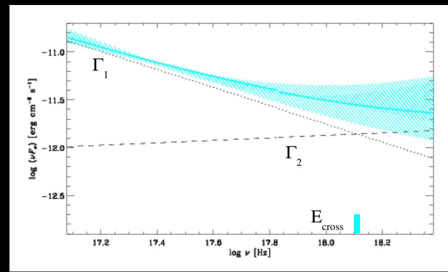

from Ferrero et al. 2006

XMM observation: time-resolved X-ray spectral analysis

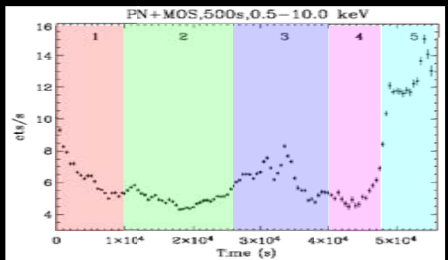

from Ferrero et al. 2006

Time-resolved spectral analysis

- light curve divided in 5 time intervals: compromise between time resolution and good photon statistics
- spectral analysis with double power-law model repeated for each time interval

Int.	Γ_1	Γ_2	E_{cross} (keV)	F_1 10^{-12} erg cm^{-2} s^{-1}	F_2 10^{-12} erg cm^{-2} s^{-1}	Synchr. (%)
1	$3.20^{+0.19}_{-0.16}$	$1.87^{+0.18}_{-0.25}$	2.01	5.99 ± 1.31	4.26 ± 1.60	58
2	$3.10^{+0.09}_{-0.11}$	$1.50^{+0.13}_{-0.22}$	2.46	5.08 ± 1.10	3.15 ± 1.33	62
3	$2.95^{+0.09}_{-0.07}$	$1.30^{+0.36}_{-0.27}$	3.74	7.93 ± 1.49	3.01 ± 1.88	72
4	$3.16^{+0.42}_{-0.26}$	$1.68^{+0.25}_{-0.34}$	1.52	4.28 ± 1.83	4.96 ± 2.04	46
5	$2.95^{+0.28}_{-0.14}$	$1.87^{+0.37}_{-0.62}$	5.34	13.01 ± 4.24	3.76 ± 1.91	78

- ➢ stronger soft (synchrotron) dominance during intervals of flaring activity (3, 5)
- ➢ significant variability of the hard (IC) component (contrary to previous results)
- ➢ soft (synchrotron) components: flatter-when-brighter behaviour (as in HBL); hard (IC) component: complex behaviour
- ➢ overall steeper-when-brighter behaviour: due to the flattening of the soft component during flares

XMM observation: time-resolved X-ray spectral analysis

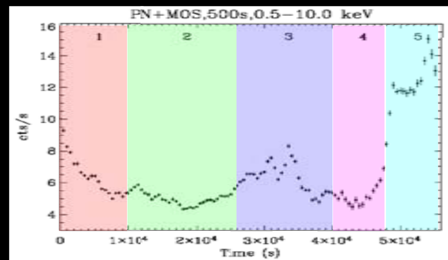

from Ferrero et al. 2006

Int.	Γ_1	Γ_2	E_{cross} (keV)	F_1 10^{-12} erg cm^{-2} s^{-1}	F_2 10^{-12} erg cm^{-2} s^{-1}	Synchr. (%)
1	$3.20^{+0.19}_{-0.16}$	$1.87^{+0.18}_{-0.25}$	2.01	5.99 ± 1.31	4.26 ± 1.60	58
2	$3.10^{+0.09}_{-0.11}$	$1.50^{+0.13}_{-0.22}$	2.46	5.08 ± 1.10	3.15 ± 1.33	62
3	$2.95^{+0.09}_{-0.07}$	$1.30^{+0.36}_{-0.27}$	3.74	7.93 ± 1.49	3.01 ± 1.88	72
4	$3.16^{+0.42}_{-0.26}$	$1.68^{+0.25}_{-0.34}$	1.52	4.28 ± 1.83	4.96 ± 2.04	46
5	$2.95^{+0.28}_{-0.14}$	$1.87^{+0.37}_{-0.62}$	5.34	13.01 ± 4.24	3.76 ± 1.91	78

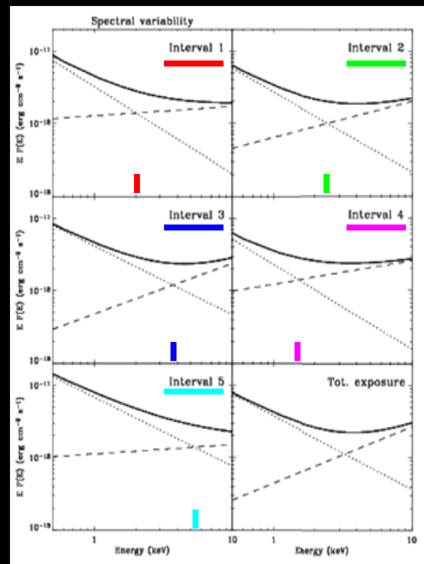

XMM observation: time-resolved X-ray spectral analysis

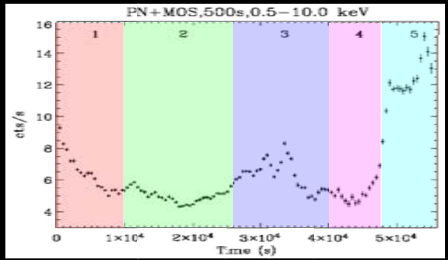

from Ferrero et al. 2006

Int.	Γ_1	Γ_2	E_{cross} (keV)	F_1 10^{-12} erg cm^{-2} s^{-1}	F_2 10^{-12} erg cm^{-2} s^{-1}	Synchr. (%)
1	$3.20^{+0.19}_{-0.16}$	$1.87^{+0.18}_{-0.23}$	2.01	5.99 ± 1.31	4.26 ± 1.60	58
2	$3.10^{+0.09}_{-0.11}$	$1.50^{+0.13}_{-0.22}$	2.46	5.08 ± 1.10	3.15 ± 1.33	62
3	$2.95^{+0.09}_{-0.07}$	$1.30^{+0.26}_{-0.27}$	3.74	7.93 ± 1.49	3.01 ± 1.88	72
4	$3.16^{+0.42}_{-0.26}$	$1.68^{+0.23}_{-0.34}$	1.52	4.28 ± 1.83	4.96 ± 2.04	46
5	$2.95^{+0.28}_{-0.14}$	$1.87^{+0.37}_{-0.62}$	5.34	13.01 ± 4.24	3.76 ± 1.91	78

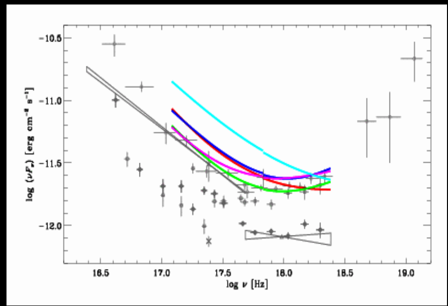

XMM SEDs superimposed to historical SEDs
(detections by HEAO-A, Einstein, ROSAT, ASCA, *Beppo*SAX)

An optical-UV and X-ray correlated flare: XMM "OM" and "PN+MOS" measurements

V
U
UVW1
UVM2

scaling to UVW1

X-ray 0.5-10 keV

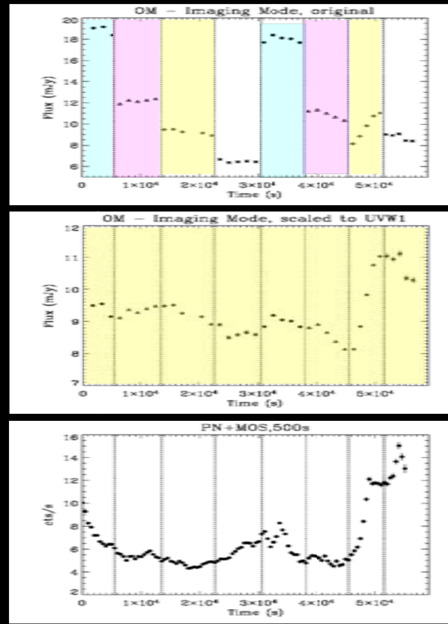

from Ferrero et al. 2006

Optical Monitor (OM) data

- imaging mode
- 38 exposures (1000-1200 s)
- V, U, UVW1, UVM2 sequences

-hyp. of power-law spectrum constant over Δt~1 ks
- spectral indices w.r.t. UVW1
- scaling of V, U, UVM2 to UVW1

➢ UV curve ≠ X-ray curve apart from the last flare

An optical-UV and X-ray correlated flare: XMM "OM" and "PN+MOS" measurements

V
U
UVW1
UVM2

scaling to UVW1

X-ray 0.5-10 keV

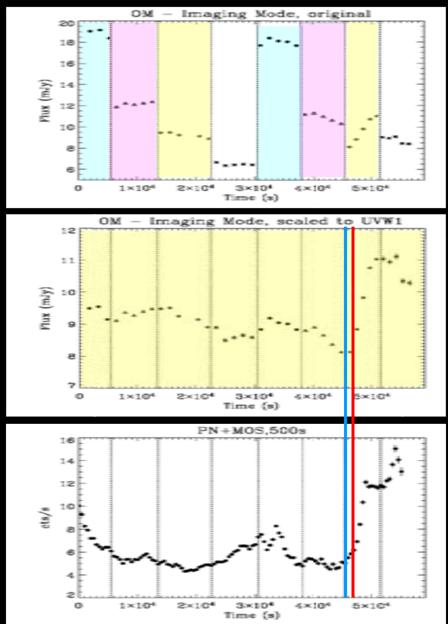

from Ferrero et al. 2006

Optical Monitor (OM) data

- imaging mode
- 38 exposures (1000-1200 s)
- V, U, UVW1, UVM2 sequences

-hyp. of power-law spectrum constant over Δt~1 ks
- spectral indices w.r.t. UVW1
- scaling of V, U, UVM2 to UVW1

➢ UV curve ≠ X-ray curve apart from the last flare

➢ Possible start of the final X-ray flare ~1 ks (~17 min) before the start of the UV flare

An optical-UV and X-ray correlated flare: ground-based optical measurements

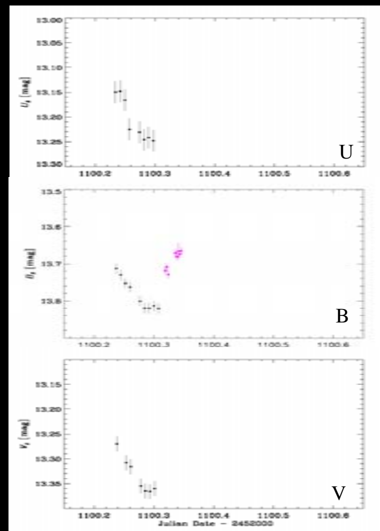

Ground-based optical observations:

UBVRI data provided by 7 optical observatories who were intensively monitoring the source during the INTEGRAL ToO of Apr. 2-7, 2004 (XMM pointing: not known)

~10 h

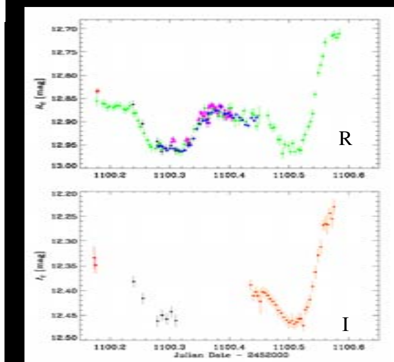

Abastumani
Maidanak
Nyröla
Tuorla
KVA
Sampurnand
Jakokoski

An optical-UV and X-ray correlated flare: ground- and space-based measurements

R-band (ground-based)

UVW1 (XMM-OM)

X-ray 0.5-10 keV (XMM, PN+MOS)

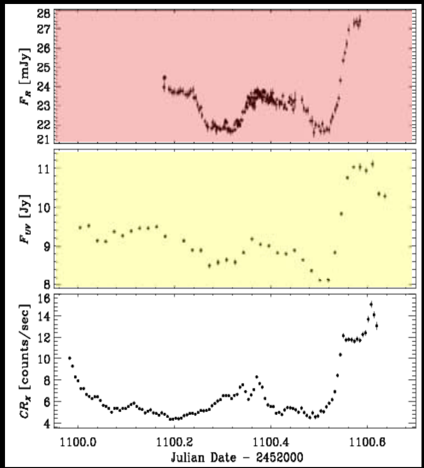

➢ Optical light curve: good match with the UV light curve; only the last flare (achromatic in "R-I") in common with the X-ray light curve

An optical-UV and X-ray correlated flare: ground- and space-based measurements

R-band (ground-based)

UVW1 (XMM-OM)

X-ray 0.5-10 keV (XMM, PN+MOS)

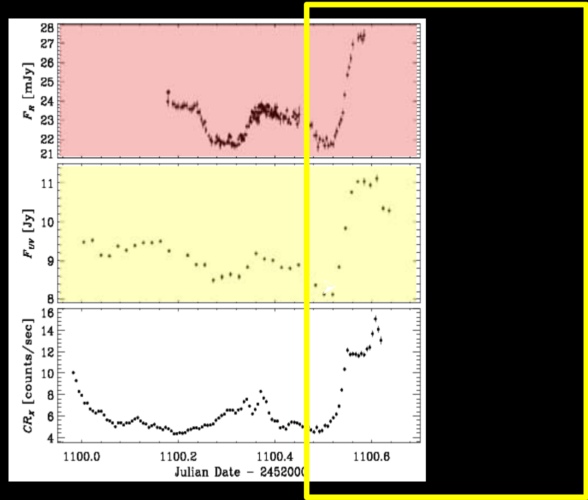

➢ Optical light curve: good match with the UV light curve; only the last flare (achromatic in "R-I") in common with the X-ray light curve

An optical-UV and X-ray correlated flare: ground- and space-based measurements

R-band (ground-based)

UVW1 (XMM-OM)

X-ray 0.5-10 keV (XMM, PN+MOS)

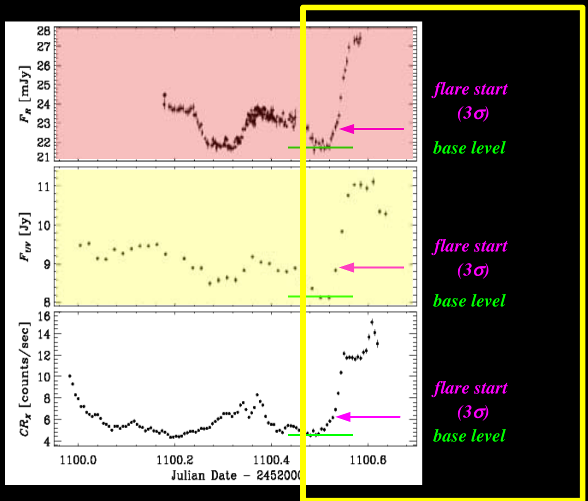

➢ Optical light curve: good match with the UV light curve; only the last flare (achromatic in "R-I") in common with the X-ray light curve

An optical-UV and X-ray correlated flare: ground- and space-based measurements

R-band (ground-based)

UVW1 (XMM-OM)

X-ray 0.5-10 keV (XMM, PN+MOS)

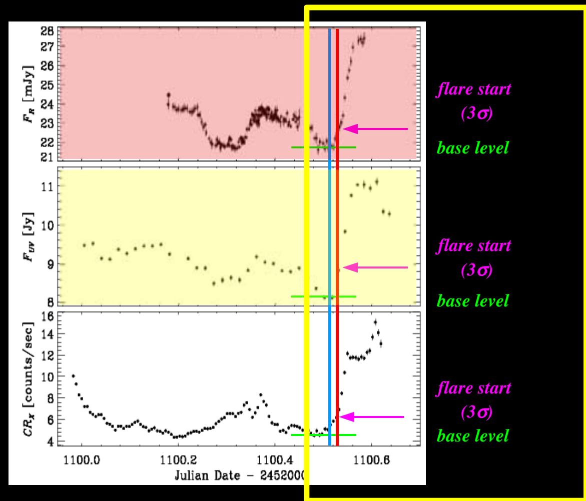

➢ Optical light curve: good match with the UV light curve; only the last flare (achromatic in "R-I") in common with the X-ray light curve
➢ Possible 1.5 ks delay of the start of the optical (R,I) flare w.r.t. the X-ray flare

An optical-UV and X-ray correlated flare: ground- and space-based measurements

R-band (ground-based)

UVW1 (XMM-OM)

X-ray 0.5-10 keV (XMM, PN+MOS)

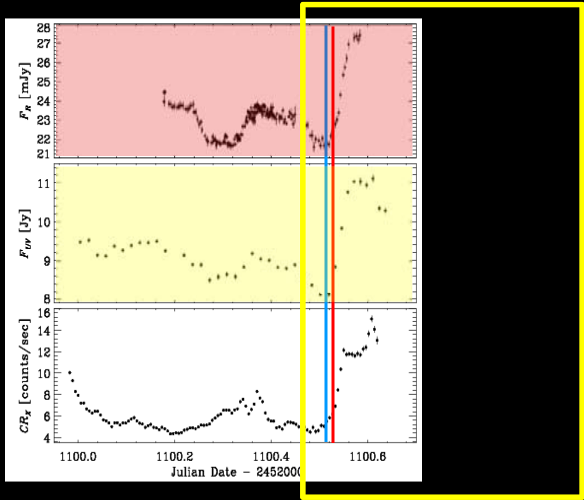

- Optical light curve: good match with the UV light curve; only the last flare (achromatic in "R-I") in common with the X-ray light curve
- Possible 1.5 ks delay of the start of the optical (R,I) flare w.r.t. the X-ray flare

An optical-UV and X-ray correlated flare: ground- and space-based measurements

R-band (ground-based)

UVW1 (XMM-OM)

X-ray 0.5-10 keV (XMM, PN+MOS)

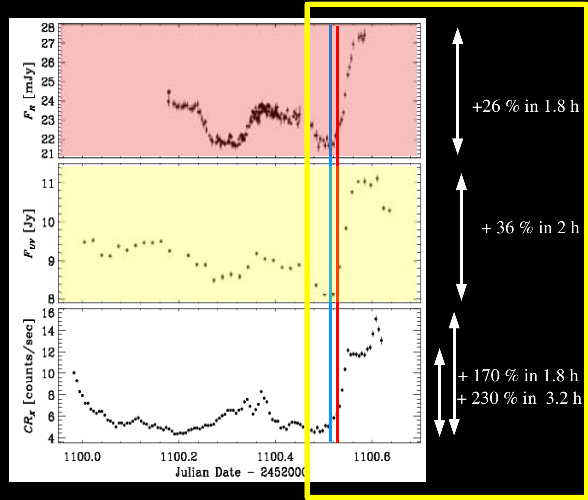

- Optical light curve: good match with the UV light curve; only the last flare (achromatic in "R-I") in common with the X-ray light curve
- Possible 1.5 ks delay of the start of the optical (R,I) flare w.r.t. the X-ray flare
- Decreasing flare amplitude from X-ray to optical frequencies

An optical-UV and X-ray correlated flare: light-curve summary

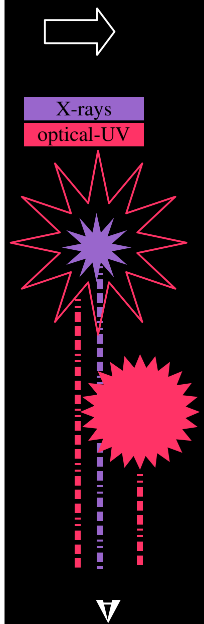

- **Overall optical-UV and X-ray light curves:**
  - * different variability patterns on time-scales ≤ ~10 hours

  ⇒ ***short-term optical and X-ray variability likely due to processes taking place in different source regions***

- **Strong X-ray flare, synchrotron dominated**
  - * optical-UV counterpart, strongly contaminating the optical-UV light curves
  - * optical counterpart possibly lagging ~1.5 ks behind the X-ray flare
  - * decreasing flare amplitude from X-ray down to optical frequencies

  ⇒ *consistency with a cooling-dominated scenario in a source region with size: R< ~2 l.h. · δ/(1+z) ~ few 100 μpc ÷ mpc*

  ⇒ *optical counterpart significant only for X-ray flares exceeding a given luminosity threshold*

- **Optical-UV intraday variability**

  ⇒ *more than one component with comparable intensity (in general difficult to disentangle)*

An optical-UV and X-ray correlated flare: comparison with previous observations

Best example of previous simultaneous intra-day optical and X-ray variability in S5 0716+71:

Nov. 1998 *Beppo*SAX and ground-based R-band observations during a faint optical-X-ray state (Giommi et al. 1999)

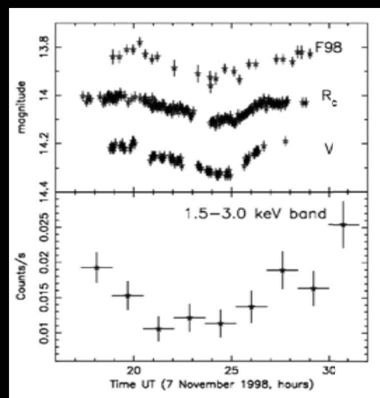

from Giommi et al. 1999

R-band optical vs soft-X-rays (1.5-3.0 keV) :

- possible 2-3 h lag of optical decay w.r.t. X-ray decay

  ⇒ interpreted as difference in cooling times or geometric effect (electrons diffusing out from an injection region while cooling) ⇒ cooling time < R/c

- simultaneous optical/X-ray rise at ~25h U.T.

⇒ ***the data quality was too poor to establish firm correlations between optical and X-ray variability***

An optical-UV and X-ray correlated flare: broadband SED evolution

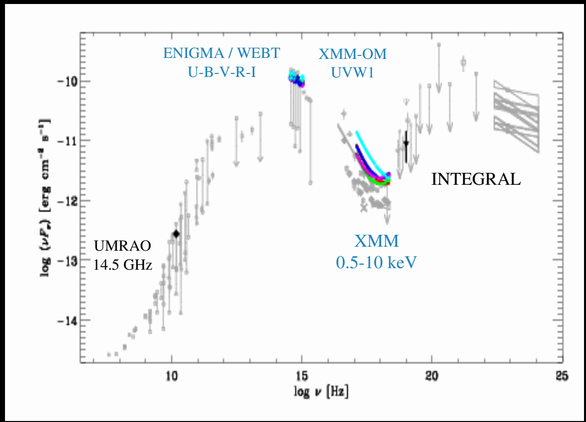

The multifrequency data collected during the XMM pointings enable, for the first time, to sudy the intra-day evolution of the optical-to-X-ray SED...

An optical-UV and X-ray correlated flare: broadband SED evolution

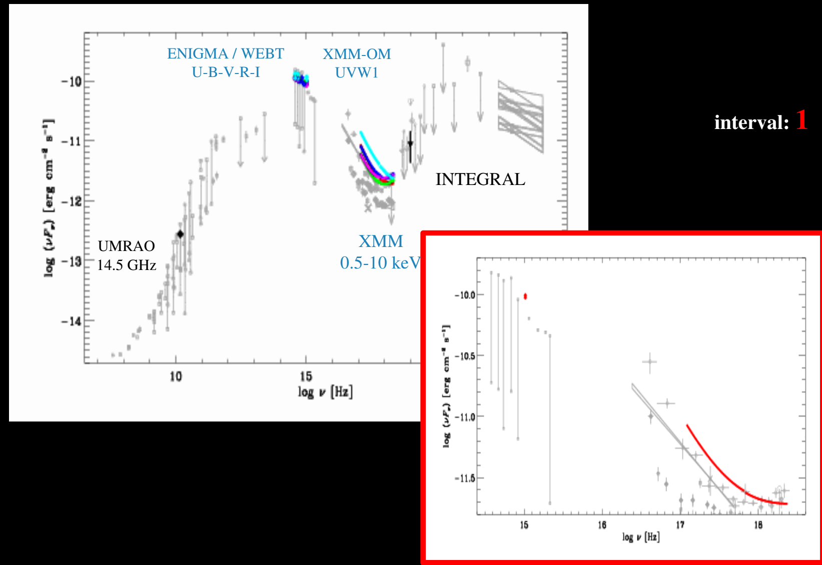

interval: 1

An optical-UV and X-ray correlated flare: broadband SED evolution

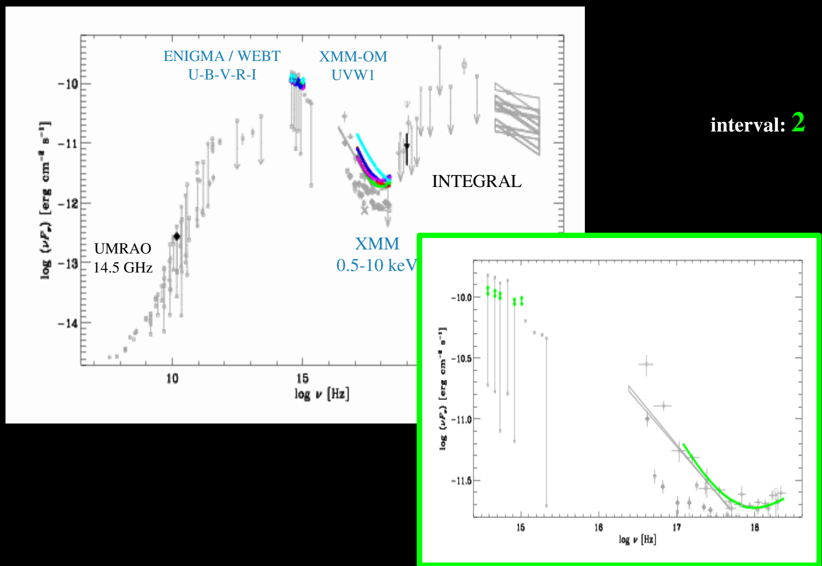

interval: 2

An optical-UV and X-ray correlated flare: broadband SED evolution

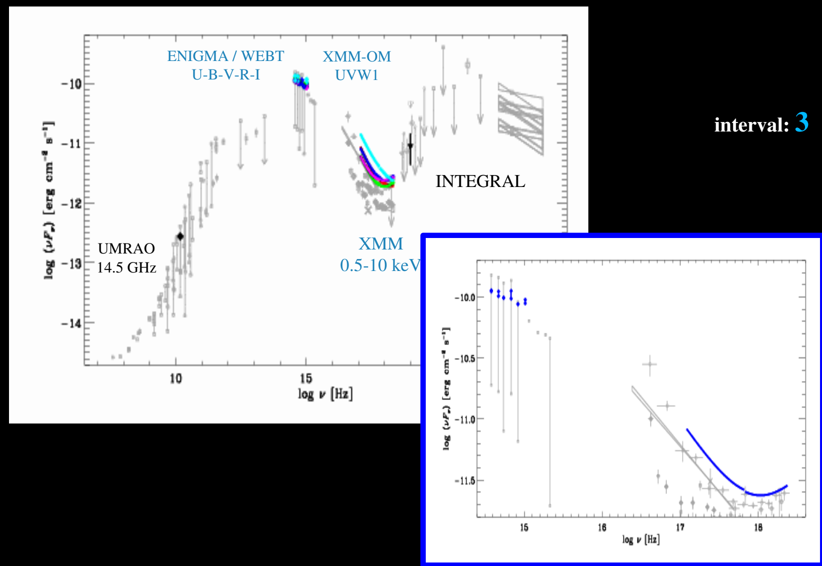

interval: 3

An optical-UV and X-ray correlated flare: broadband SED evolution

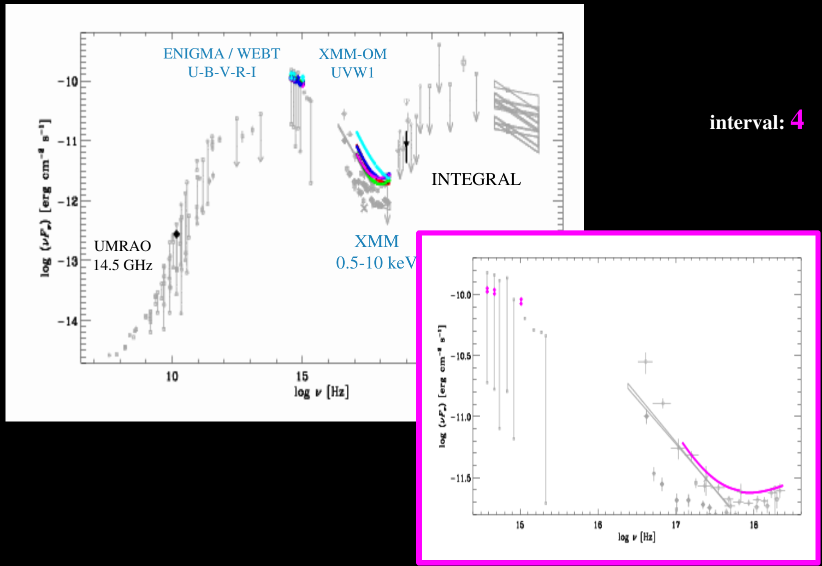

interval: 4

An optical-UV and X-ray correlated flare: broadband SED evolution

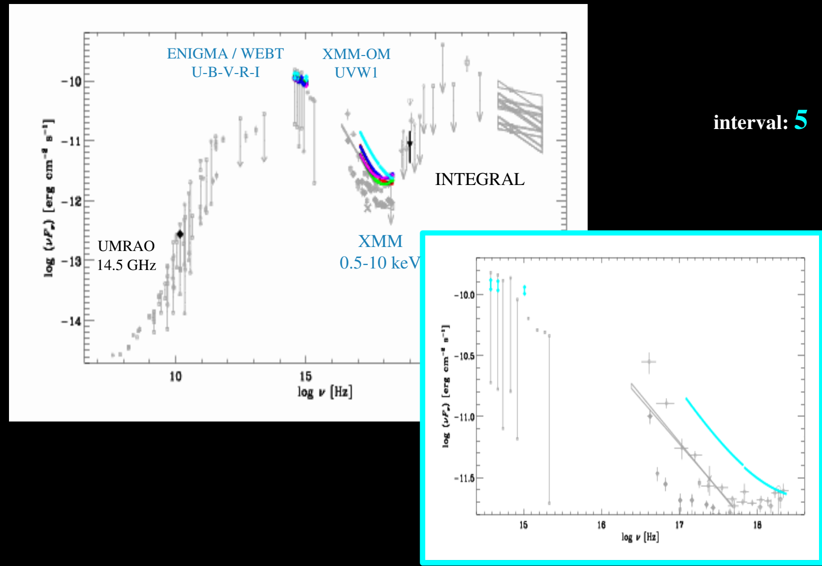

interval: 5

An optical-UV and X-ray correlated flare: broadband SED evolution

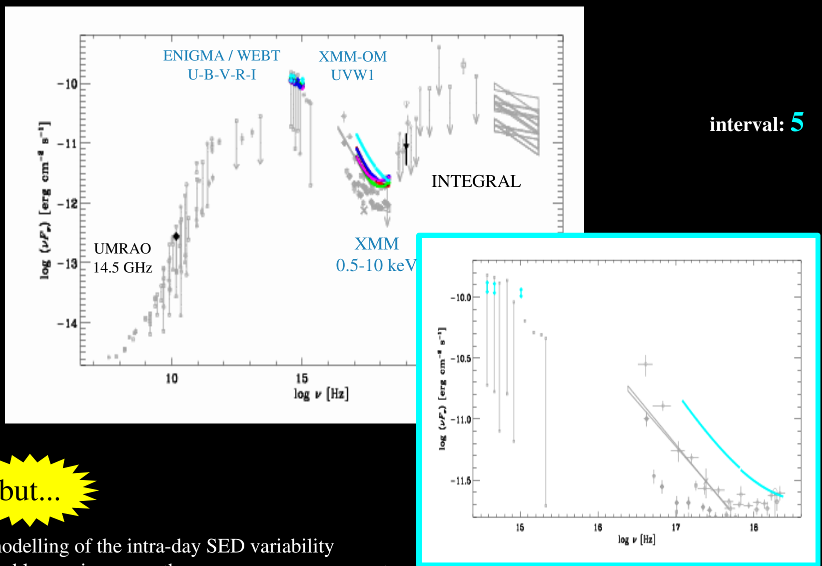

interval: 5

but...

... modelling of the intra-day SED variability probably requires more than one source component

Summary

0716+714 long-term variability during 2003-2004

- detection of two historical outbursts
- no correlation between colour and brightness
- *flatter-when-brighter* chromatism of the main flux bursts
- confirmation of the long-term brightnening of the source discovered by Nesci et al. (2005)
- confirmation of the increase of the frequency of the major outbursts present in the 2002-2003 dataset by Nesci et al. (2005)

  ⇒ possible time-dependent beaming effect as responsible of the intensification of the activity

0716+714 short-term variability: *simultaneous X-ray and optical observations in April 2004*

- brightest X-ray state ever detected for this source
- time-resolved spectral analysis: synchrotron dominance during flaring states; significant short-term variability of the IC component
- detection of the optical-UV counterpart of a strong X-ray flare of (possible soft lag ~1.5 ks)
- presence of more than one IDV component in the optical light curves
- intra-day optical to X-ray SED evolution: a challenge for the emission models

Thanks a lot for your attention

and for the collaboration!

Multi-frequency flux density and VLBI Observations of rapidly variable AGN

Status and preliminary results

T. Krichbaum, I. Agudo,
K. Gabanyi, S. Britzen, N. Marchili, et al.

H. Ungerechts, H. Wiesemeyer, C. Thum, et al.

J. Liu, J.L. Han, et al.

Polarimetric VLBA monitoring during core campaign in Nov. 2003

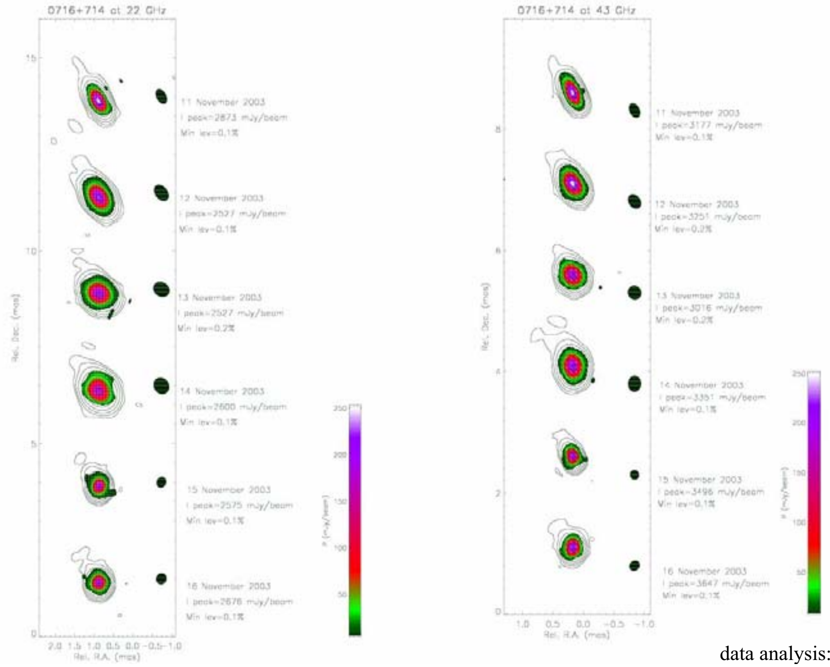

data analysis: I. Agudo

11 cm Effelsberg monitoring in August 2006

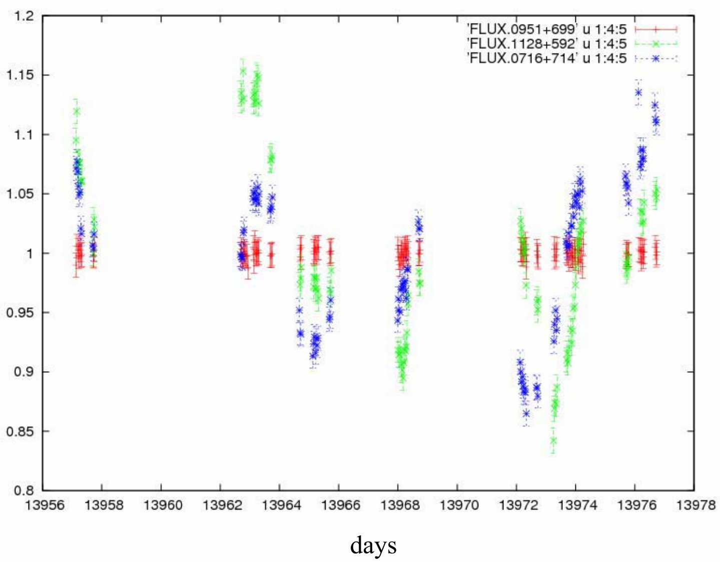

Regular monitoring of IDV sources with the 25m Urumqi telescope (China)

3-5 days of continuous blocktime scheduled every 4-6 weeks

reach rms accuracy of 1 %

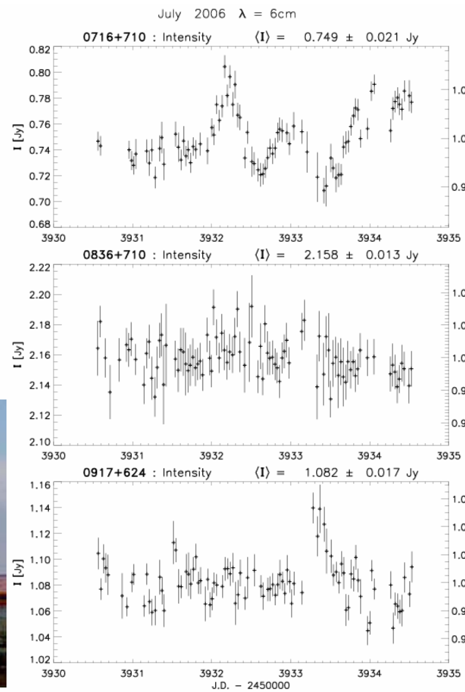

A new rapid IDV source: J1128+59

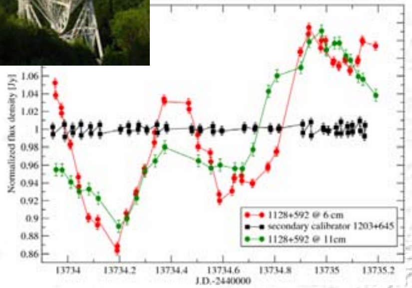

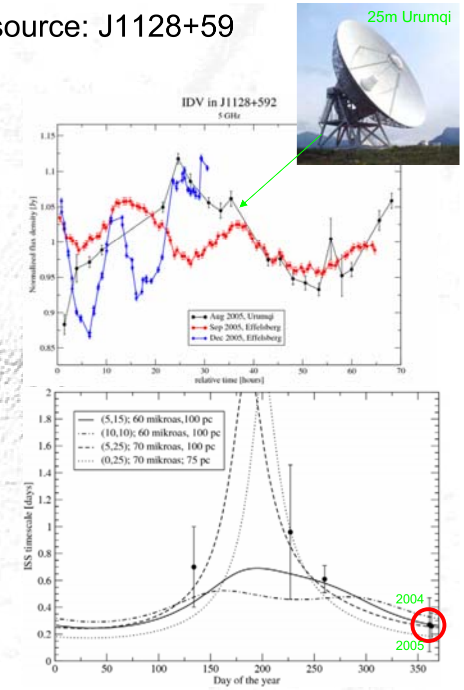

Is there an annual modulation pattern ?

Gabanyi et al. 2007, in prep.

Multi-frequency monitoring of 3C454.3 with the Effelsberg and IRAM telescopes

T.P. Krichbaum, et al. (MPIfR)
H. Ungerechts, H. Wiesemeyer, C. Thum, et al. (IRAM)

Aim: Follow the spectral evolution after major flare in Spring 2005

Spectral Evolution of 3C454.3 after Optical Outburst in May

data: Effelsberg, Pico Veleta, SMA (still preliminary)

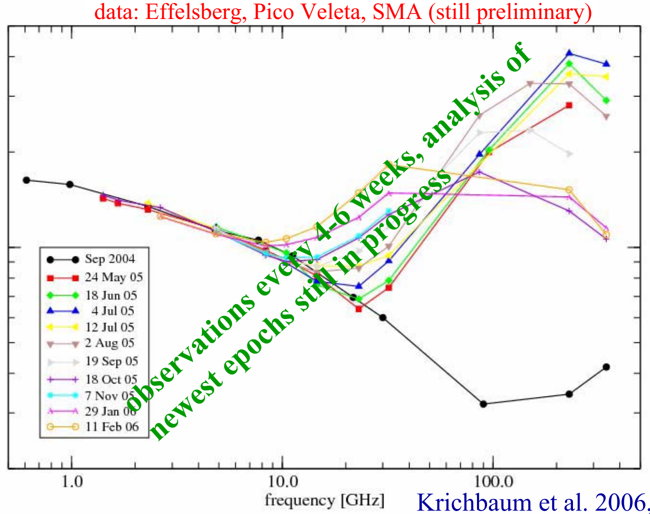

Krichbaum et al. 2006, in prep.

3C454.3: Polarisation Angle Variations

(Pico Veleta, VLA, Michigan)

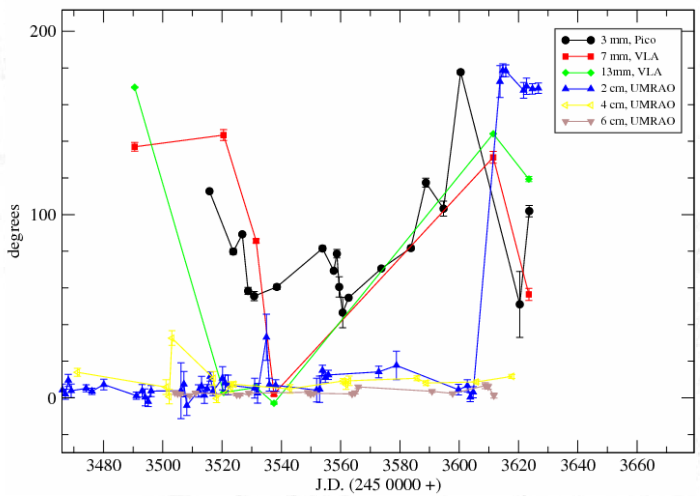

Krichbaum, Wiesemeyer et al. 2006, in prep.

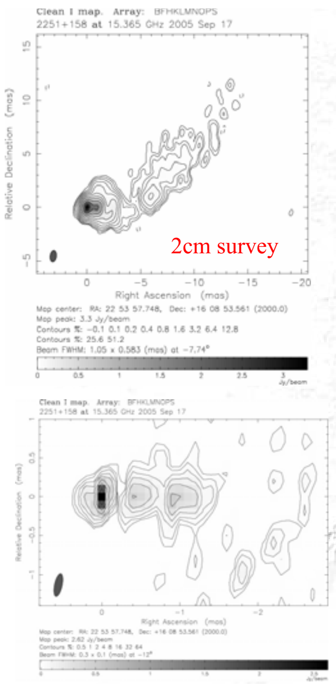

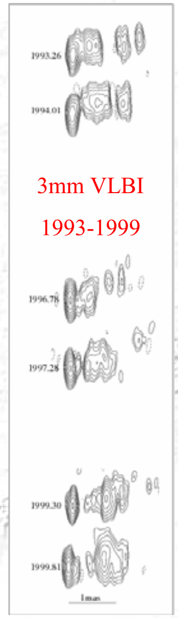

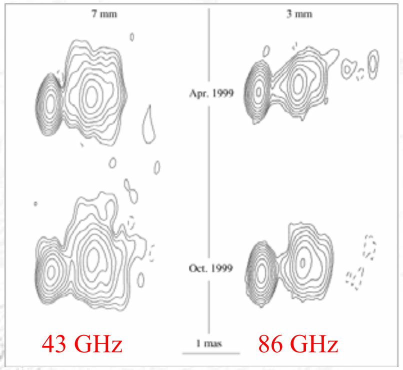

15 GHz (2cm VLBA survey

43 GHz (VLBA)

86 GHz (CMVA, GMVA)

→ quasi simultaneous epochs allow to determine spectral properties

Pagels et al. 2004 and Krichbaum et al. 2006

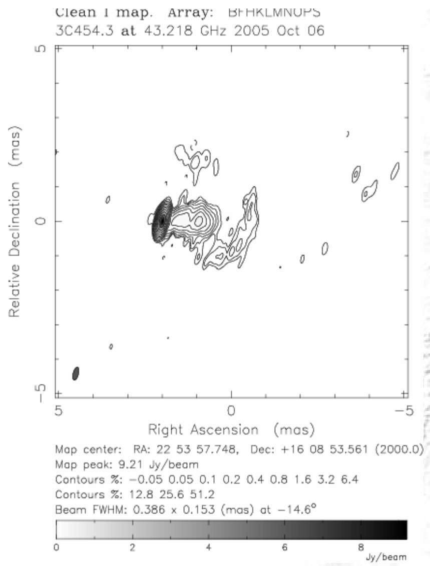

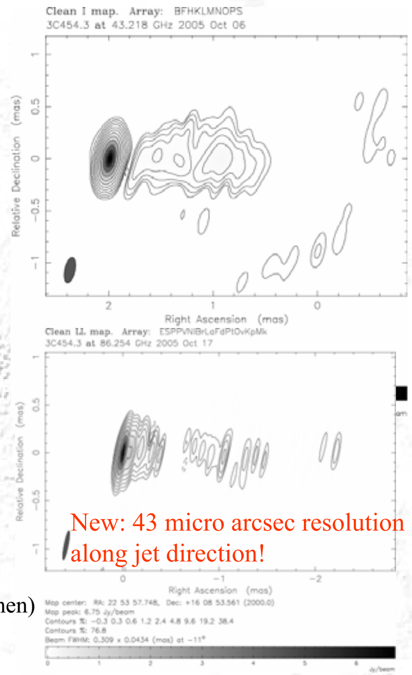

43 GHz (VLBA, A. Marscher, & T. Savolainen)

86 GHz (GMVA, Krichbaum et al.)

3mm polarimetric monitoring of OJ287 with IRAM 30m

- To help providing new data to fix or rule out the models and to help establishing the possible casual connection between the second optical flare and the radio flares
- We have proposed a monitoring of OJ287 with the new IRAM 30m polarimeter (XPOL)
- with 86 GHz measurements every 15 days during more than 1.5 yr
- As we observe 4-Stokes parameters => circ. pol. densely time sampled for an AGN for the first time at 3mm
- Our observations will also support the interpretation of mm-VLBI monitorings
- Highest rated proposal for the last deadline
- 4 months of observations already performed
- Almost 50% data initially rejected due to bad weather (mainly) and technical problems (part of these data will be recovered in the future)

Agudo et al. 2006

3mm polarimetric monitoring of OJ287 with IRAM 30m

Preliminary results:

- Crude data reduction. Inst. pol. cal. and error bars (still very conservative) will be improved in the future.
- Evidence of significantly large variability in Stokes I only.
- pL about 2% -7%
- EVPA about -20° to 10°
- pC tends to be negative but consistent with null circular polarization within the present error bars.

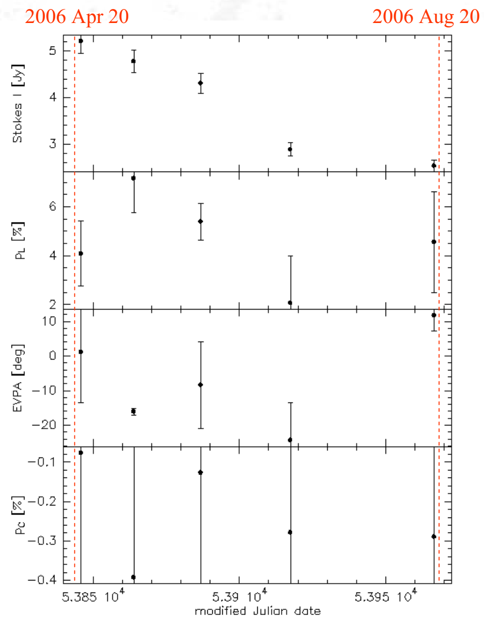

Agudo et al. 2006

3mm polarimetric monitoring of OJ287 with IRAM 30m

Future:

- Continuation of the observations for another 1yr-1.5 yr
- Proposal for the next deadline in preparation
- Optimization of the calibration strategy
- Recovery of data from non-optimum weather-condition observations

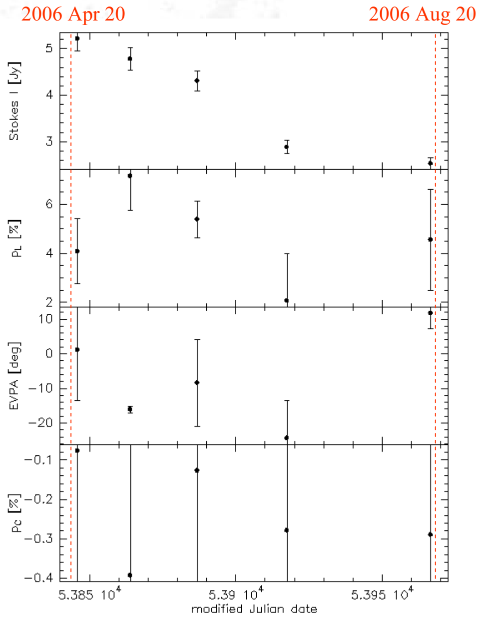

Agudo et al. 2006

NRAO 150: A misaligned quasar with a rotating jet

- Intense radio-mm source
- First catalogued by Pauliny-Toth et al. (1966) at 1.4 GHz
- Monitored at radio-mm λ since beginning of the eighties
- ~12 Jy at 1.3cm and ~7 Jy at 3mm

Metsähövi 1 and 1.3 cm

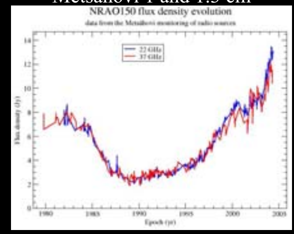

Terasranta et al. (2004)

Pico Veleta 1, 2 and 3 mm

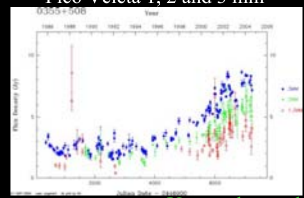

Ungerechts et al.

- cm-VLBI scales shows a jet extended up to ~30 mas to the North-East

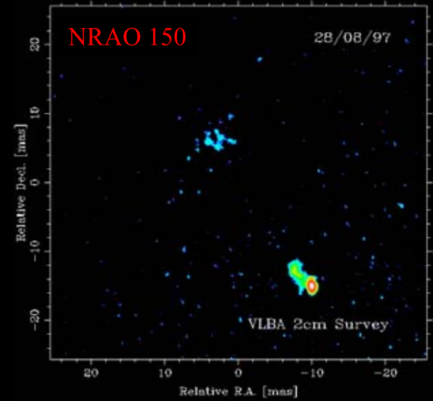

Kellermann et al. (1998)

VLBI results: ~120º of inner to outer jet misalignment

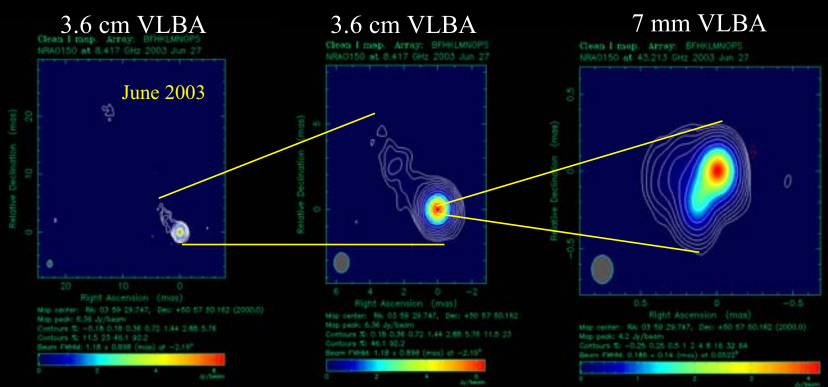

- New 3.6 cm and 7 mm-VLBA observations reveal a strong misalignment (of ~120º) within the first 0.5 mas
- Question: What produces this strong misalignment?
- Answer: Jet bend, alignment of the jet with line of sight and projection effects
- Another question: What produces the jet bend? Answer: 3mm VLBI monitoring

Agudo et al., in preparation

VLBI results: Fast jet structural position angle rotation

3 mm-VLBI images
GMVA and CMVA

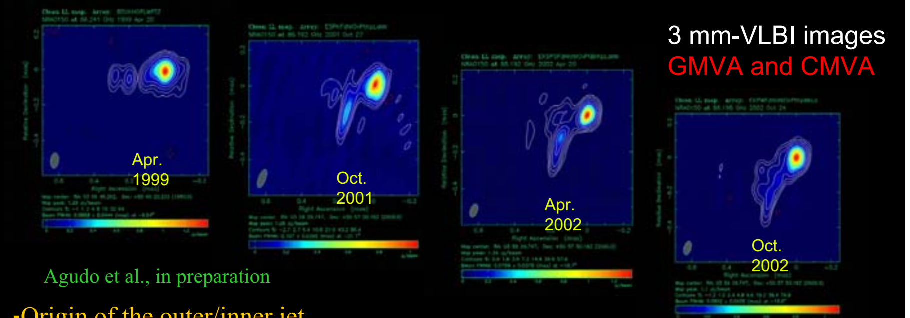

Agudo et al., in preparation

- Origin of the outer/inner jet misalignment
- Rotation of the innermost 0.5 mas of the jet with an angular speed of ~10º/yr
- Change in the rotation direction of the jet before April 2004, which allows for the estimation of possible periodicity

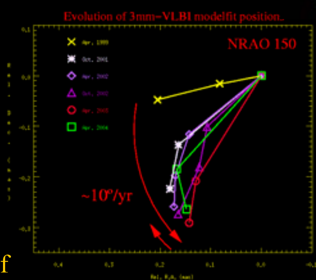

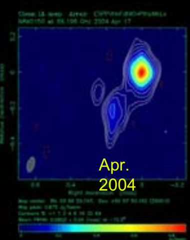

Agudo et al. 2006

VLBI results: Is NRAO 150 rotating periodically?

Metsahövi 1 and 1.3 cm

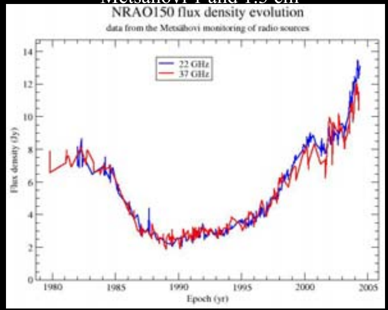

Terasranta et al. (2004)

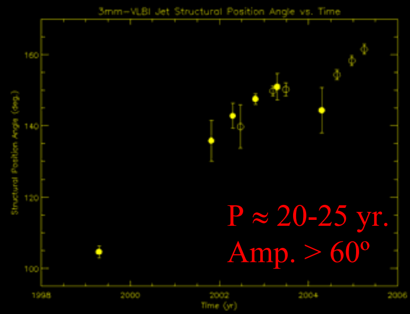

- If the jet rotation is correlated with the single-dish light curves of the source:
    - Possible periodic behaviour
    - P ≈ 20-25 yr
- It needs to be confirmed and constrained

Agudo et al. 2006

OJ is faint! (T. Pursimo, NOT, 29-Aug-2006: R ≈ 15.4)

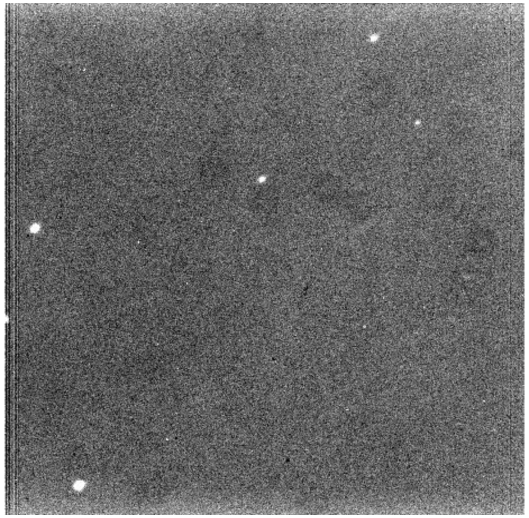

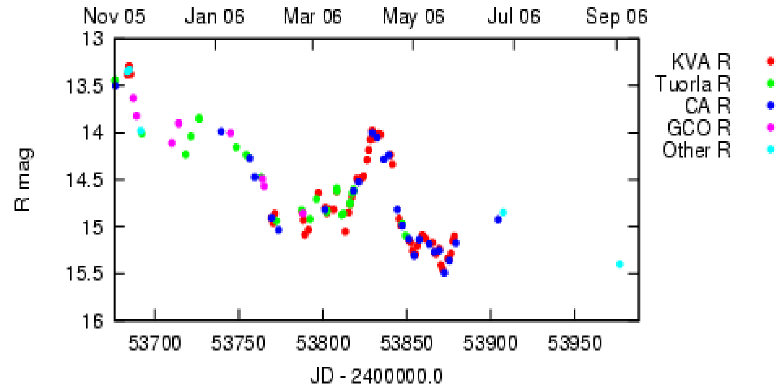

H_α monitoring at the VLT

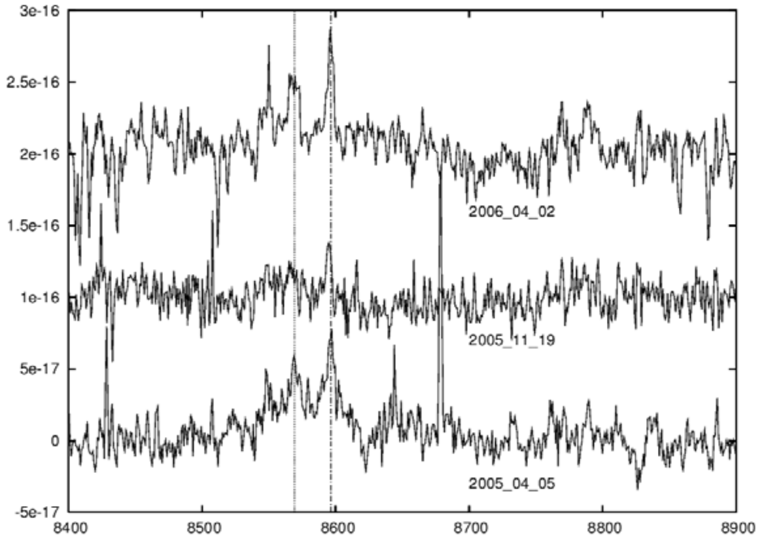

Sitko & Junkkarinen 1985:

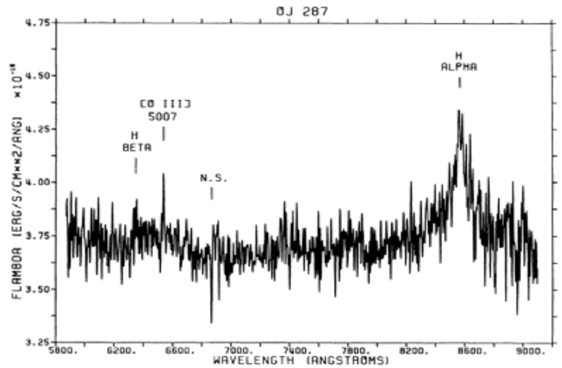

Kidger et al. 1995:

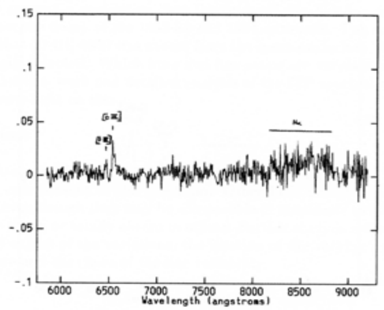

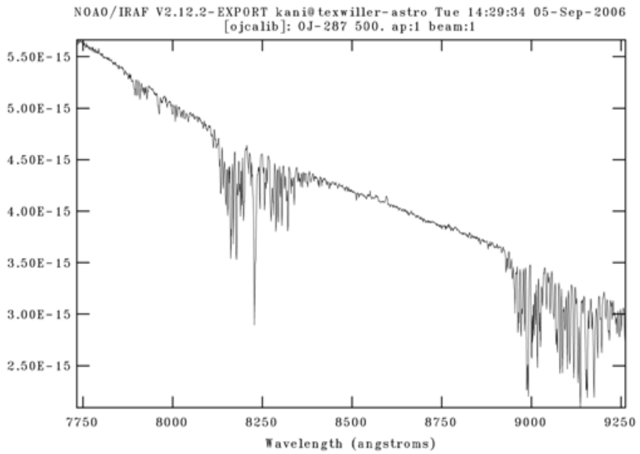
NOAO/IRAF V2.12.2-EXPORT kani@texwiller-astro Tue 14:29:34 05-Sep-2006
[ojcalib]: OJ-287 500. ap:1 beam:1
5.50E-15
5.00E-15
4.50E-15
4.00E-15
3.50E-15
3.00E-15
2.50E-15
7750
8000
8250
8500
8750
9000
9250
Wavelength (angstroms)

Stefano Ciprini

1. University of Perugia (Torino Observatory node), Italy
2. Tuorla Observatory (University of Turku), Finland
(EC Young Researcher Training Network ENIGMA)

An *"fast"* update about the XMM-Newton and coordinated MW campaign on OJ 287

8th ENIGMA Meeting
Sept. 06-08, 2006 – Helsinki University of Technology and Metsähovi Radio Observatory, Otaniemi, Espoo, SUOMI-FINLAND

XMM-Newton observations and coordinated core MW campaign on OJ 287

Goals:

❑ Study the spectral-temporal behaviour of OJ 287 on both short and long time scales, and in different brightness states (before and during the possible cyclic outburst).

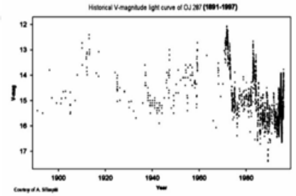

❑ X-ray data likely provide information on the high-energy (inverse Compton, IC) spectral component, while radio-to-optical observations map the behaviour of the synchrotron bump.

❑ Possibly to clarify underlying physics, and relevance of geometrical and energetic models.

❑ Search for multifrequency correlations.

❑ To challenge a satellite-triggered coordinated MW campaign on a well-know and peculiar blazar.

http://www.astro.utu.fi/OJ287MMVI/

* MMVI = 2006

OJ 287: XMM-Newton proposals

❑ 2 XMM-Newton observations (Cycle AO-4, PI: Stefano), and coordinated core WEBT campaign (CM: Stefano) performed in 2005. Satellite pointing dates: April 12, and Nov. 3-4, 2005. *Paper in preparation.*

❑ A 3rd XMM-Newton observation granted (Cycle AO-5, PI: Stefano) to be scheduled in a day between Nov.15-Nov.21, 2006 (43ksec). *MW core campaign announcement next week.*

Visibility of OJ 287 by XMM-Newton in 2005:

Source name	Other names	Redshift	EGRET detection	X-rays past observations	X-rays integral flux [erg cm^{-2} s^{-1}]	XMM AO-4 source visibility periods	Optical visibility window†
OJ 287	PKS 0851+202 PG 0851+202	$z = 0.306$	YES	Einstein,EXOSAT,ROSAT ASCA,*Beppo*SAX	$1.35\text{-}5.0 \times 10^{-12}$ (2-10 keV) (ASCA, SAX)	2005.Apr.12 - 2005.May.05 2005.Oct.16 - 2005.Nov.18	Oct-May

† Calculated for the mean latitude of the WEBT and ENIGMA collaboration telescopes.

The 2 XMM pointings performed in 2005:

April 12, 2005

Target_Name	RA	Dec	Position_Angle	
OJ 287	08:54:48.87	+20:06:30.6	285:05:17.8	
XMM Obs_Duration	XMM Obs: **Start Time**	XMM Obs: **End Time**	Satellite Revolution	IB
40000 sec	2005-04-12 at 12:55 UT	2005-04-13 at 00:03 UT	0978	E3

November 3-4, 2005

Target - PI	RA	Dec	Position_Angle	
OJ 287 - S. Ciprini	08:54:48.87	+20:06:30.6	104:13:22.6	
XMM Obs_Duration	XMM Obs: **Start Time**	XMM Obs: **End Time**	Satellite Revolution	IB
51000 sec	2005-11-03 at 20:59 UT	2005-11-04 at 11:09 UT	1081	E3

XMM-Newton Satellite

XMM-Newton has three mirror modules:
- Instruments behind:
  1) RGS-1 and MOS-1
  2) RGS-2 and MOS-2
  3) pn

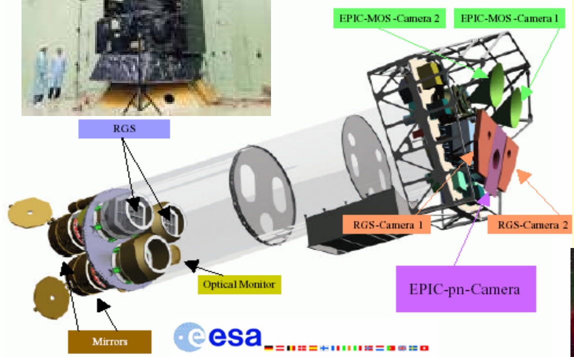

- EPIC: MOS1, MOS2 and pn
- RGS: RGS-1, RGS2
- OM: Optical Monitor

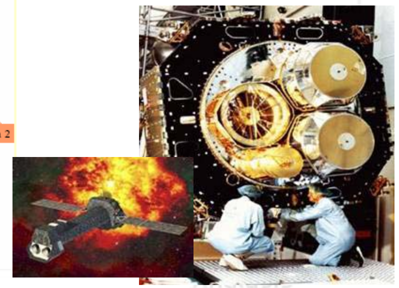

Other ongoing OJ 287 observations/campaigns

❑ Long term 2005-2008 monitoring project (ENIGMA Campaign) on OJ 287 (in the footsteps of the OJ-94 project, Aimo, Leo, Kari, Jochen, Stefano...).

❑ Optical photometry and polarimetry monitoring program on OJ 287 ongoing (Jochen, Kari).

❑ MAGIC ToO observations of OJ 287 performed in Nov. 2005 (Elina, no detection).

❑ Effelsberg radio IDV observations (4-days, Apr.12 and Nov. 8-9-10, 2005, Lars). *Paper in advanced stage.*

❑ VLBA and global 3mm-VLBI radio-structure/polarization observations performed (April 2005, Ivan). More VLBA & Global 3mm-VLBI observations ongoing (period 2005-2007, Tuomas).

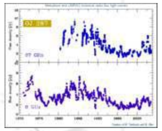

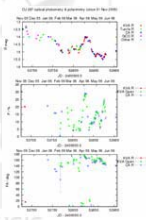

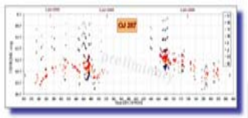

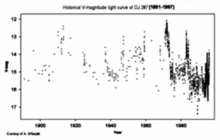

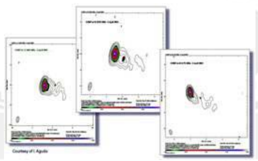

OJ 287: previous broadband SEDs

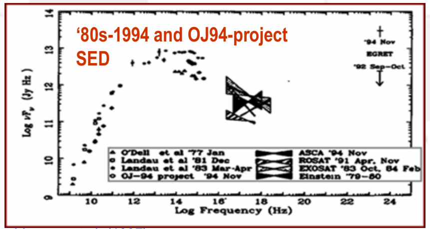

Idesawa et al. (1997)

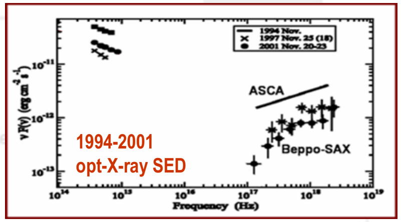

Massaro et al. (2003)

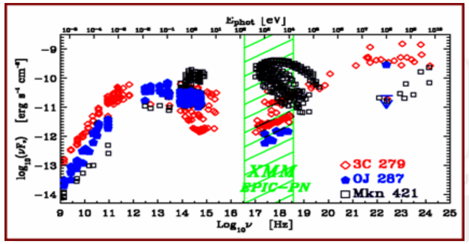

Comparison among the SED of OJ 287 SED, with the SED of a HBL (TeV blazar) and a FSRQ prototype (Mkn 421 and 3C 279).

Source name	Other names	EGRET detection	X-rays past observations	X-rays integral flux [erg cm^{-2} s^{-1}]
OJ 287 z = 0.306	PKS 0851+202 PG 0851+202	YES	Einstein,EXOSAT,ROSAT ASCA,BeppoSAX	1.35-5.0×10^{-12} (2-10 keV) (ASCA, SAX)

XMM-Newton coordinated MW campaign participants 1

Institutes/Observatories participating in the MW coordinated campaign (XMM pointing-1/part-1 MW campaign list):

Optical Observatories:
❑Osaka Kyoiku University Observatory - Kashiwara, Osaka, Japan (K. Sadakane)
❑Lulin Observatory - Lulin, Taiwan (W. P. Chen)
❑Xinglong Station of NAOC - Yanshan Mountains, China, (J.-H. Wu)
❑ARIES Sampurnanand Telescope - Naini Tal, Uttaranchal, India (R. Sagar, G. Krishna)
❑Abastumani Astrophysical Observatory - Mt. Kanobil, Georgia, (O. Kurtanidze)
❑Crimean Astrophysical Observatory - Nauchny, Crimea, Ukraine (Y. Efimov, V. Larionov)
❑Çanakkale Onsekiz Mart University Observatory - Çanakkale, Turkey (A. Erdem)
❑Jakokoski Observatory - Jakokoski, Finland (P. Pääkkönen)
❑Nyrölä Observatory - Nyrölä, Finland (A. Oksanen, K. Nilsson)
❑Tuorla Observatory - Piikkio, Finland (L. Takalo, A. Sillanpää)
❑Catania Observatory - Catania, Italy (A. Frasca)
❑Campo Imperatore Observatory - L'Aquila, Italy (V. Larionov)
❑Armenzano Observatory - Armenzano, Assisi, Italy (D. Carosati)
❑Perugia Observatory - Perugia, Italy (G. Tosti, S. Ciprini)
❑Torino Observatory - Torino, Italy (C. Raiteri, M. Villata)

Optical (cont.):
❑Heidelberg Observatory - Heidelberg, Germany (J. Heidt)
❑Michael Adrian Observatory- Trebur, Germany (J . Ohlert)
❑Agrupacio Astronomica de Sabadell - Sabadell, Spain (J. A. Ros)
❑KVA Telescope - La Palma, Canary Islands, Spain (L. Takalo, A. Sillanpää)
❑Nordic Optical Telescope - La Palma, Canary Islands, Spain (T. Pursimo)
❑Mt. Lemmon KASI Observatory - Mount Lemmon, Arizona, USA (L. Chung-Uk)
❑Kitt Peak SARA Observatory - Kitt Peak, Arizona, USA (J. Webb)
❑Tenagra Observatories - Sonoran desert, Arizona, USA (A. Sadun)
❑Coyote Hill Observatory - Wilton, California, USA (C. Pullen)

❑Radio-mm:
❑RATAN-600 (Special Astrophys. Obs.) (576 m) - Zelenchukskaya, Russia (Y. Kovalev)
❑Metsähovi Radio Telescope (14 m) - Metsähovi, Finland (M. Tornikoski, A. Lahteenmaki)
❑Noto Radio Observatory - Noto, Siracusa, Italy (C. Raiteri, P. Leto)
❑Effelsberg Radio Telescope (100 m) - Effelsberg, Germany (T. Krichbaum, L. Fuhrmann)
❑IRAM Millimeter Telescope (30 m) - Pico Veleta, Spain (T. Krichbaum, H. Ungerechts)
❑Univ. of Michigan Radio Astron. Obs. (UMRAO) (26 m) - Dexter, Michigan, USA (M. Aller)

XMM-Newton coordinated MW campaign participants 2

Institutes/Observatories participating in the MW coordinated campaign (XMM pointing-2/part-2 MW campaign list):

Optical/NIR Observatories:
❑Osaka University - Osaka, Japan (K. Torii)
❑Sobaeksan KASI Optic. Astr.Obs. - Sobaeksan, Korea (C.-U. Lee)
❑Lulin Observatory - Lulin, Taiwan (W.-P. Chen)
❑Tsinghua University - Beijing, China (J. Li)
❑Xinglong Station of NAOC - Yanshan Mountains, China, (J.-H. Wu)
❑ARIES Sampurnanand Tel. - Naini Tal, Uttaranchal, India (R. Sagar, G. Krishna)
❑Mount Maidanak Observatory, Ulugh Beg Astronomical Institute - Mount Maidanak, Uzbekistan (M. A. Ibrahimov)
❑Abastumani Astrophysical Observatory - Mt. Kanobil, Georgia, (O. Kurtanidze)
❑Crimean Astrophysical Obs. - Nauchny, Crimea, Ukraine (Y. Efimov, V. Larionov)
❑Çanakkale Onsekiz Mart University Obse. - Çanakkale, Turkey (A. Erdem)
❑Saint Petersburg State Univ. Obs. - St. Petersburg, Russia (V. M. Larionov)
❑Bulgaria National Astron. Obs. - Rozhen, Bulgaria (E. Ovcharov, A. Kostov)
❑Jakokoski Observatory - Jakokoski, Finland (P. Pääkkönen)
❑Tuorla Observatory - Piikkio, Finland (L. Takalo, A. Sillanpää)
❑MonteBoo Obs., Masaryk University - Brno, Czech Republic (F. Hroch)
❑Catania Observatory - Catania, Italy (A. Frasca)
❑Campo Imperatore Obs. - Assergi, L'Aquila, Italy (A. Arkharov)
❑Armenzano Observatory - Armenzano, Assisi, Italy (D. Carosati)
❑Porziano Observatory - Porziano, Assisi, Italy (D. Capezzali)
❑Perugia Observatory - Perugia, Italy (G. Tosti, S. Ciprini)

Optical (cont.):
❑Torino Observatory - Torino, Italy (C. Raiteri, M. Villata)
❑Heidelberg Lander. - Heidelberg, Germany (L. Ostorero, D. Emmanoulopoulos)
❑Michael Adrian Observatory- Trebur, Germany (J . Ohlert)
❑KVA Telescope - La Palma, Canary Islands, Spain (L. Takalo, A. Sillanpää)
❑Nordic Optical Telescope - La Palma, Canary Islands, Spain (T. Pursimo)
❑INAOE Tonantzintla Obs. - Tonantzintla, Puebla, Mexico (O. Lopez-Cruz)
❑Mt. Lemmon KASI Obs. - Mount Lemmon, Arizona, USA (C.-U. Lee)
❑Ohio University MDM Obs. - Kitt Peak , Arizona, USA (M. Boettcher)
❑Kitt Peak SARA Obs. - Kitt Peak, Arizona, USA (J. Webb)
❑Tenagra Observatories - Sonoran desert, Arizona, USA (A. Sadun)
❑National Astr. Obs. of San Pedro Mártir - Baja California Peninsula, Mexico (E. Benitez, D. Dultzin-Hacyan.)
❑Coyote Hill Observatory - Wilton, Sacramento, California, USA (C. Pullen)

Radio-mm:
❑RATAN-600 (Special Astr. Obs.) (576 m) Zelenchukskaya, Russia (Y. Kovalev)
❑RT-22 Crimean Astr.l Obs. (22m) - Simeiz, Crimea, Ukraine (A. Volvach)
❑Metsähovi Radio Tel. (14 m) - Metsähovi, Finland (M. Tornikoski, A. Lahteenmaki)
❑Noto Radio Obs. (32m) - Noto, Siracusa, Italy (P. Leto, C. Raiteri)
❑Effelsberg Radio Tel. (100 m) - Effelsberg, Germany (T. Krichbaum, L. Fuhrmann)
❑IRAM Millimeter Tel. (30 m) - Pico Veleta, Spain (T. Krichbaum, H. Ungerechts)
❑Univ. of Michigan Radio Astr. Obs. (UMRAO) (26 m) - Dexter, Michigan, USA (M. Aller)

Beware of the weather conspiracy 1

Bad space weather: 1st XMM obs. (April 12, 2005) affected by high background radiation and stopped. *EPIC pn*: the excellent camera collected enough photons to construct a spectra. *RGS*: no detection. *OM*: UV-opt. observations performed. Time lost added to the 2nd pointing.

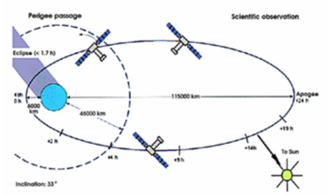

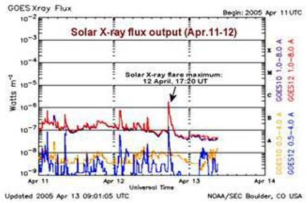

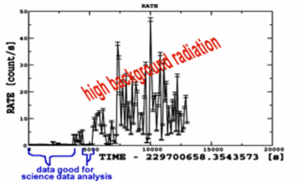

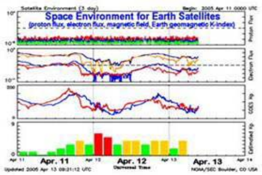

Beware of the weather conspiracy 2

Bad atmospheric weather: Optical ground-based observations obstructed by bad weather in Europe during the 1st (April 12, 2005) XMM-Newton pointing.

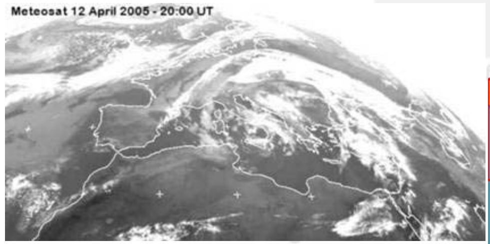

5 Optical observatories in center Italy (2 amateur, 3 professional) alerted/involved personally for April 12… but bad luck with weather!

OJ 287 XMM-Newton: X-ray EPIC images

EPIC: large frame + medium filter used. Data processed with XMM-SAS v. 6.5.
Intervals of high background filtered. Spectral analysis of PN + MOS1+MOS2 data with XSPEC.

April 12, 2005

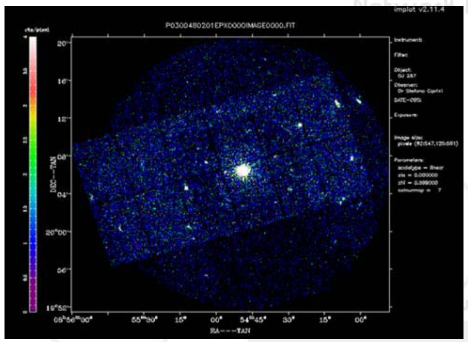

Nov. 3-4, 2005

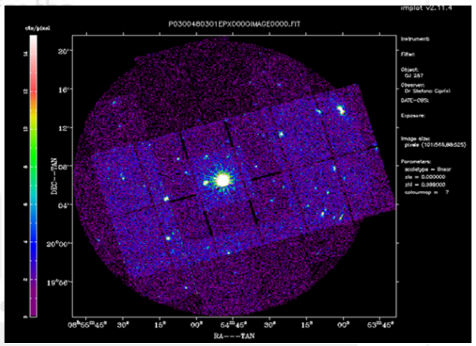

OJ 287 XMM-Newton: X-ray EPIC spectrum Apr. 12, 2005

Date: April 12, 2005 - OJ 287, z=0.306.
XMM-Newton *EPIC: PN* + *MOS1* + *MOS2* spectra
Model: single power law + galactic absorption in the 0.2-10 KeV range

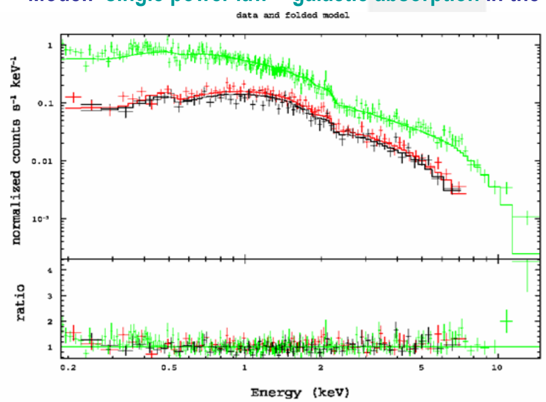

H column density:
$N_H = 3.09 \times 10^{20}$ cm^{-2}

Power-law photon index:
$\Gamma = 1.628 \pm 0.023$

Reduced chi-squared:
$\chi_r^2 = 1.035$, d.o.f.=367

Flux density (2-10 KeV):
$F_{2-10keV} = (2.47 \pm 0.8) \times 10^{-12}$ erg s^{-1} cm^{-2}

OJ 287 XMM-Newton: X-ray EPIC spectrum Nov. 3-4, 2005

Date: November 3-4, 2005 - OJ 287, z=0.306.
XMM-Newton *EPIC: PN* + *MOS1* + *MOS2* spectra
Model: broken power law + galactic absorption in the 0.2-10 KeV range

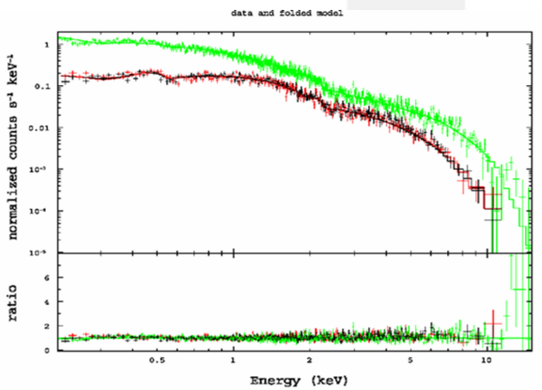

H column density:
$N_H=3.09 \times 10^{20}\ cm^{-2}$

Broken power-law photon indexes:
$\Gamma_1=2.65(-0.07/+0.12)$
$\Gamma_2=1.79 \pm 0.02$
break energy: 0.69 KeV

Reduced chi-squared:
$\chi_r^2=1.030$, d.o.f.=927

Flux density (2-10 KeV):
$F_{2-10keV}=(1.82\pm0.07)\times10^{-12}$ erg s^{-1} cm^{-2}

Preliminary summary on the X-ray observations

- Apr.12 (XMM 1st obs.): Best fit: simple single power law component (IC?).
- Nov.3-4 (XMM 2nd obs.): Best fit: broken power law component (break ~0.7 keV), (Synch.tail+IC ? Break signature between the synchrotron and IC components ?)
- X-ray observations provided information on the high-energy (IC) spectral component.
- Different brightness states, flux variations: $F_{2-10keV}=2.47\times10^{-12}$(1st), and $F_{2-10keV}=1.82\times10^{-12}$(2nd), erg s^{-1} cm^{-2} (previous obs.: fluxes in the range $1.35-5.0\times10^{-12}$ erg s^{-1} cm^{-2}).
- Spectral variability: single/broken power law, slope variation.

OJ 287 XMM-Newton: OM opt-UV observations

- Optical Monitoring instrument (OM). Summary of the observations obtained:

	UVW2	UVM2	UVW1	U	B	V
lambda (A)	2120	2310	2910	3440	4500	5430
Num. of images (Apr.12):	1	2	2	1	1	1
Num. of images (Nov.3-4):	0	0	8	1	1	1

Example of 2 ultraviolet (UV) images

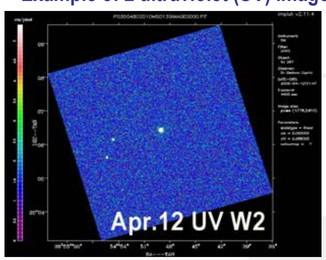

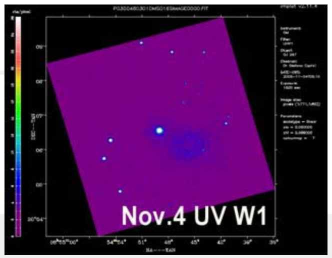

The "usual" optical finding chart

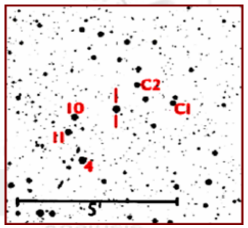

OJ 287 XMM-Newton: OM opt-UV observations

	UVW2	UVM2	UVW1	U	B	V
lambda (A)	2120	2310	2910	3440	4500	5430

Preliminary results:

- Agreement of the U,B,V calibrated OM mags with the reported comparison stars values. (XMM-OM "space"-mags are suitable to make a nice comp. stars calibration sequence for the OJ 287 field in opt. UBV filters).
- High brightness of OJ 287 in UV bands during both the pointings (synch. peak in UV, or UV therm. bump, or...?).

Apr.12, 2005: OJ 287 magnitudes

Preliminary values

OM-band	MAG	ERR
V	[illegible]	0.01
B	[illegible]	0.01
U	[illegible]	0.01
UV-W1	[illegible]	).01
UV-W1	1	.01
UV-M2	1	.01
UV-M2	1	.01
UV-W2	1	01

Nov.3-4, 2005: OJ 287 magnitudes

Preliminary values

OM-band	MAG	ERR
V	[illegible]	0.01
B	[illegible]	0.01
U	[illegible]	0.01
UV-W1	[illegible]	0.01
UV-W1	[illegible]	0.01
UV-W1	[illegible]	0.01
UV-W1	[illegible]	).01
UV-W1	[illegible]	).01
UV-W1	1	.01
UV-W1	1	.01
UV-W1	1	.01

OJ 287: optical/NIR coordinated extended campaing: data galore!

Extended-campaign/monitoring: some month around the 2 XMM pointing dates. 2 observing (night-time visibility) seasons. Part1 + part2, total period: Oct. 2004 – April 2006.

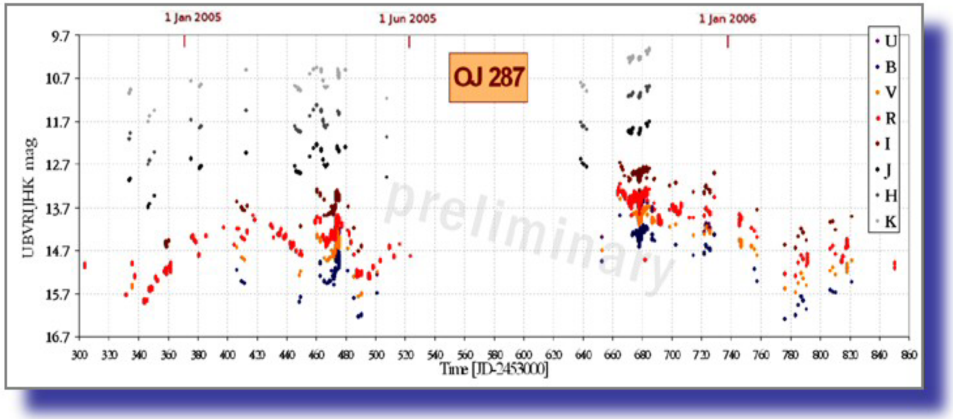

OJ 287: XMM pontings and part1+part2 optical light curves

During both the 2 GO XMM-Newton observations performed, OJ 287 was flaring in the optical bands. …*The source was not shy when observed by XMM!*

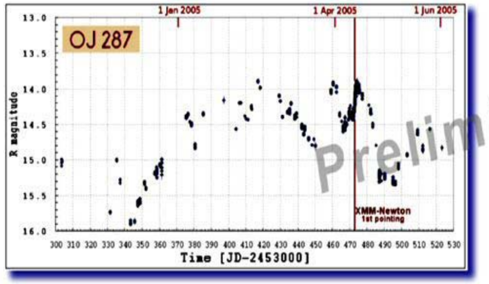

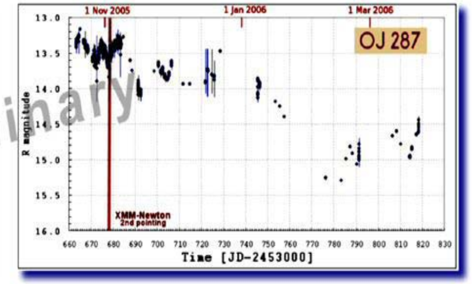

- Part 1 period data: Oct. 2004 - May 2005. Part 2 period data: Oct. 2005 – April 2006. Monitoring observations + intensive WEBT campaign around the 2 XMM-pointing date.
- Optical outburst and high brightness during the 2nd XMM pointing (Oct.-Nov. 2005).

OJ 287 part-1 MW campaign: optical light-curve

Oct. 2004 - May 2005. Monitoring observations + intensive WEBT core campaign (5 days, Apr. 10-14, 2005) around the 1st XMM-pointing date (April 12, 2005):

- Intermediate/high brightness level. Brightness increased of 2 mag in about 2.5 months.
- Optical flare during the pointing: increase of ~ 0.8 mag in 8 days, large drop of ~ 1.4 mag in 13 days.
- Apr.12: almost 0.3 mag brightness increase in less than 9 hours!

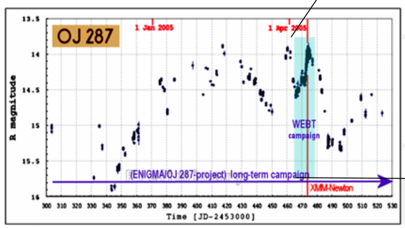

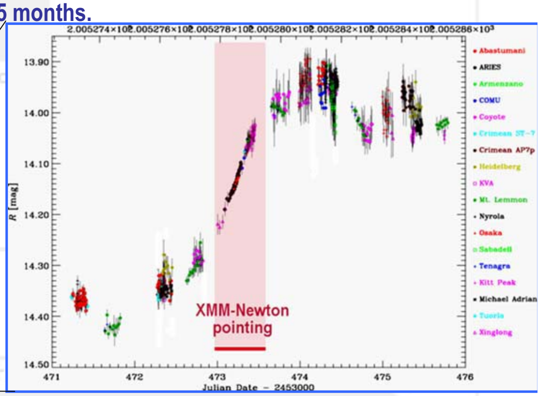

OJ 287 part-1 campaign: some radio observations

OJ 287: April 2005, radio flux and structure:

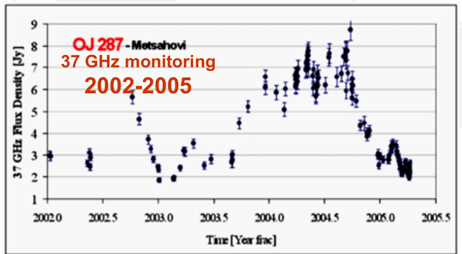

Courtesy of A. Lähteenmäki

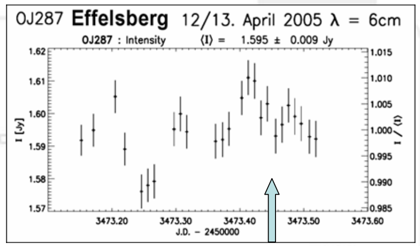

Courtesy of L. Fuhrmann

IDV ~ 3%

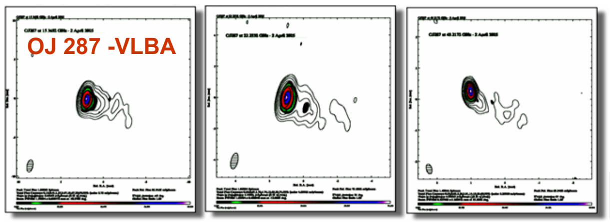

VLBA radio structure/polarization observations in 3 bands (April 2, 2005).

Courtesy of I. Agudo

OJ 287 part-2 MW campaign: optical light-curve

Oct. 2005 – Apr. 2006. Monitoring observations + intensive WEBT core campaign (about 20 days) around the 2nd XMM-pointing date (Nov.3-4, 2005):

- OJ 287 showed a persisting outburst (about 1 month, R-band peaks around mag=13.2/13.3) .

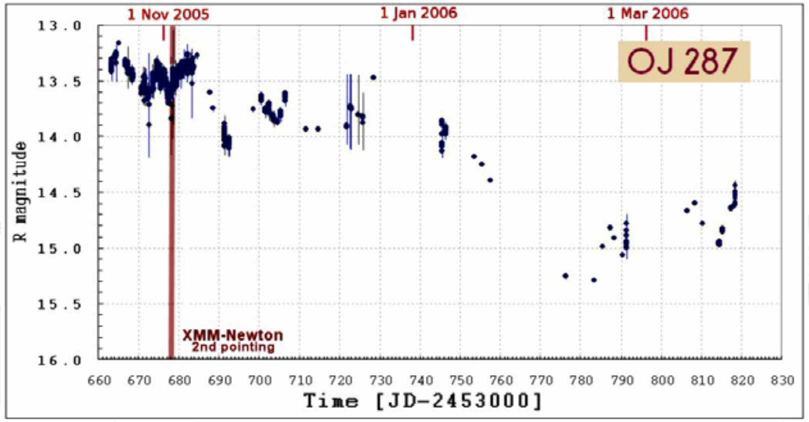

OJ 287 part 2 MW campaign: Oct.-Nov. 2005 optical surprise

Oct. Nov. 2005 optical light curve: a quite amazing optical outburst showing wiggling time-structure and persistence (about 1 month).

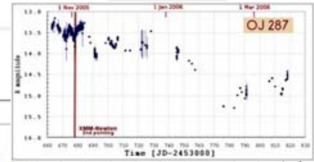

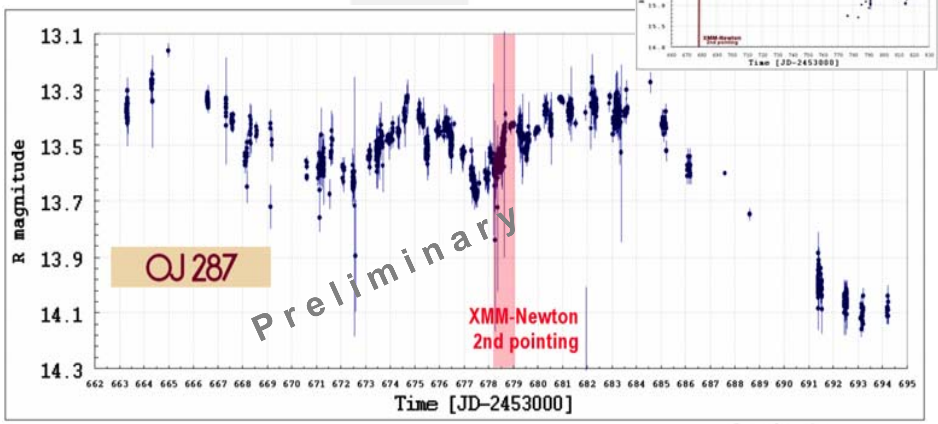

OJ 287 part 2 MW campaign: Oct.-Nov. 2005 optical surprise

Oct. Nov. 2005 optical light curve: optical brightness increasing during this 2nd XMM ppinting date too.

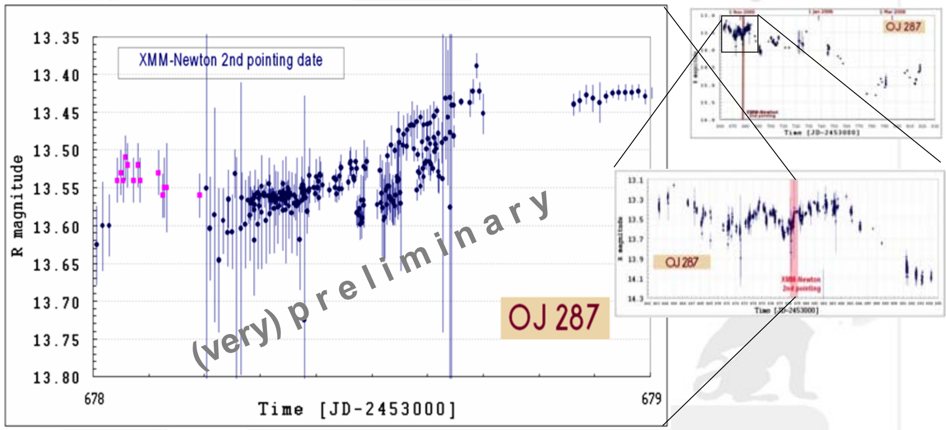

OJ 287 XMM-Newton MW-campaign: few comments

- The OJ 287 MW campaign was a challenge. It was the first time too. Much work needed: the XMM GO proposal (2 stages for each of the 2 proposals accepted); MW observations requests and tuning; information support-interaction with the ground based obs. (e.g. about 300 email received); reduction of satellite and optical data (about 3700 data points only in the R-band); data assembling; data analysis; results publication…
- MW campaigns are beautiful but do not forget: - time needed; - manpower; - possible and useful funding (data analysis and campaign management help).
- Reduced final radio data are easier to handle with respect to heterogeneous optical data coming usually from very different (professional and amateur) observatories.
- Optical data can better provide temporal variability information (light curves) because of the narrow spectral extension and long-term databases (3-4 time decades can be investigated).
- The long-term monitoring at radio/optical bands is important to characterize blazars variability on different timescales. Models profit of temporal variability information on several time decades, and of SEDs containing simultaneous radio-optical spectra.
- Satellite triggered campaigns are very appealing for ground-based observers (amateur or not).

Farewell

8th ENIGMA Meeting

Sept. 06-08, 2006 – Otaniemi, FINLAND

Broad-Band Spectra of GPS/CSS Sources

Łukasz Stawarz

(& Luisa Ostorero, Stefan Wagner, et al.)

Landessternwarte Heidelberg, Heidelberg, Germany

Max-Planck-Institut für Kernphysik, Heidelberg, Germany

Obserwatorium Astronomiczne UJ, Kraków, Poland

Radio Spectra – Examples

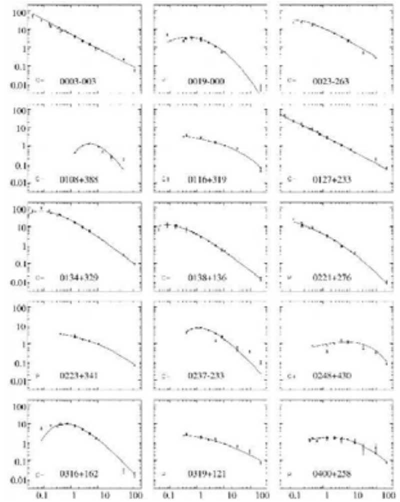

General Characteristics

'GHz Peaked Spectrum' (GPS):

- $\nu_{\rm p} \sim 0.5 - 10\,$GHz
- $LS \lesssim 1\,$kpc

'Compact Steep Spectrum' (CSS):

- $\nu_{\rm p} \lesssim 0.5\,$GHz
- $LS \sim 1 - 10\,$kpc

GPS/CSS Population:

- Nuclei of GPS and CSS objects classified as RGs, QSOs, Sy 1s, or Sy 2s.
- GPS/CSS similar to classical doubles (FR IIs) $\Rightarrow$ 'Compact Symmetric Objects' (CSOs) if $LS \lesssim 1\,$kpc, or 'Medium Symmetric Objects' (MSOs) if $LS \sim 1 - 10\,$kpc.
- GPS/CSS with a 'core–jet' morphology $\Rightarrow$ 'true' GPS/CSS objects or 'regular' radio-loud quasars viewed in projection?
- About 10% of radio sources found in high-frequeny radio surveys belongs to the GPS class, while 30% is classified as CSS objects.

$\nu_{\rm p} - LS$ Anticorrelation

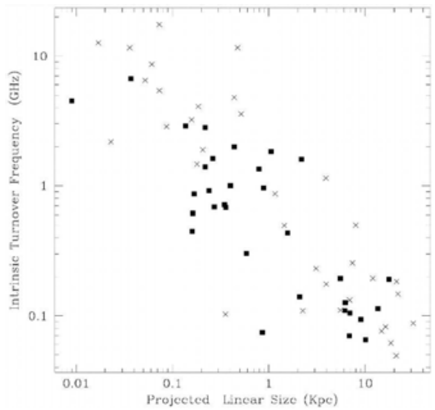

O'Dea & Baum 1997

- $\nu_{\rm p} \propto LS^{-0.65}$, however with a large scatter.
- The observed correlation implies unification of GPS and CSS populations.
- Continuous distribution up to the observationally limited $\nu_{\rm p} \sim 10\,$GHz suggests an unnoticed population of sources with $\nu_{\rm p} > 10\,$GHz ('High Frequency Peakers').
- *(Question: what does it mean if most of the sources from the sample are not realy GPS/CSS sources?)*

Radio Powers

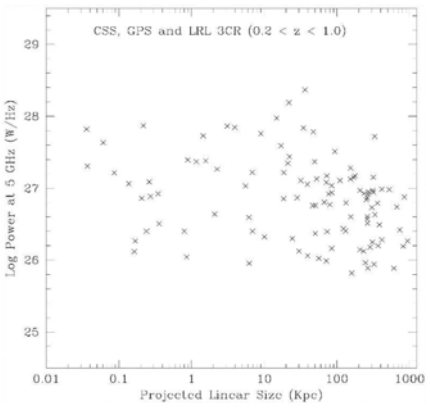

O'Dea 1998

- The 'true' GPS/CSS sources have to be *intrinsically* very powerful in radio, because Doppler and projection effects seem to be minor.
- Radio powers at 5 GHz always exceed the FR I/FR II division, $L_{5\,\mathrm{GHz}} \sim 10^{25}$ W Hz^{-1}, and reach $\sim 10^{29}$ W Hz^{-1} in some cases.
- Since they are as powerful as classical doubles but much smaller, GPS/CSS objects can be either young version of the extended radio sources (*Phillips & Mutel 1982*) or examples of radio-loud AGNs 'frustrated' by the ambient medium (*van Breugel et al. 1984*).

Ages of GPS/CSS Sources

- Spectral ageing analysis of radio lobes gives the ages
  .
  $< 10^4$ yrs for GPS sources ($B_{\mathrm{eq}} \sim 10$ mG), and
  $\sim 10^4 - 10^5$ yrs for CSS objects ($B_{\mathrm{eq}} \sim 1$ mG),
  .
  with the injection spectral indices ranging from 0.35 up to 0.8 (*Murgia et al. 1999*).
- The spectral ages are consistent with the kinematic ages for the advanced velocities on average $v_{\mathrm{adv}} \sim 0.3c$.
- Such high advanced velocities were in fact detected in a number of GPS/CSS sources (*Gugliucci et al. 2005*). The ram-pressure arguments suggest density of the ambient medium $n_{\mathrm{e}} < 1$ cm^{-3} (typical for the extended radio sources).
- This suuports the 'youth' scenario, and contradicts the 'frustration' scenario, since the latter requires total masses of cold ambient gas in a range $10^{10} - 10^{11}\,M_{\odot}$ within the host galaxies (which would be then similar to the amount of gas present in ultraluminous infrared galaxies, but much larger than amount of gas in hosts of other radio-loud AGNs).

Spectral Turnover

- Spectral turnover due to either synchrotron self-absorption (SSA) or free-free absorption (FFA) through a screen of dense ambient matter.
- The sources' parameters obtained by means of applying *both* models to observational data are roughly realiable and consistent with the other constraints for many particular objects, mostly due to observational limitations; problems were noted in either cases, and the general requirement in both models is an inhomogeneous structure of the absorbing medium.
- The observed spectral indices below the peak frequency are usually $\alpha_{\mathrm{low}} \geq -2$ (where the flux density is $S_\nu \propto \nu^{-\alpha}$), in some cases are bit flatter and close to the standard value $-5/2$ predicted by the homogeneous SSA model, while in the other cases are even consistent with the exponential cutoff predicted by the simplest version of the FFA model.
- The variety of the low-frequency spectral indices indicates therefore inhomogeneity of the absorbing medium, as mentioned above, and/or superposition of several emission components with different physical parameters.
- The fact that in many cases $\alpha_{\mathrm{low}} < -1/3$, i.e. that the low-frequency continua are flatter than the flattest optically thin synchrotron spectrum which can be produced, indicates that some absorption has to be present.

Template Radio Spectrum (?)

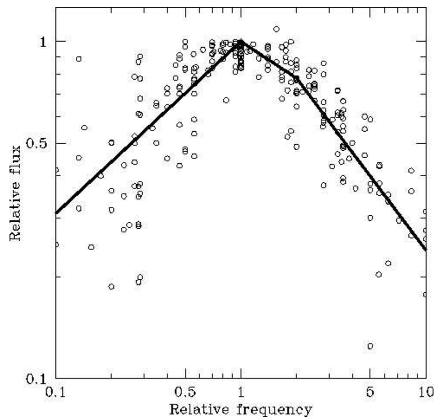

De Vries et al. 1997

- The average spectral indices for the analyzed sample of GPS/CSS sources are $\alpha_{\mathrm{low}} = -0.51(\pm 0.03)$ and $\alpha_{\mathrm{high}} = +0.73(\pm 0.06)$ below and above the peak frequency, respectively.
- The values of α_{high} are characterized by a very broad distribution between $+0.5$ and $+1.2$.
- There may be also a flat spectral plateau between ν_{p} and $2 \times \nu_{\mathrm{p}}$ in the template GPS/CSS spectrum, with average power-law slope $\alpha_{\mathrm{flat}} = +0.36(\pm 0.05)$.

Ambient Medium

- In many objects there are strong evidences for the FFA due to nuclear disk/torus-like structure of the obscuring material with < 100 pc size and $N_{\rm H}$ up to $\sim 10^{23}$ cm^{-2} (*Peck et al. 1999, Kameno et al. 2000, Marr et al. 2001, Mutoh et al. 2002, Kameno et al. 2003*).
- GPS sources exhibit (very) low polarization of their radio fluxes ($few\%$, if any), while radio continua of CSS objects a bit higher. This is most likely due to Faraday depolarisation. The observed RM has a very broad scatter in the GPS/CSS sample, from very large, $RM \sim 10^4$ rad m^{-2}, to very small, $RM \lesssim 10^2$ rad m^{-2}. Faraday screen seems to be associated with the optical line-emitting clouds interacting with jets (*Cotton et al. 2003, 2006*).
- Very broad HI absorption lines are often detected in GPS/CSS objects (at much higher rate than in extended radio galaxies), with the hydrogen column densities (anticorrelating with the sources' sizes) in a range between $N_{\rm H} \sim 10^{22}$ cm^{-2} down to $N_{\rm H} \sim 10^{19}$ cm^{-2} *Vermeulen et al. 2003, Pihlström et al. 2003, Gupta et al. 2006*). Detailed studies of a few objects indicate that the HI absorption lines are well associated with optical emission lines, and thus arise most likely in the atomic cores of Narrow Line Region (NLR) clouds distributed within ~ 1 kpc radius around active nuclei, and interacting with the expanding radio source (*Labiano et al. 2006, Vermeulen et al. 2006*).

Infrared-To-Optical

- GPS/CSS sources have the same MFIR strenghts as extended sources with comparale radio powers and redshifts, i.e., $\langle L_{50\,\mu{\rm m}}\rangle \sim 3 \times 10^{45}$ erg s^{-1} for $\langle L_{5\,{\rm GHz}}\rangle \sim 10^{44}$ erg s^{-1} in the case of GPS/CSS radio galaxies (*Heckman et al. 1994, Hes et al. 1995, Fanti et al. 2000*).
- Host galaxies of GPS/CSS sources are very similar to host galaxies of powerful (3CR) classical doubles when observed in NIR, being evolved ellipticals with some morphological indications of relatively recent merger events (*De Vries et al. 1998, 2000*). Very often they exhibit also kpc-scale optical emission aligned with the main axis of radio source, with line luminosities of about $L_{\rm opt}^{\rm ext} \sim 10^{42} - 10^{43}$ erg s^{-1}, and outflow velocities of $v_{\rm out} \sim 10^8$ cm s^{-1} (*De Vries et al. 1999, Axon et al. 2000, O'Dea et al. 2002, Labiano et al. 2005*).
- At near UV frequencies, GPS/CSS sources, similarly to classical doubles, exhibit complex spectra composed from nebular continuum, nuclear light, and starburst component (*Tadhunter et al. 2002*). GPS/CSS quasars possess often acrretion disk-related UV-bumps, with the luminosities of $L_{\rm UV} \geq 10^{46}$ erg s^{-1}, the value characteristic for powerful quasars in general.

Dusty Tori

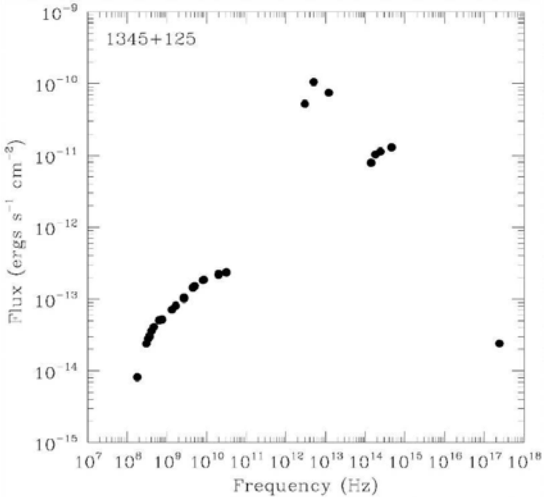

X-rays

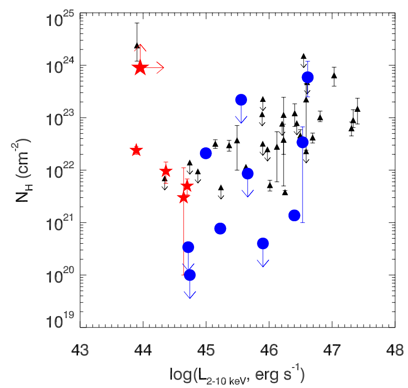

Guainazzi et al. 2006: GPS galaxies (stars), GPS/CSS quasars (circles), RL QSOs (triangles).

- X-ray observations show that GPS/CSS sources are heavily obscured rather than intrinsically weak in X-rays (*Guainazzi et al. 2006, Vink et al. 2006, Siemiginowska et al. 2006*).
- The X-ray obscuration is consistent with the presence of obscuring nuclear tori, just like in the case of extended and powerful radio-loud AGNs: $N_{\rm H}$ ranges from $\sim 10^{21}$ cm^{-2} up to $\geq 10^{23}$ cm^{-2}.
- In some cases excess hard X-ray emission reported (CSS objects 3C 48, PKS 2004-447, and 3C 303.1; *Worrall et al. 2004, Gallo et al. 2006, O'Dea et al. 2006*).

X-ray Spectra – Examples

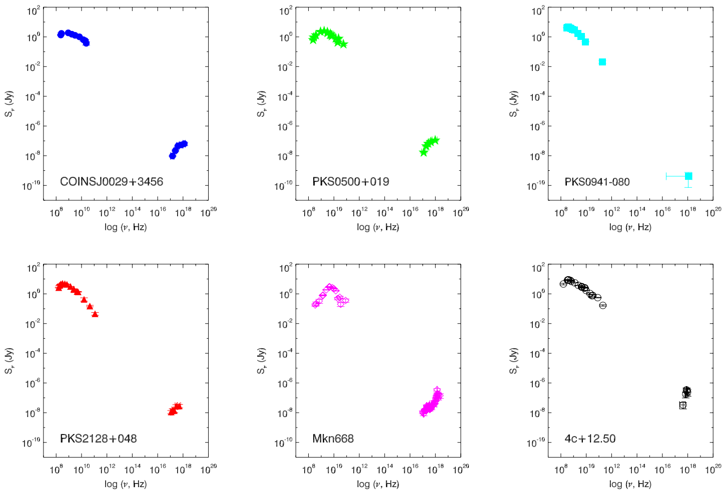

Not Frustrated! Although Obscured, Depolarized (and FFA-ed ?)

- A number of authors interpreted small sizes of GPS/CSS sources in terms of an efficient confinement of expanding radio structure by dense galactic environment, associated in a natural way with NLR (*van Breugel et al. 1984, Gopal-Krishna & Wiita 1991*).
- This interpretation was believed to explain nicely at the same time the characteristic for the GPS/CSS class spectral turnover and neglegible radio polarisation, as results of FFA and Faraday rotation/depolarisation, respectively, on clumpy NLR screen surrounding the discussed radio structures.
- However, since GPS/CSS objects are as powerful in radio as classical doubles, the postulated confinement requires the environment much denser than described above. Such significantly denser environments of GPS/CSS sources were indeed claimed previously, but are not supported by the most recent multiwavelength studies.
- On the other hand, GPS/CSS sources do interact strongly with the clumpy/multi-phase ambient medium, are heavily obscured and depolarized, and so can be indeed FFA-ed (*De Young 1993, 1997, Bicknell et al. 1997, Carvalho 1994, 1998*).
- Still, the FFA absorption models cannot explain *easily* the observed $\nu_{\rm p} - LS$ anticorrelation (but see *Bicknell et al. 1997*).

They are young! (And SSA-ed ?)

- 'Youth' scenarios differ in the
  assumed profiles for the ambient medium density, $\rho(r)$,
  assumed self-similar/non self-similar lobes' evolution,
  assumed constant jet power/jet intermittency
  (see *Phillips & Mutel 1982, Carvalho 1985, Fanti et al. 1995, Readhead et al. 1996, Begelman 1996, Reynolds & Begelman 1997, Alexander 2000, Snellen et al. 2000, Perucho & Marti 2002, Kawakatu & Kino 2006*).
- Therefore, evolution of the sources' parameters (radio luminosity, hotspots' velocities, etc) are different in different models.
- Usually, the youth scenarios associate spectral turnover to the SSA process, although such an association is not required.
- The evolutionary models with spectral turnover due to SSA cannot explain *easily* the observed $\nu_{\rm p} - LS$ anticorrelation.

Cocoon's Evolution

All the models describing evolution of GPS/CSS sources start from the set of equations introduced by *Begelman & Cioffi (1989)*:

(1)
$$L_{\rm j} = c\,\rho(LS)\,v_{\rm h}^2\,A_{\rm h} \quad , \quad p = \rho(l_{\rm c})\,v_{\rm c}^2 \quad , \quad 3\,p\,V = 2\,L_{\rm j}\,t \quad ,$$
$$v_{\rm h} = \frac{d\,LS}{dt} \quad , \quad v_{\rm c} = \frac{d\,l_{\rm c}}{dt} \quad , \quad \frac{d\,V}{dt} = 2\pi\,l_{\rm c}^2\,v_{\rm h} \quad .$$

For the given jet power $L_{\rm j}$ and ambient medium density profile $\rho(r)$, as well as for the parameter of choice LS, the number of variables is larger than the number of equations (1). To close the system, we follow *Kawakatu & Kino (2006)*, who introduced a general scalling

(2)
$$l_{\rm c}^2 \propto t^X \quad .$$

In addition, we restrict our analysis to young GPS/CSS sources, which evolve in a central plateau of the galactic gaseous halo, and which are young $t \leq 10^5$ yr. Thus, we set the ambient density profile as $\rho = m_{\rm p}\,n_0$ with the expected $n_0 \sim 0.1\,{\rm cm}^{-3}$, and fix $X = 1$ to reproduce the appropriate *'1D'* jet evolution found in the numerical analysis of *Scheck et al. (2002)*. Such a choice gives $v_{\rm h} \propto LS^0$ (as required by observations), $v_{\rm c} \propto LS^{-1/2}$, $p \propto LS^{-1}$, $l_{\rm c} \propto LS^{1/2}$, $V \propto LS^2$, $t \propto LS$, and $A_{\rm h} \propto LS^0$.

Cartoon by *Kino & Kawakatu (2006)*

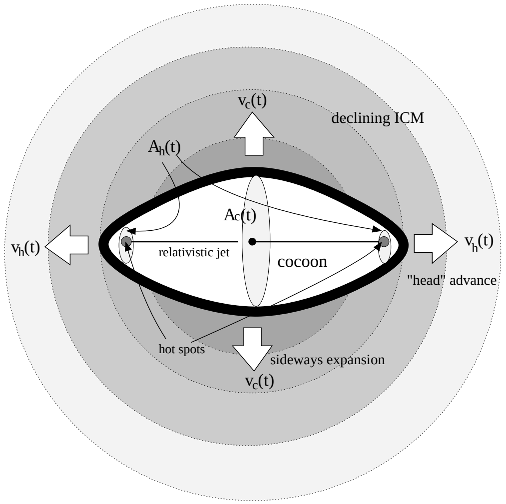

Cocoons' Magnetic Field

We assume that the cocoons of GPS/CSS objects, just like cocoons of extended powerful radio sources, are close to the minimum power condition. In general, one can parameterize magnetic field energy density in the cocoon as $U_{\rm B} = \eta \, p$, with $\eta \leq 1$. For example, in the case of energy equipartition between the lobe's ultrarelativistic electrons, ultrarelativistic protons and magnetic field, one has $\eta = 1$. Thus,

(3) $$U_{\rm B} = \eta \left(\frac{L_{\rm j} \, m_{\rm p} n_0 \, v_{\rm h}}{6\pi} \right)^{1/2} LS^{-1} \approx 10^{-4} \, \eta \, L_{\rm j,\,45}^{1/2} \, n_{-1}^{1/2} \, \beta_{0.3}^{1/2} \, LS_1^{-1} \quad {\rm erg\,cm^{-3}} \quad ,$$

where $L_{\rm j,\,45} \equiv L_{\rm j}/10^{45}$ erg s^{-1}, $n_{-1} \equiv n_0/0.1$ cm^{-3}, $\beta_{0.3} \equiv v_{\rm h}/0.3\,c$, and $LS_1 \equiv LS/1$ pc. This, with the expected n_{-1}, $\beta_{0.3} \sim 1$, gives the cocoon's magnetic field intensity

(4) $$B = (8\pi \, U_{\rm B})^{1/2} \approx 0.05 \, \eta^{1/2} \, L_{\rm j,\,45}^{1/4} \, LS_1^{-1/2} \quad {\rm G} \quad .$$

For $L_{\rm j,\,45} \geq 1$ and $\eta \sim 1$ one therefore obtains $B \sim 10$ mG and $B \sim 1$ mG for the GPS ($LS \sim 0.01 - 1$ kpc) and CSS ($LS \sim 1 - 10$ kpc) objects, respectively, consistently with observational constraints.

Scaling Laws

Assuming that the terminal shock injects power-law electron energy distribution $N_{\rm e}(\gamma) = N_0 \, \gamma^{-s}$ (with *fixed spectral shape*) to the expanding lobe, and that $U_{\rm e} \propto U_{\rm B}$ (with $U_{\rm B}$ as given above), one can find the bolometric synchrotron luminosity

(5) $$L_{\rm syn} \propto U_{\rm B} \, U_{\rm e} \, V \propto LS^0$$

The monochromatic synchrotron power measured at some fixed observed frequency $\nu^{\star}$ (and thus produced by the electrons with different eneregies at different times of observation, because of a change in the magnetic field intensity) scales as

(6) $$[\nu^{\star} L_{\nu^{\star}}] \propto B^{(s-3)/2} \, U_{\rm B} \, U_{\rm e} \, V \propto LS^{(3-s)/4}$$

The characteristic SSA frequency scales as

(7) $$\nu_{\rm ssa} \propto LS^{-x} \quad {\rm with} \quad x = (s+2)/(2s+8) = 0.3 - 0.36$$

for $s = 1 - 3$, while the observed power at such SSA frequency scales as

(8) $$[\nu_{\rm ssa} L_{\nu_{\rm ssa}}] \propto B^{(s-3)/2} \, \nu_{\rm ssa}^{(3-s)/2} \, U_{\rm B} \, U_{\rm e} \, V \propto LS^{y} \quad {\rm with} \quad y = (3-s)/(2s+8) = 0.2 - 0$$

Intrinsic Turnover?

The electrons can undergo 1st order Fermi acceleration at the jet terminal (reverse) shock if they are able to be scattered by the turbulence at both sides of the shock front. In the case of the cold protons carrying bulk of the kinetic energy of powerful jets on large ($>$ pc) scales the maximum frequency of the Alfv'enic turbulence is set by the cold proton gyrofrequency $\Omega_{\rm p}$. This implies that the electrons which can undergo 1st order Fermi acceleration at the jet head have to be already ultrarelativistic. Indeed, taking the appropriate resonance condition for the electron–Alfvén wave interaction $\lambda \sim r_{\rm e}$, where λ is the wavelength of a turbulent mode and $r_{\rm e} = \gamma \, m_{\rm e} c^2 / e \, B_{\rm HS}$ is the electron gyroradius for the hotspot magnetic field $B_{\rm HS}$, together with the dispertion relation for the non-compressive Alfvén waves $\omega^2 = v_{\rm A}^2 \, k^2$, where $k = 2\pi/\lambda$, $v_{\rm A} = \beta_{\rm A} \, c$ is the Alfvén velocity, and $\omega < \Omega_{\rm p}$, one obtains (see *Bell 1978*)

(9) $$\gamma_{\rm cr} \approx \beta_{\rm A} \, \Gamma_{\rm j} \, \frac{m_{\rm p}}{m_{\rm e}}$$

In the above, we put the cold protons' gyrofrequency $\Omega_{\rm p} = e \, B_{\rm HS} / \Gamma_{\rm j} \, m_{\rm p} c$, where $\Gamma_{\rm j}$ is the jet bulk Lorentz factor, since the cold protons carrying bulk of the jet kinetic energy are shocked at the jet head to the average energy $\Gamma_{\rm j} \, m_{\rm p} c^2$ (assuming only mildly-relativistic advance velocity of the hotspot itself).

Turnover Frequency

Is it therefore possible that the turnover frequency observed in GPS/CSS sources is due to the electrons with Lorentz factors $\gamma_{\rm cr}$? With the magnetic field intensity as given previously, this frequency would read as

(10) $$\nu_{\rm p} = \frac{e\,B\,\gamma_{\rm cr}^2}{4\pi\,m_{\rm e}c} \approx 60\,\beta^2_{\rm A,\,-1}\,\Gamma^2_{\rm j,\,5}\,\eta^{1/2}\,L^{1/4}_{\rm j,\,45}\,LS_1^{-1/2} \quad {\rm GHz} \quad ,$$

where $\Gamma_{\rm j,\,5} \equiv \Gamma_{\rm j}/5$ and $\beta_{\rm A,\,-1} \equiv \beta_{\rm A}/0.1$.

.

Note three important features in the above formula:

- values of $\nu_{\rm p}(LS)$ as required;
- weak dependance on $L_{\rm j}$;
- anticorrelation $\nu_{\rm p} \propto LS^{-0.5}$ *almost* as the observed one $\nu_{\rm p} \propto LS^{-0.65}$.

.

If, in addition, $\Gamma_{\rm j} \propto LS^{-0.065}$....

What About the 'Classical' Hotspots?

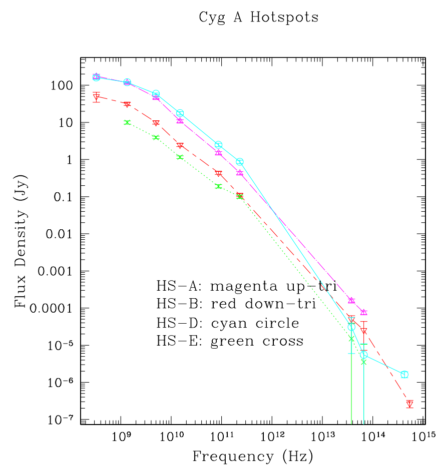

Spectral turnover for $\gamma_{\rm cr} \sim 10^3$ is indeed the case! (*Carilli et al. 1991, Harris et al. 2006*).

How to Check It?

In the case of powerful radio sources infrared emission of dusty tori is likely to dominate the other photon fields on scales between 1 pc and 1 kpc. Energy density of this emission at the distance r from the galactic center can be estimated as

(11) $$U_{\rm IR} = \frac{L_{\rm IR}}{4\pi\,c\,r_{\rm d}^2}\,\frac{1}{1+(r/r_{\rm d})^2} \quad ,$$

where $L_{\rm IR}$ is the torus luminosity (which is typicaly some small ζ fractions of the accretion-related UV luminosity of the active center, $L_{\rm IR} \sim \zeta\,L_{\rm UV}$), and $r_{\rm d} = (L_{\rm UV}/4\pi\,\sigma_{\rm SB}\,T_{\rm d}^4)^{1/2}$ is the characteristic scale of the torus with the temperature $T_{\rm d}$ (*Sikora et al. 2002, Błażejowski et al. 2000, 2004*). For powerful quasars $L_{\rm UV} \sim 10^{46} - 10^{47}$ erg s^{-1}, $\zeta \sim 0.1$, and $T_{\rm d} \sim 10^3$ K, what is consistent with the typical MFIR emission observed from GPS/CSS sources. Since $r_{\rm min}$ is expected to be much smaller than the distances considered here,

(12) $$r_{\rm d} \sim L^{1/2}_{\rm IR,\,45}\,\zeta_{-1}^{-1/2}\,T_3^{-2} \quad {\rm pc} \quad ,$$

where $L_{\rm IR,\,45} \equiv L_{\rm IR}/10^{45}$ erg s^{-1}, $\zeta_{-1} \equiv \zeta/0.1$, and $T_3 \equiv T_{\rm d}/10^3$ K, one can restrict the analysis to $LS > r_{\rm d}$, obtaining $U_{\rm IR}(LS > r_{\rm d}) \sim 3 \times 10^{-4}\,L_{\rm IR,\,45}\,LS_1^{-2}$ erg cm^{-3}.

Comptonisation of the IR Torus Emission

Emission due to comptonisation of the IR photons produced by the dusty torus within the radio cocoon is expected to peak at the characteristic frequency

(13) $$\varepsilon_{\rm ic,\,cr} = \varepsilon_{\rm IR}\,\gamma_{\rm cr}^2 \sim 100\,\beta^2_{\rm A,\,-1}\,\Gamma^2_{\rm j,\,5} \quad {\rm keV} \quad ,$$

with the luminosity

(14) $$L_{100\,{\rm keV}} \sim \frac{U_{\rm IR}}{U_{\rm B}}\,L_{\rm p} \quad .$$

Such an emission can be strong enough to be detected by SWIFT/SUZAKU, since

(15) $$\frac{U_{\rm IR}}{U_{\rm B}} \sim 3 \times L_{\rm IR,\,45}\,\eta^{-1}\,\xi_{-1}^{1/2}\,L_{\rm p,\,44}^{-1/2}\,LS_1^{-1} \quad ,$$

where we have introduced the efficiency factor in converting jet power to the radio (peak) luminosity of the cocoon, $\xi \equiv L_{\rm p}/L_{\rm j}$, and put $\xi_{-1} \equiv \xi/0.1$, $L_{\rm p,\,44} \equiv L_{\rm p}/10^{44}$ erg s^{-1}. Note, that for the observed $\langle L_{\rm IR,\,45}\rangle \sim 3$ and $\langle L_{\rm p,\,44}\rangle \sim 1$, and the expected GPS/CSS parameters $\eta,\ \xi_{-1} \sim 1$, this reads as $\langle U_{\rm IR}/U_{\rm B}\rangle \sim 10\,LS_1^{-1}$.

To Conclude:

Single power-law spectra of ultrarelativistic electrons is just a zero-order approximation.

.

for example 3C 273 jet:

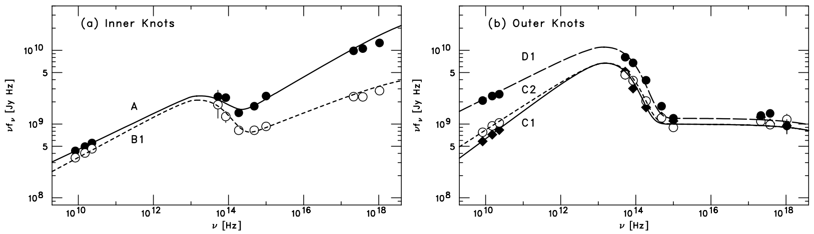

(*Uchiyama et al., 2006*)

Spectral energy distributions and 37 GHz monitoring of BL Lacertae objects

Elina Nieppola (eni@kurp.hut.fi)
Metsähovi Radio Observatory

M. Tornikoski, A. Lähteenmäki,
E. Valtaoja

The 8th ENIGMA meeting,
September 6 – 8 2006

Outline

- Introduction
- Spectral energy distributions (SEDs) using multifrequency data
- Metsähovi BL Lac observing project
- 37 GHz BL Lac data publication
- Future

Introduction

- BL Lacertae objects (BL Lacs) – a subgroup of blazars
- BL Lacs are divided into subclasses
  - Observational basis: RBLs (radio-selected) and XBLs (X-ray-selected)
  - Physical basis: LBLs (low-energy) and HBLs (high-energy)
  - IBLs (intermediate) in between

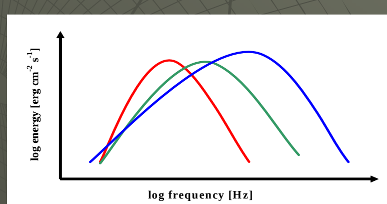

SEDs of BL Lacs

- SEDs of 304 objects determined using mf-data
  - Main data source CATS database (http://cats.sao.ru)
  - Parabolic fit to the synchrotron component (observer's frame)
  - → division to LBL / IBL / HBL
    - Nieppola, Tornikoski & Valtaoja 2006, A&A, 445, 441

SEDs of BL Lacs

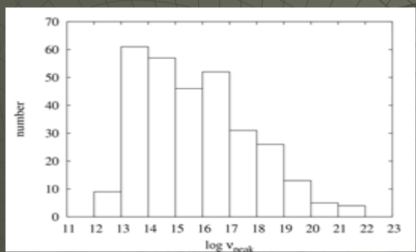

- Dividing boundaries:
  - log ν_{peak} < 14.5 → LBL
  - 14.5 < log ν_{peak} < 16.5 → IBL
  - log ν_{peak} > 16.5 → HBL
- Result: 98 LBLs, 96 IBLs, 110 HBLs

SEDs of BL Lacs

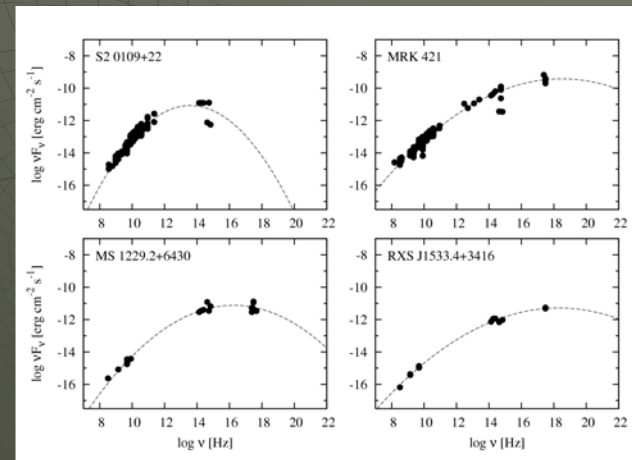

SEDs of BL Lacs

- Division of observational classes to physical ones:
  - → X-ray surveys discover also LBLs

	LBL	IBL	HBL
RBL	84%	10%	6%
IBL	22%	36%	42%
XBL	21%	25%	54%

SEDs of BL Lacs

- Clear negative correlation between radio luminosity and log ν_{peak}, but:
- No correlation between log ν_{peak} and luminosity at ν_{peak} → inconsistent with the "blazar sequence" scenario (Fossati at al. 1998, MNRAS, 299, 433)

SEDs of BL Lacs

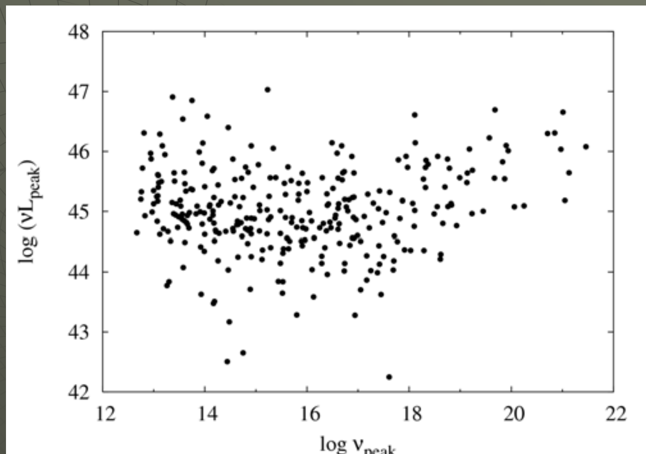

Metsähovi BL Lac observing project @ 37 GHz

- Started in December 2001 (ongoing)
- Source sample of 398 BL Lac objects mostly from Veron-Cetty & Veron BL Lac catalogue (9th ed., 2000)

Metsähovi BL Lac observing project @ 37 GHz

- Main objective: to get an idea of the high radio frequency behaviour of different types of BL Lacs (especially IBLs and XBLs)
- Some powerful objects monitored before as a part of the extragalactic sources monitoring project

Metsähovi BL Lac observing project @ 37 GHz

- Main benefit: Planck extragalactic foregrounds
  - The foreground sources must be removed from the CMB maps
  - Metsähovi gives a preview of what Planck is expected to see

37 GHz BL Lac data publication

- First data publication of the extended BL Lac source list (Nieppola et al. 2006, submitted)
- More than 3000 datapoints @ 37 GHz
- All 398 observed at least once, 34% detected at S/N > 4

37 GHz BL Lac data publication

- Detection rates by class:
  - 77% of LBLs detected, 37% of IBLs and 15% of HBLs
- Most observed sources: BL Lac, OJ 287, Mrk 421, AO 0235+164, S5 0716+714
- Still, 96% of the sample have been observed < 10 times

37 GHz BL Lac data publication

- Observing intervals vary
  - For objects with > 5 observations the mean interval is 124 days
- The mean fractional variability index of the sample $\Delta S=0.31$
  - Almost half of the sample increased their flux level to twice their S_{min}

37 GHz BL Lac data publication

- No dependence between ν_{peak} and fractional variability can be established

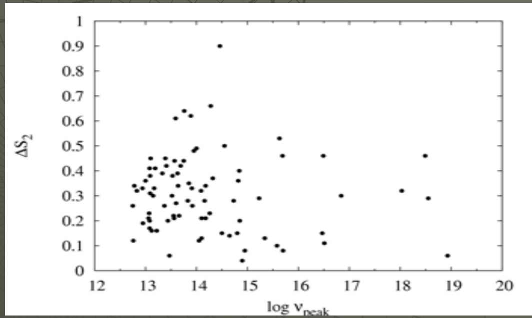

37 GHz BL Lac data publication

- Unprecedented data set for BLOs at high frequencies
  - The main result: HBLs & IBLs cannot be overlooked when estimating the foreground contamination
  - The ratio of detections vs. non-detections is ~ 20% → fair chance of a random detection

Future

- Analysis of the long-term radio variability of BL Lacs (continuation of Hovatta et al., in preparation)
  - Limited sample, only Metsähovi monitoring sources
  - Time scales and flare analysis
- SEDs
  - Dependence of ν_{peak} and other properties
    - Doppler factors
    - viewing angles, etc.

Kinematics of radio jets

….*some ideas about task 4*

Team in Bonn

Ivan Agudo
Emmanouil Angelakis

Thomas Krichbaum
Nicola Marchili
Nadia Kudryavtseva
Veronika Meyer
Arno Witzel
Anton Zensus
et al.
....

Uwe Bach

Lars Fuhrmann

This talk is .....

- By no means complete!
- Possibly (radio)-biased
- Not exclusively referring to ENIGMA-related publications
- … and based on a personal recollection !

Task 4: Variations of Source Structure and Flux

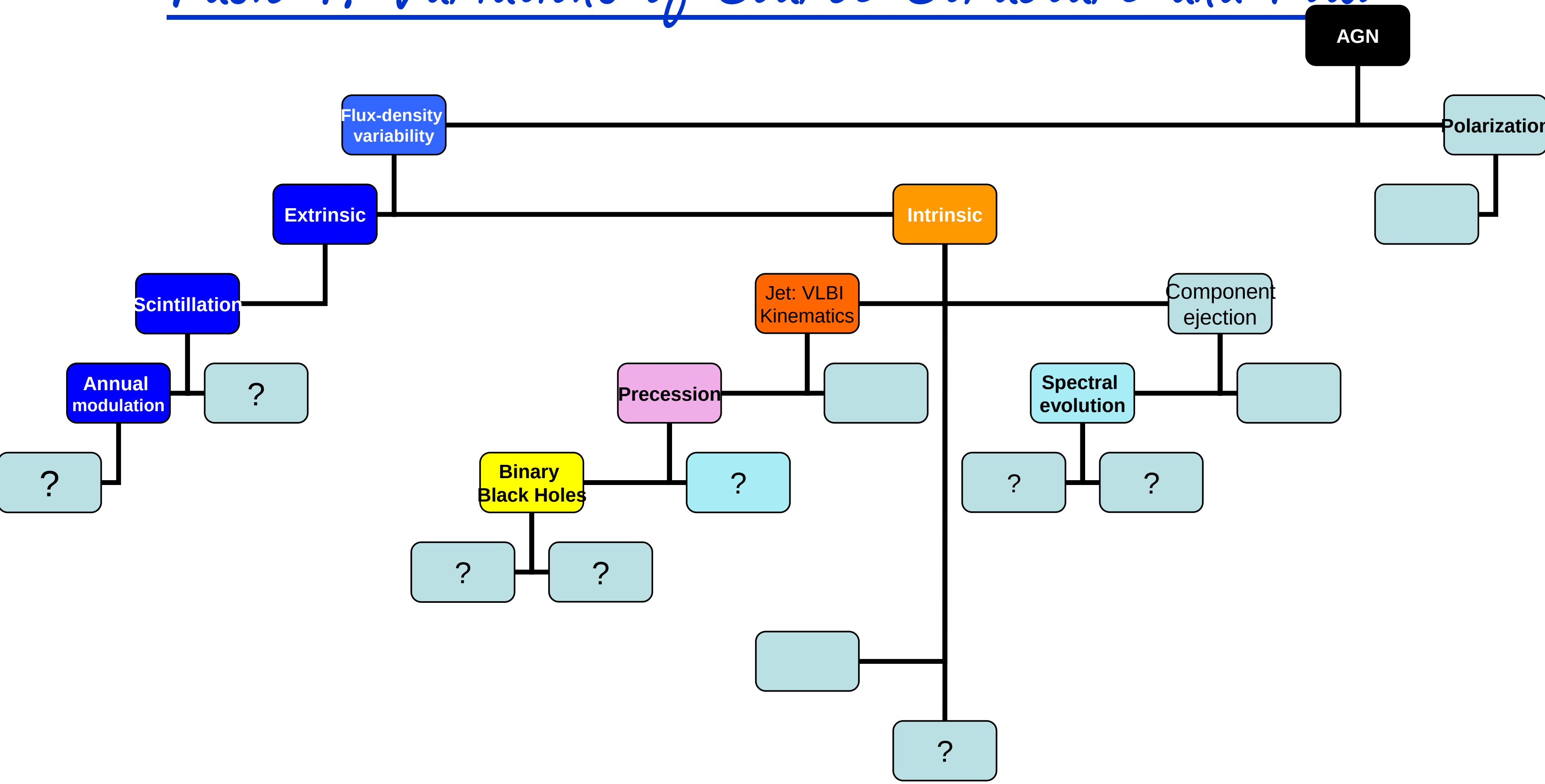

3C 120 (and its implications)

Marscher et al., 2002, Nature

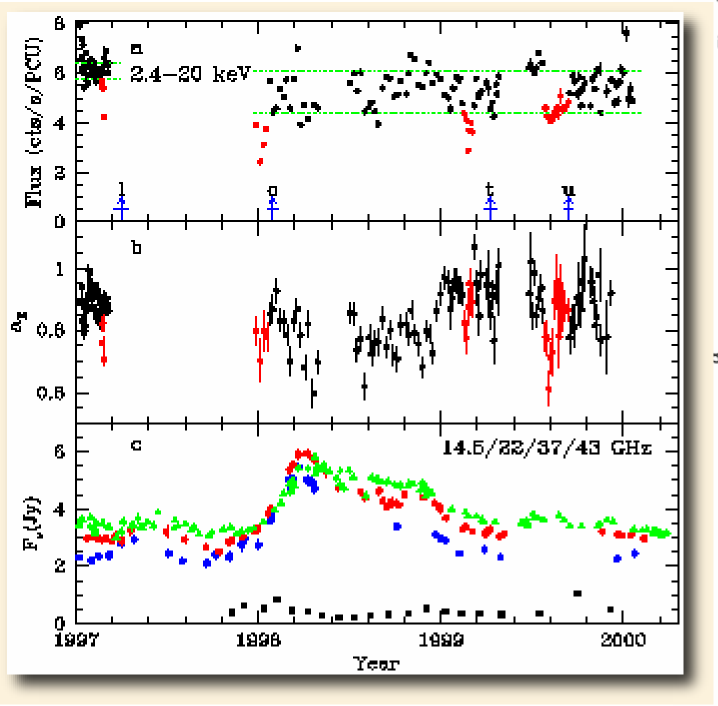

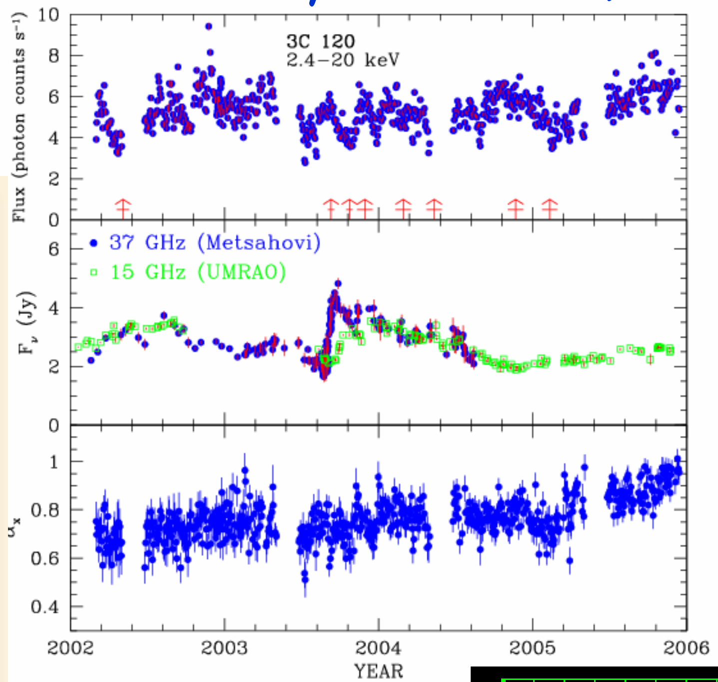

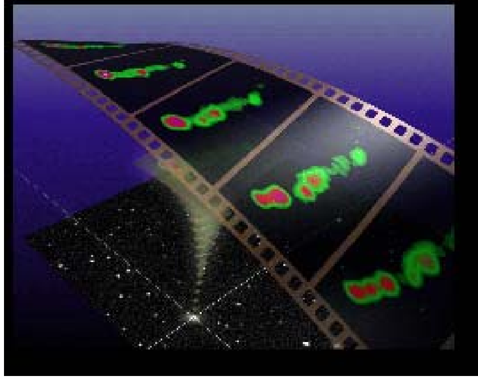

P. Ogle et al. 2005, Astrophysical Journal, 618, 139

Gomez et al.; 3C120, 43 GHz, VLBA

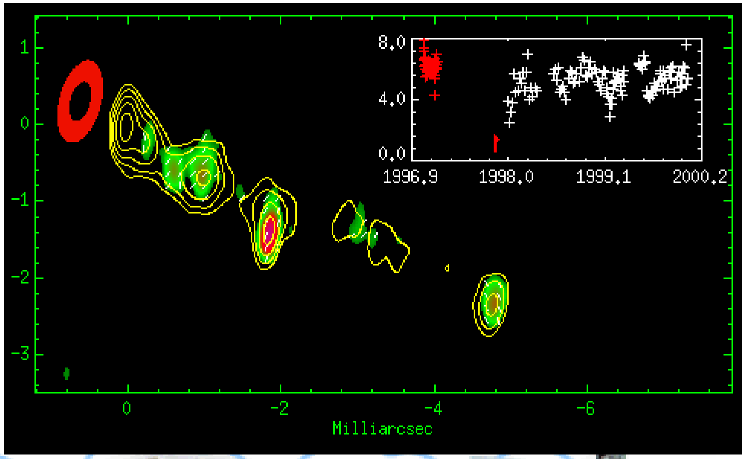

IDV, IDV, IDV, IDV

IDV-observations with Urumqi

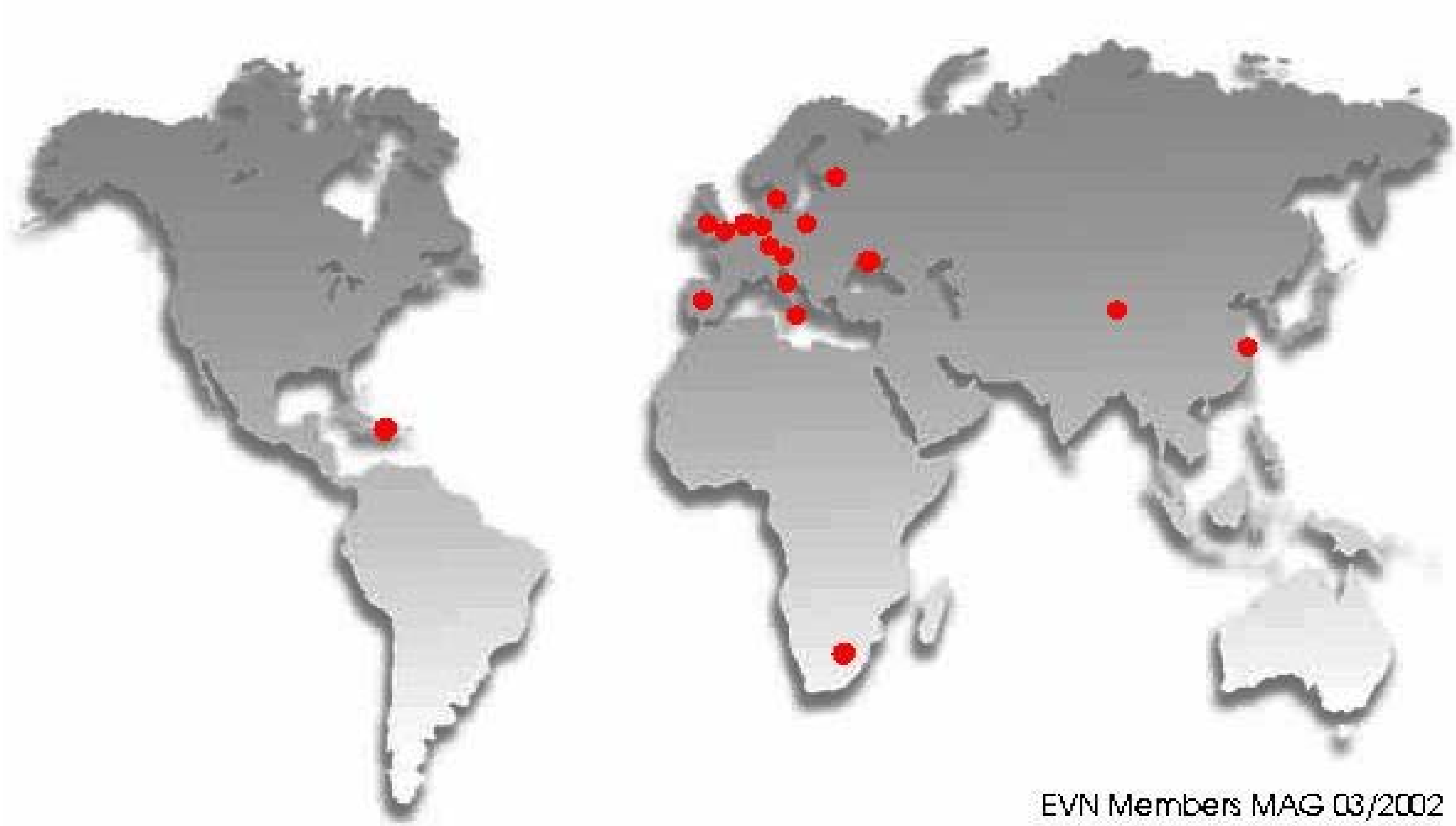

Effelsberg + Urumqi monitoring

Effelsberg

Urumqi

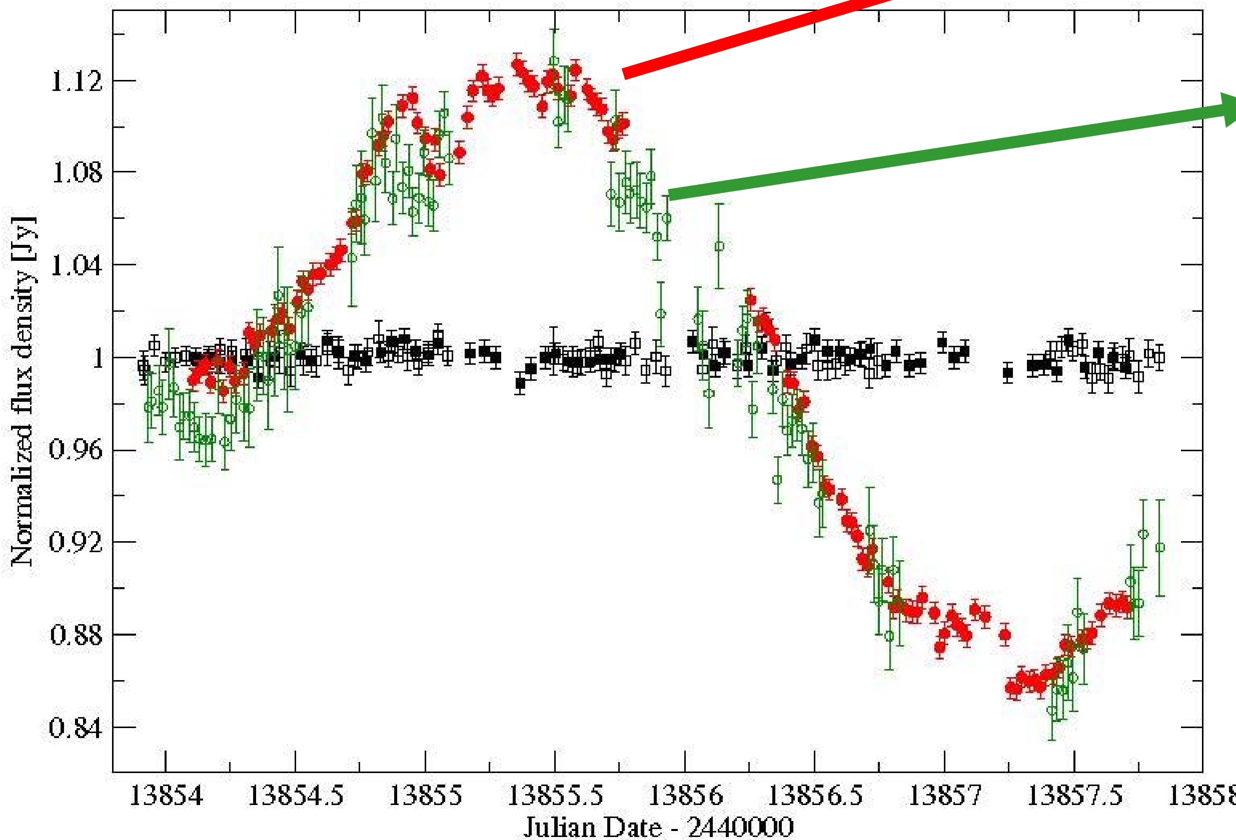

N. Marchili, K. Gabanyi, T. Krichbaum, et al.

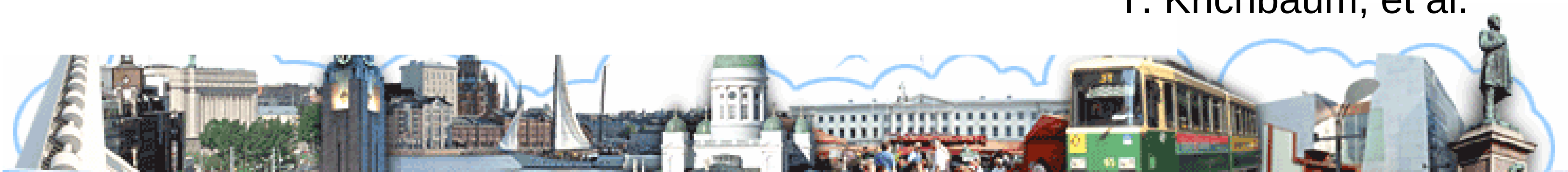

Scintillation: Annual modulation

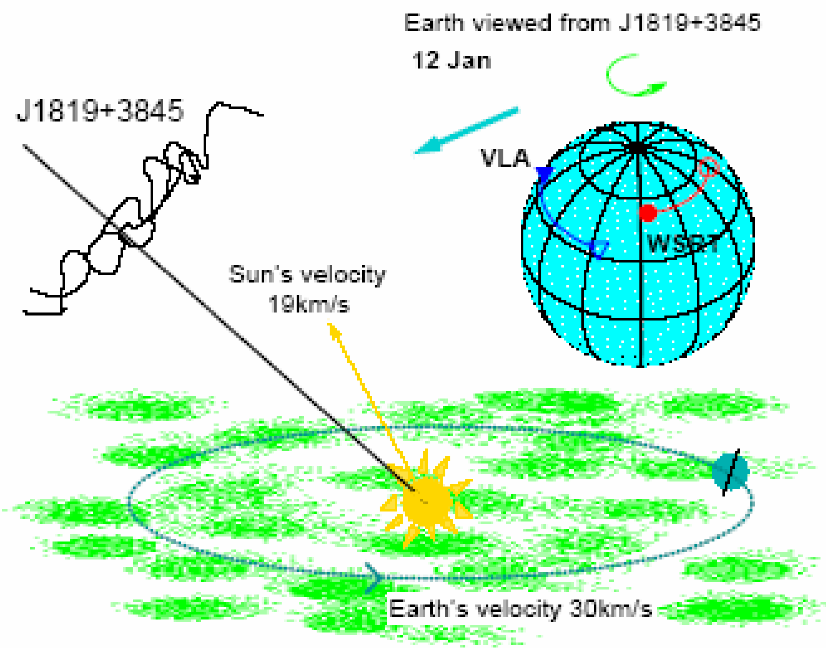

- Currently being succesfully modelled for the source 1128+592 (Gabanyi, Krichbaum, Marchili, et al.)

Already claimes for 0917+624 (e.g., Rickett et al.), J 1819+3845 (Dennett-Thorpe & de Bruyn 2003), PKS 1257-326 (Bignall et al. 2003), PKS 1519-273 (Jauncey et al. 2003), maybe 0954+658 (L. Fuhrmann et al.)

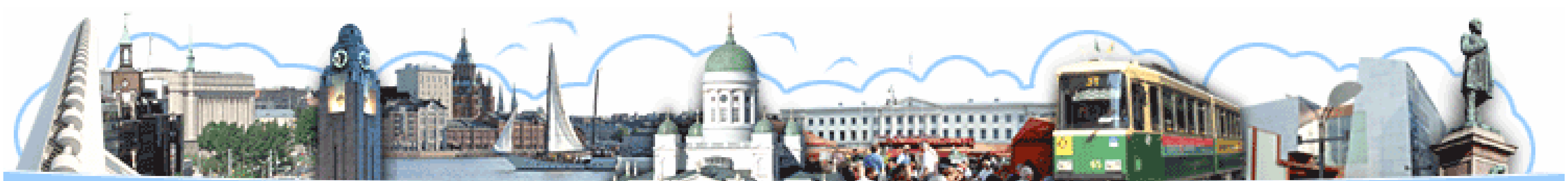

Flux-dens

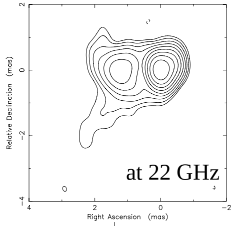

2005+403

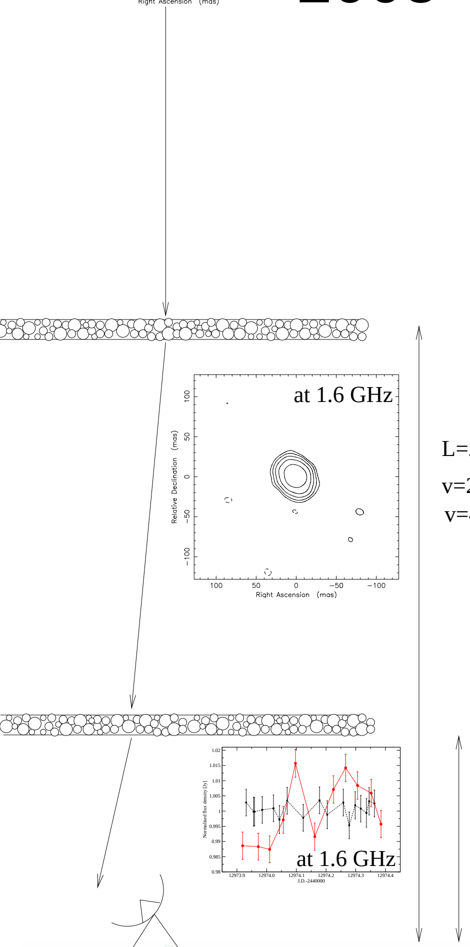

L=2.35 kpc

v=200 km/s t=12 days a

v=47 km/s t=52 days at

9 pc < L < 40 pc

50 km/s < v < 220 kı

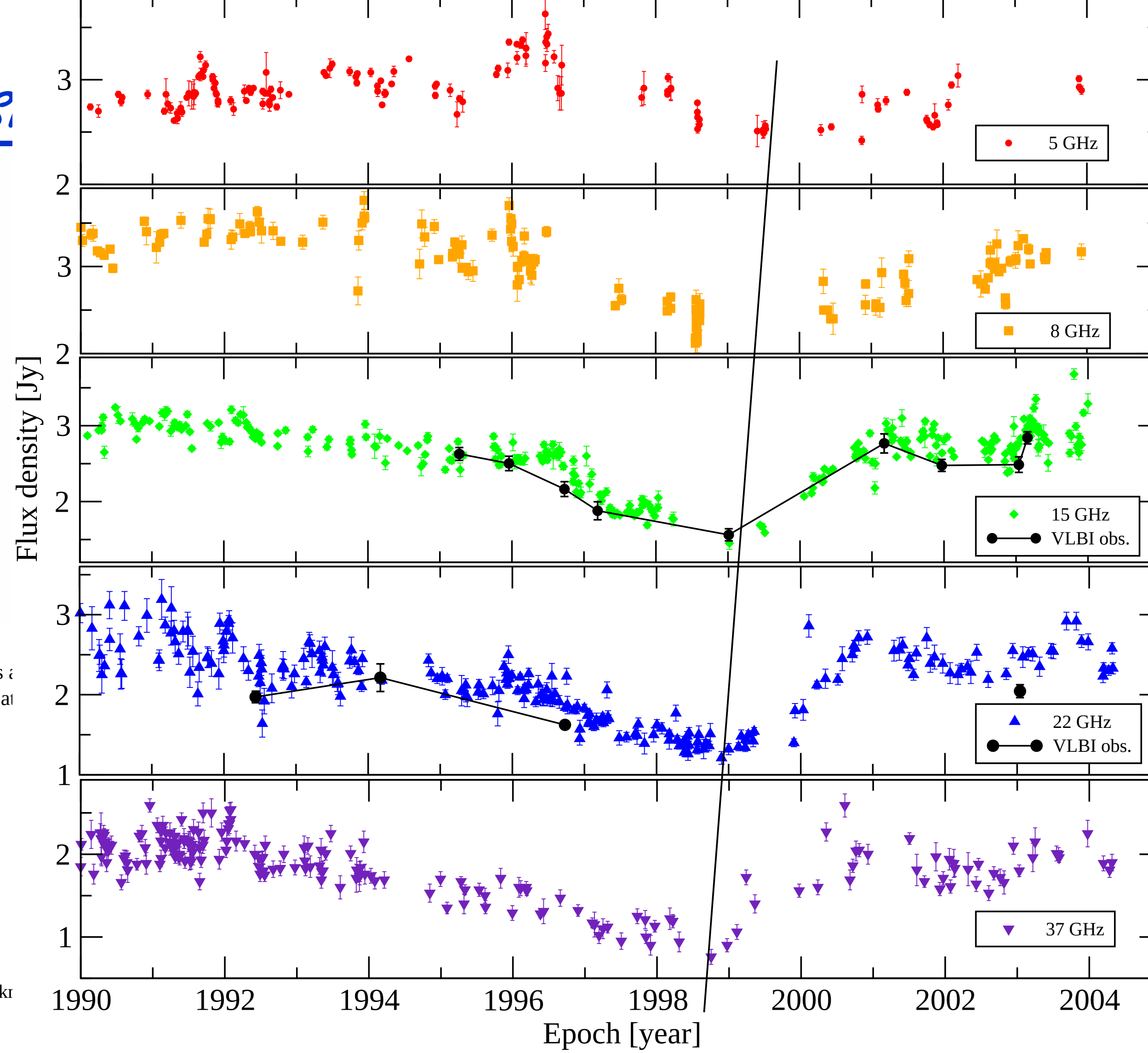

Gabanyi et al. 2006

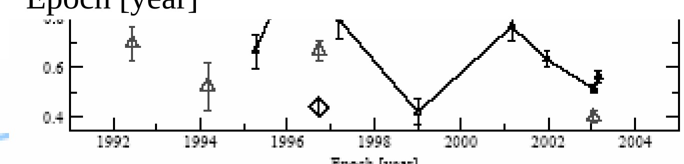

Helical Structures .....

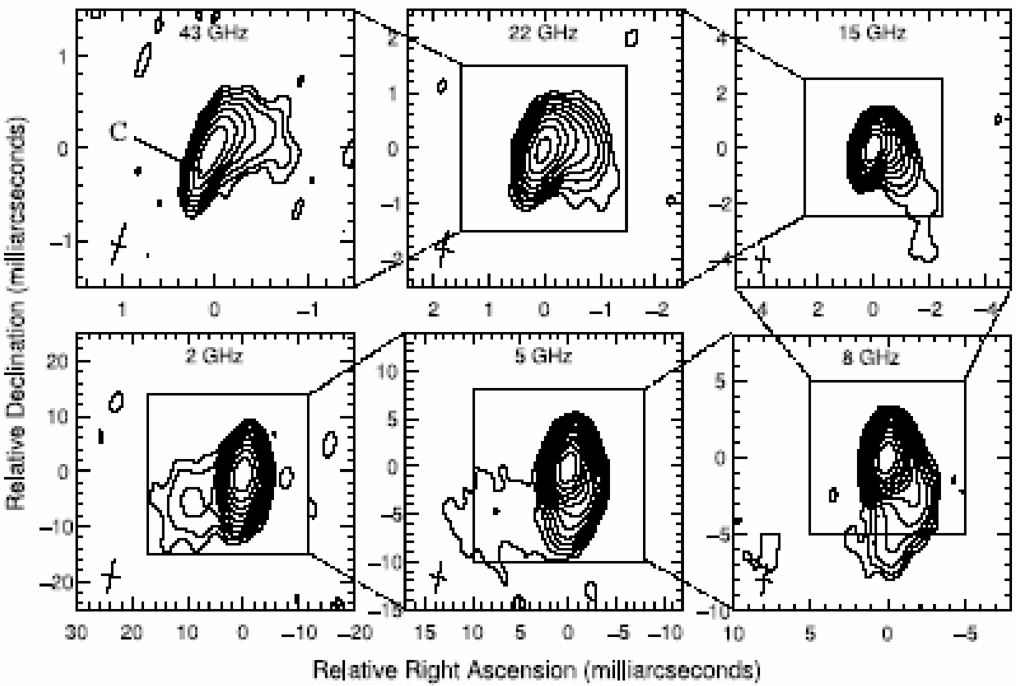

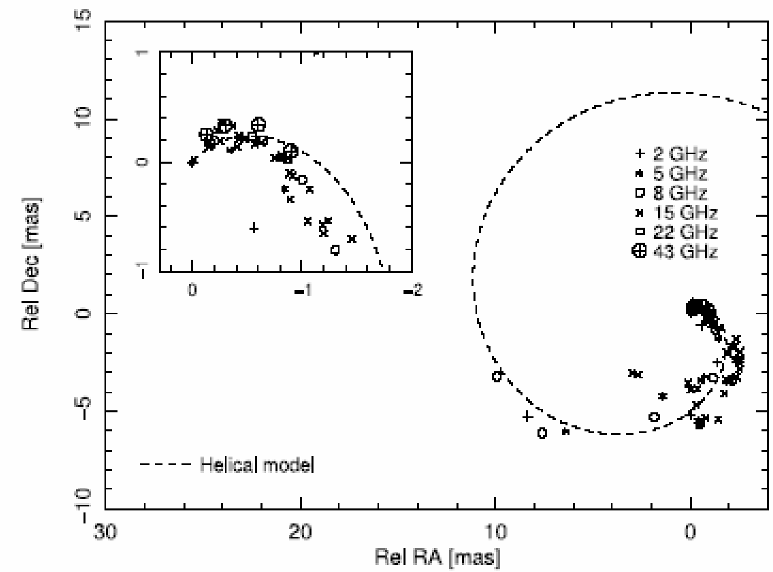

FIG. 12.—Best-fit trajectory and component centroid positions at different frequencies for the model describing a low-frequency helical fundamental mode of Kelvin-Helmholtz instability.

Savolainen et al., 2006ApJ...647..172

2136+141

Rotating something?

NRAO 150; etc.

7 degrees per year;

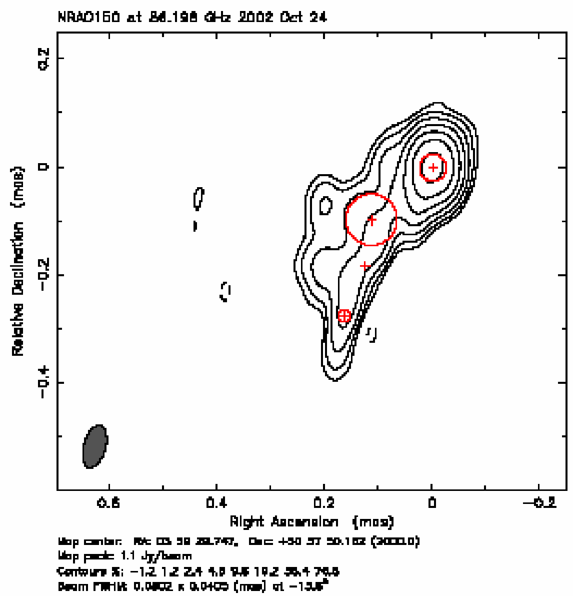

Fig. 4. 3 mm–VLBI image of NRAO 150 taken on October 2002. The positions of the fitted Gaussian components are indicated by the crosses and the circles (of radius equal to the FWHM of each Gaussian) symbolize their size.

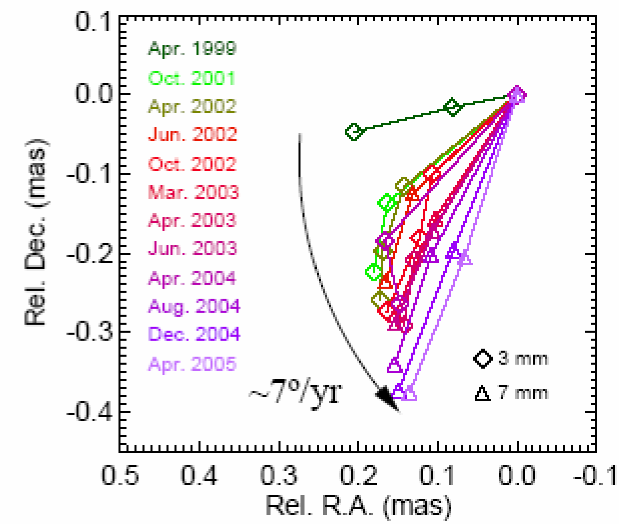

Fig. 6. Position –with respect to the core of the jet emission– of the inner model–fit components in NRAO 150. Only results from observations performed between 1999 and 2005 at 3 mm and 7 mm are drawn. The plot shows a fast change of the jet initial direction with a mean angular speed of ~ 7°/year.

Agudo et al. 2005, Agudo et al. in prep.

Highest-Resolution Radio Astronomy

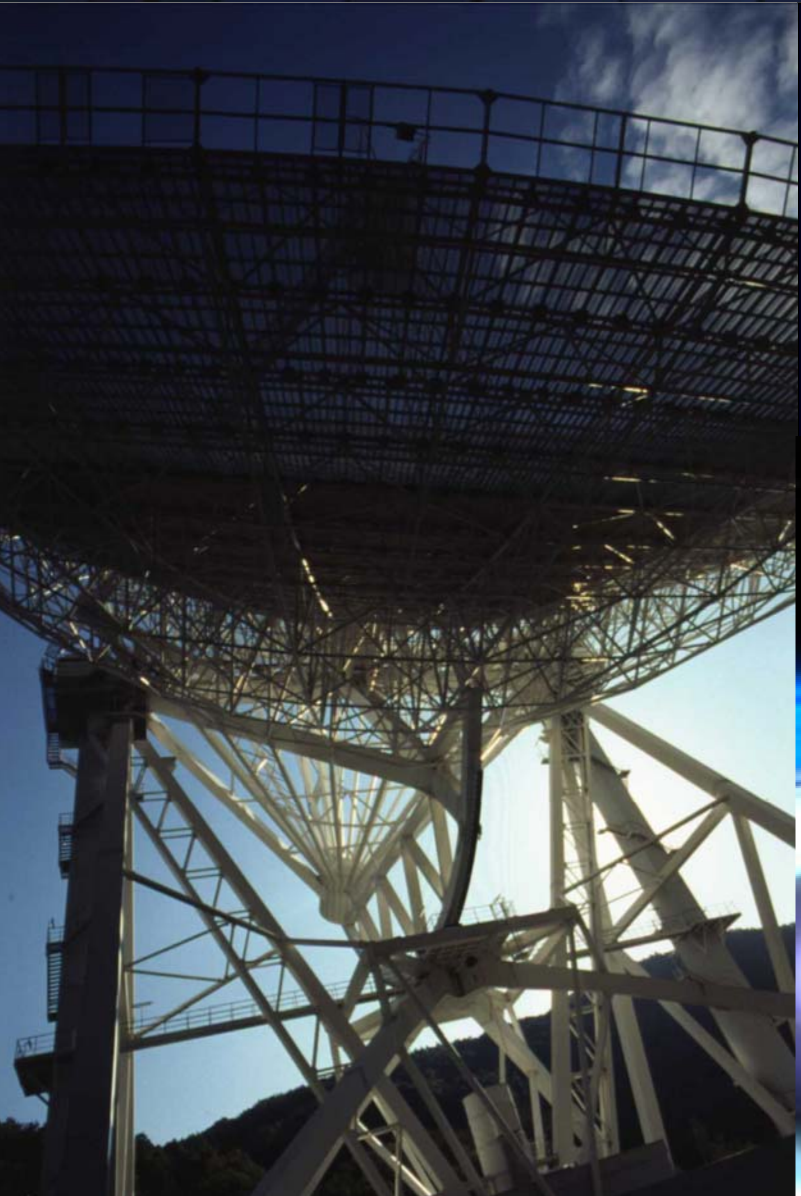

The Quest for the Black Hole

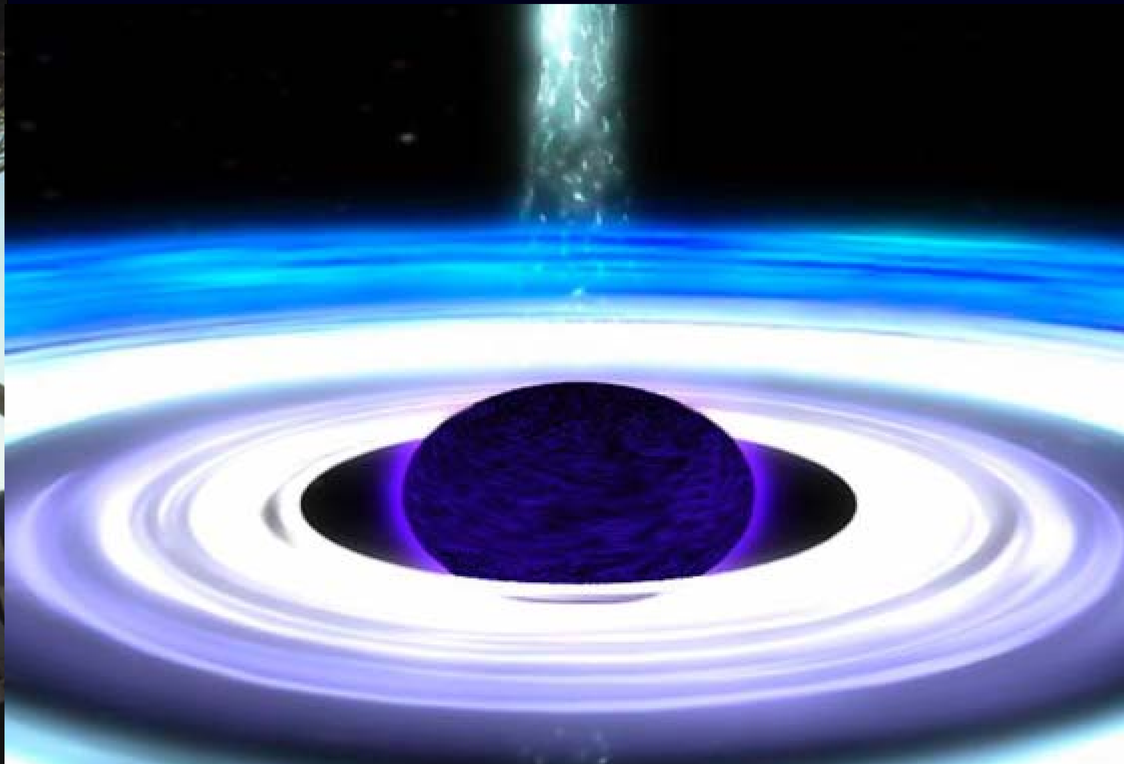

EGRET

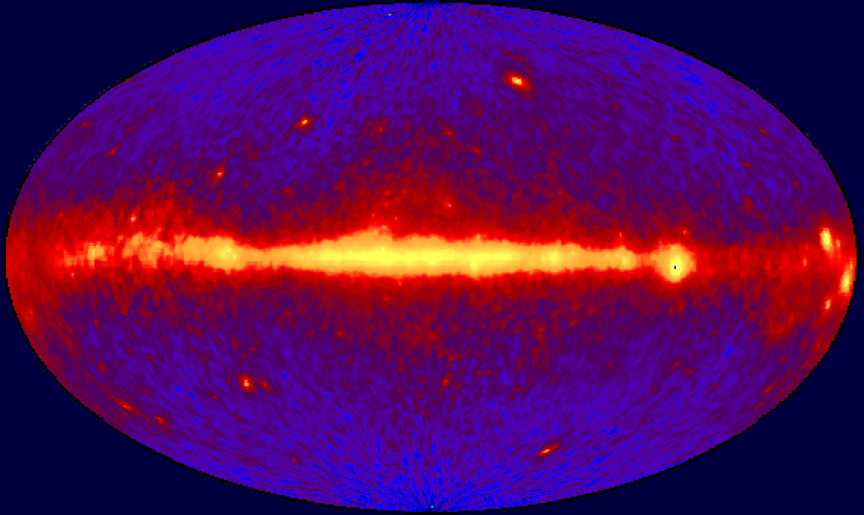

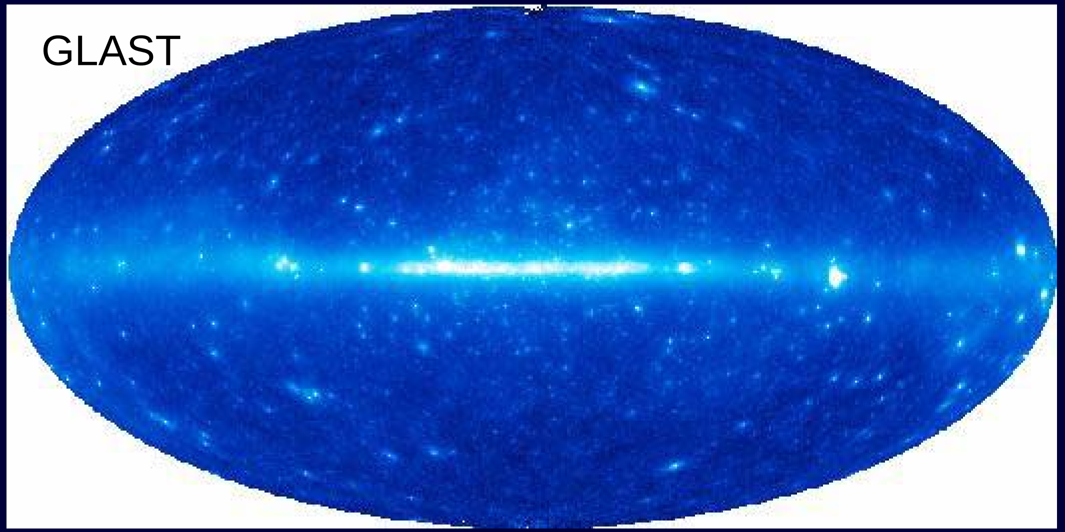

LAT All-Sky Map (E > 100 MeV, 1 year) Simulated,S. Digel

Supermassive Binary Black Holes
in different evolutionary stages?

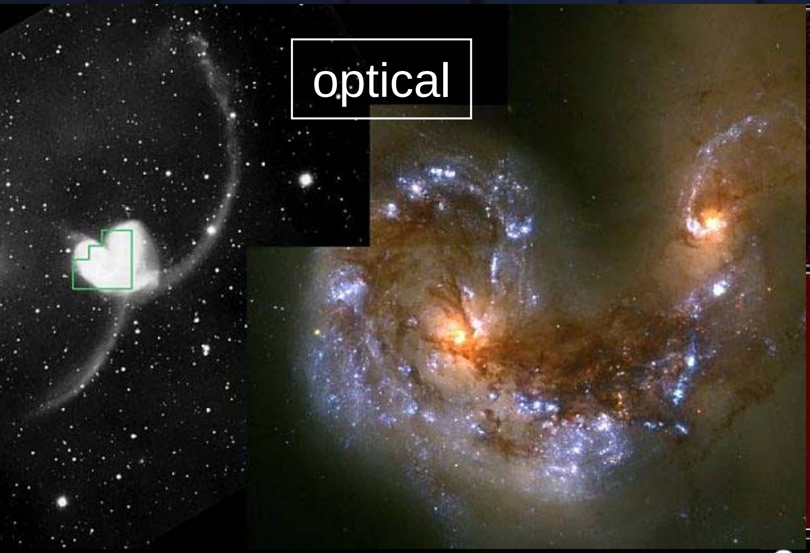

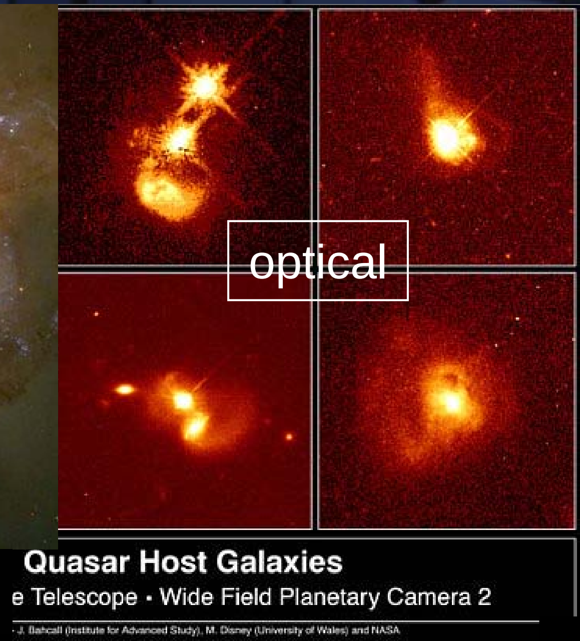

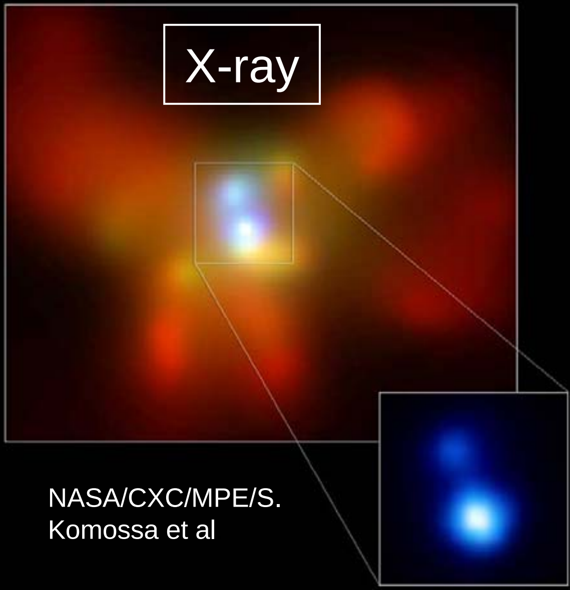

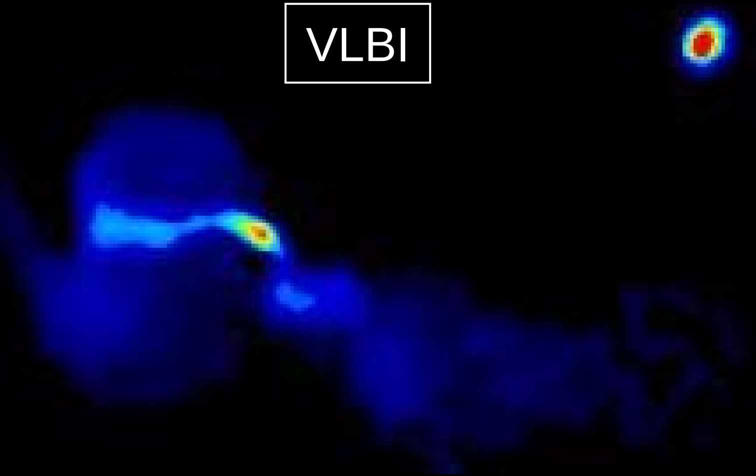

Hardcastle et al. 1996

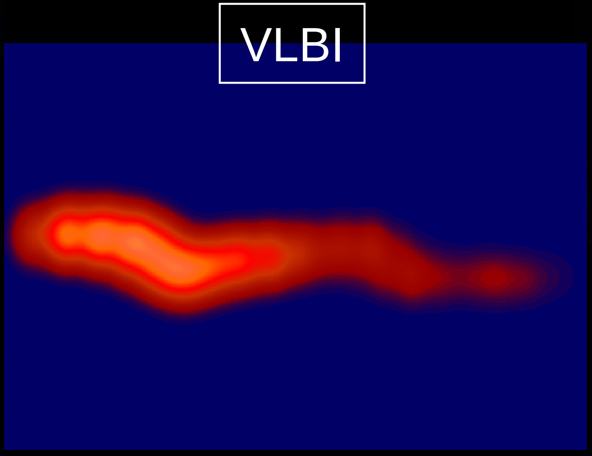

Lobanov & Roland 2004

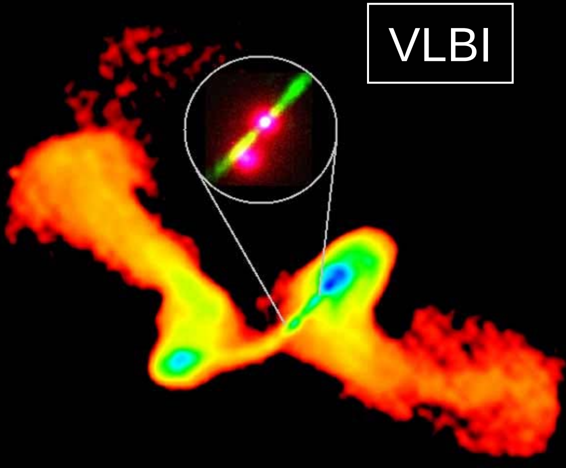

Murgia et al.

Supermassive Binary Black Holes: when OJ287 fails to flare ...

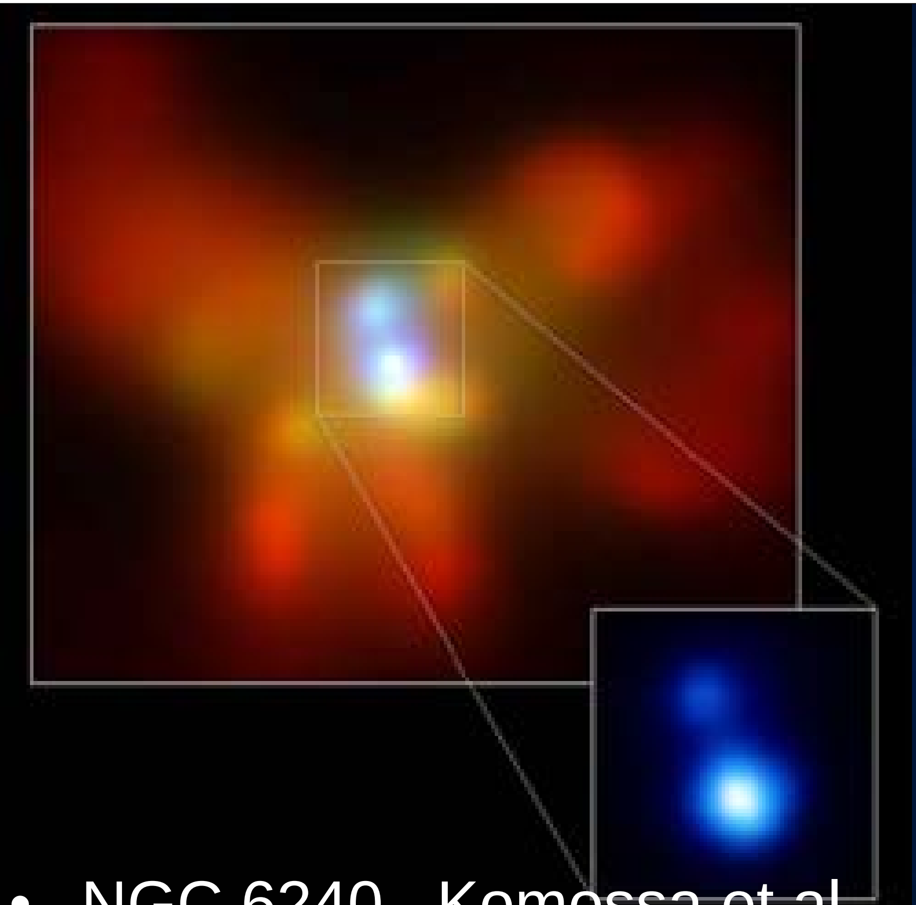

- NGC 6240 , Komossa et al.
- 3000 light years apart
- "starburst" galaxy
- Merger: 30 million years ago

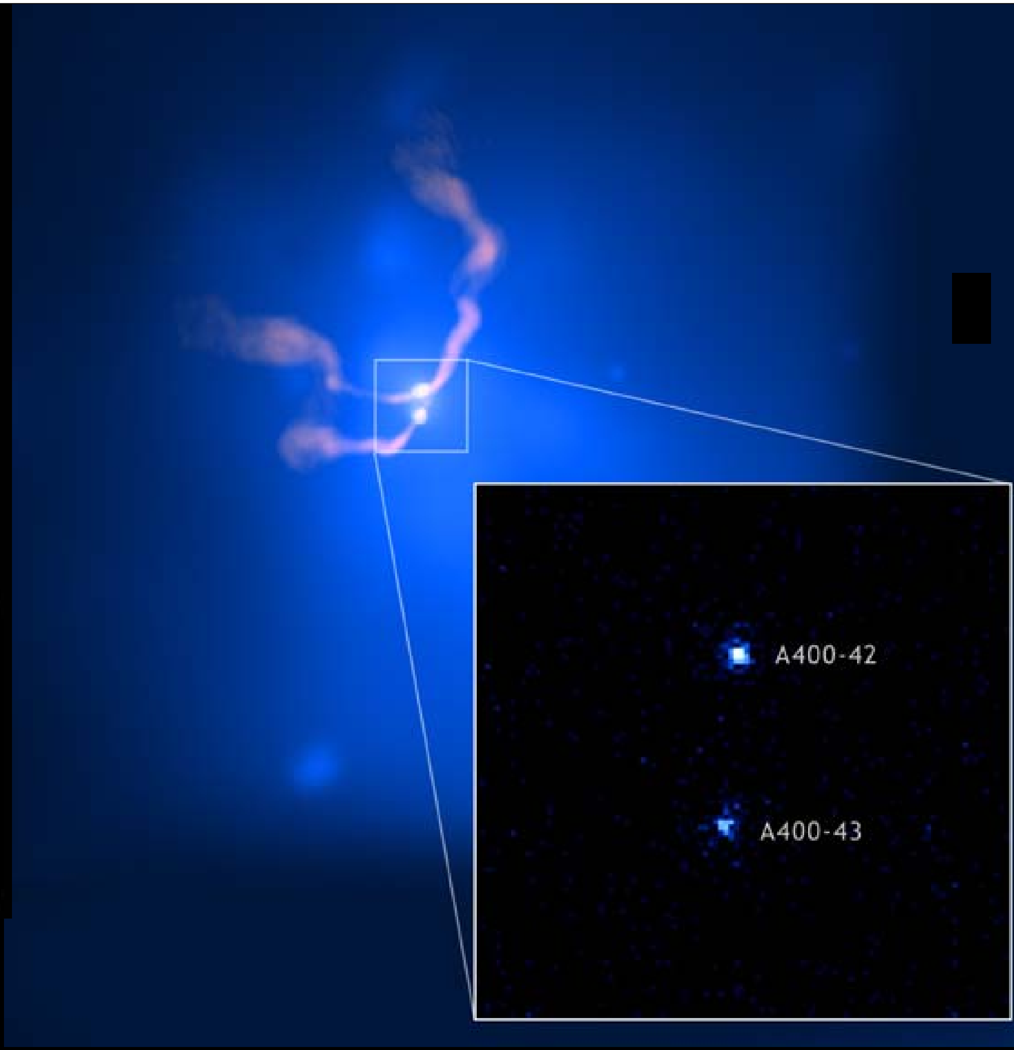

3C75 in Abell 400, X-ray,Radio

F.N. Owen, C.P. O'Dea, M. Inoue, & J. Eilek

Supermassive Binary Black Hole in 3C345

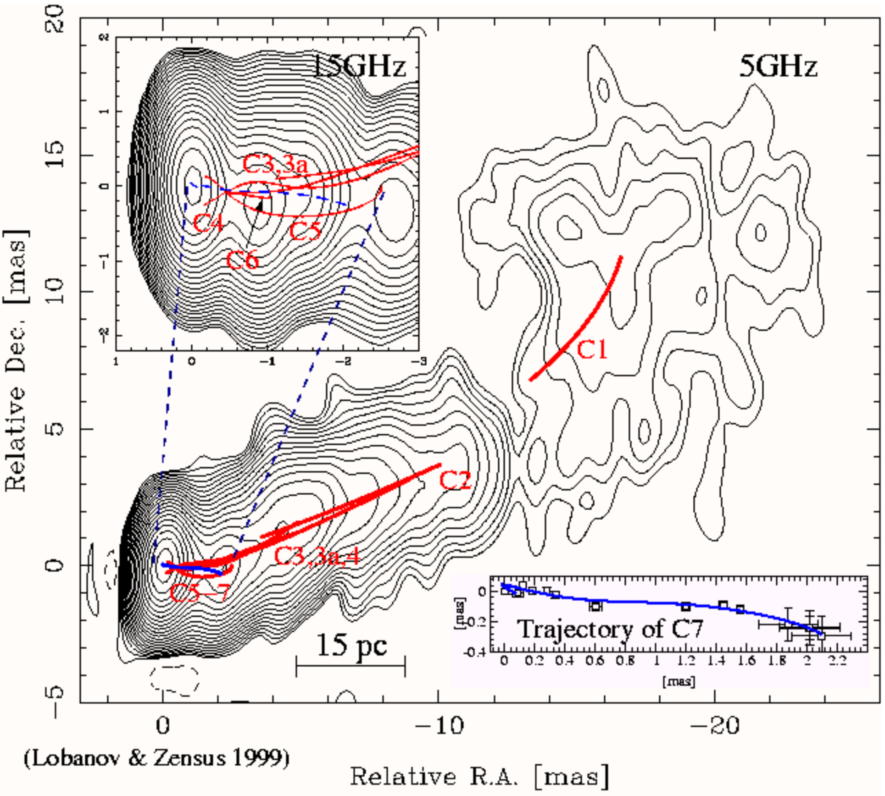

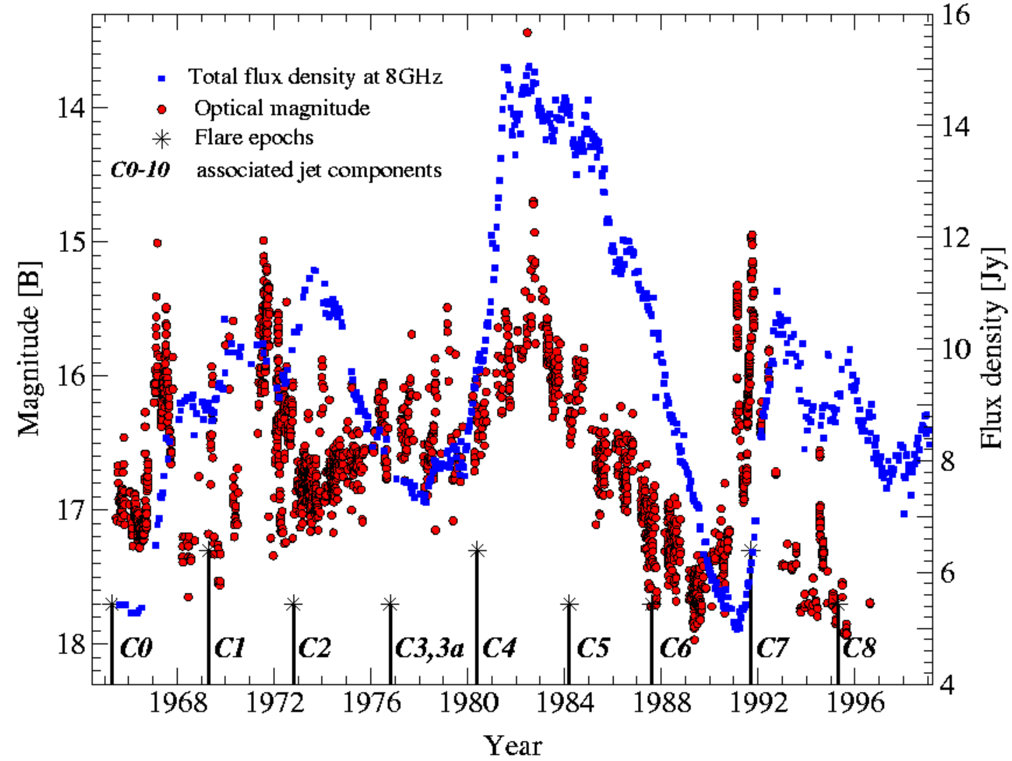

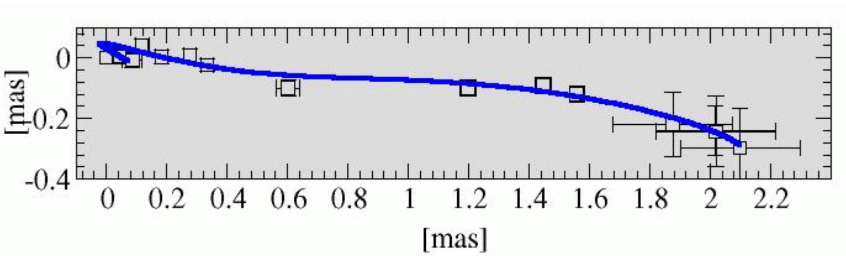

Optical data: 1965- (>2500)
Radio data: 1965- (>3000)
VLBI data: 1979- (>280)

Lobanov & Roland 2005

0716+714

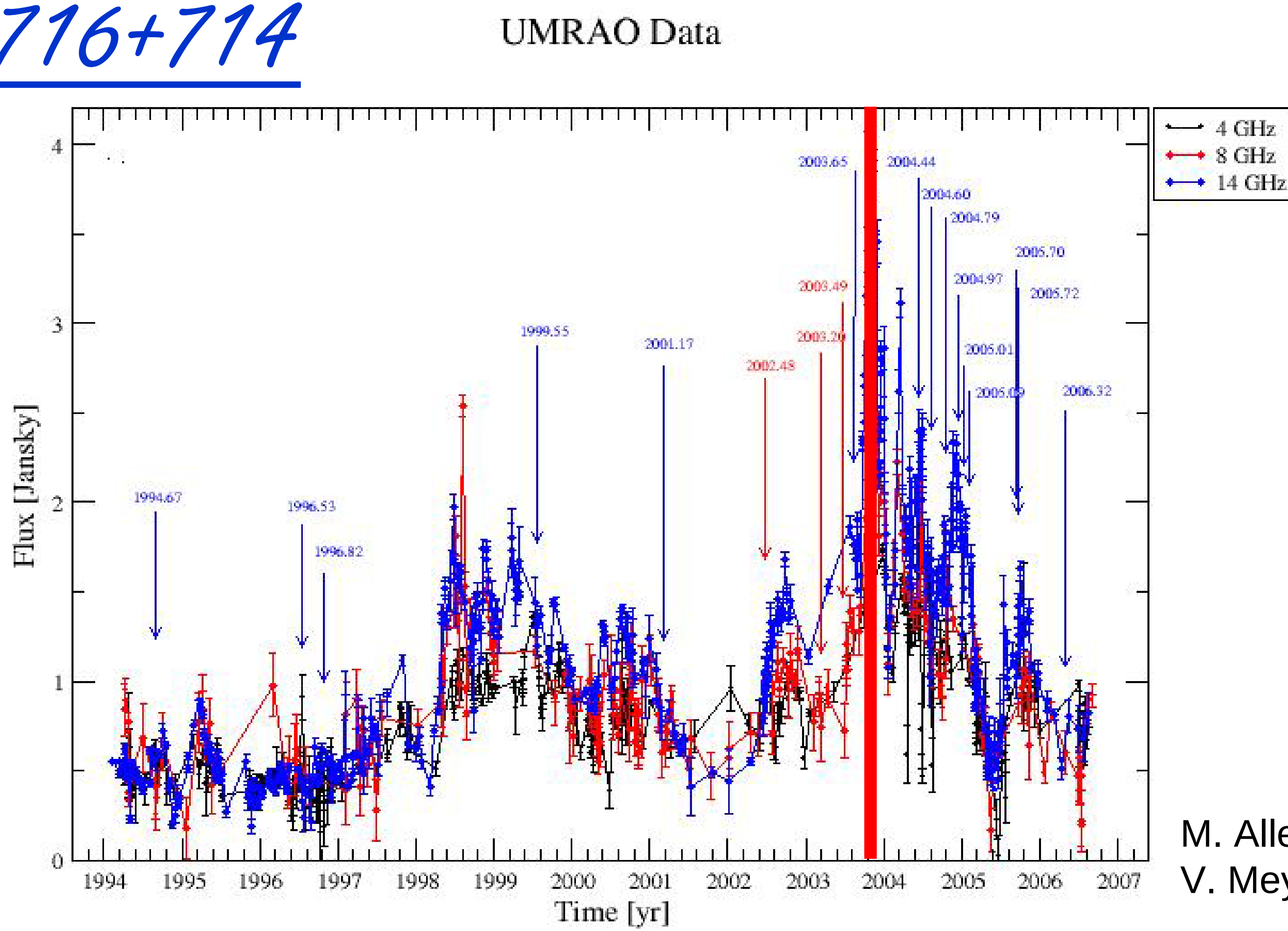

M. Aller
V. Meyer

Thanks!!

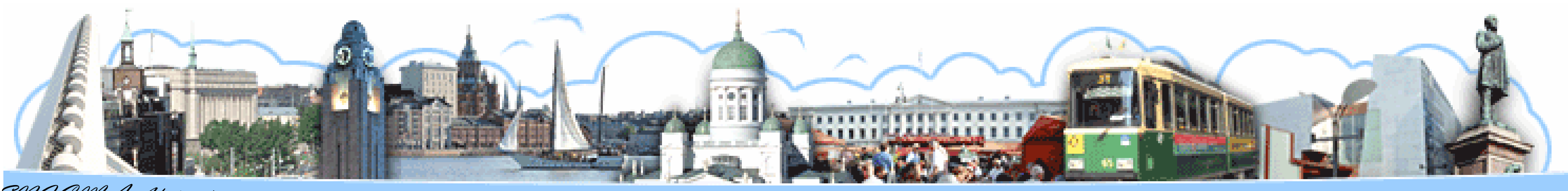

High Precision (Optical) Photometry

What have we learnt and where are we going?

CIT, Ireland

LSW, Germany

Boyden Observatory, South Africa

Kryoneri Observatory, Greece

Niall Smith (CIT)

Blazars

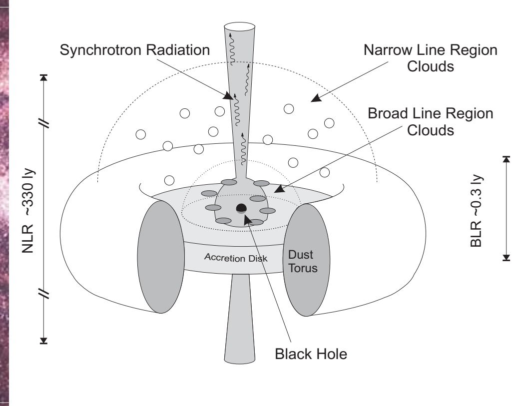

PG 0954+51

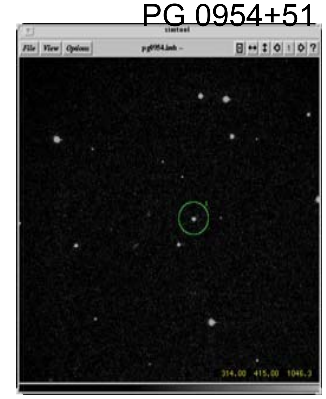

Field of AP Lib

AP Lib

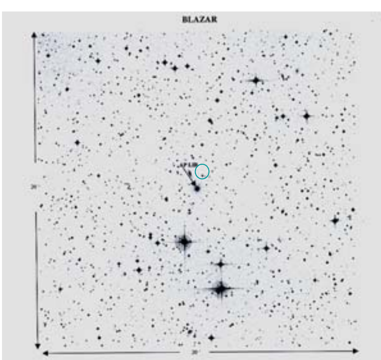

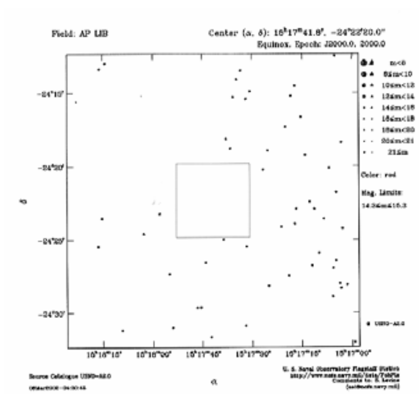

Field of B2 2134+23

B2 2134+23

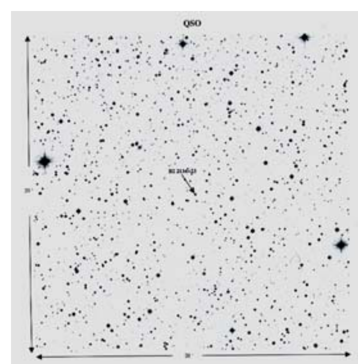

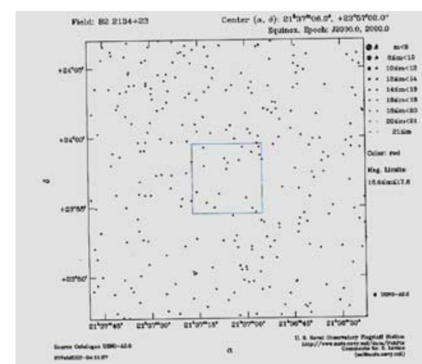

Science Drivers

The ONLY way to infer structures on timescales of light-minutes in AGN is with photometry / spectroscopy

Blazars are lineless → photometry

> Photometry on timescales of minutes can probe structures which are three orders of magnitude smaller than even proposed space-borne mm-VLBI

Science Drivers

RELIABLE detection/characterisation of

microflares (ultra-rapid events lasting few minutes)

rapid, small-amplitude events (T_B >> 10^{12} K)

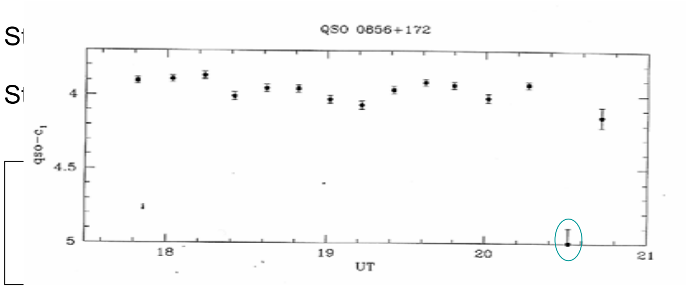

Technical Drivers

RELIABLE CCD photometry of blazars

- during major flares (rare)
- during "quiescent" phases (more common)

PRECISE CCD photometry of blazars

- at mmag level

TIMESCALE of minutes (sampling of seconds)

Long TIME-SERIES to make statistically significant statements

Photon-Limited Detection

Simple example:

If stellar image covers 10 pixels on CCD with a well depth of 350,000 electrons

then

total electron count is 3,500,000

yielding

photometric error of 0.58mmag (~0.06%)

The lure of EMCCDs ……

EMCCD SNR Equation

$$SNR = Q.I.t.F_n.\left[Q.t.F_n.(I + B_{SKY}) + (N_r/G)^2\right]^{-0.5}$$

G = Gain of the Gain Register

F_n = Multiplication Noise factor = 0.5

With G set sufficiently high, this term goes to zero

BUT

Readout speed and readout noise are decoupled

Architecture of EMCCDs

EMCCD readout architecture uses a GAIN REGISTER

- E2V – L3 Vision
- TI – Impactron

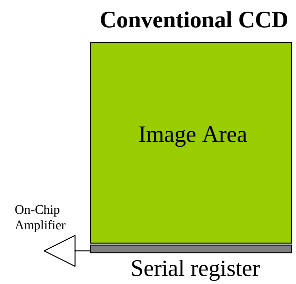

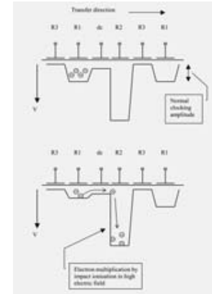

EMCCD Engineering Campaigns

2.2m telescope at Calar Alto

7 nights Jan/Feb 2003
6 nights Sept 2003

65,949 science frames in January

367,069 science frames in September

L3 (Andor)

At 4 frames/s a 6-day run generates 690 GIGABYTES of data

Ultracam "Mini-Campaign"

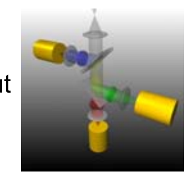

- 3-channel camera capable 4 Mb/s readout
- Three 1k x 1k frame-transfer CCDs
- Observations taken in November 2003 on 4.2m WHT at La Palma in Service Mode
  - Windowed to 100x80 pixels
  - 46,000 science frames per filter = 138,000 frames of data
  - 2 hours of data
- Only one reference star selected by service astronomer
- Similar follow-up observations taken in May 2004

PG0716+714 – EMCCD

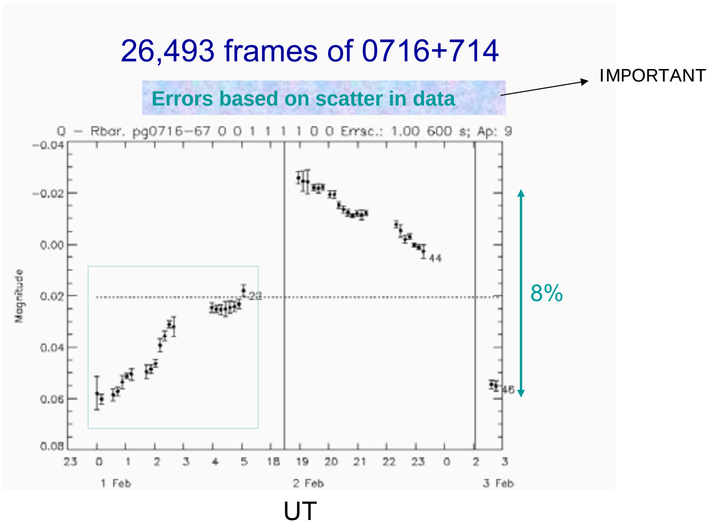

PG0716+714 – Ultracam

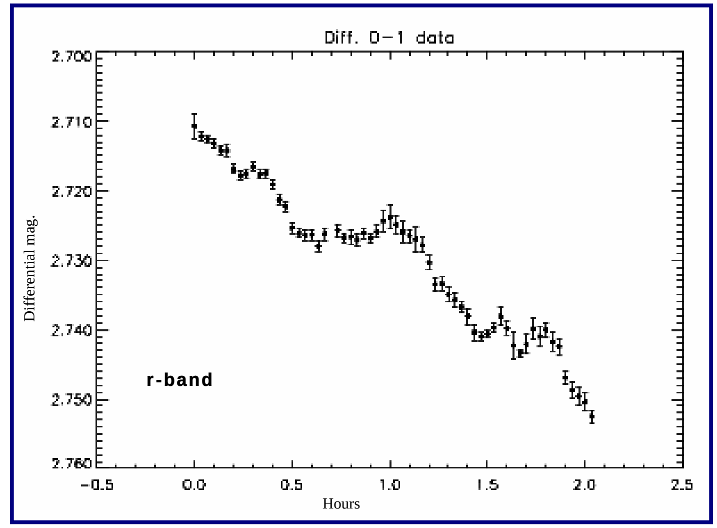

Generation of Lightcurves

Output is piped to IDL program "qvar"

- performs differential photometry using a master reference star (composed of 4-8 stars typically)
- provides statistical tests of variability
- allows different background determination methods to be used
- tracks variations in fwhm, position, apparent magnitude, airmass
- allows rejection of variable stars or data points affected by cosmic rays
- adjust parameters and "see what happens"

FLATTEN
FLATTEN
FLATTEN

Comparison of results?

- Best Photometric precision achieved was +/-1 *mmag* on either 2.2m or 4.2m
- Good S/N on each frame

Summed Image of the field of 0716+71

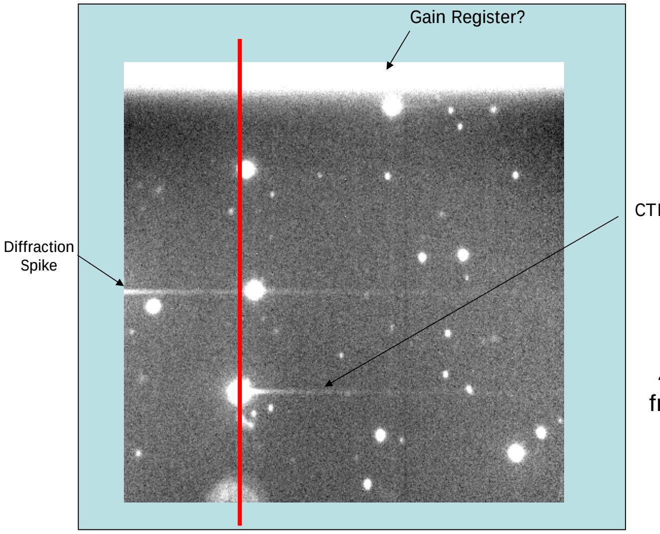

4572 frames

Laboratory Photometric Tests

EMCCD

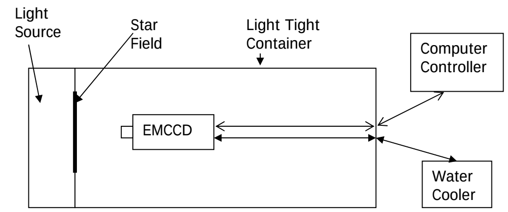

Photometric Analysis

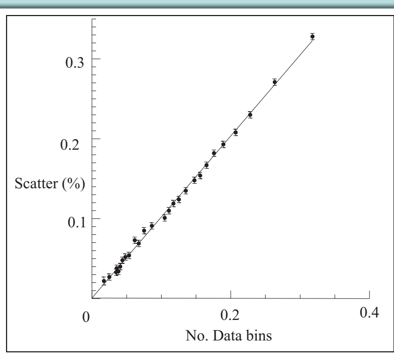

Limiting Scatter in Star1 = 0.01%

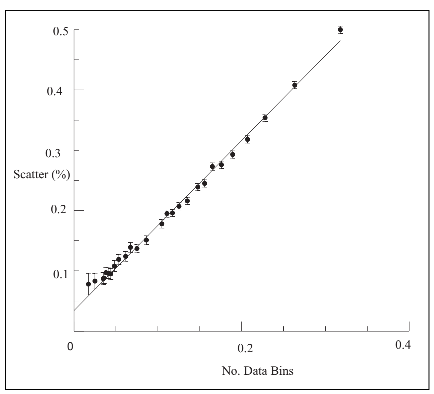

Limiting Scatter in Star2 = 0.03%

Limit to Photometric Precision?

What limits <u>instrumental</u> photometric precision?

- Many parameters to combine
  - Gain, clock voltages, shift speed, etc.

<u>Clock Induced Charge (CIC)</u>

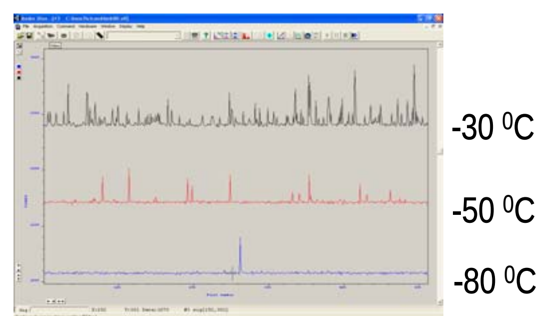

CIC Measured Quantitatively

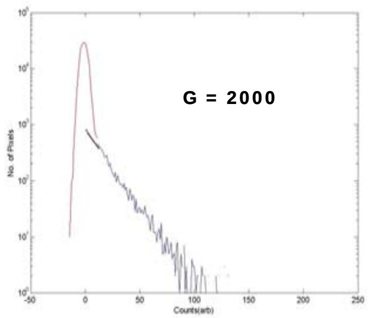

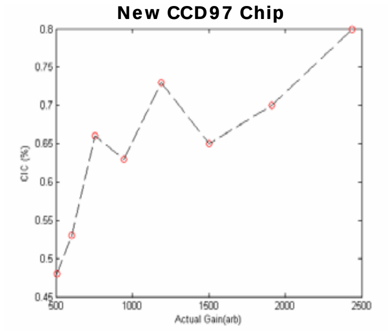

540 frames (1.4 x 10^7 pixels)

CIC < 1%

Removing Multiplication Noise – Photon Counting

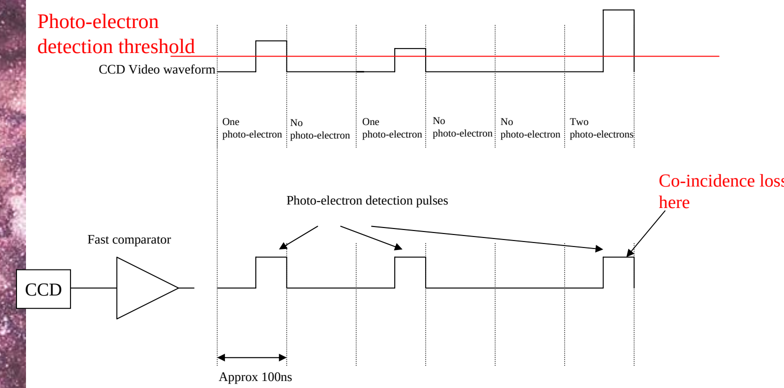

$$SNR = Q.I.t.\left[Q.t.(I + B_{SKY})\right]^{-0.5}$$

Noiseless Detector !

Is the EMCCD the limit??

- Photon statistics
- Sampling
  - inherent plate scale (3 pixels for FWHM)
    - undersampling is really not a good idea – ever!
  - intra-pixel sensitivity
  - changes in seeing
  - crowded fields
    - “pointy” PSF’s are bad
    - non-Gaussian PSF’s are bad

Is the EMCCD the limit??

- Comparison stars
  - magnitudes (relative to each other and the source)
  - colour (relative to each other and the source)
  - number
  - isolation (or otherwise)
  - intrinsic stability
- Isolation of object
  - PSF-fitting is inherently an approximation
- Host galaxy contribution
- Optimum aperture
  - variations in PSF across chip

Is the EMCCD the limit??

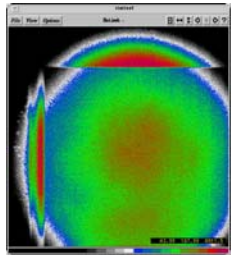

- Flatfielding
  - integrated counts in the flatfield
  - dangers of a “master flat”
  - flatfield spectrum is not the same as the source
- Tracking accuracy
  - ideally remove the need for flatfielding in differential photometry
- Focussing
  - changes PSF and can lead to non-linear behaviour of object and/or stars
  - defocussing doesn’t help in wide-fields as it leads to PSF overlaps of possibly many sources

Next Phase – Testing Emission Models

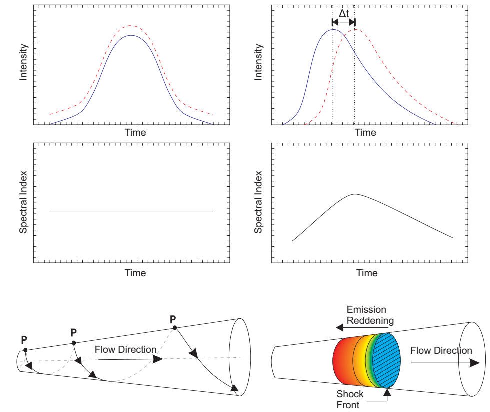

Two Channel Photometer

TOφCAM (**T**wo-Channel **O**ptical ***Ph***otometric ***I***maging **Cam**era) – pronounced “*toffee- cam*”

Potentially 160 TBytes of high quality data

Funded by Science Foundation Ireland

160 Nights Observation

– Greece – Kryoneri (1.2m)

– Greece – Aristarchos (2.3m)

– South Africa – Boyden (1.5m)

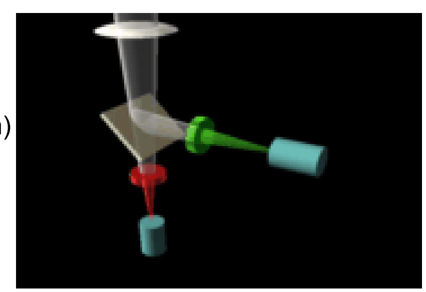

First light early 2007

Optical Layout

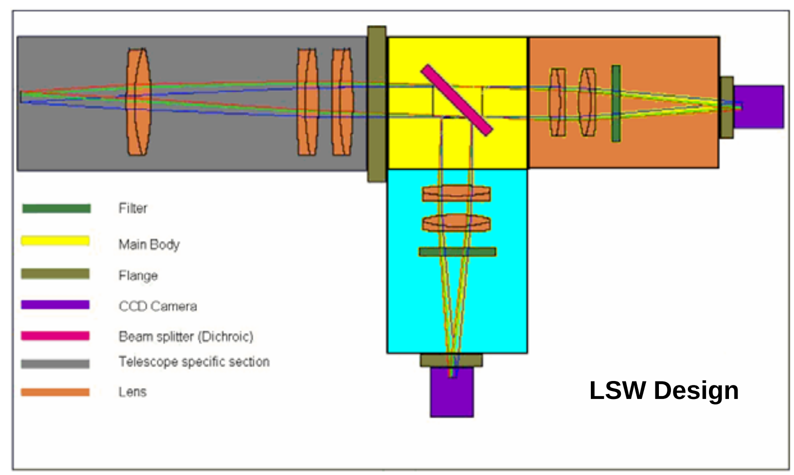

Mechanical Design

- Design and Fabrication - Mechanical Engineering Dept in CIT
- Design
  - Compact, lightweight, simple (no moving parts)
  - Rigid chassis
  - Optics fixed, except one changeable filter
  - Collimator optics fitted per telescope
  - Generally have all day to make changes - no need for quick release/easy access!!

Detectors

- E2V CCD97-00 L3 sensors
- Back illuminated
- Frame Transfer
- Thermoelectrically cooled

Active Pixels	512 x 512
Pixel size (µm)	16 x 16
Image area (mm)	8.2 x 8.2
Well depth (e⁻)	160,000
Readout Rate (MHz)	10
Frame Rate (frames per sec)	34
Read Noise (e⁻)	< 1
Dark Current @ -85 °C (e⁻/pix/sec)	0.001
Gain	1000
Peak QE (%)	90
Cooling Temperature (°C)	-100

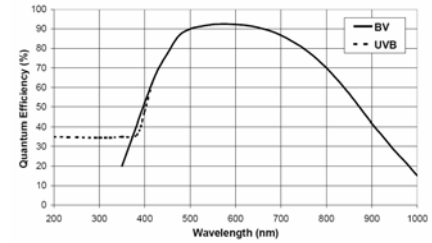

Data Acquisition

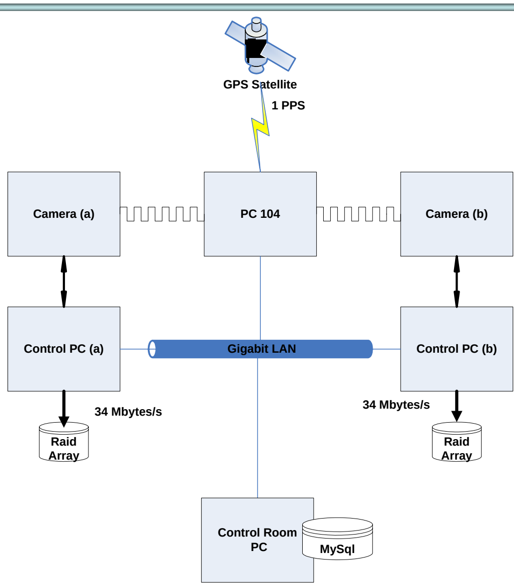

- Timing
  - GPS
  - 1PPS
  - ms resolution
  - PC104 controlling triggering and logging of timestamps
- 2 camera control PCs
  - P4, 2 GB RAM
  - Raid 0 SATA HDs
  - 4 x 200 GB drives
  - Data stream to disk
  - Removable HDs
- Control PC (GUI)
  - TCP/IP over Ethernet communication
  - Remote access
- Live Photometry

Thoughts

<u>Reduction Methodologies</u>

Is there an optimum way?

<u>Intensive monitoring</u>

Access to guaranteed time
What type of equipment available?
Harmonising the results through calibration.

<u>Coordinated monitoring</u>

How do we decide upon targets?
Are flaring sources always best?

A few more thoughts

- Requirements of high precision photometry are somewhat at odds with those of optical photometry aimed at supporting a large multiwavelength campaign
- Community mostly interested in multiwavelength campaigns
- Need a network of telescopes as identical as possible (detectors, optical elements) with precision timing
- Long data trains
- We plan to use 2 EMCCDs with two identical filter sets to test how similarly we can determine the lightcurve of a source from two different locations

Kryoneri Telescope Project

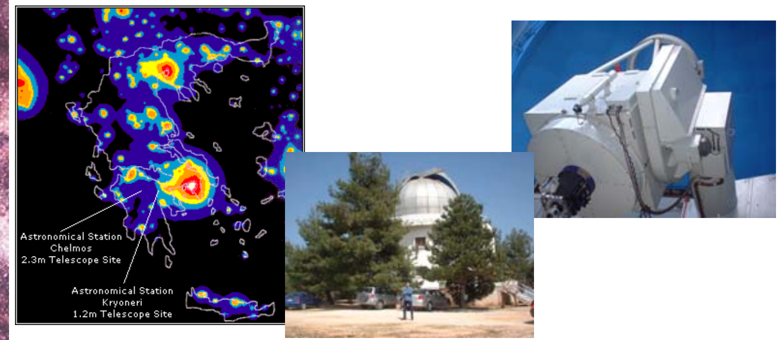

- Agreement in place with Institute of Astronomy & Astrophysics, Athens
- Now have secured funding to robotise the 1.2m Kryoneri Telescope

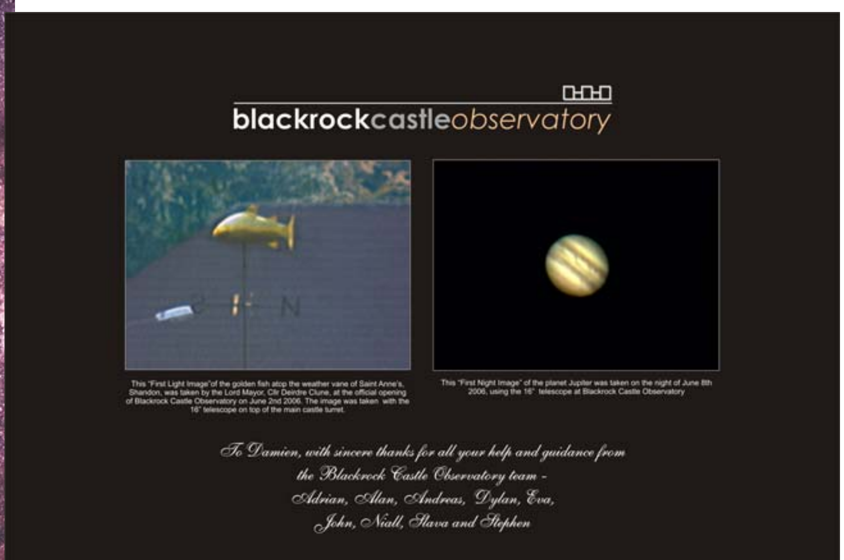

Thankyou for your attention

Quasar Host Galaxies in the FORS Deep Field

Carolin Villforth
Landessternwarte Heidelberg, Germany

8. ENIGMA-Meeting
6.9.-8.9.2006
Espoo, Finland

Contents

Cosmology and Magnitude System

- cosmology is: $H_0 = 70 km/s/Mpc, \Omega_m = 0.3, \Omega_\Lambda = 0.7$, unless otherwise stated
- all magnitudes are in Vega-system

Motivation

Falomo et al. 2005

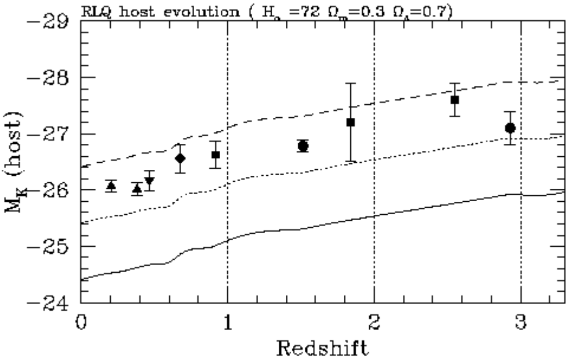

Motivation

Falomo et al. 2005

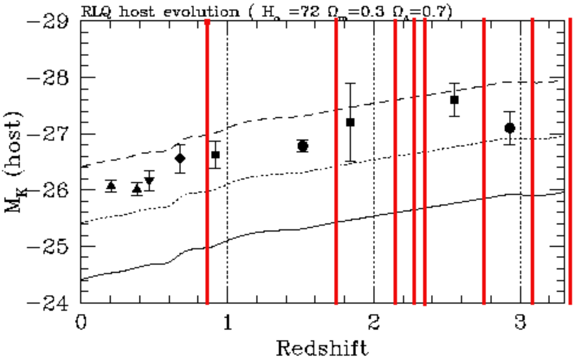

$\Longrightarrow$ our quasars lie in a very interesting redshift range!

The FORS Deep Field

- field around high-redshift (z=3.3650) radio-loud (?) QSO Q0103-260
- size of field: 6.8'x6.8'
- about 9000 objects in photometric catalog
- spectroscopy for about 350 objects, including all 8 identified quasars

The FORS Deep Field - FDF vs. HDF

Heidt et al. 2003

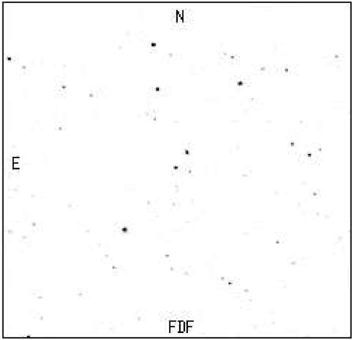

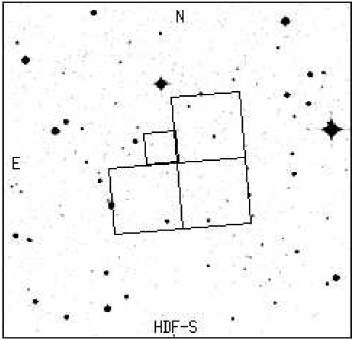

- FDF is distinctly larger than HDF $\Longrightarrow$ better statistics
- FDF contains far less bright stars than HDF

The FORS Deep Field - Data

filter	telescope	exposure time [s]	FWHM ["]	50% compl. limit
U	VLT	44400	0.97	25.64
B	VLT	22660	0.60	27.69
g	VLT	22145	0.87	26.86
R	VLT	26400	0.75	26.68
I	VLT	24900	0.53	26.37
J	NTT	4800	1.20	23.60/22.85
Ks	NTT	4800	1.24	21.57/20.73
F814W	HST	2400	0.12	?

The FORS Deep Field - Redshift Distribution

Appenzeller et al. 2004
photometric redshifts

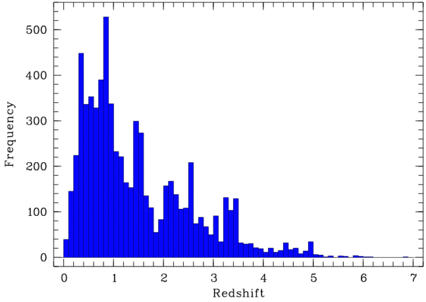

Noll et al. 2004 (∼350 objects)
spectroscopic redshifts

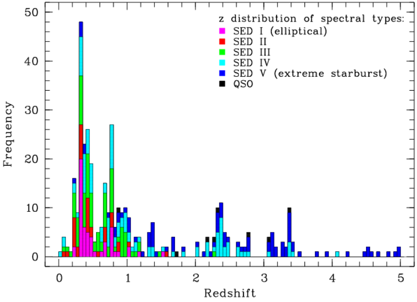

The QSO-Sample

FDF-ID	z	m_I	M_B	M_B $H_0 = 50$ $\Omega = 0$	type	radio
FDF0809	0.8650	21.4	-20.65	-21.29	QSOI	RQQ
FDF1837	2.2540	22.9	-21.88	-22.79	QSOI	RQQ
FDF2229	2.1560	20.8	-23.57	-24.56	QSOI	RQQ
FDF2633	3.0780	22.8	-22.33	-23.59	QSOI	RQQ
FDF4683	3.3650	18.6	-27.19	-28.53	QSOI	RLQ
FDF5962	1.7480	21.9	-22.29	-23.15	QSOI	RQQ
FDF6007	2.7515	24.1	-21.10	-22.27	TypeII	RQQ
FDF6233	2.3215	23.9	-19.73	-20.77	BAL	RQQ

Data Analysis

- construction of Point Spread Function (PSF) (IRAF)
- fitting the object (kimage)
  - fitting the central point source
  - fitting a core+galaxy-model
- error simulations (fitsimul, to be done)

Fits

different models are fitted to each object:

- core-fit(AGN): scaled PSF is fitted
  3 free parameters: magnitude, x- and y-position
- core+galaxy-fit: scaled PSF(AGN) + either disk (β=1) or bulge (β=0.25) galaxy model
  3 free parameters: magnitude of core, magnitude of galaxy, effective radius of galaxy, coordinates fixed, β fixed
- FDF0809: additional fit with 5 free parameters, additionally ellipticity and position angle of galaxy

Results

- for 4 out of 8 quasars, the host galaxy could be resolved

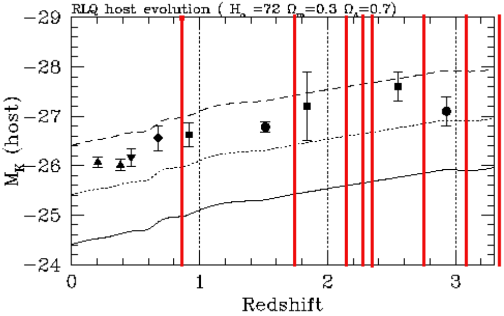

- redshifts of resolved host galaxies lie between z=0.8650 and z=2.7515

Results

- for 4 out of 8 quasars, the host galaxy could be resolved

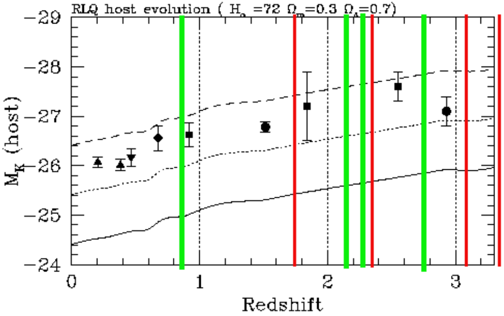

- redshifts of resolved host galaxies lie between z=0.8650 and z=2.7515

Resolved Objects: FDF0809

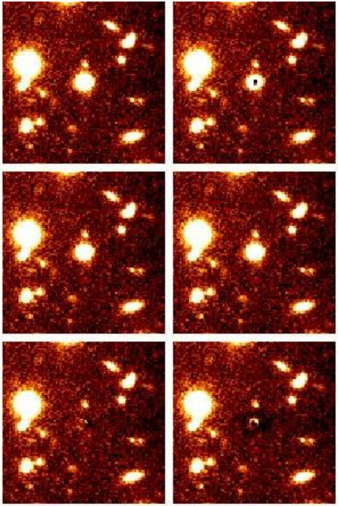

- z=0.8650
- type: QSO
- resolved in all filters
- clearly better fits for disk-model
  $\Longrightarrow$ simulation of spectra
- k-corrected absolute magnitudes (galaxy) in I:
  M(disk) = -22.22, M(bulge) = -23.12

Simulation of Spectra - Result for FDF0809 (I)

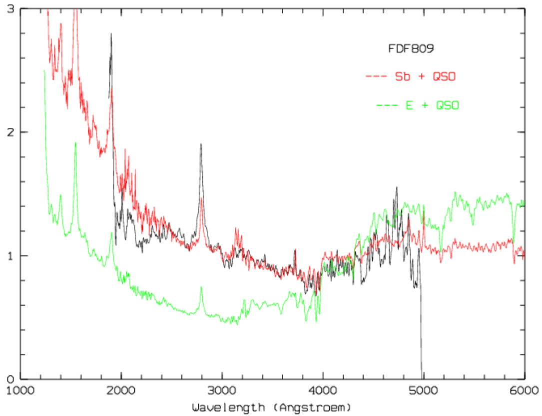

$\Longrightarrow$ disk galaxy is clearly preferred

Simulation of Spectra - Result for FDF0809 (B)

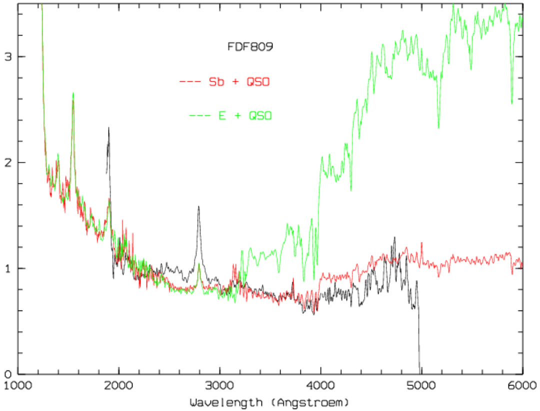

$\Longrightarrow$ disk galaxy is clearly preferred

Resolved Objects: FDF1837

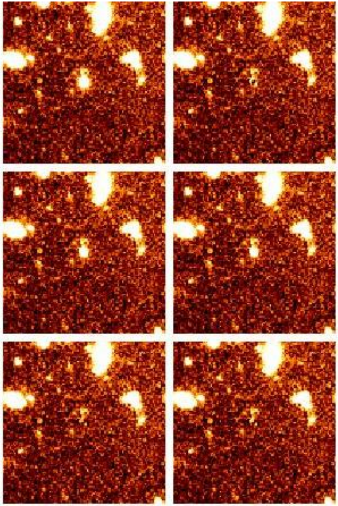

- z=2.2540
- type: QSO
- resolved in filters UBgRI
- slightly better fits for disk-model
- k-corrected absolute magnitudes (galaxy) in I:
  M(disk) = -23.89, M(bulge) = -26.29

Resolved Objects: FDF2229

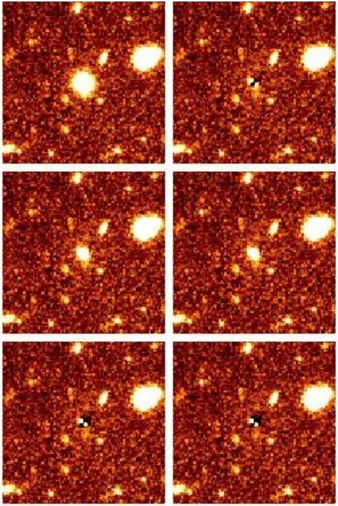

- z=2.1560
- type: QSO
- resolved in filters UBgRI
- slightly better fits for disk-model
- k-corrected absolute magnitudes (galaxy) in I:
  M(disk) = -24.66, M(bulge) = -26.76

Resolved Objects: FDF6007

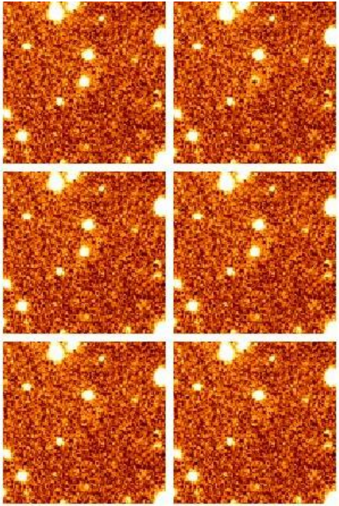

- z=2.7515
- type: TypeII Quasar
- resolved in filters BgRI and F814W(HST)
- no model preferred in fits
- k-corrected absolute magnitudes (galaxy) in I:
  M(disk) = -22.90, M(bulge) = -26.80

Unresolved Objects: FDF2633

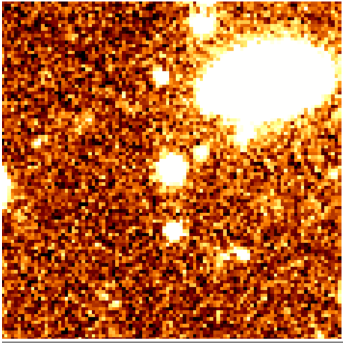

- z=3.0780
- type: QSO
- not resolved
- problems due to close-by elliptical galaxy
- close-by galaxy was fitted to improve the fits

Unresolved Objects: FDF2633

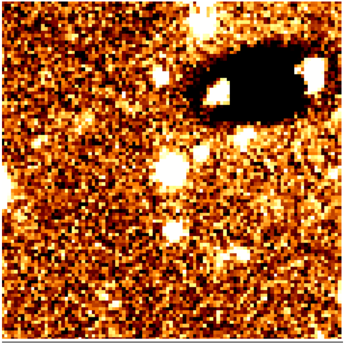

- z=3.0780
- type: QSO
- not resolved
- problems due to close-by elliptical galaxy
- close-by galaxy was fitted to improve the fits

Unresolved Objects: FDF2633

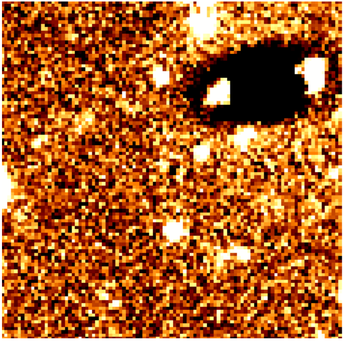

- z=3.0780
- type: QSO
- not resolved
- problems due to close-by elliptical galaxy
- close-by galaxy was fitted to improve the fits

Unresolved Objects: FDF4683

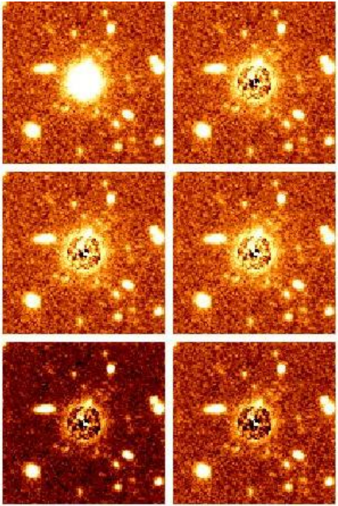

- z=3.3650
- type: QSO
- not resolved
- problems due to brightness of quasar
- PSF does not work as it is built out of distinctly fainter PSF-stars

Comparison of k-corrected Absolute Magnitudes

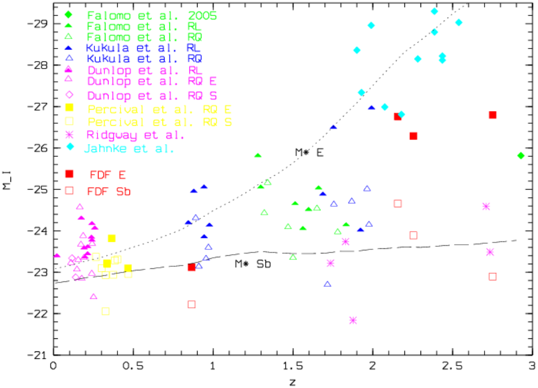

k-corrections (redshift) by Bicker et al. 2004, k-corrections (different filters) by Poggianti 1997

Comparison of k- and e-corrected Absolute Magnitudes

e-corrections by Bicker et al. 2004, passive evolution
cosmology is: $H_0 = 70 km/s/Mpc, \Omega_0 = 0.1$

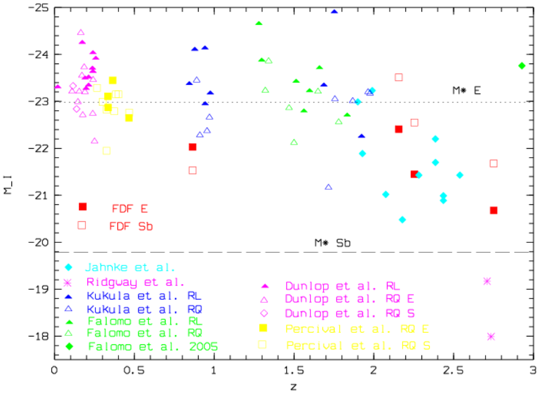

Evolution of Elliptical Quasar Host Galaxies (e-corrected)

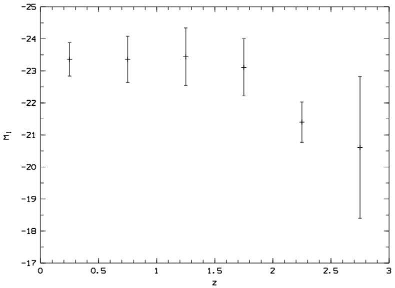

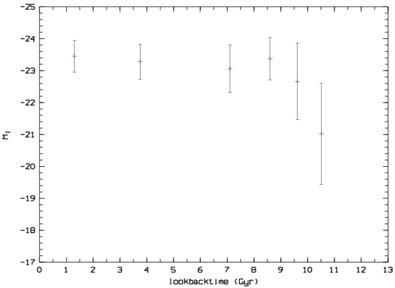

cosmology is: $H_0 = 70 km/s/Mpc, \Omega_0 = 0.1$

$\Longrightarrow$ absolute magnitude of elliptical quasar host galaxies decreases beyond z≈2

Evolution of Elliptical Host Galaxies of RLQ and RQQ (e-corrected)

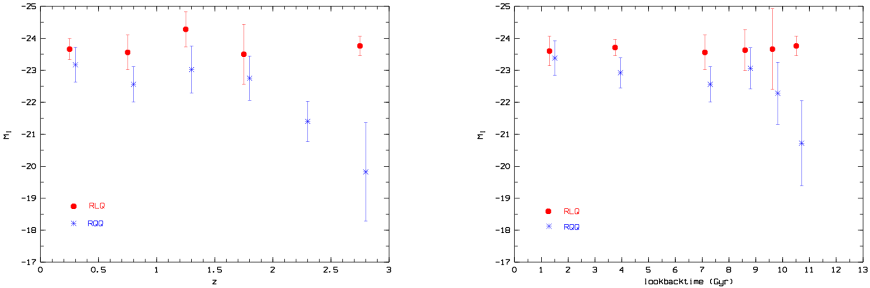

cosmology is: $H_0 = 70km/s/Mpc, \Omega_0 = 0.1$

$\Longrightarrow$ host galaxies of RLQ and RQQ evolve differently

Mass of Central Black Hole - Method

M_{BH} in nearby elliptical galaxies correlates with properties of galaxies

- we used these correlations to measure M_{BH} for the resolved host galaxies
- correlations are from the paper Novak et al. 2006, used correlations are based on data from Bettoni et al. 2003, Marconi & Hunt 2003, Gebhardt et al. 2003 and McLure & Dunlop 2002
- correlations use M_B, M_R and M_J of galaxy
- e-corrected absolute magnitudes are used, as the correlations are based on z≈0 data $\Longrightarrow$ values are only upper limits!!!

Mass of Black Hole - Plot

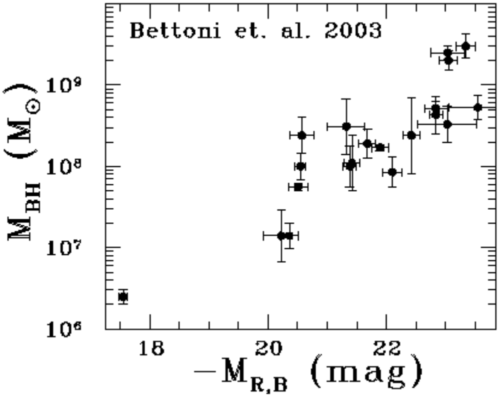

Novak et al. 2006

Mass of Central Black Hole - Results

object $\rightarrow$ $\downarrow$ paper (filter) $\downarrow$	FDF0809	FDF1837	FDF2229	FDF6007
Gebhardt(B)	(8.48)	6.76	9.45	7.27
Marconi&Hunt(J)	(7.39)	–	–	–
Bettoni et al.(R)	(8.39)	7.35	7.53	7.45
McLure&Dunlop(R)	(8.29)	7.35	7.51	7.44
average	(8.1)	7.2	8.2	7.4

$log(M_{BH}/M_{\odot})$ for resolved objects using different correlations

Conclusions and Outlook

- elliptical quasar host galaxies were less luminous at redshifts higher than z≈2
- host galaxies of RLQ and RQQ evolve differently
  - host galaxies of RLQ are more luminous, their absolute e-corrected magnitude stays constant up to z≈3
  - host galaxies of RQQ are less luminous, their absolute e-corrected magnitude decreases distinctly beyond z≈2
- open questions:
  - why do host galaxies of RQQ and RLQ evolve differently??
  - what happens beyond z≈3 ??

⟹ future observations at even higher redshifts need excellent resolution and very deep images

Colors of the Resolved Host Galaxies - Methods

investigation of galaxy type using colors

- colors, calculated using apparent magnitudes of L_* galaxies are plotted over redshift
- colors of resolved galaxies are plotted into the same diagram
- possible influences due to forbidden or semi-forbidden lines: these lines may come from expanded regions but belong to the core
  $\Longrightarrow$ magnitude of galaxy is overestimated

Colors of the Resolved Host Galaxies - Plots

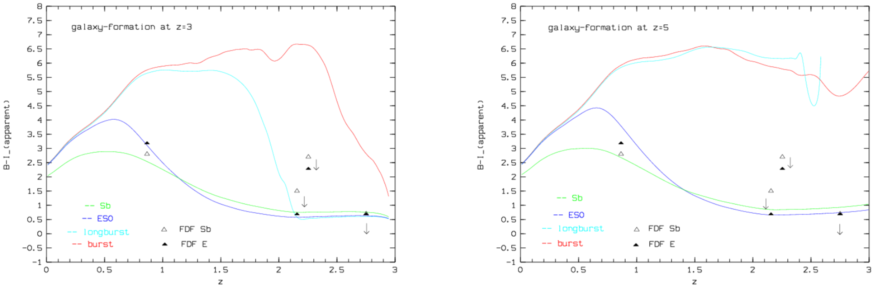

color: B-I

red is up, blue is down

arrows mark possible influences due to lines

Colors of the Resolved Host Galaxies - Plots

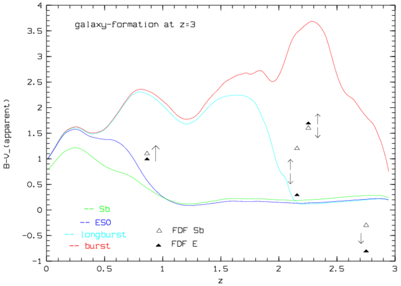

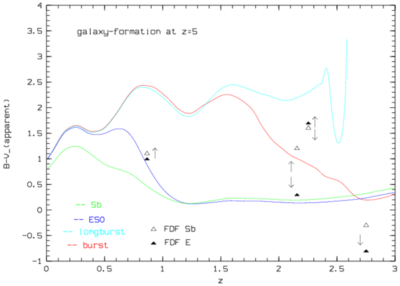

color: B-V

red is up, blue is down

arrows mark possible influences due to lines

Colors of the Resolved Host Galaxies - Plots

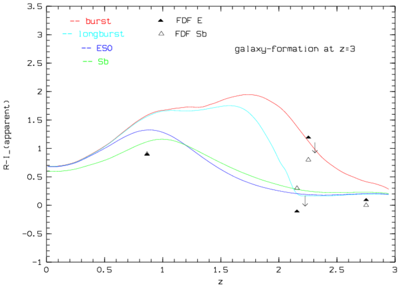

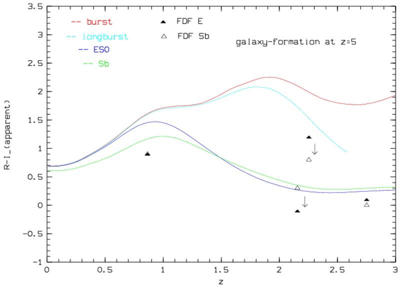

color: R-I

red is up, blue is down

arrows mark possible influences due to lines

Colors of the Resolved Host Galaxies - Plots

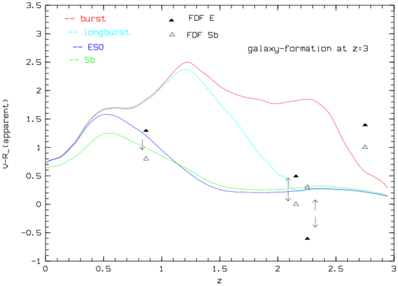

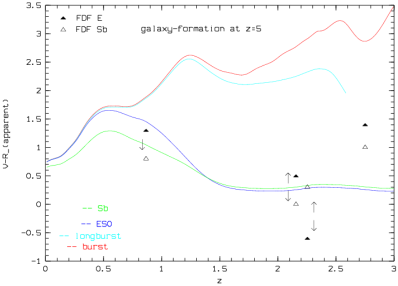

color: V-R

red is up, blue is down

arrows mark possible influences due to lines

Colors of the Resolved Host Galaxies - Plots

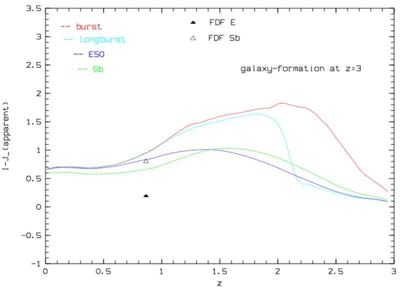

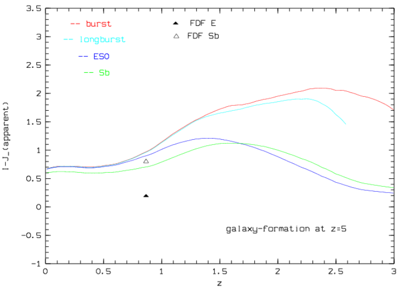

color: I-J

red is up, blue is down

arrows mark possible influences due to lines

Colors of the Resolved Host Galaxies - Results

- FDF0809: compatible with galaxy types E/S0 or Sb, no distinction between galaxy formation at z=3 or z=5
- FDF1837, FDF2229, FDF6007: compatible with types longburst, E/S0 and Sb at z=3 or E/S0 and Sb at z=5

Calculation of Star Formation Rate

SFR is calculated using rest-frame UV-fluxes

- method used is from the paper by Kennicutt 1998
- wavelength-range: rest-frame 1250-2500 Å
  $\Longrightarrow$ this range is dominated by young stars
  $\Longrightarrow$ can be used to calculate SFR
- $SFR(M_\odot/yr) = 1.8 \times 10^{-27}\{\frac{d_l^2 \times 10^{-0.4(m_{AB}+48.6)}}{1+z}\}$
- flux of forbidden or semi-forbidden lines was subtracted (may come from extended region but belong to central point source)
- problem: formula does not work properly if SFR changes on time-scales smaller than 10^8yr
  $\Longrightarrow$ this is likely in very young galaxies!!!
  $\Longrightarrow$ method will be tested on model galaxies

Star Formation Rate - Results

object(filter used)->	0809(B)	1837(R)	2229(R)	6007(I)
object(e)	1.8	0.03-4.7	15.8-33.0	6.9
object(d)	1.8	0.07-8.2	14.9-30.1	4.4
burst(z=3)	0.4	0.07	0.06	15.2
burst(z=5)	0.4	0.04	0.04	0.07
longburst(z=3)	0.5	391.2	300.9	288.8
longburst(z=5)	0.3	0.05	0.05	-
E/S0(z=3)	6.5	170.8	157.9	240.3
E/S0(z=5)	2.6	68.0	57.3	87.2
Sb(z=3)	5.4	8.2	8.3	6.6
Sb(z=5)	4.9	6.8	6.9	6.0

Simulation of Spectra - Method

simulating the FORS spectroscopy using fitted models

- flux ratio (central point source to galaxy) is calculated in a 1" slit (corresponding to FORS spectroscopy)
- template spectra for QSO, SeyfertII, E/S0 and Sb are calibrated in the used filter transformed to the rest frame of the object
- template spectra for QSO/SeyfertII and galaxy are weighted using the flux ratio and added up

$\Longrightarrow$ simulated spectrum is compared to measured spectrum

Simulation of Spectra - Result for FDF0809 (I)

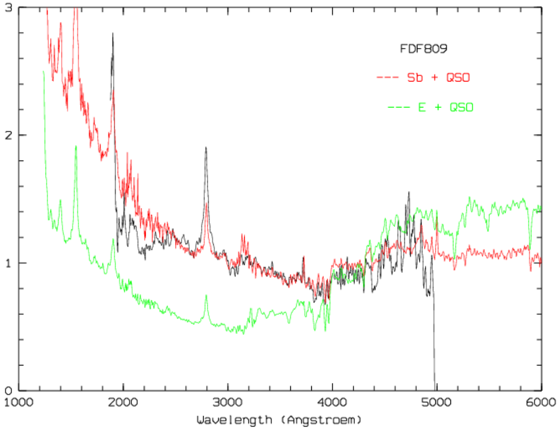

Simulation of Spectra - Result for FDF0809 (B)

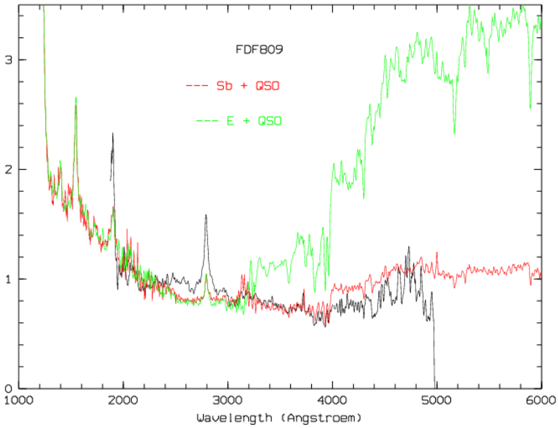

Simulation of Spectra - Result for FDF1837 (I)

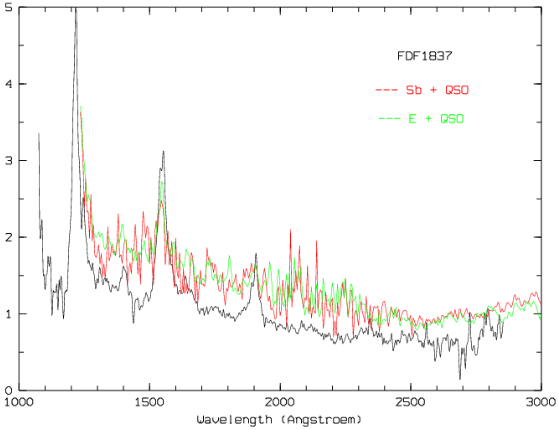

Simulation of Spectra - Result for FDF2229 (I)

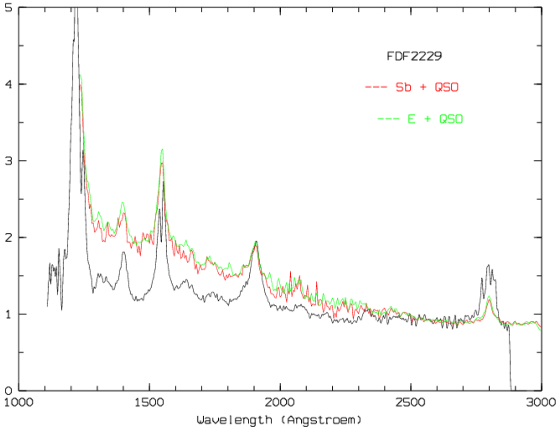

Simulation of Spectra - Result for FDF6007 (I)

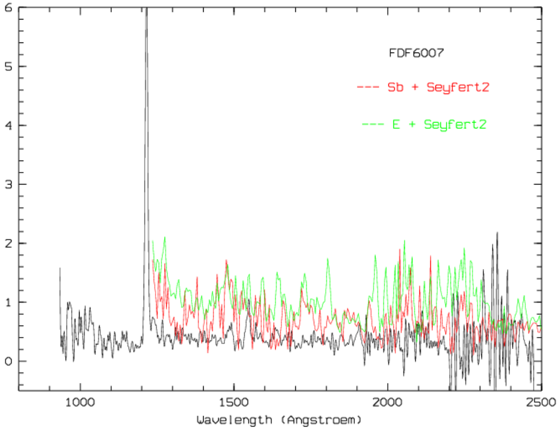

Conclusions - FDF0809

- disk-model was clearly preferred in fits
- simulation of spectrum yielded excellent results for Sb, but strong deviations for E/S0
- colors of host galaxy are consistent with Sb or E/S0
- SFR: 1.8 $M_{\odot}/yr$
- $M_{BH} \leq\sim 10^8 M_{\odot}$
  $\Longrightarrow$ host galaxy is clearly identified as disk galaxy

Conclusions - FDF1837

- disk-model was slightly preferred in fits
- simulation of spectrum could neither exclude E/S0 nor Sb
- colors of host galaxy rule out bursts and longburst at high redshifts (z=5)
- SFR: 0.03-8.2 $M_{\odot}/yr$, value is only reasonable if SFR does not change on small time scales (e.g. Sb)
- $M_{BH} \leq 10^7 \sim 10^8 M_{\odot}$

Conclusions - FDF2229

- disk-model was slightly preferred in fits
- simulation of spectrum could neither exclude E/S0 nor Sb
- colors of host galaxy rule out bursts and longburst at high redshifts (z=5)
- SFR: 15-33 $M_{\odot}/yr$, value is only reasonable if SFR does not change on small time scales
- $M_{BH} \leq\sim 10^8 M_{\odot}$

Conclusions - FDF6007

- no model preferred in fits
- simulation of spectrum could neither exclude E/S0 nor Sb
- colors of host galaxy show strong deviations from all models in 2/4 colors, other two only rule out bursts and longburst at high redshifts (z=5)
- SFR: 4.4-6.9 $M_{\odot}/yr$, value is only reasonable if SFR does not change on small time scales
- $M_{BH} \leq 10^7 \sim 10^8 M_{\odot}$

VHE observations with the MAGIC telescope

- Imaging Air Cherenkov Technique – How does it work?
- MAGIC telescope
  - short introduction
  - How is the data analysed?

IACT: Imaging Air Cherenkov Technique

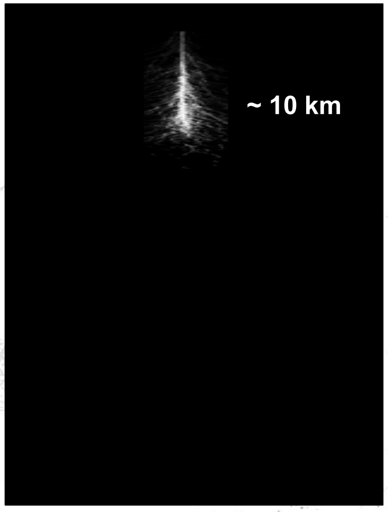

particle shower

Cherenkov
e

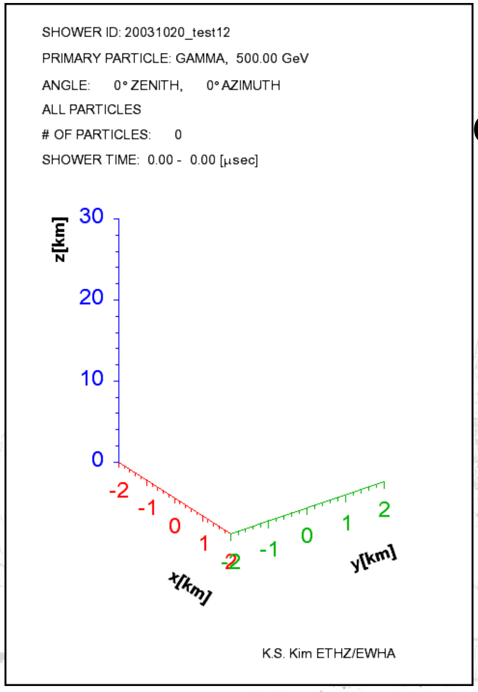

particle shower

IACT: Imaging Air Cherenkov Technique

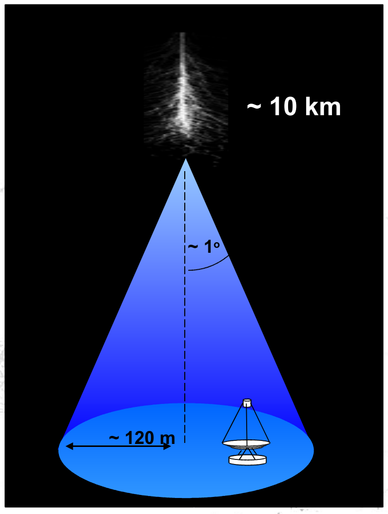

emission of cherenkov light

IACT: Imaging Air Cherenkov Technique

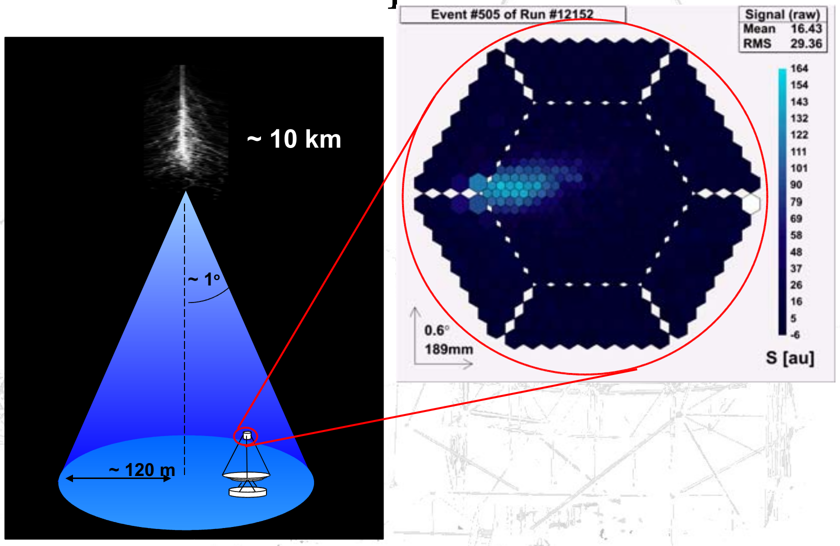

MAGIC Telescope: Major Atmospheric Gamma-ray Imaging Cherenkov Telescope

MAGIC Telescope:

MAGIC Telescope

- Observatorio Roque de los Muchachos, La Palma, 2200 m a.s.l.
- isochronous mirror, diameter: 17 m
- weight: ~70 t
- tracking accuracy < 0.1°
- fast repositioning (GRBs) 180°/30sec

MAGIC Telescope

- PMT camera (577 pixels)
  small pixels: 0.1°
  large pixels: 0.2°
- optical cables
- digitization with 300MHz FADCs into ring buffer
- trigger (signal above threshold, time coincidence, pattern recognition)
- => data acquisition:
  rate: 200-300Hz
  read out time: 50ns
  pulse integration: 5-10ns

MAGIC Telescope

- background:
  hadron, myons, ...
- gammas/background <1/1000
- energy range: > 100 GeV
- sensitivity: 1 Crab/5 min
- zd-range:
  low energies: < 35°
  higher energies: < 60°
- observations during moon
- observation modes:
  on/off-mode, wobble-mode

MAGIC Telescope

- 577 pixel · 30 byte/pixel
  => ~17.3kB / event
- 200 events/s · 17.3kB/event
  => ~3.5MB/s
- 1.5TB/month => increasing with new read out and second telescope => ~20TB/month)

- changing conditions (environment, hardware)

=> flexible, robust, automatic analysis

MAGIC Telescope

- results 1-2 days after data taking
- consistent analysis for all data
- results and status available in a database
- long term study of quality parameters
- test bench for development of new methods

=> first step towards a cherenkov observatory

MAGIC Telescope

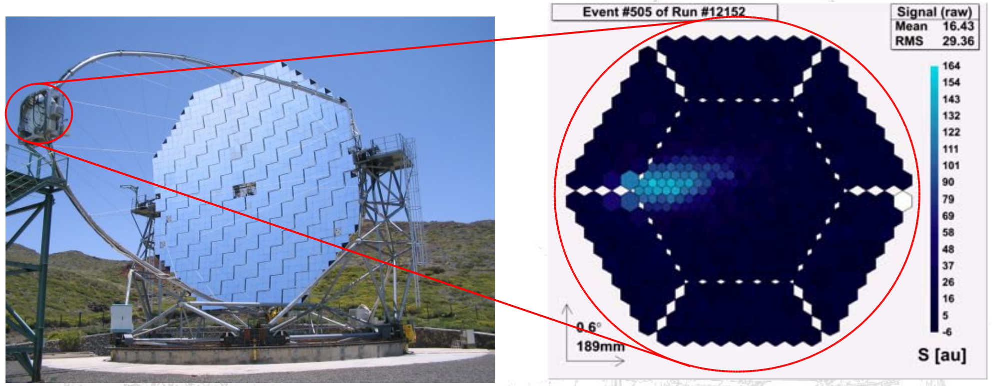

Analysis

- calibration
- calculation of image parameter
- quality cuts
- background suppression
- reconstruction of shower origin
- energy reconstruction, spectrum

Analysis

- calibration
  - relative calibration with light pulses
  - absolute calibration with myons

Analysis

- calibration
  - relative calibration with light pulses

Analysis

- calibration
  - relative calibration with light pulses
  - absolute calibration with myons

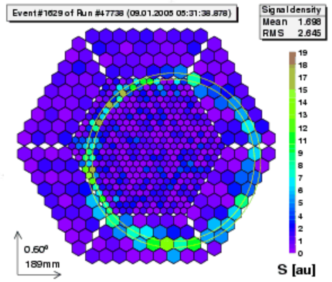

Analysis

- calibration
- calculation of image parameters
  - image cleaning
  - calculation of parameters describing the shower image
  - calculation of myon parameters

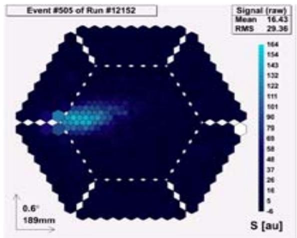

image cleaning

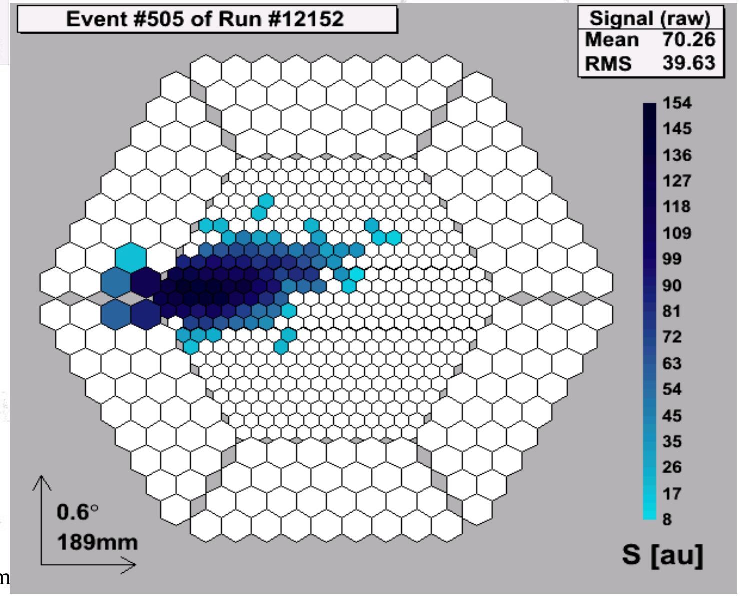

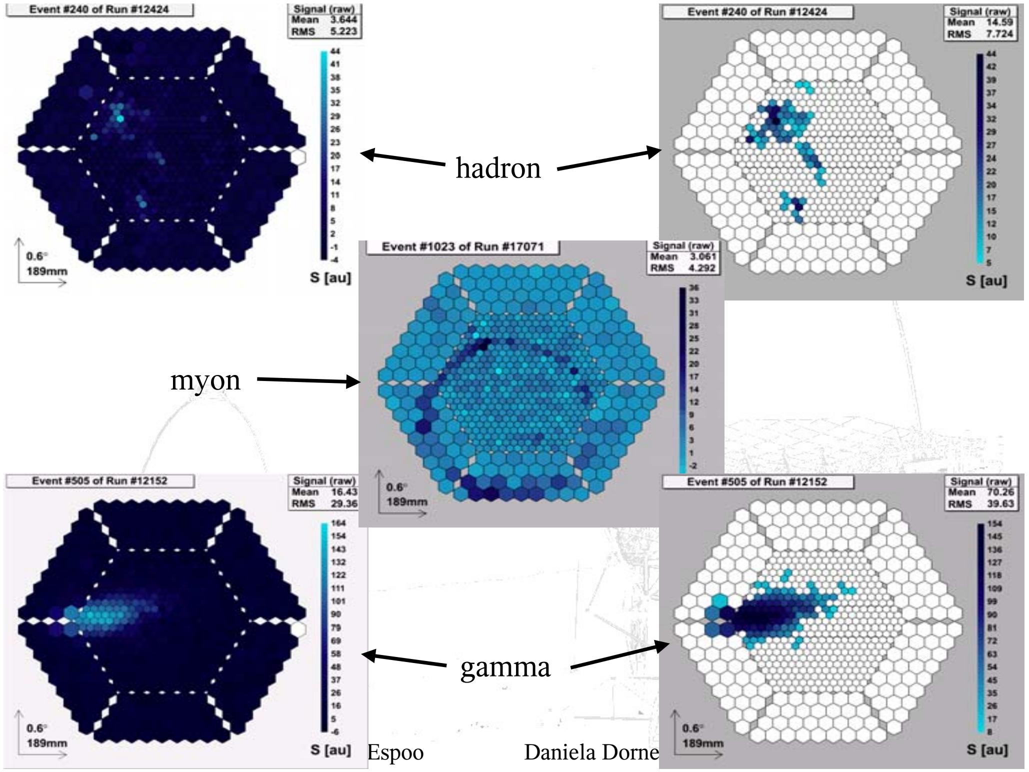

image parameters

- size:
total number of photons of the shower

- standard deviations of the light distribution: width, length

- direction of the shower

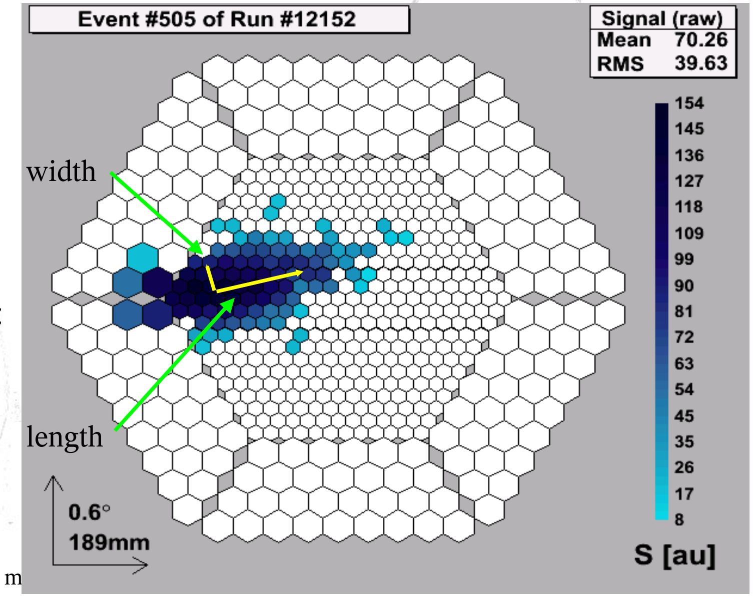

Analysis

- calibration
- calculation of image parameter
- quality cuts – exclude data with bad quality
  quality parameters for all data are available from the automatic analysis
  - weather
  - telescope performance (e.g. point spread function)

Analysis

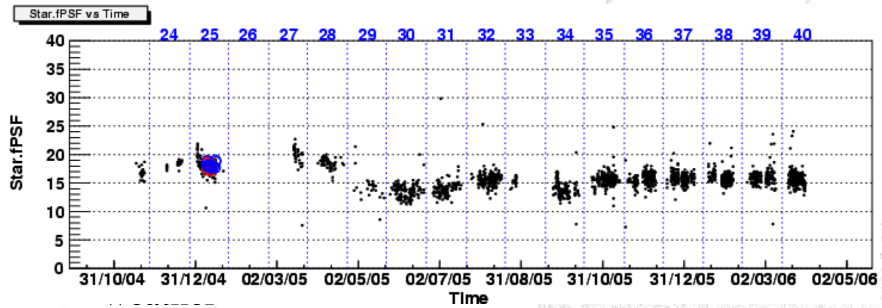

- telescope performance (e.g. point spread function)

Analysis

- calibration
- calculation of image parameter
- quality cuts
- background suppression

gamma or hadron?
different image parameters

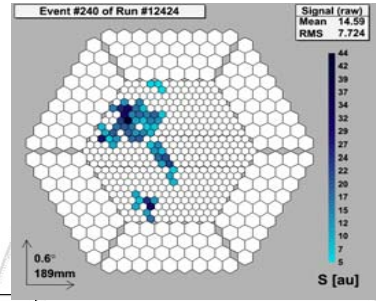

methods for background suppression:
- static cuts
- dynamic cuts
- random forrest
- neural net

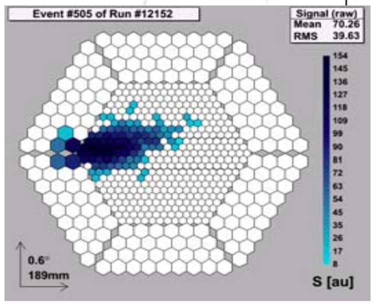

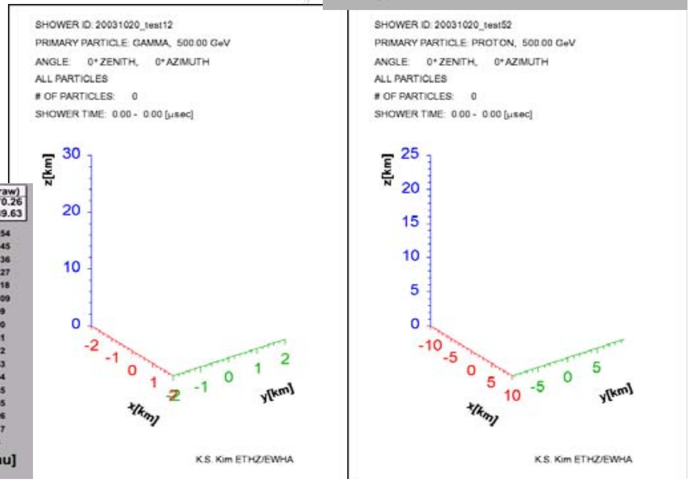

Analysis

- calibration
- calculation of image parameter
- quality cuts
- background suppression
- reconstruction of shower origin

Analysis

- calibration
- calculation of image parameter
- quality cuts
- background suppression
- reconstruction of shower origin

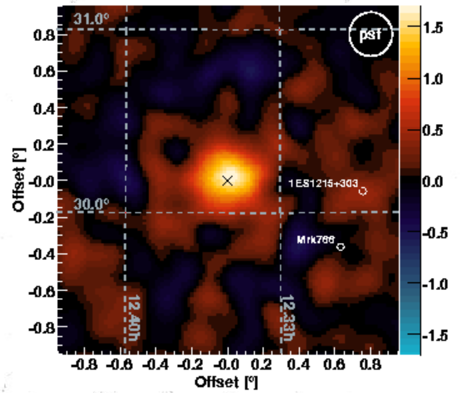

Analysis

- calibration
- calculation of image parameter
- quality cuts
- background suppression
- reconstruction of shower origin
- energy reconstruction, spectrum
  - reconstruction of energy by comparison with simulated showers

Results – see next talks

- Elina Lindfors: Discovery of VHE gamma-rays from Mkn 180 triggered by an optical outburst
- Thomas Bretz: Overview of AGN observation with the MAGIC telescope


Discovery of VHE emission from Mrk 180
Triggered by an optical outburst
E.Lindfors & D. Mazin on behalf of the MAGIC collaboration
ENIGMA Meeting, 8th September 2006, Otaniemi

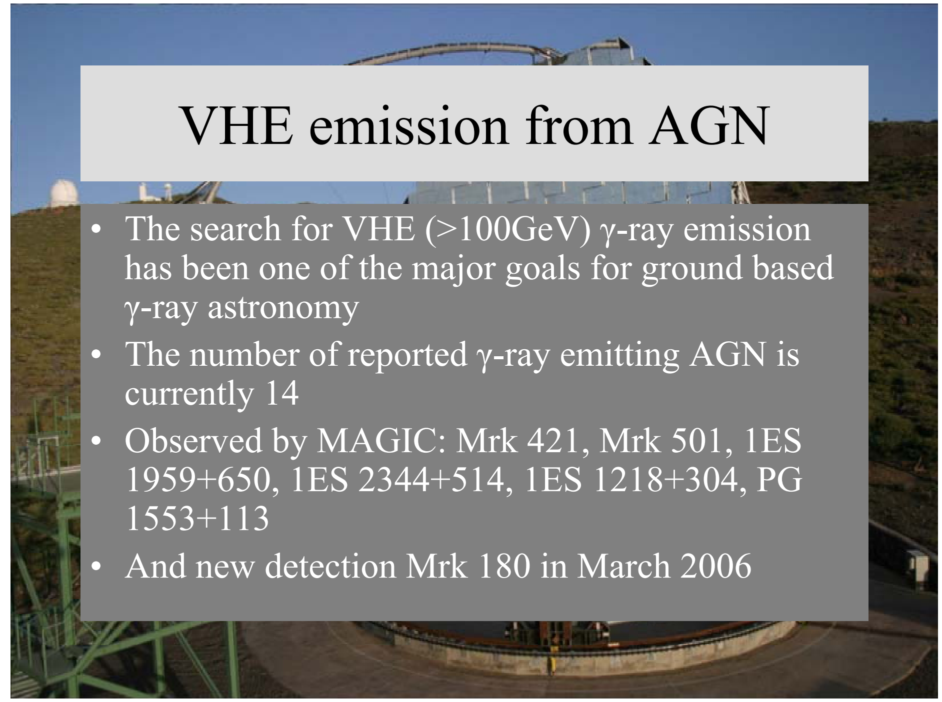
VHE emission from AGN
• The search for VHE (>100GeV) γ-ray emission has been one of the major goals for ground based γ-ray astronomy
• The number of reported γ-ray emitting AGN is currently 14
• Observed by MAGIC: Mrk 421, Mrk 501, 1ES 1959+650, 1ES 2344+514, 1ES 1218+304, PG 1553+113
• And new detection Mrk 180 in March 2006

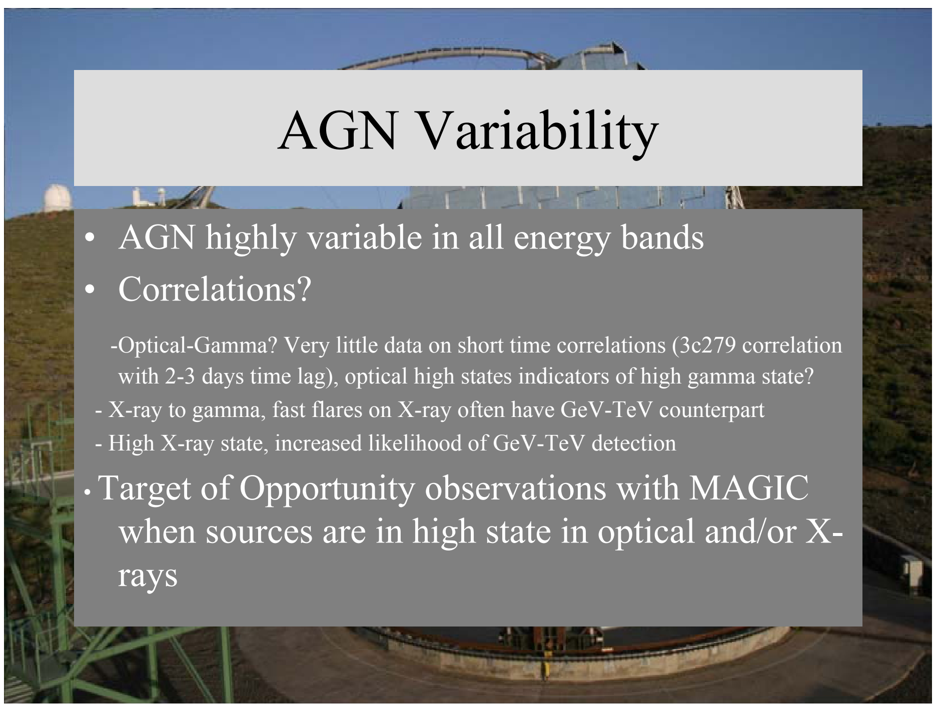
AGN Variability
• AGN highly variable in all energy bands
• Correlations?
-Optical-Gamma? Very little data on short time correlations (3c279 correlation with 2-3 days time lag), optical high states indicators of high gamma state?
- X-ray to gamma, fast flares on X-ray often have GeV-TeV counterpart
- High X-ray state, increased likelihood of GeV-TeV detection
• Target of Opportunity observations with MAGIC when sources are in high state in optical and/or X-rays

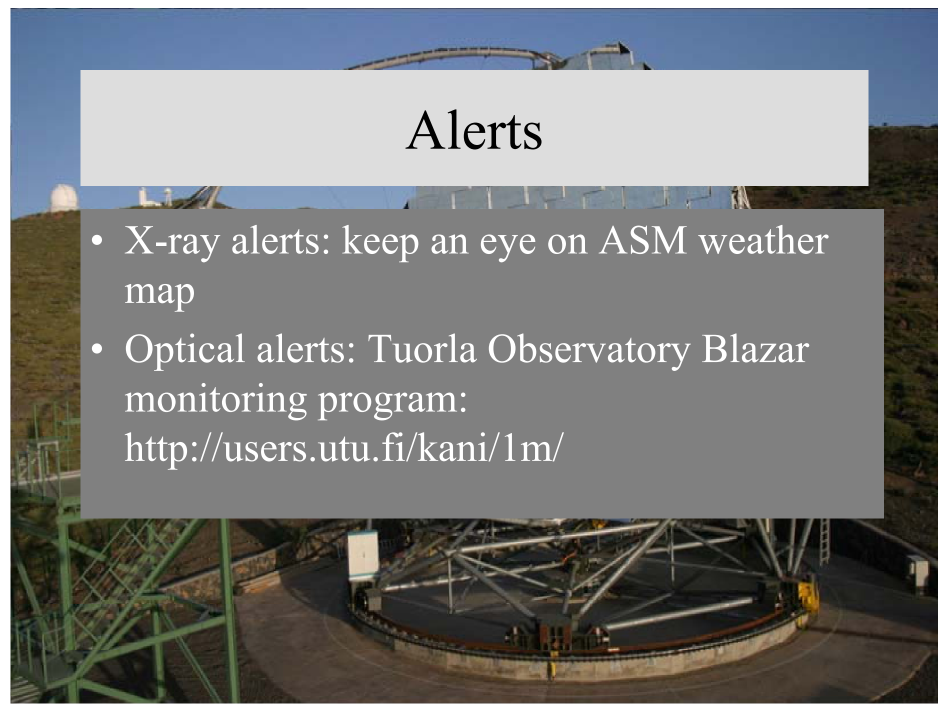
Alerts
• X-ray alerts: keep an eye on ASM weather map
• Optical alerts: Tuorla Observatory Blazar monitoring program: http://users.utu.fi/kani/1m/

Mrk 180

- Well-known HBL z=0.045
- Bright host galaxy (R=14.17±0.02) much fainter core (R=15.79 ±0.02) (Nilsson et al. 2003)
- Only upperlimits from EGRET, Whipple and HEGRA

Mrk 180 underwent an optical outburst in March 2006

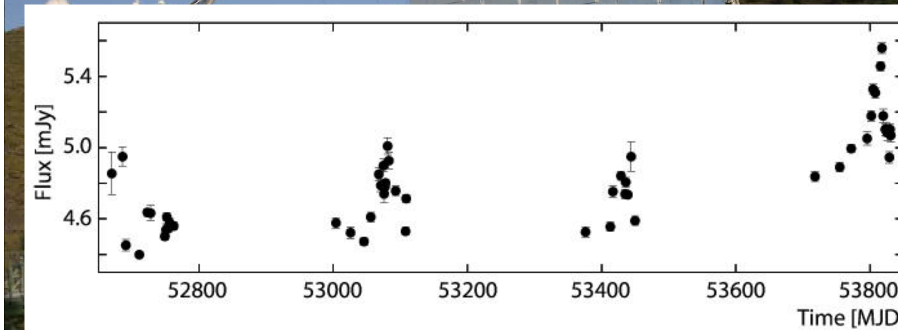

0.2mag

Quasi-simultaneous UMRAO data shows no evidence of flaring

Mrk 180 (March 2006)

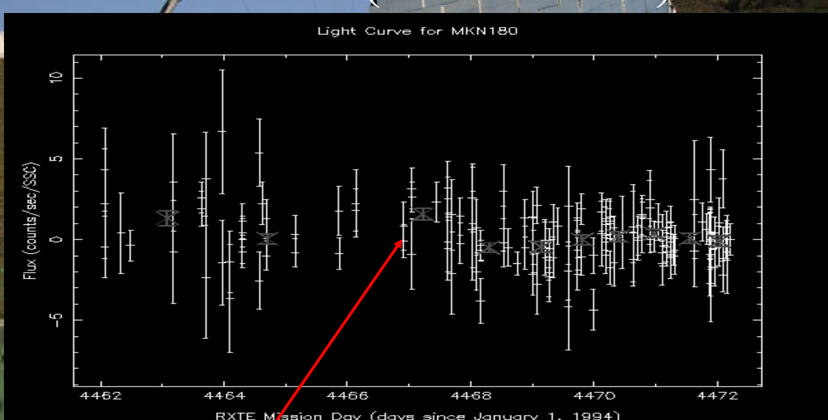

Alert was given

MAGIC Observations

- Started 23rd of March
- Observed from 23rd to 31st of March (scheduled telescope shutdown 1st of April)
- Total observation time 12.4 hours, observation conditions mostly good, but few nights there was some high clouds.
- Observations done in Wobble mode
- Runs with unusual trigger rates rejected => total observation time reduced to 11.1 hours
- ZA=39°-44°

Data Analysis

- Done by D.Mazin
- Using standard analysis and calibration programs for the MAGIC telescope.
- γ/hadron separation was done using random forest
- Number of excess events : difference between the source and background region in θ² distributions, three background regions

θ² distribution

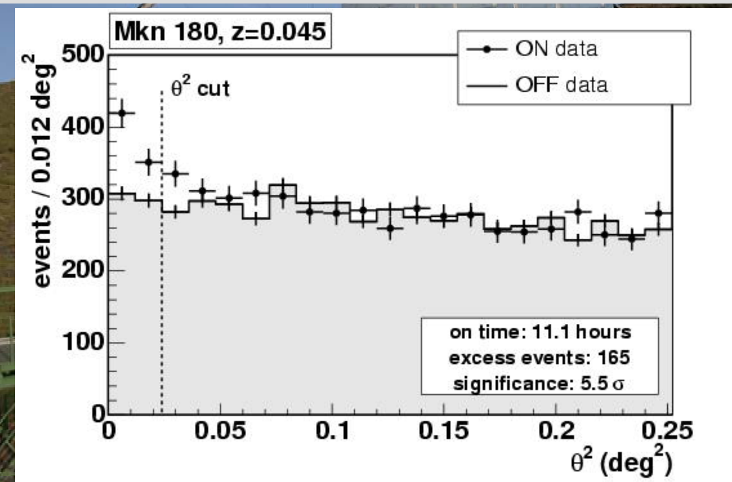

θ=angular distance between the source position in the sky and the resconstructed arrival position of the shower

No evidence of flux variability, the fit to the nightly integrated flux is consistent with a constant emission: χ^2/ndf = 7.1/6

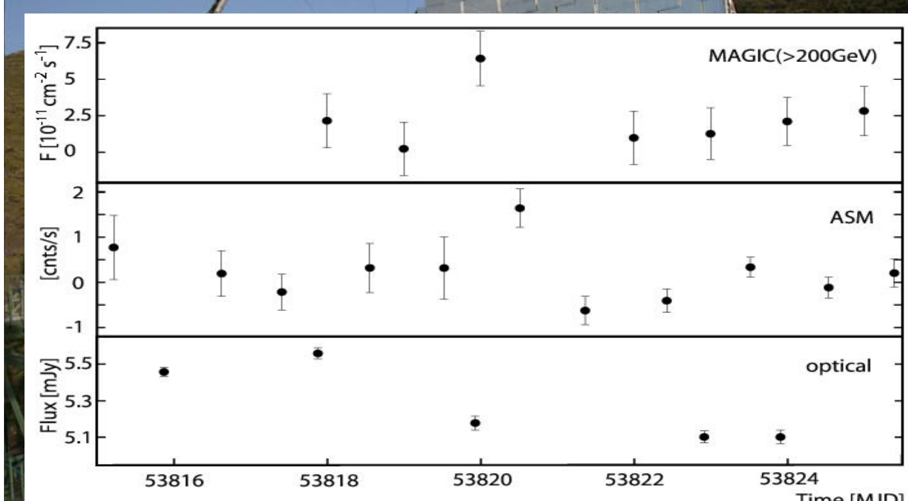

The measured and the de-absorbed energy spectrum of Mrk 180

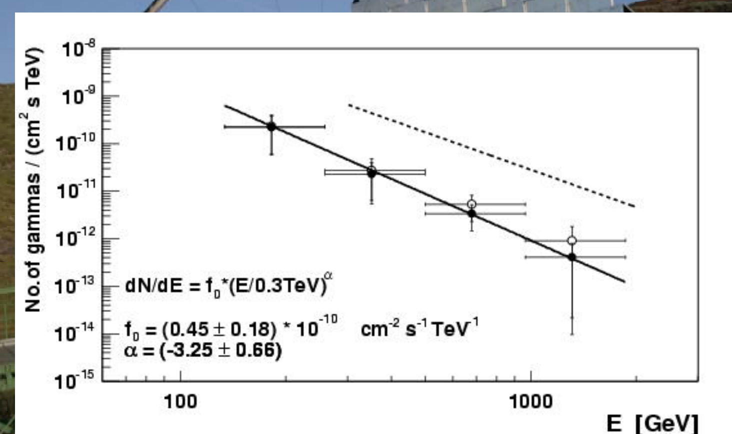

The observed integral flux above 200 GeV is 1.27 $*10^{-11}$ ergs /cm²/s (or 11% of Crab flux)

-Errors statistical only: The systematic error about 50% for the absolute flux level and 0.2 fo the spectral index

-Results of independent cross-check analysis were in good agreement with the numbers reported here.

-VHE gamma-rays partially absorbed by low energy photons of the evolving extragalactic background light, the effect is small for photons with energies below 1TeV

-Used the best-fit model of Kneiske et al. 2004

-The deabsorbed spectrum has slope –2.8±0.7

The spectral energy distribution of Mrk 180

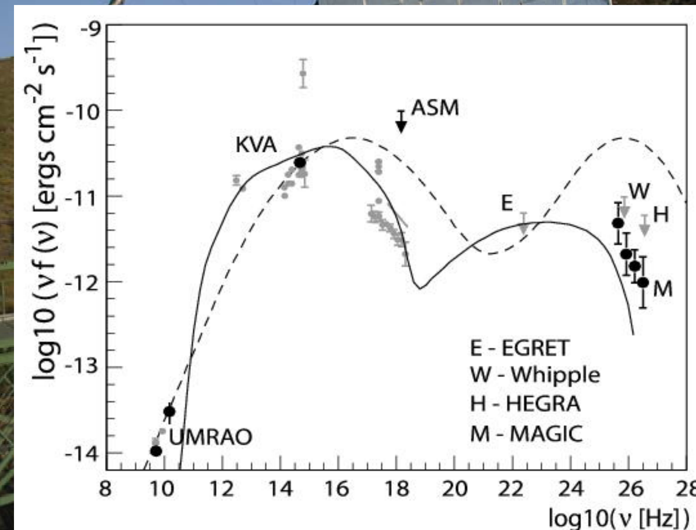

Does the detection present a flaring state?

- Flare in optical, hint of flare in X-rays
- Observed flux factor of 30 above the prediction of Costamante and Ghisellini model, their model calculation is based on quiescent synchrotron spectrum

But...

- The source has not been observed in low optical state with MAGIC and we are below the upper limits from other experiments, so we have nothing to compare to.
- Although MAGIC lightcurve can be considered suggestive it is statistically consistent with constant emission.

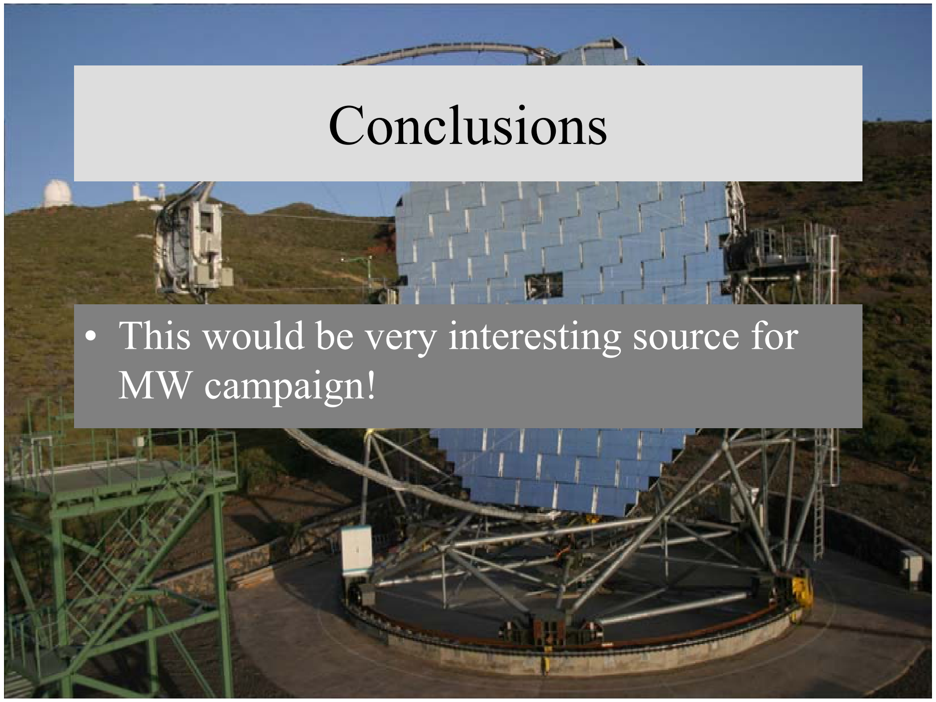
Conclusions
• This would be very interesting source for MW campaign!

Thomas Bretz

Observations of extragalactic sources above **100GeV** with the **MAGIC** telescope

Introduction

...the following talk is about AGN observed with the MAGIC telescope...

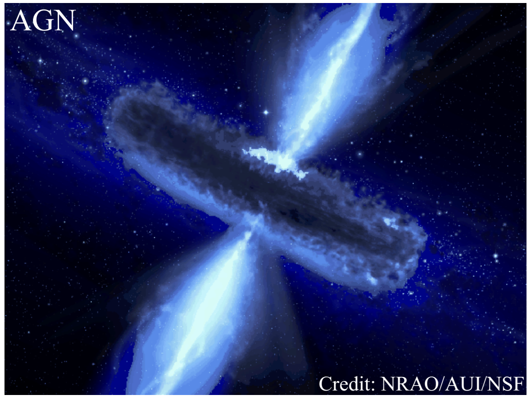

Artist view

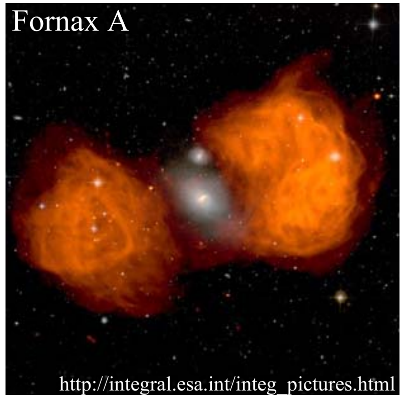

Multiwavelengthpicture in false colors

Introduction - What is an AGN?

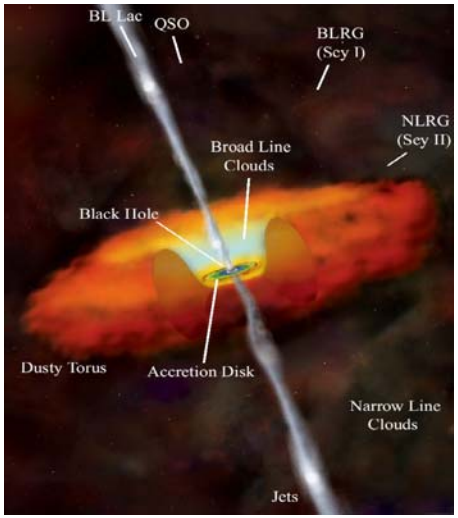

- ENIGMA...?

Contents

- Markarian 421 – spectrum
- Markarian 501 – lightcurve
- Markarian 180 -> Elina
- 1ES2344+514 – detection
- 1ES1959+650 – SED

- 1ES1218+304
  - detection
  - spectrum
  - intrinsic spectrum
  - spectral energy distribution

- PG1553+113
- GRB050713a; GRB050904

MAGIC

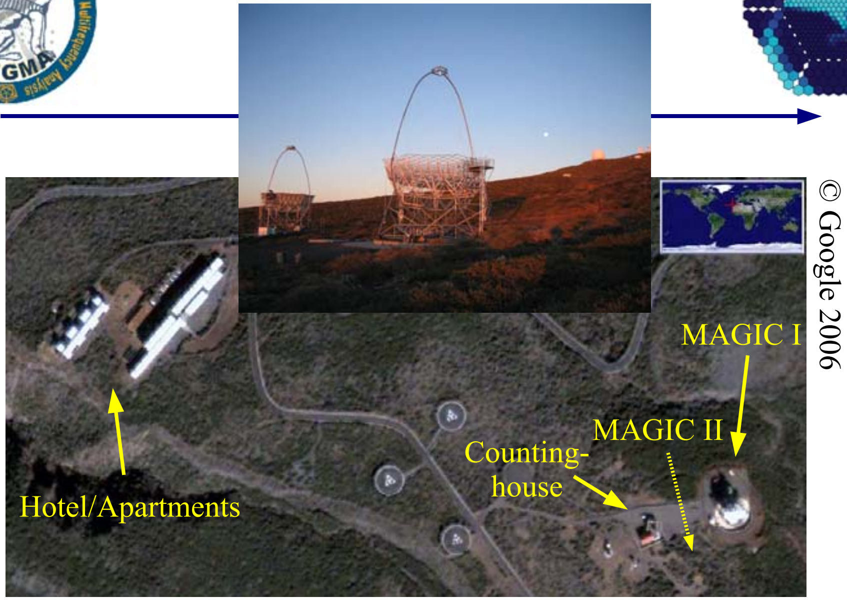

Observation Period: Since fall 2004; z.Zt. Cycle 1 (April 2005 – April 2006)

Markarian 421 (z=0.031)

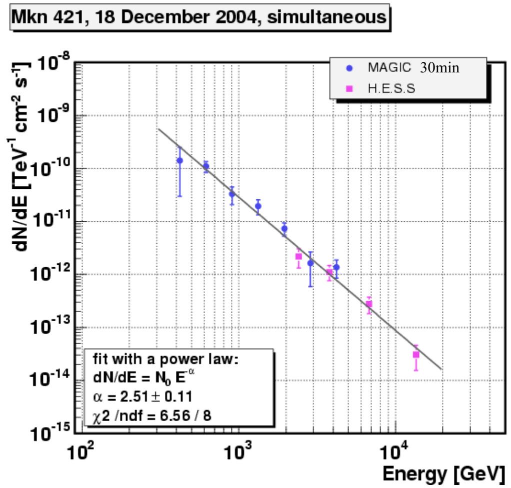

- Observation period: 2004-2006
  - Significance » 40 (*Li/Ma*)
- Simult. observations (H.E.S.S.)
  - 18. December 2004
  - 1.5h
  - Significance 10.1
    - Measurements fit well
    - Spectrum over 1.5 order of magnitude

Markarian 421 (z=0.031)

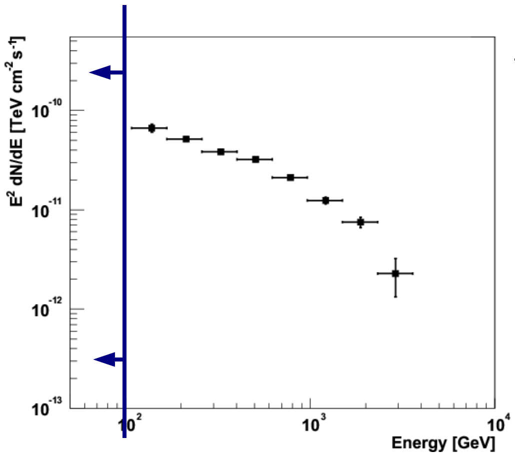

Results of the observations:

- Peak-energy ≤100GeV
- Indirect measurement of the absorption due to the evolving extragalactic background light
- Correlation of X-ray and gamma-flux

ApJ 2006, submitted (astro-ph/0603478)

Markarian 421 (z=0.031)

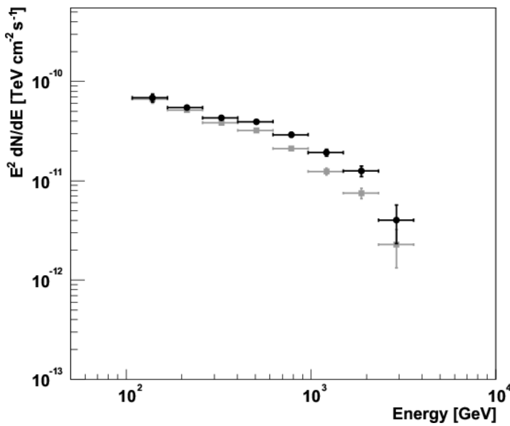

Results of the observations:

- Peak-energy ≤100GeV
- Indirect measurement of the absorption due to the evolving extragalactic background light
- Correlation of X-ray and gamma-flux

ApJ 2006, submitted (astro-ph/0603478)

Markarian 421 (z=0.031)

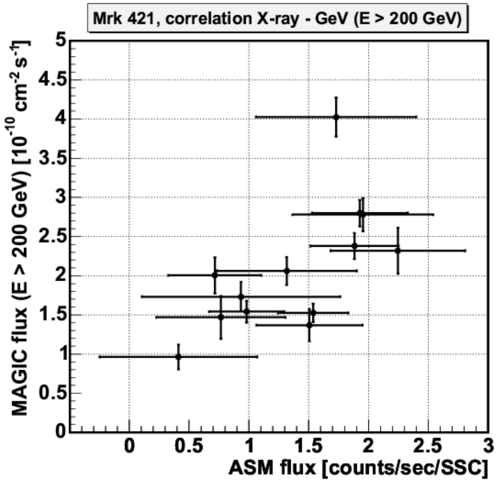

<u>Results of the observations:</u>

- Peak-energy ≤100GeV
- Indirect measurement of the absorption due to the evolving extragalactic background light
- Correlation of X-ray and gamma-flux

ApJ 2006, submitted (astro-ph/0603478)

Markarian 501 (z=0.033)

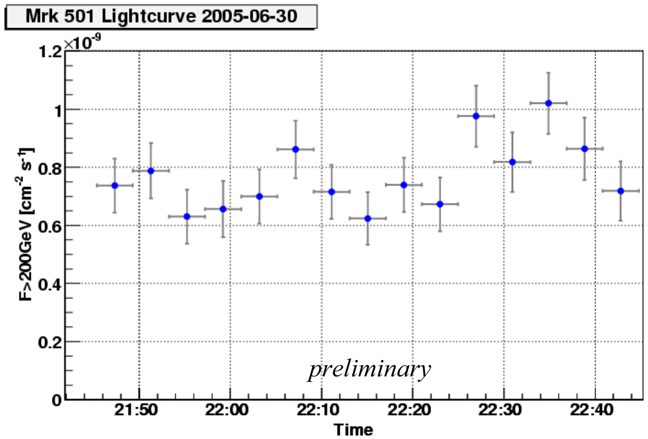

- Resolution of the time-variability <5min
- Probability for the flux being consistent with a constant flux only 5%
- Flux-variations 30%-50%

Markarian 501 (z=0.033)

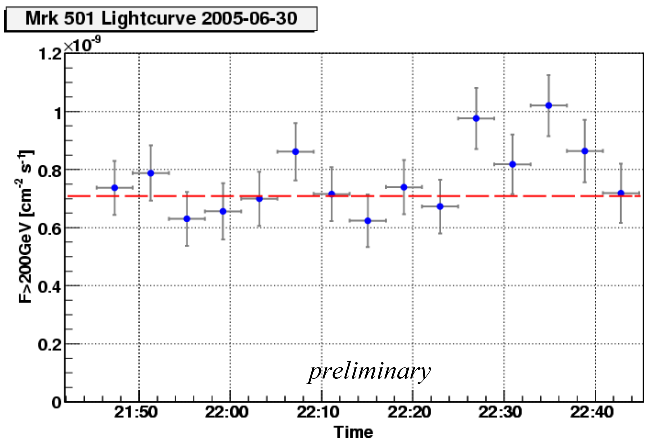

- Resolution of the time-variability <5min
- Probability for the flux being consistent with a constant flux only 5%
- Flux-variations 30%-50%

see also Bednarek, Protheroe 1999 MNRAS 310, p.577ff

1ES 2344+514 (z=0.044)

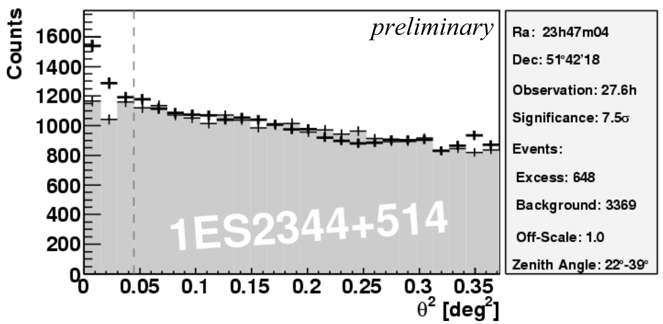

- Known to emit at VHE (Whipple)
- 3. Aug. – 31. Dec. 2005
- Low flux state
- Extension of the VHE-spectrum below 350GeV

in preparation

1ES 1959+650 (z=0.047)

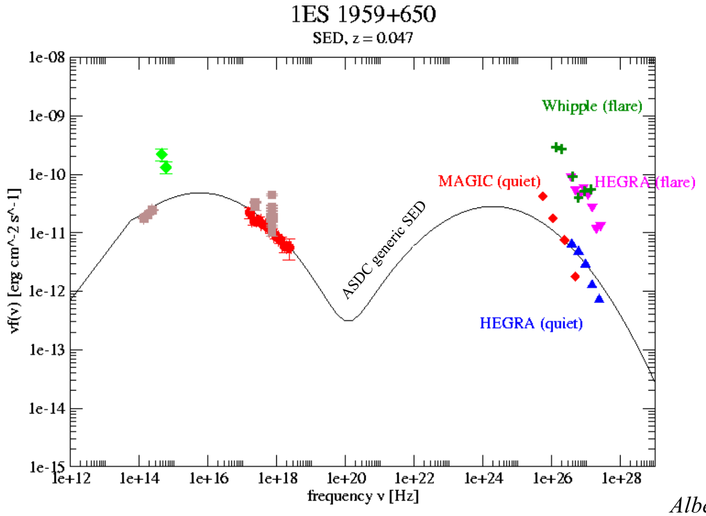

- Sept./Oct. 2004: 6.5h
- Significance 8.2

- Orphan flare (Whipple)
- Spectrum extended to lower enegies
- low flux state (quiescent state?)
- fits well with *HEGRA-quiet*
- X- and Gamma-ray luminosität similar

PhD thesis N.Tonello, 2/2006
Albert et al., ApJ 2006, 639, p.761ff

1ES 1218+304 (z=0.182)

- 9.-15. January 2005
- 6,4 sigma (Li/Ma) for the emission at the position of 1ES1218+304
- 560 excess events / 8,2h
- Signal consistent with PSF (~0.12°)

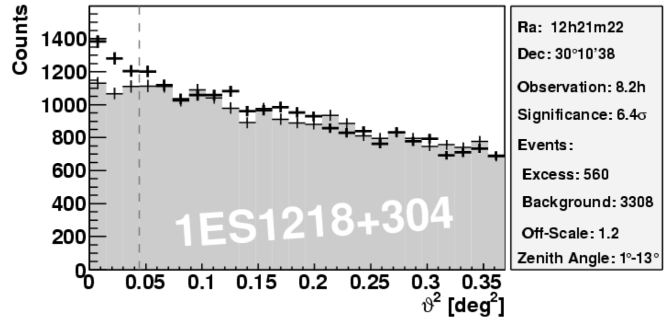

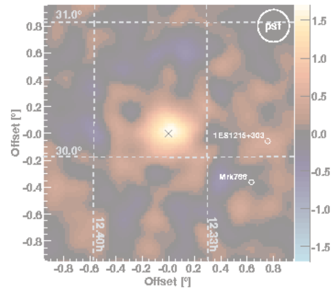

T.Bretz, PhD thesis
Albert et al., ApJ 642, 2006

Result of the data analysis

- 9.-15. January 2005
- 6,4 sigma (Li/Ma) for the emission at the position of 1ES1218+304
- 560 excess events / 8,2h
- Signal consistent with PSF (~0.12°)

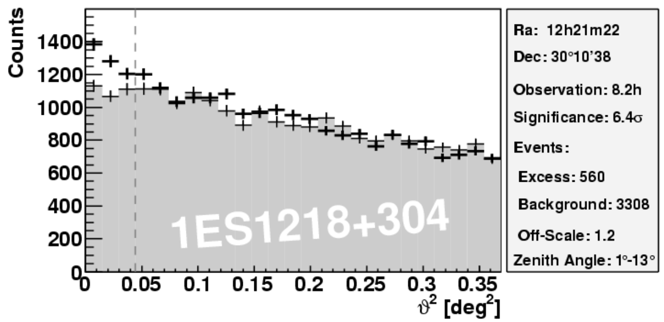

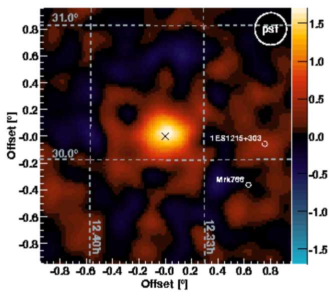

T.Bretz, PhD thesis
Albert et al., ApJ 642, 2006

Result of the data analysis

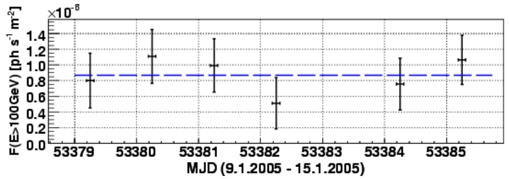

- Lightcurve consistent with constant flux

$$(8{,}7 \pm 1{,}4) \cdot 10^{-7} s^{-1} \cdot m^{-2}$$

T.Bretz, PhD thesis
Albert et al., ApJ 642, 2006

Result of the data analysis

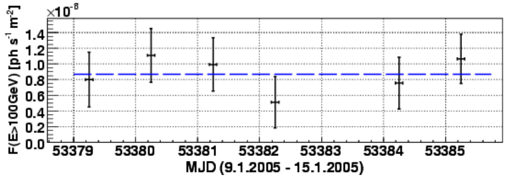

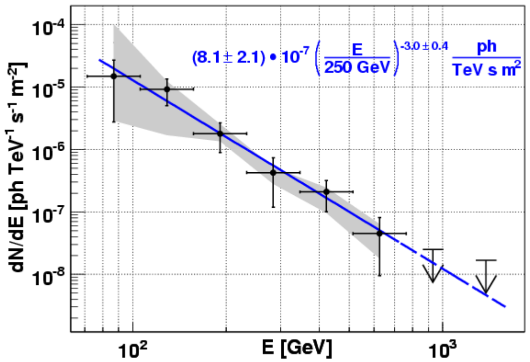

- Lightcurve consistent with constant flux
  $(8{,}7\pm1{,}4)\cdot10^{-7}s^{-1}\cdot m^{-2}$
- Statistical error
- Systematic error from analysis (gray area)
- Differential spectrum consistent with apower law:
  $(8{,}1\pm2{,}1)\cdot10^{-7}(E/250\,GeV)^{3{,}0\pm0{,}4}s^{-1}m^{-2}TeV^{-1}$

  - first new AGN emitting at 100GeV-300GeV (peak energy ~120GeV)

T.Bretz, PhD thesis
Albert et al., ApJ 642, 2006

Correction for absorption due to the metagalactic radiation field

- Pair production of gammas with diffuse metagalactic photons
  - eg. star light, reemission from dust, etc.

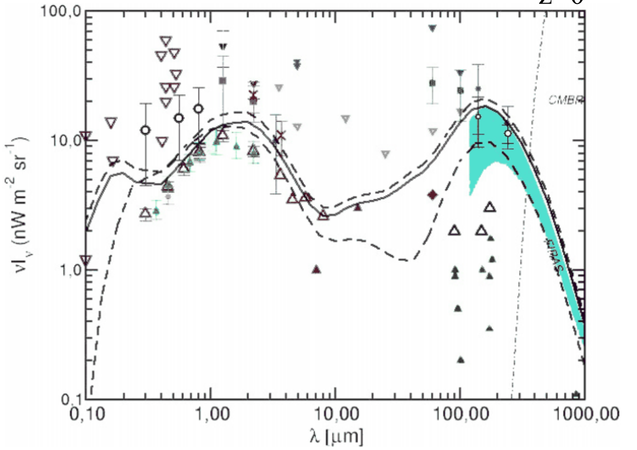

(Kneiske et al., A&A 386, 2002)

Correction for absorption due to the metagalactic radiation field

- Pair production of gammas with diffuse metagalactic photons
  - eg. star light, reemission from dust, etc.

Pair production condition:

$$E_{LE}\cdot E_{HE}>2\cdot(m_e c^2)^2$$

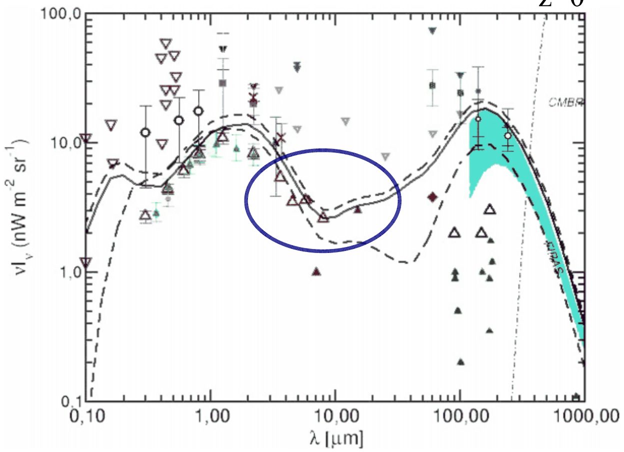

(Kneiske et al., A&A 386, 2002)

Correction for absorption due to the metagalactic radiation field

- *Fazio-Stecker-Relation*:
  - Gamma-horizont (Attenuation by 1/e)

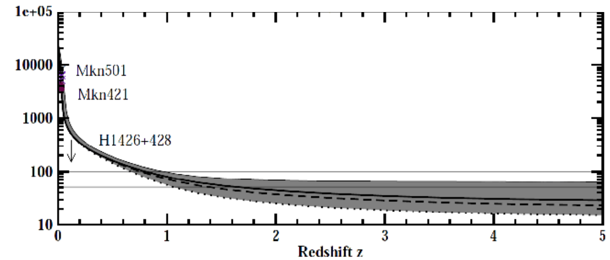

Correction for absorption due to the metagalactic radiation field

- *Fazio-Stecker-Relation*:
  - Gamma-horizont (Attenuation by 1/e)

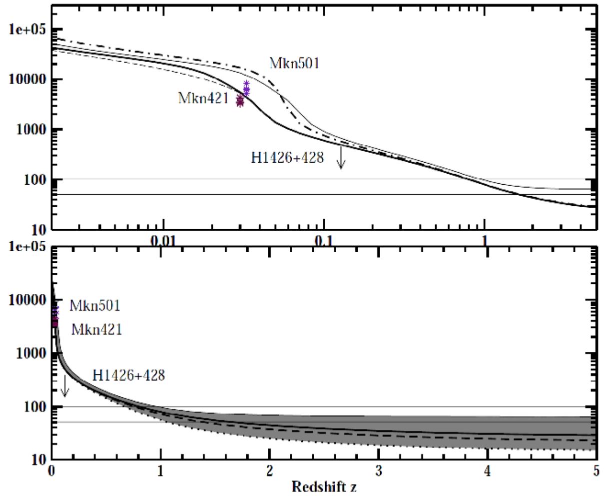

Correction for absorption due to the metagalactic radiation field

- *Fazio-Stecker-Relation*:
  - Gamma-horizont (Attenuation by 1/e)
- For **z=0.182** we get a cut-off at ~400GeV

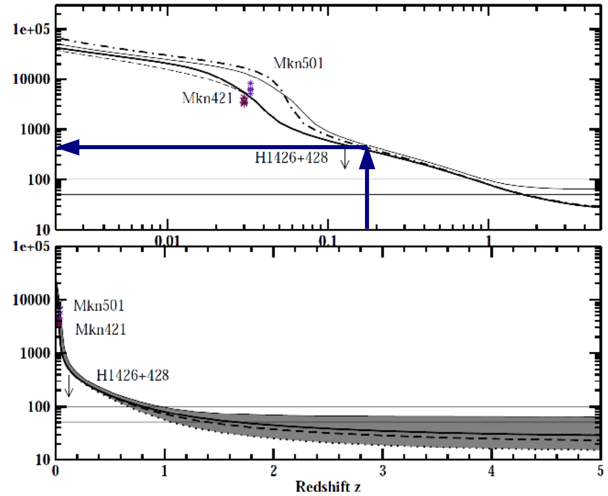

(Kneiske, Bretz, A&A 413, 2004)

Correction for absorption due to the metagalactic radiation field

- *Fazio-Stecker-Relation*:
  - Gamma-horizont (Attenuation by 1/e)
- For **z=0.182** we get a cut-off at ~400GeV
  - Correction of the spectrum for the attenuation

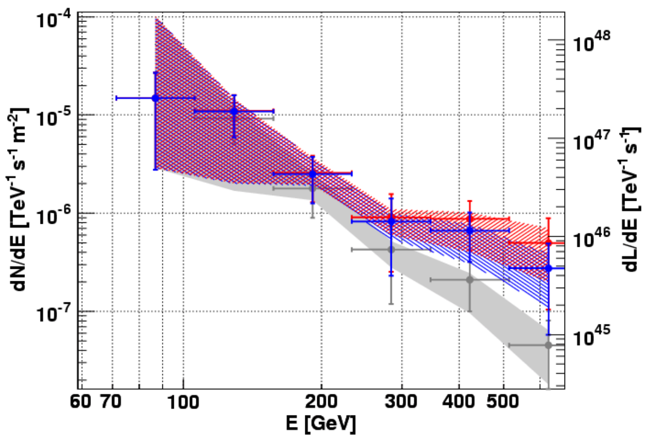

T.Bretz, PhD thesis

Including of the new data points into the known spectral energy distribution

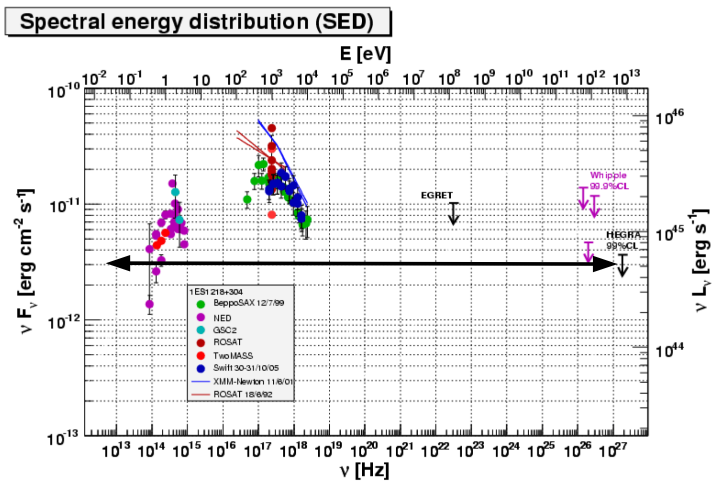

Radio | optical | X-ray | γ-ray (VHE)

T.Bretz, PhD thesis

Including of the new data points into the known spectral energy distribution

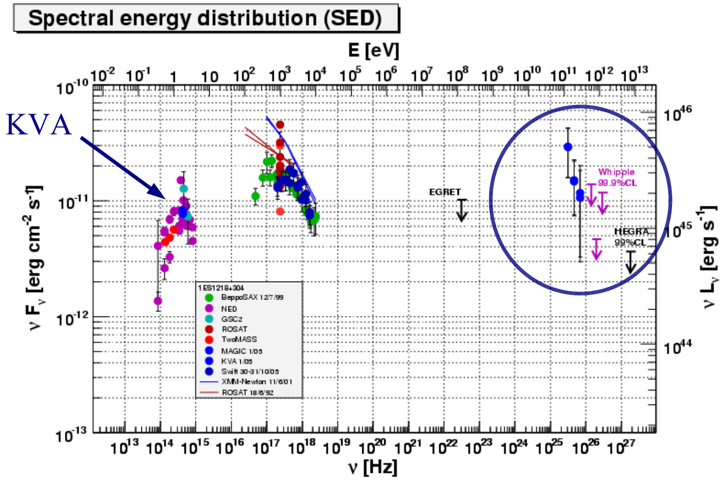

T.Bretz, PhD thesis

SSC-model fit

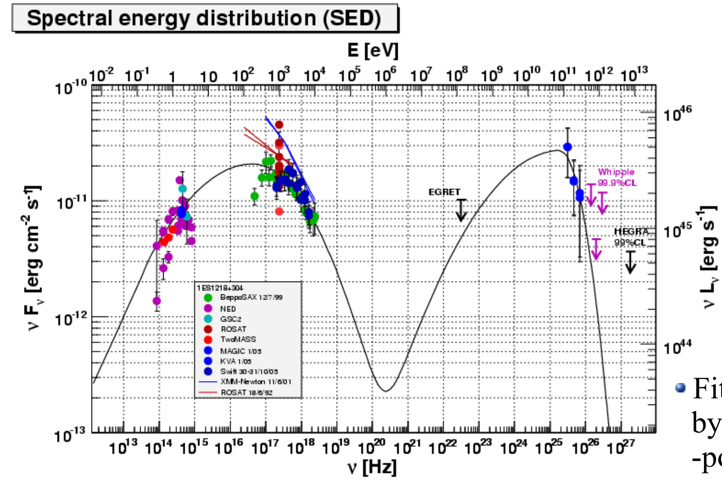

- Fit-Parameter restricted by peak-height and -position

(Model: Ghisellini, Maraschi, Dondi, A&AS 120, 1996) (Tavecchio, ApJ 509, 1998)

SSC-model fit

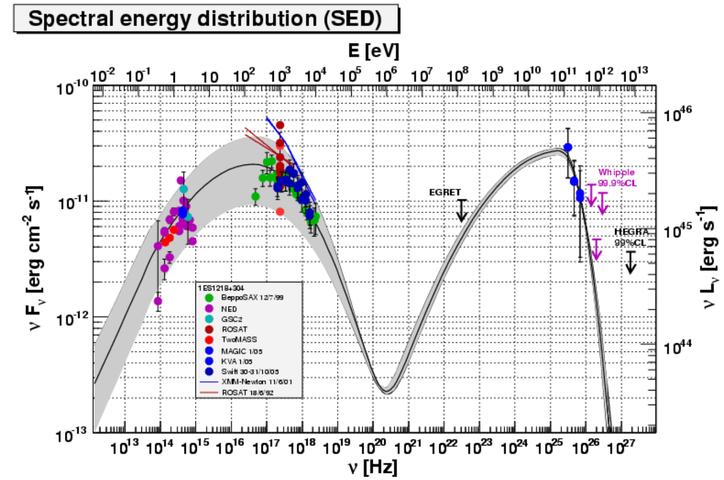

T.Bretz, PhD thesis

Comparison with blazar sequence

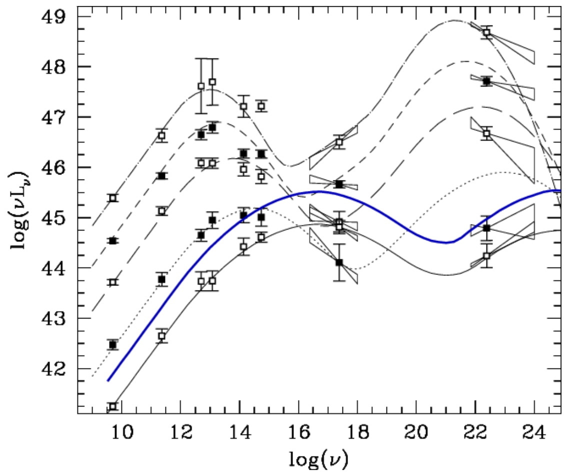

- The spectrum of 1ES1218+304 fits into the sequence
- But it is on the upper edge of the bin
- A similar source with a slightly higher luminosity would violate the sequence.

T.Bretz, PhD thesis

PG 1553+113 (z>0.09)

Combined signal 2005/2006

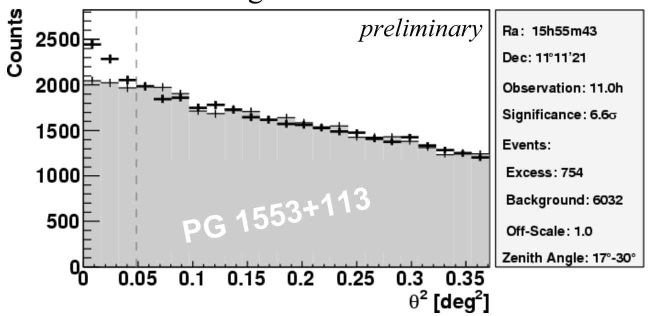

Observations:

- 3.-13. May 2005 (~some days before H.E.S.S.)
  - Significance > 3
- Follow-up observations: 29. Jan. – 9. March 2006
  - Significance > 5

PG 1553+113 (z>0.09)

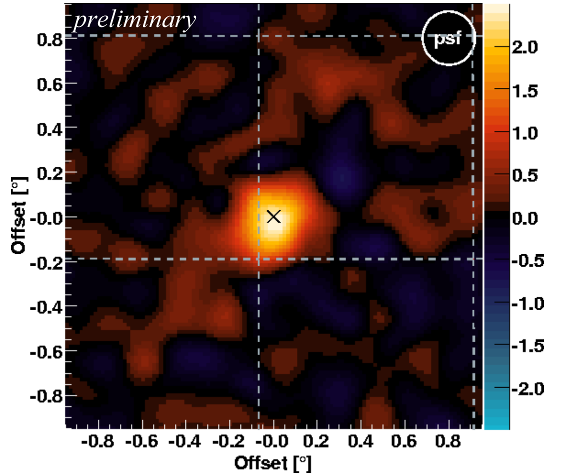

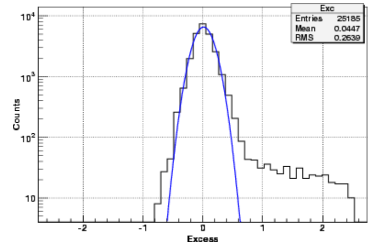

Gamma-ray Bursts (z>1?)

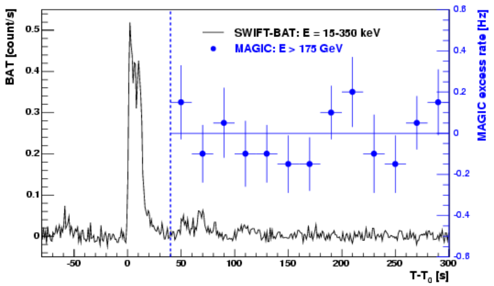

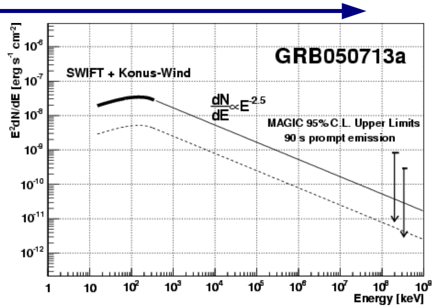

- 12 GRB observed since April 2005 (10x Afterglow-, 2x Prompt-emission)
- Typical repositioning time <25 seconds
- Prompt emission (050713a; 050904)
  - Time for repositioning <10 seconds (!)
  - No significant signal

ApJ 2006, accepted (astro-ph/0602231)

Conclusion

- Talking about AGN you should not forget the TeV part of the spectrum
- There are now more and more sources known to emit at TeV energies
- MAGIC is able to measure down to 100GeV at best conditions
  - **TeV spectra should be included in MWL discussions**

Taking a view at Blazars from another angle

Stefan Wagner, LSW Heidelberg

ENIGMA set out to study AGN through variability.

Being humans, this implied that we worry about small-scale emission regions (Δt ~ 30 yrs ~ 10 pc)

How relevant are these scales?
Where is(are) the emitting region(s)?
Cross-identifications and decomposition

Taking a view at Blazars from another angle

We said *AGN, but mostly discussed Blazars.*
Their variability is most spectacular (relativistic aberation).
For addressing the questions ...

How relevant are these scales?
Where is(are) the emitting region(s)?
Can we cross-identify and decompose?

... Blazars (believed to be seen jet-on) are not ideal.
According to unification, FRI sources are off-axis Blazars

M 87

The first (1918), the closest (in the north), brightest (most bands), and best studied jet

Off-axis (7-30 deg) Blazar

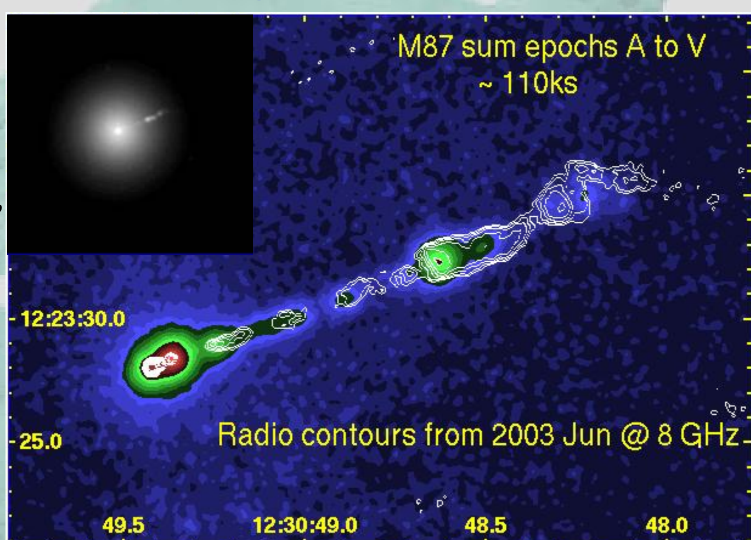

D.Harris, 2006

Sizes and IDV

In IDV discussions it is often argued that radio-sources are synchrotron self-absorbed at radio frequencies on the linear scales that are inferred from radio-IDV.

This has never been proven.

In M87 it was shown to be incorrect:
1 light-day corresponds to ~3 10^15cm, taking different angles between M87 and IDV sources into account, this corresponds to ~10^17cm, approaching resolved scales in highest resolution VLBI studies of M87

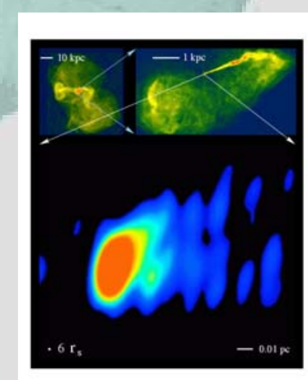

... Monitoring II: Fluxes

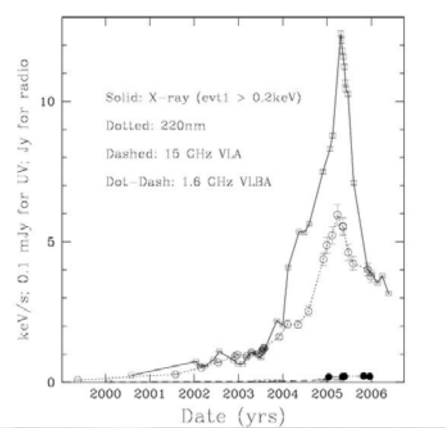

Radio, optical, xrays, gamma-rays

show variations on scales of months

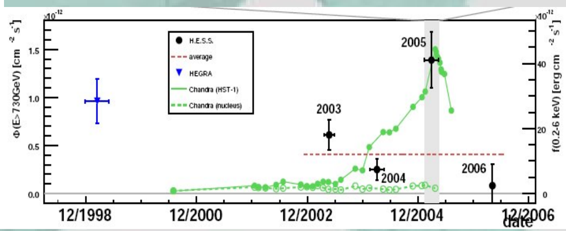

... Monitoring III: Flares

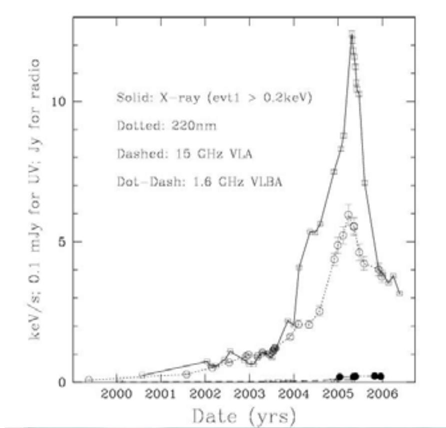

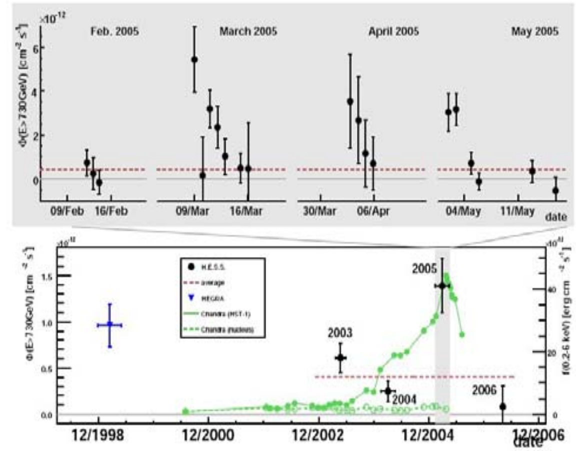

The Black Hole

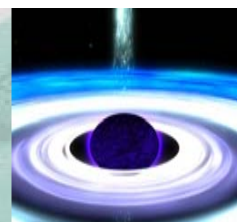

Short time scales <=> Small distances?

10^16cm ~ few R_g

Kerr Black Hole in magnetic field will develop large electric potential and huge EM force, accelerating charged particles to very high energies (Slane et al., 1980)

Problem: B ~ 10000 G required for $1M_9$

Do we know magnetic fields?

The jet

M 87 is an off-axis Blazar
Central parsec-scale jet base would be similar to
on-axis Blazars (D is reduced by an order of magnitude)

VHE gamma-rays will be produced in a similar way, the time-scales are reduced by an order of magnitude. The spectra and SED would be similar.

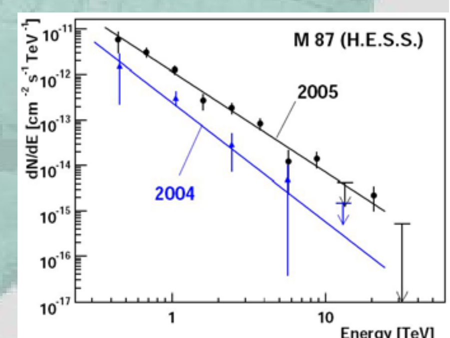

The knot HST-1

Similar long-term light-curves suggest gamma-ray emission from HST-1.
Some sub-volume has to be even more compact than morphological limit.

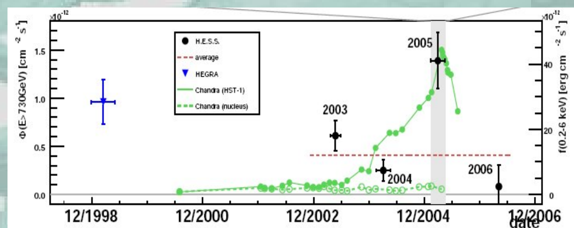

Also the site of rapidly variable component?

Fast variations

Fast variations in VHE gamma-rays were detected in 2005 (high level) only (up to now)

Possibly a selection effect
(would have been hard to detect at lower level)

No variations on similar timescales have been seen at X-ray/optical/IR/radio wavebands
(few simultaneous observations, though)

Not many reported searches on these time-scales.

But they are expected in IC models!

Musings

How relevant are these scales?
Very (50% amplitudes)
Note these are volume filling factors of 10^-20
enormous dynamic ranges in emissivity

Where is(are) the emitting region(s)?
Anywhere
One-two-many (HST-1, knot A, base of jet)?
When seen end-on, superpositions of many
One source of VHE emission?
All sites emit X-ray, optical, and radio emission

Musings

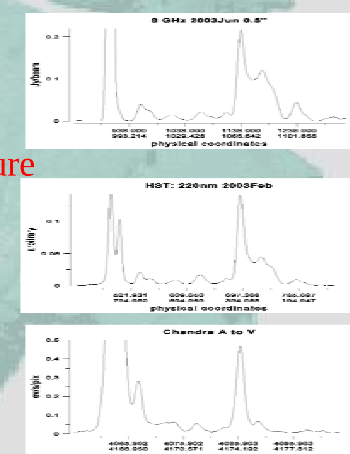

Where is(are) the emitting region(s)?
All of them may have compact substructure
Superposition of many components along the los
timing-noise
SED superposition

Cross-identifications and decomposition
What is quiescent emission?
Jet-emission between knots (dynamic range problem)
timing noise, isolated flares, => lots to be done

Ever more riddles

Dissipation of bulk kinetic energy in the jets of powerful blazars

K. Katarzynski & GG

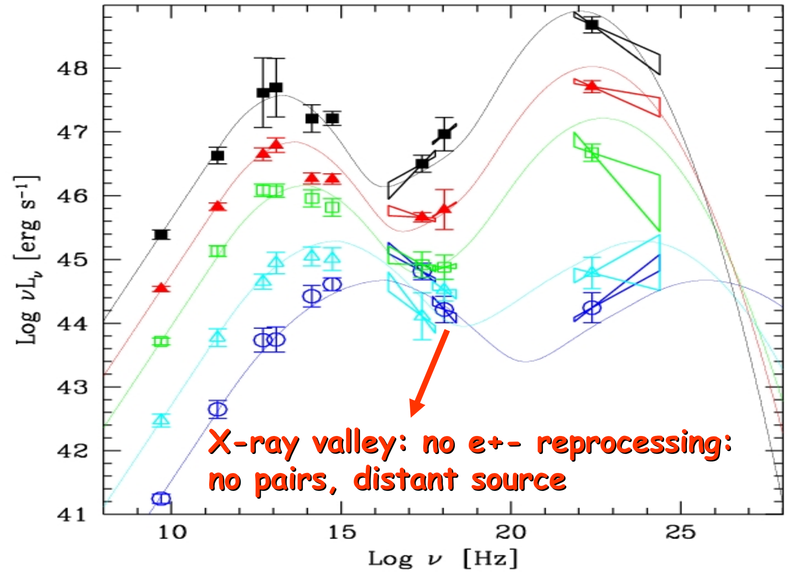

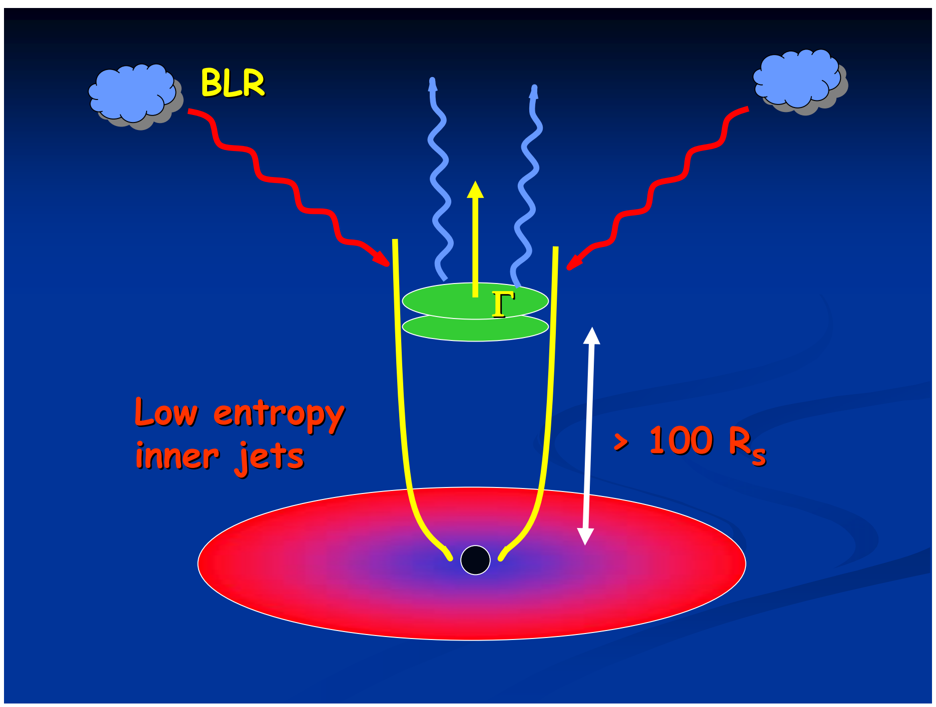

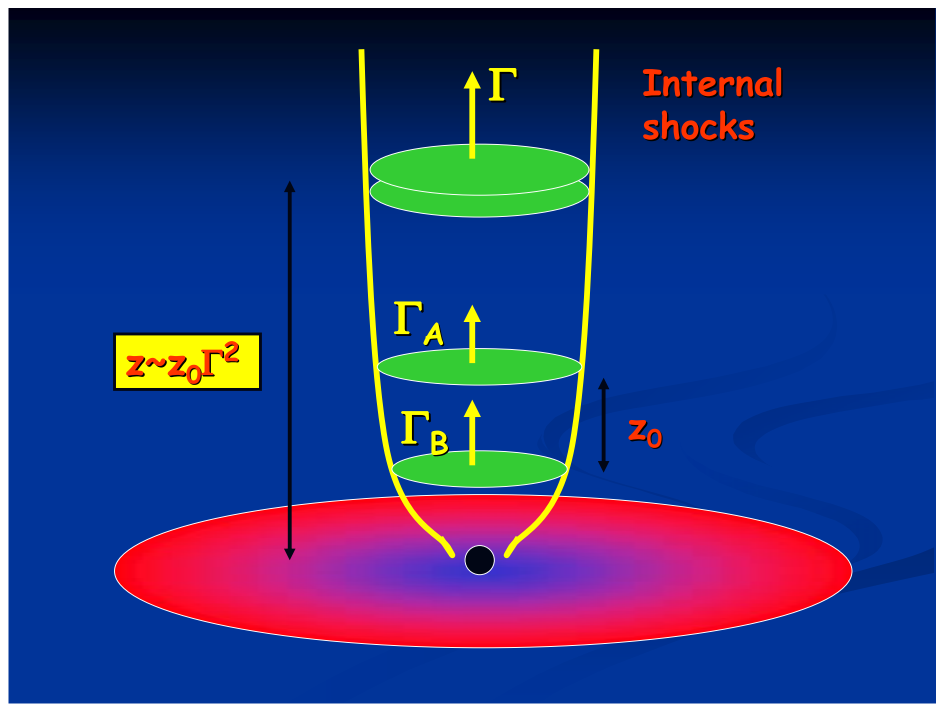

What happens if Γ changes?

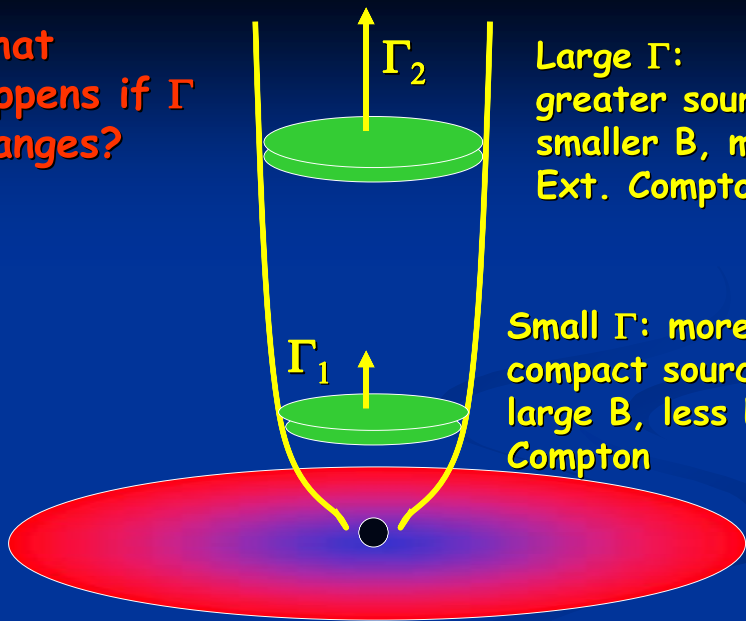

Large Γ: greater source, smaller B, more Ext. Compton

Small Γ: more compact source, large B, less Ext. Compton

Main assumptions

- The jet always produces blobs of constant bulk kinetic energy: $E=\Gamma M$ is constant
- The amount of energy given to the emitting electrons is the same
- Also the magnetic energy is the same: $E_B=VU_B=$ constant
- The blob is spherical, $R=\psi z=\psi\Gamma^2 z_0$

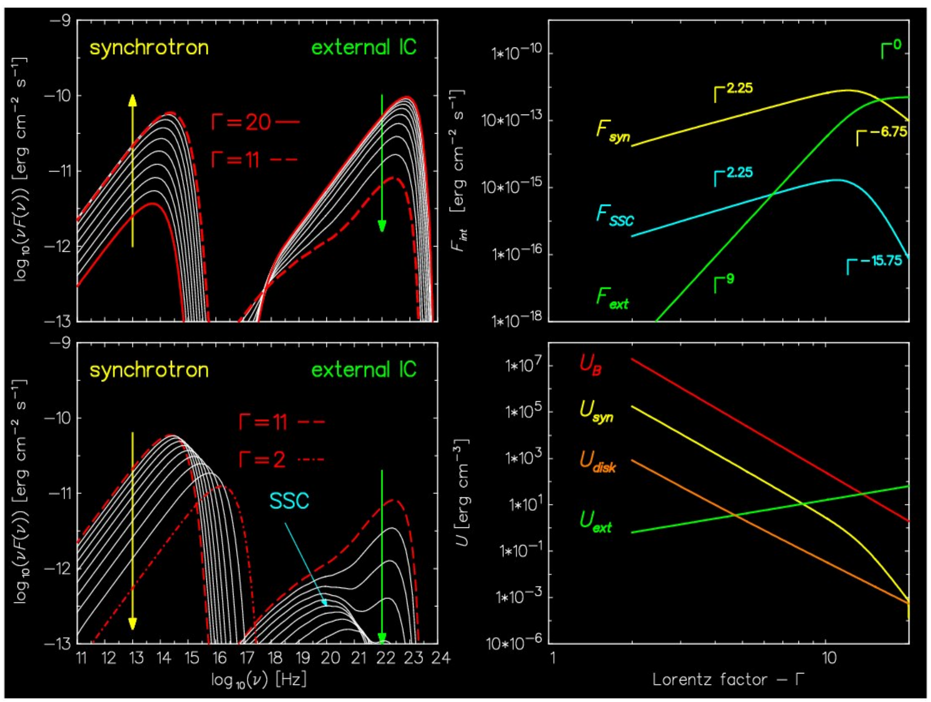

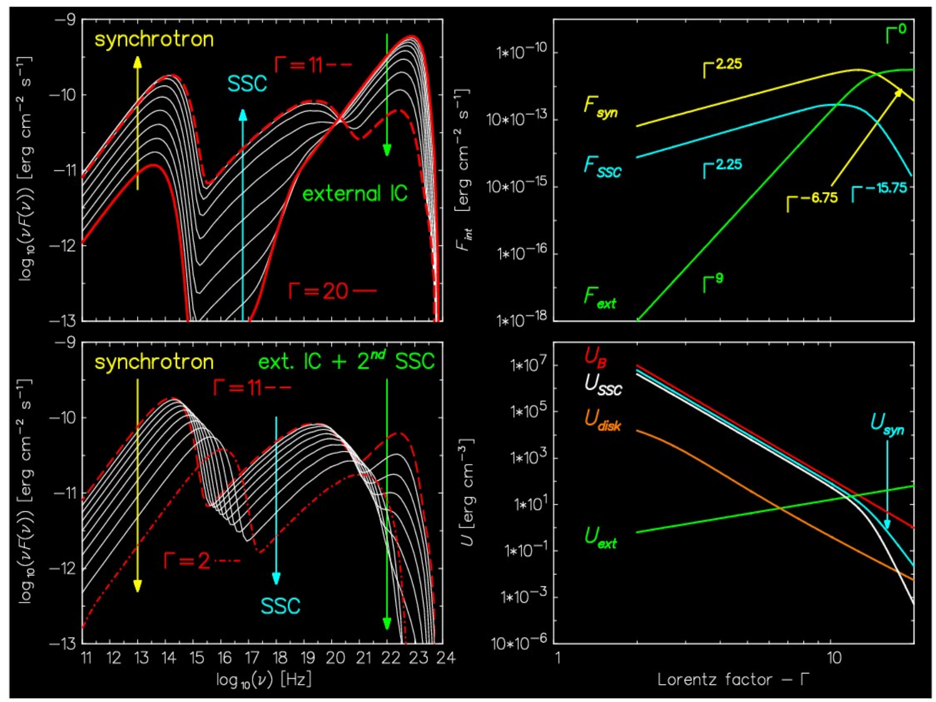

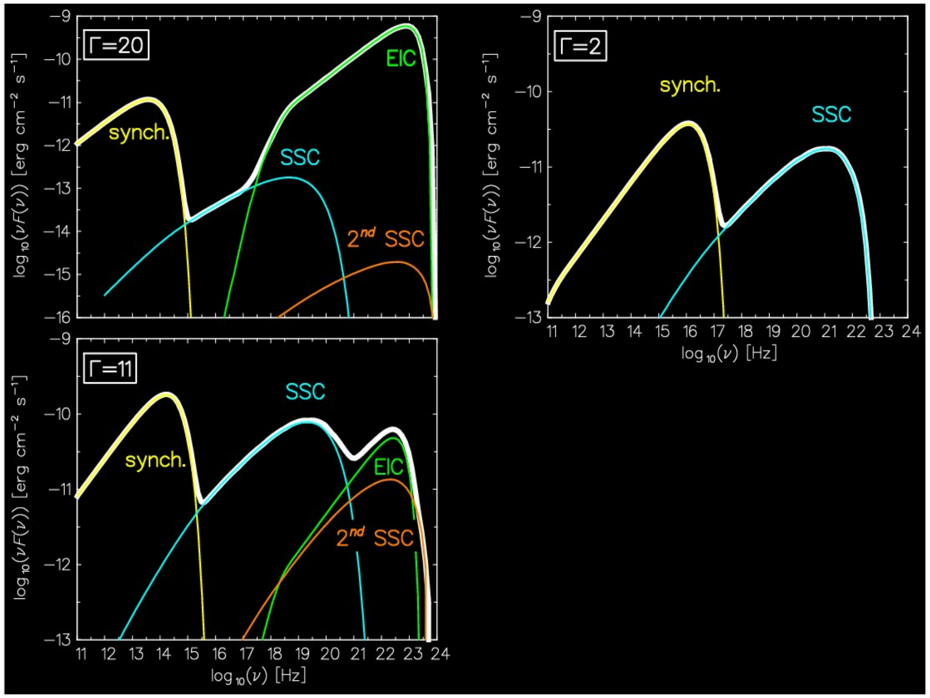

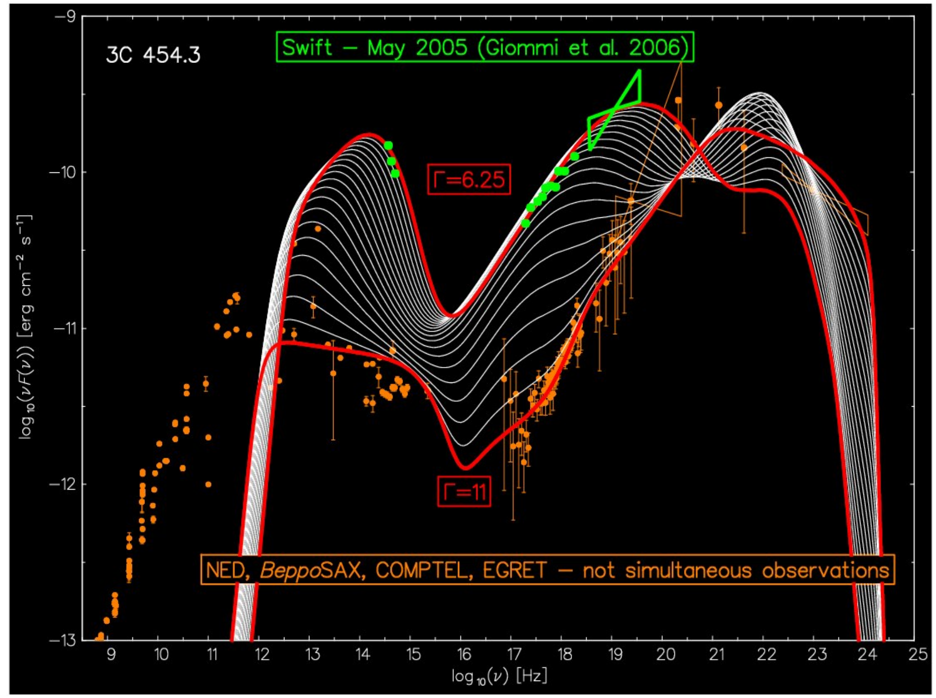

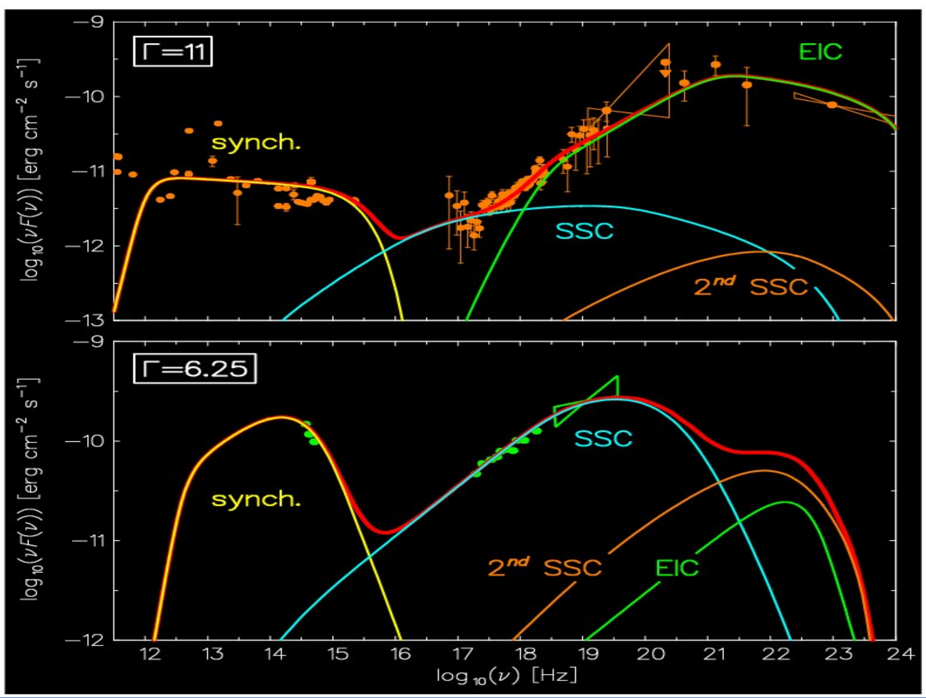

Conclusions

1. "Early" dissipation is possible
2. Dramatic changes even if the jet works with the same efficiency
3. "Economic" way for strong variability
4. 3C 454.3 can be explained without invoking a large variation of the jet power
5. Small Γ may be the rule. May explain why EGRET detected 1/4 of strong radio blazars.
6. Easily testable by AGILE and GLAST

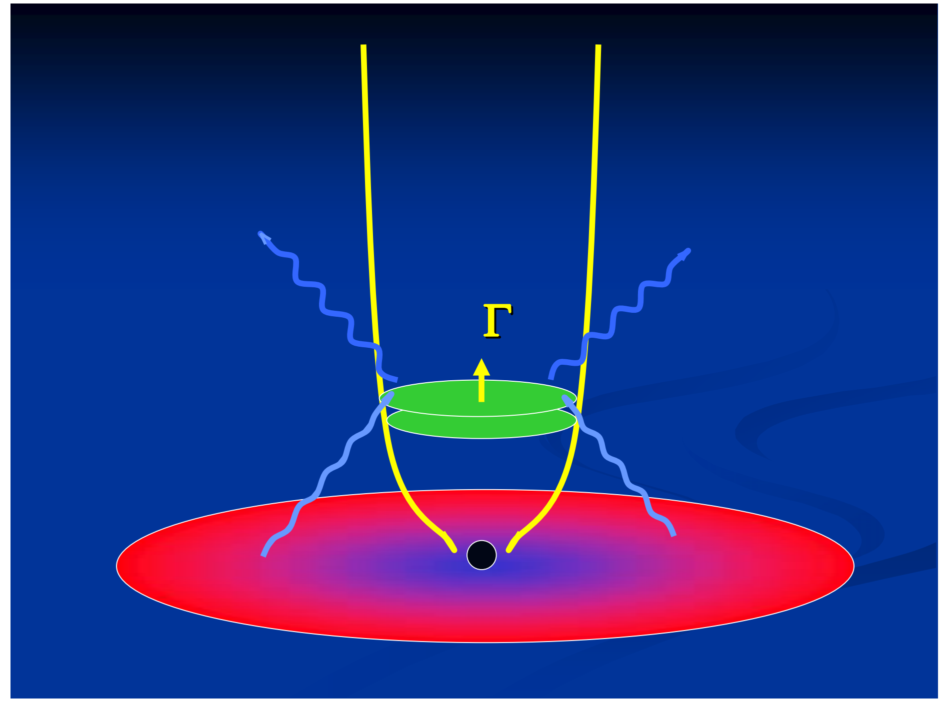
Γ

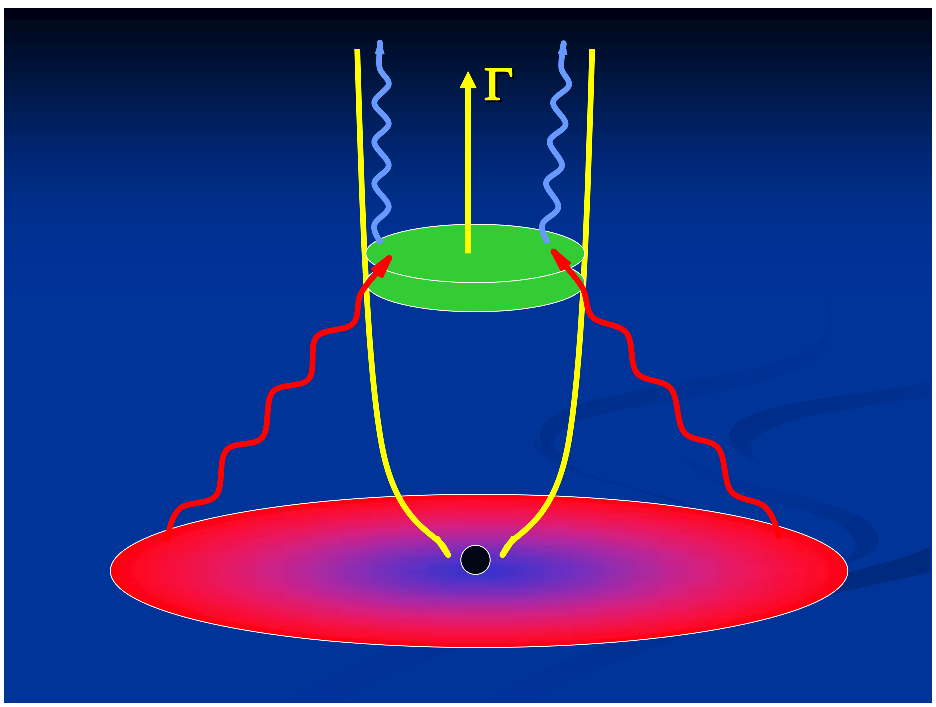
Γ

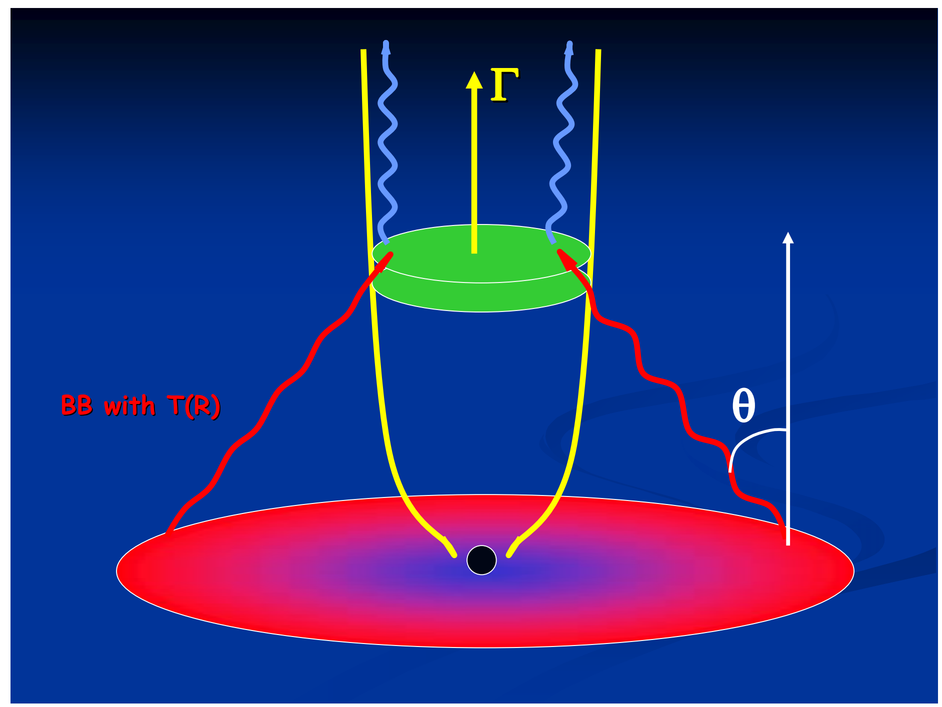
Γ
BB with T(R)
θ

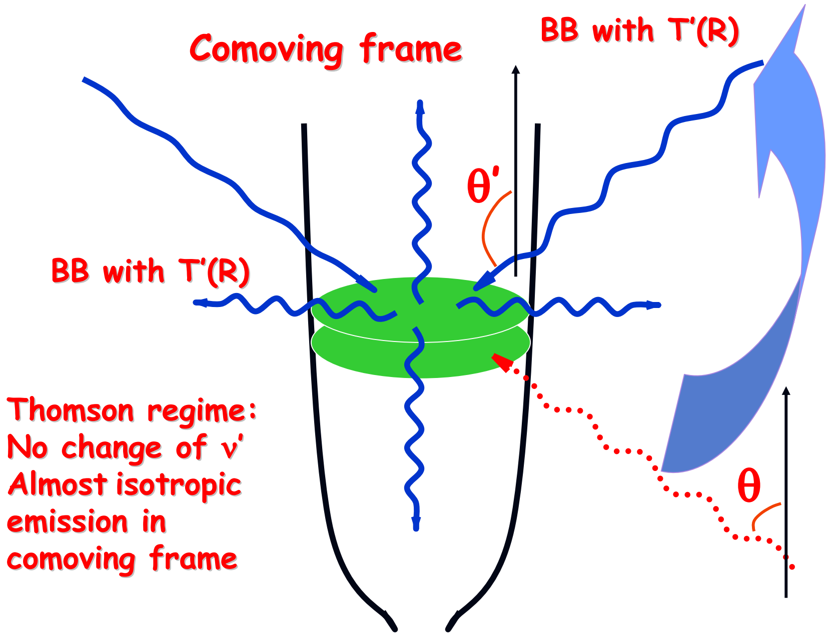

Comoving frame
BB with T'(R)
θ'
BB with T'(R)
Thomson regime:
No change of ν'
Almost isotropic
emission in
comoving frame
θ

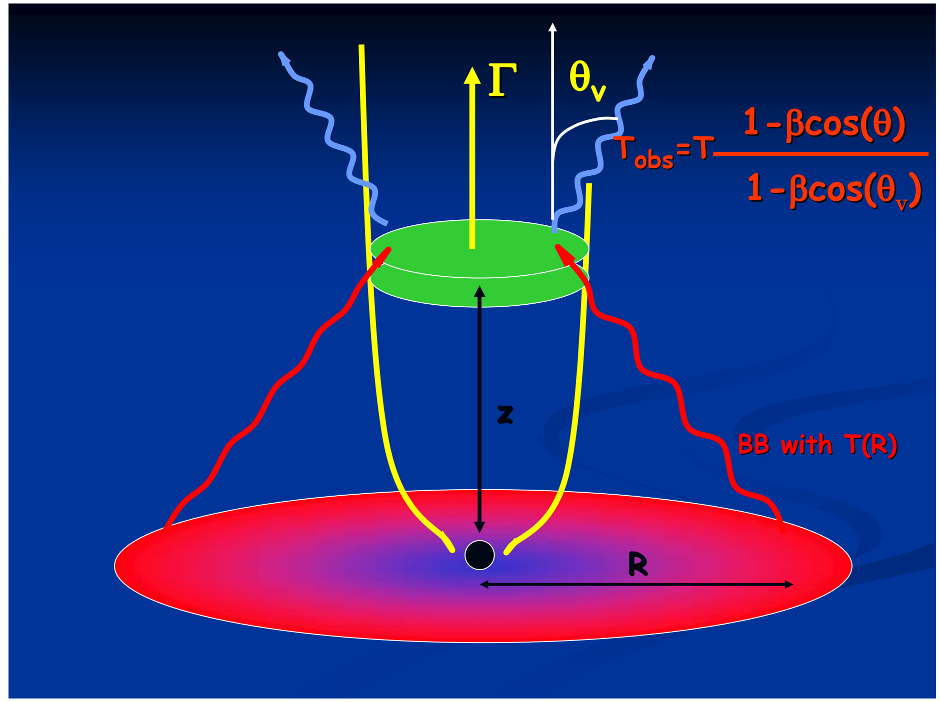

Γ
θ_v
$T_{obs}=T\frac{1-\beta\cos(\theta)}{1-\beta\cos(\theta_v)}$
z
BB with T(R)
R

Dual-frequency polarization observation of the 4C71.07 jet

The ongoing search for helical magnetic fields

Andreas Papageorgiou, Cork institute of Technology

8th ENIGMA meeting, Espoo, Finland – 6 Sep 2006

The Jet

- 4C71.07 (0836+710)
- z= 2.17 - 1 mas = 4 *h-1* pc (*qo*=0.5, *Ho*=100 *h* km /s /Mpc)
- Strongly polarized in all wavelengths
- Can be traced up to 180 mas from the core (0.3GHz)
- pc-scale jet, straight, continuous structure, a few knots, Faraday corrected MVPA parallel to jet direction.

- Observation presented here: 1997.9 – 8 &15GHz

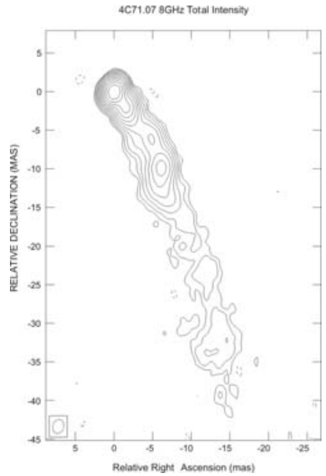

The aim of the observation

- Original proposal:
  - Study the faraday corrected MVPA behaviour at the jet's knots.
- My aim:
  - Compare transverse polarization structure with Helical field predictions.

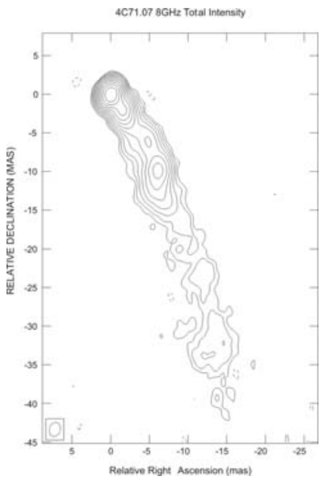

Total Intensity images

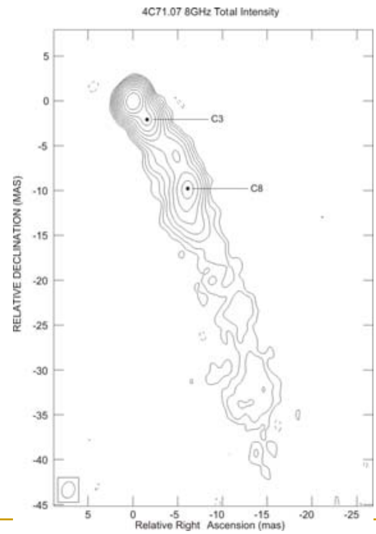

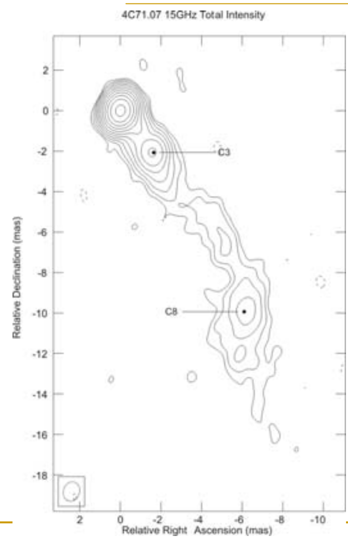

Polarized Intensity and EVPA

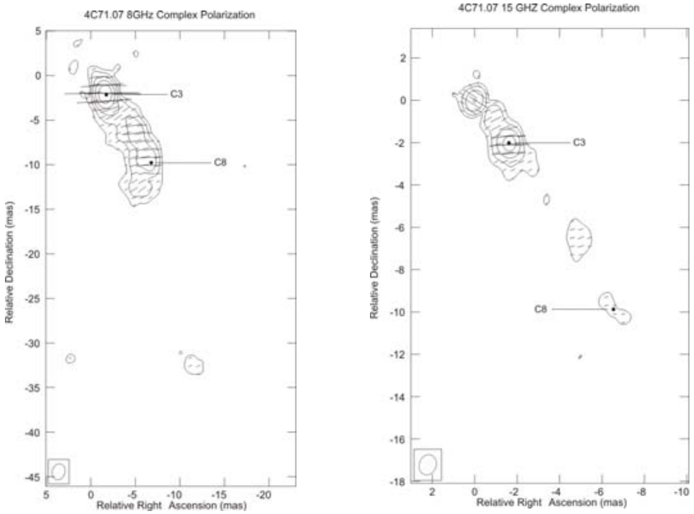

Fractional polarization

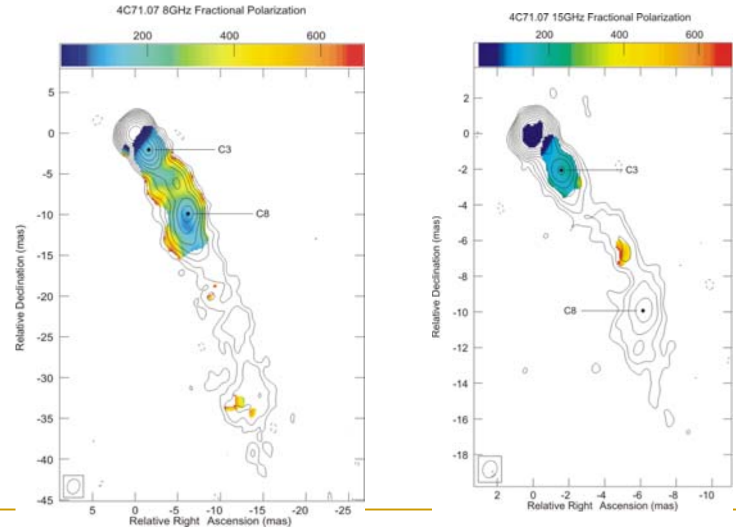

Rotation Measure & MVPA

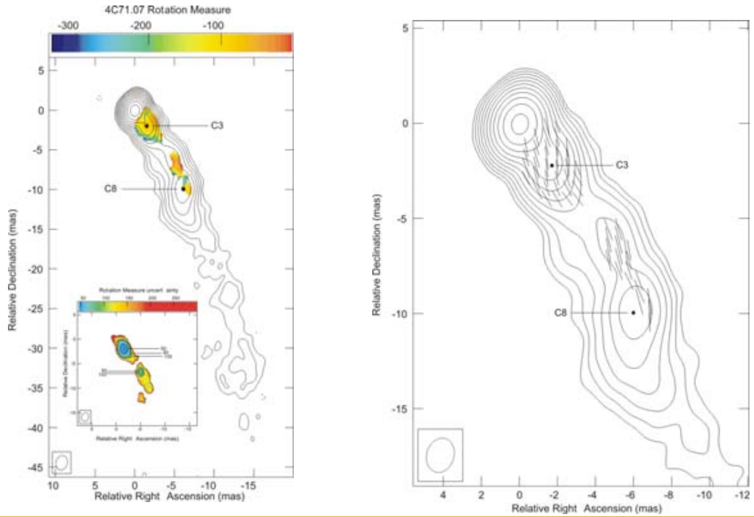

Component evolution

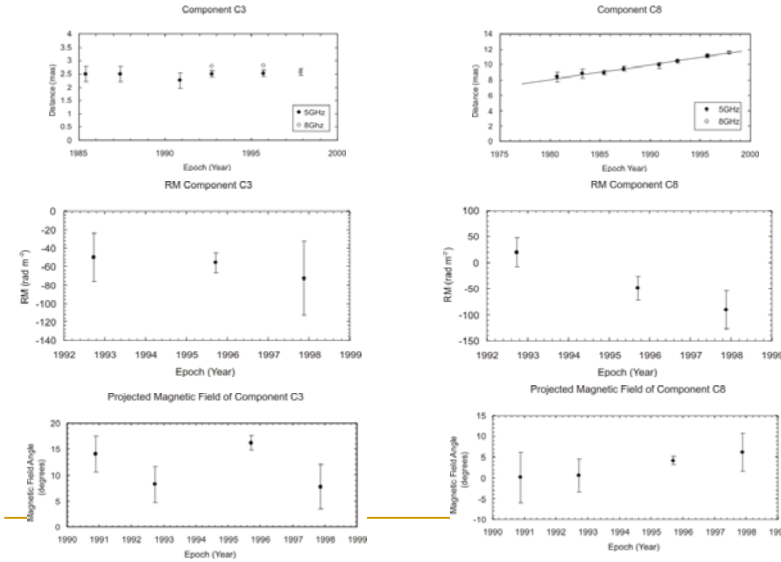

Comparison with Helical field model

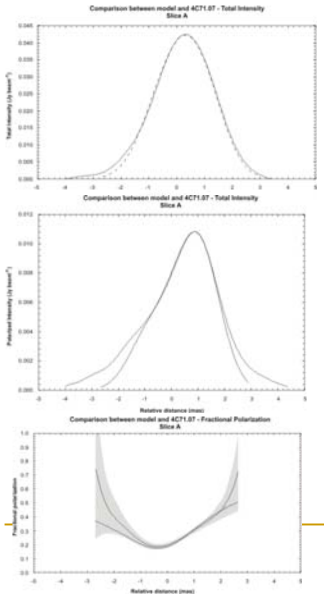

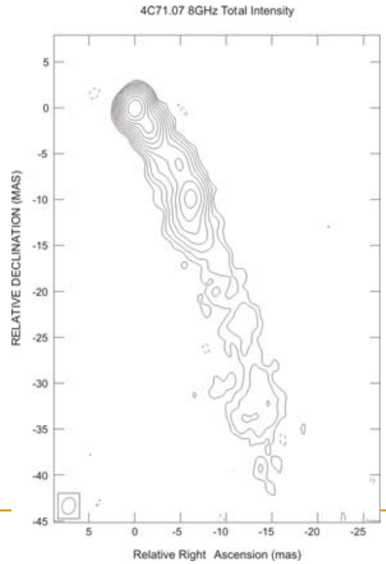

Helical field models

- Currently, two approaches
  - Asymmetries in transverse I, P, MVPA
  - Asymmetries in Faraday RM
- As it is, the two different methods probe different regions of jets
  - Former: Field geometry from synchrotron emitting jet.
  - Later: Field geometry of the medium surrounding the synchrotron emitting jet
- Should these geometries be the same?

Future work

- Regarding 4C71.07
  - 1.6 GHz VSOP polarization observation (Epoch 2001)
  - Will provide RM with higher accuracy (~ 3-5 rad/m^2) → Better look at the RM asymmetry presented here.
  - Add a 4th point at the Component C8 RM evolution (Maybe, just maybe, the RM is decreasing, will have to get my SF analysis software out)
- Generaly
  - Look for data on more sources to compare with Helical field models
  - Sources should preferably be continuous, long with no bends

Final note on Helical Fields

- WHY BOTHER?
- Questions:
  - Are they really there?
  - Is there evidence for them?
- If yes:
  - Are they common?
  - Is there any preference in pitch angles?
  - How do pitch angles evolve along the jet?

ENIGMA 8th meeting
6 – 8 September, 2006
Helsinki, Finland

The multi-wavelength polarization VLBI structure of 3 BL Lacertae objects

Vladislavs Bezrukovs
Cork Institute of Technology,
Irish team

Introduction

- **1308+326**
  - Intensity and polarization model fitting;
  - Helical B Field in the jet?
  - Polarization rotation in 43 GHz.
- **0828+493**
  - Intensity and polarization model fitting;
  - Helical B Field in the jet?
- **1803+784**
  - Intensity and polarization model fitting;
  - Helical B Field in the jet?
  - RM gradient in the jet.

1308+326
(November 2002)

1308+326. Model fitting.

15 GHz map
Intensity (mJy)
1) 1510.8
2) 184.1
3) 137.0
4) 148.0
5) 44.9

Polarization (mJy) and PA (deg)
1) 57.9 96.578
2) 10.9 63.087
3) 18.5 -5.44

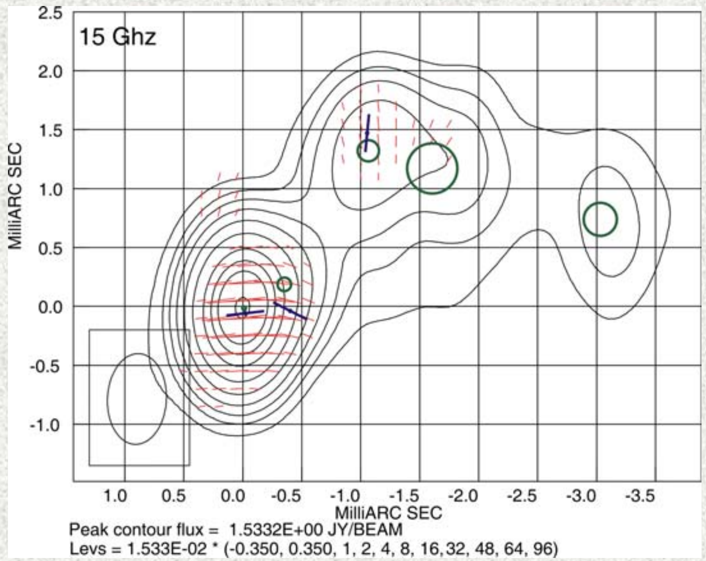

1308+326. Model fitting.

22 GHz map
Intensity (mJy)
1) 1811.0
2) 161.0
3) 163.0
4) 57.4
5) 53.7

Polarization (mJy) and PA (deg)
1) 57.9 67.08
12) 1.5 54.37
3) 15.1 -26.23

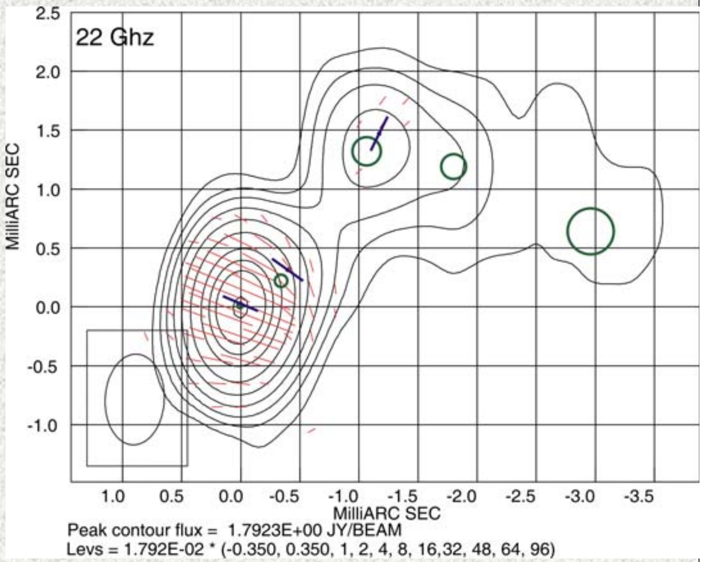

1308+326. Model fitting.

43 GHz map
Intensity (mJy)
1) 1310.0
1b) 230.5
2) 82.8
3) 113.2

Polarization (mJy) and PA (deg)
1) 98.6 33.592

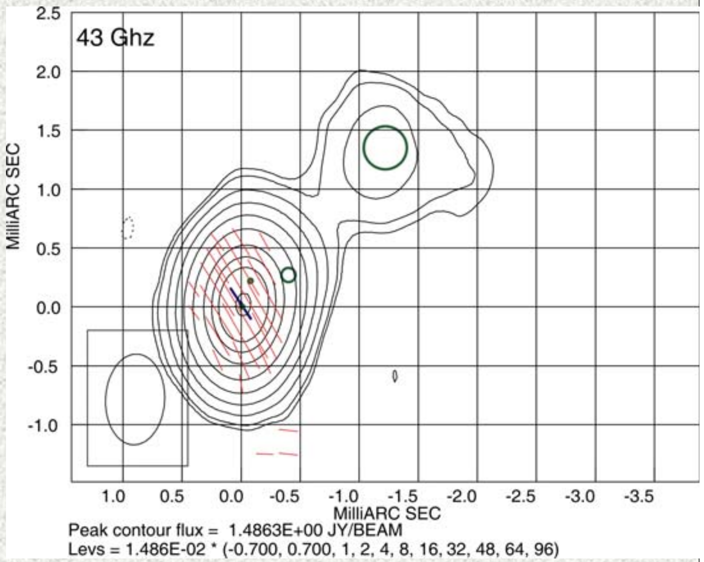

1308+326. Model fitting.

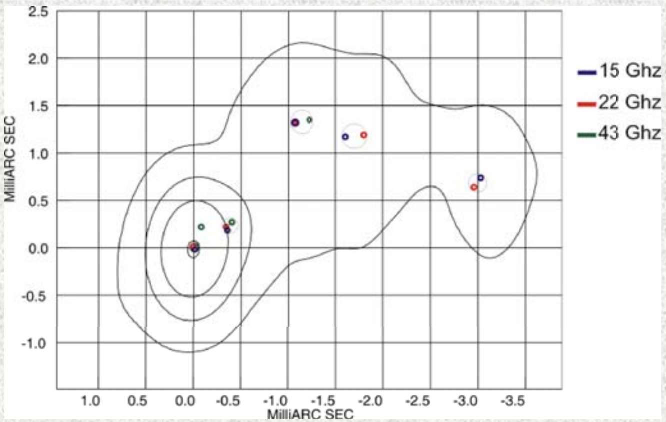

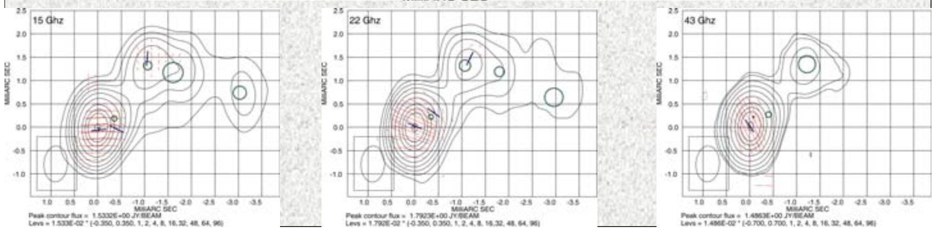

1308+326. Spectral index maps.

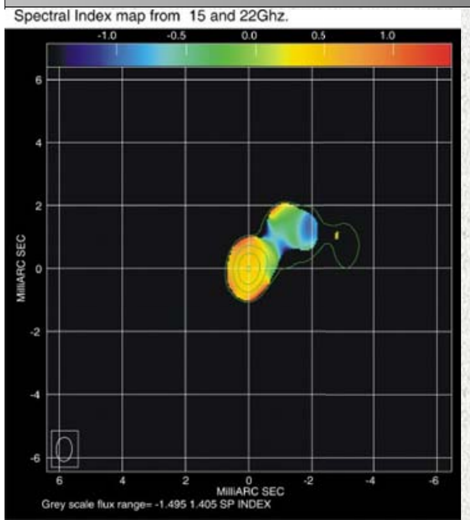

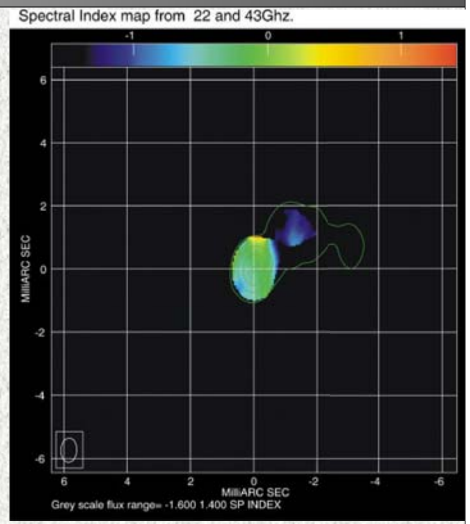

Spectrum in core region positive -> **core optically thick**

Spectrum in core region negative -> **core optically thin**

1308+326. Rotation measure.

Why we rotate polarization angle in 43 GHz to 90^o?

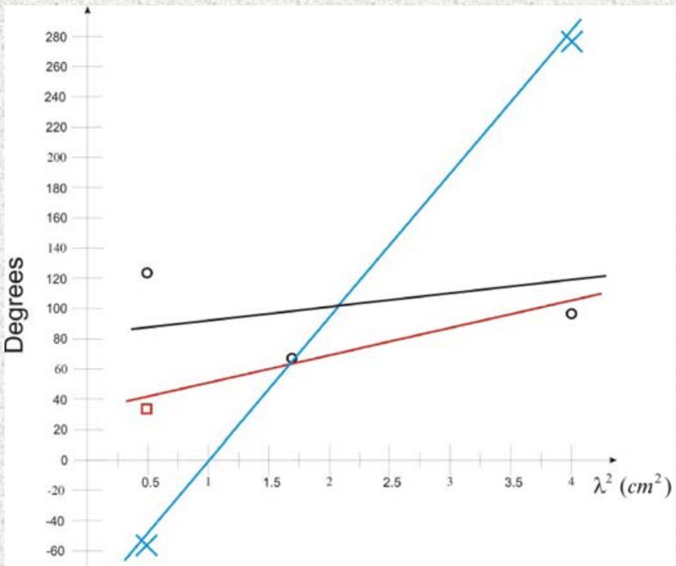

1308+326. Rotation measure.

Rotation measure map maded form 15, 22 and 43 Ghz.

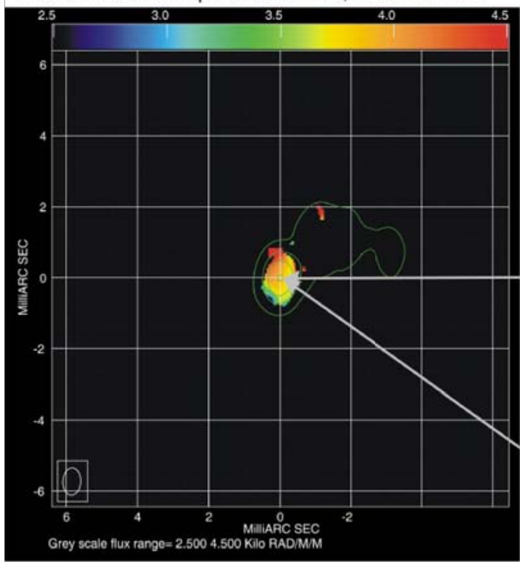

Rotation measure in core center,
RM calculated using map

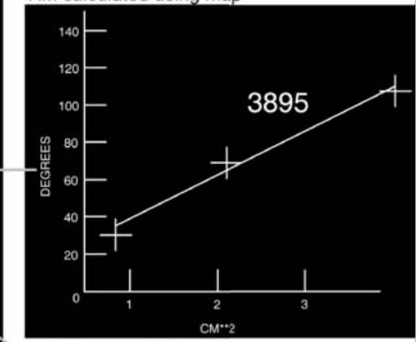

$\sim 3220 \frac{rad}{m^2}$

(RM calculated using
model fitting PA values)

1308+326. November 2002 epoch compare with MOJAVE data.

15 GHZ Intensity map with
polarization sticks

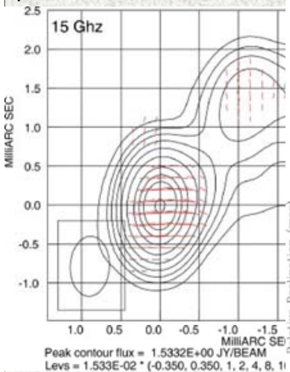

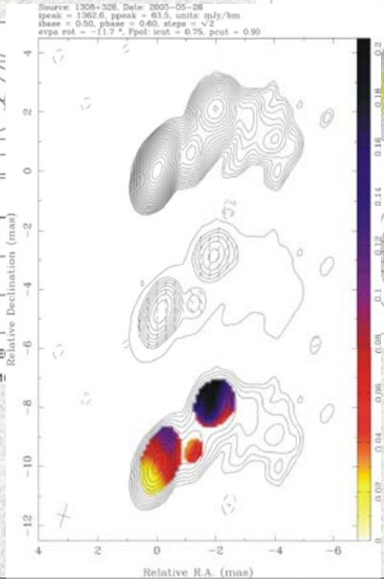

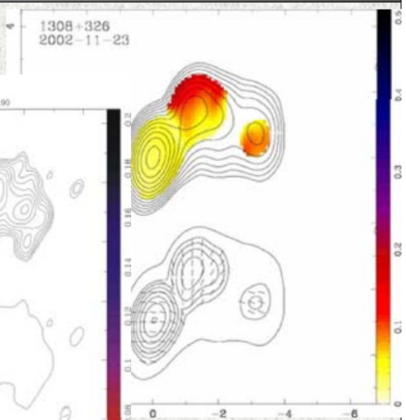

MOJAVE Sample

0828+493
(November 2004)

0828+493. Model fitting.

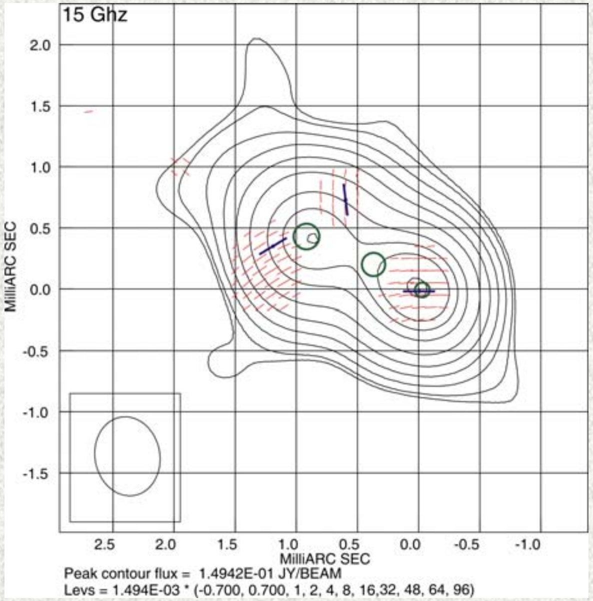

15GHz map

Intensity (mJy)

1) 153.4
2) 65.9
3) 134.8

Polarization (mJy) and PA (deg)

1) 2.3 94.132
2) 2.9 121.132
3) 2.4 7.132

0828+493. Model fitting.

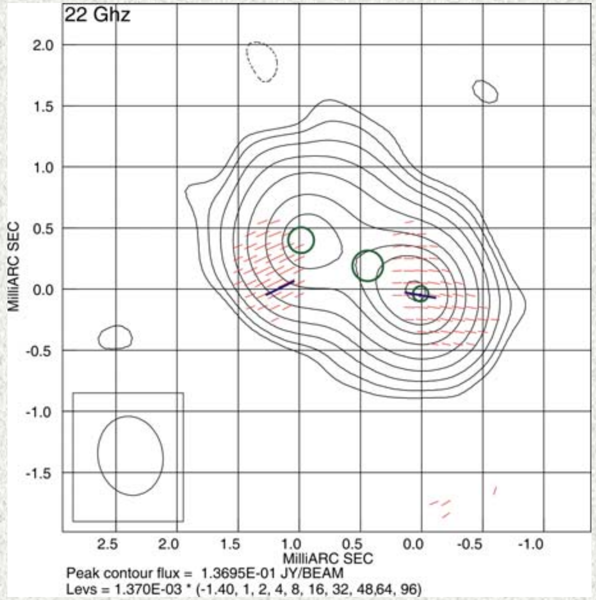

22GHz map

Intensity (mJy)

1) 143.6
2) 79.2
3) 100.2

Polarization (mJy) and PA (deg)

1) 2.2 80.06
2) 3.2 116.06

0828+493. Model fitting.

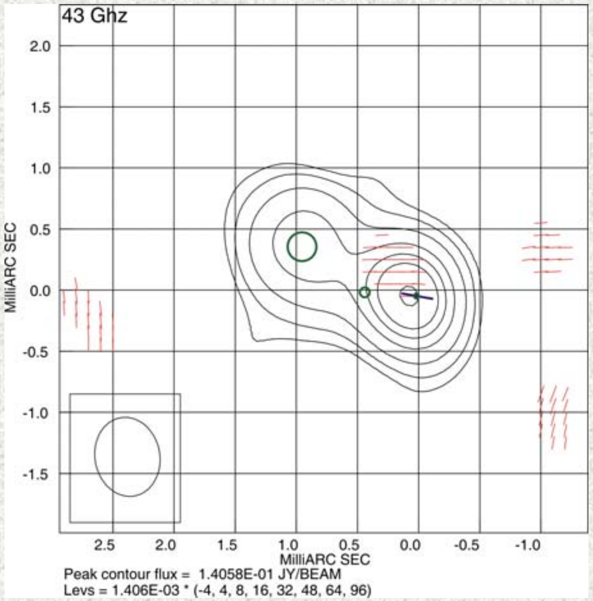

43GHz map

Intensity (mJy)

1) 114.2
2) 51.5
3) 103

Polarization (mJy) and PA (deg)

1) 4.09 89.146

0828+493. Model fitting.

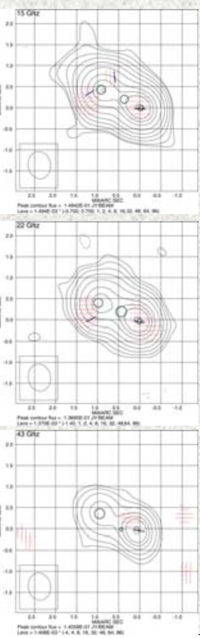

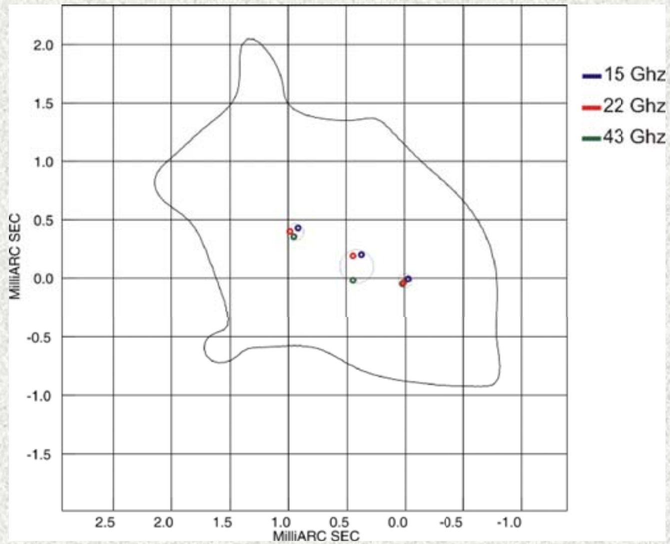

0828+493. Rotation Measure.

RM made from 15 and 22 GHz.

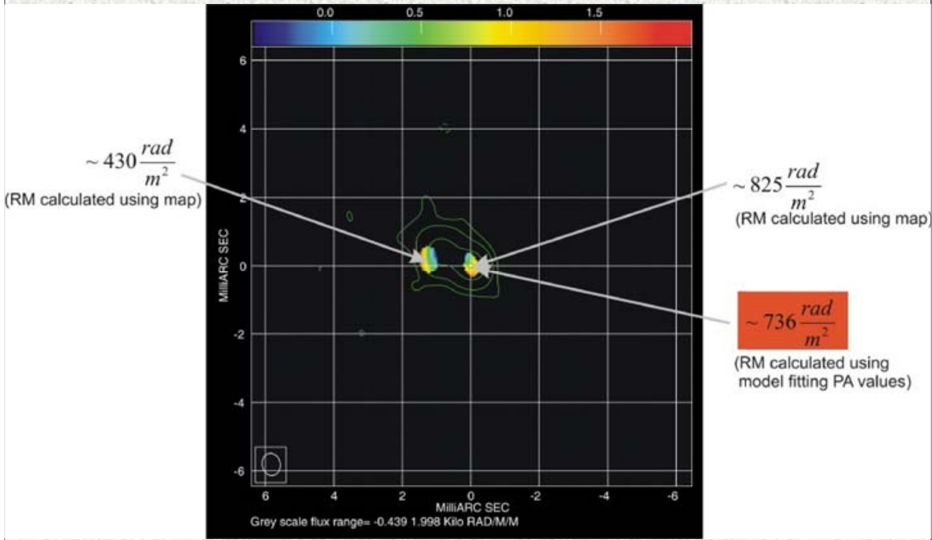

1803+784
(May 2004)

1803+784. Model fitting.

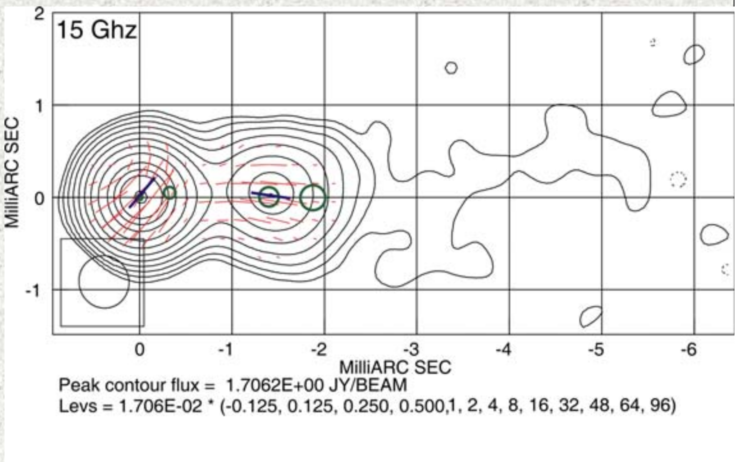

15 GHz map

Intensity (mJy)

1) 1709.0
2) 174.6
3) 278.4
4) 47.9

Polarization (mJy) and PA (deg)

1) 57.4 139.74
2) 33.9 81.74

1803+784. Model fitting.

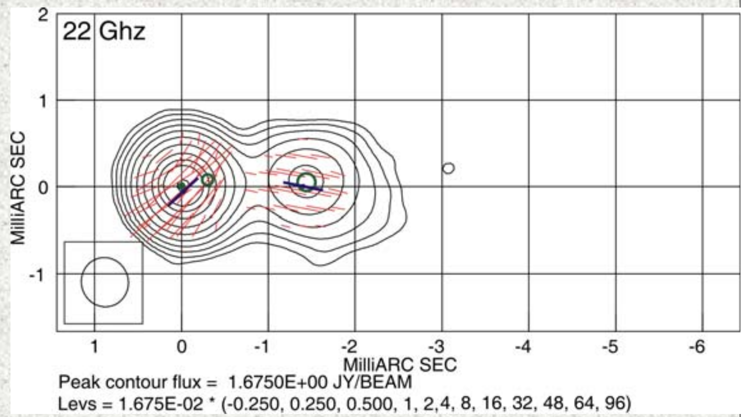

22 GHz map

Intensity (mJy)

1) 1688.7
2) 144.5
3) 270.0

Polarization (mJy) and PA (deg)

1) 60.7 132.87
2) 28.6 78.81

1803+784. Model fitting.

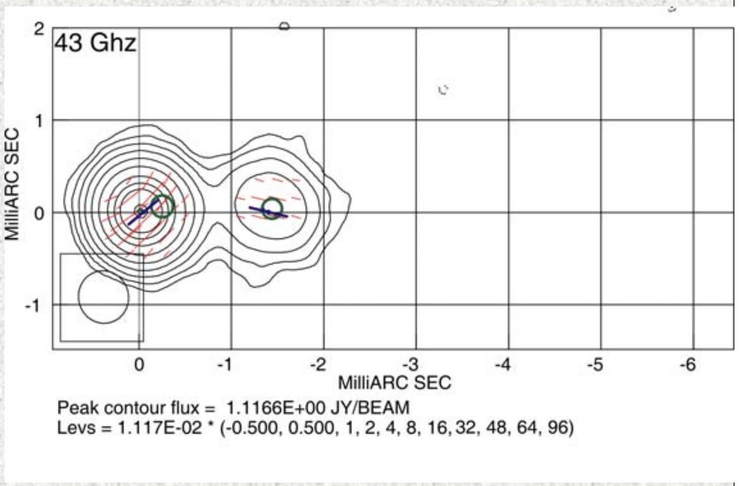

43 GHz map

Intensity (mJy)

1) 1091.0
2) 146.0
3) 173.0

Polarization (mJy) and PA (deg)

1) 37.0 129.65
2) 12.7 76.4

1803+784. Model fitting.

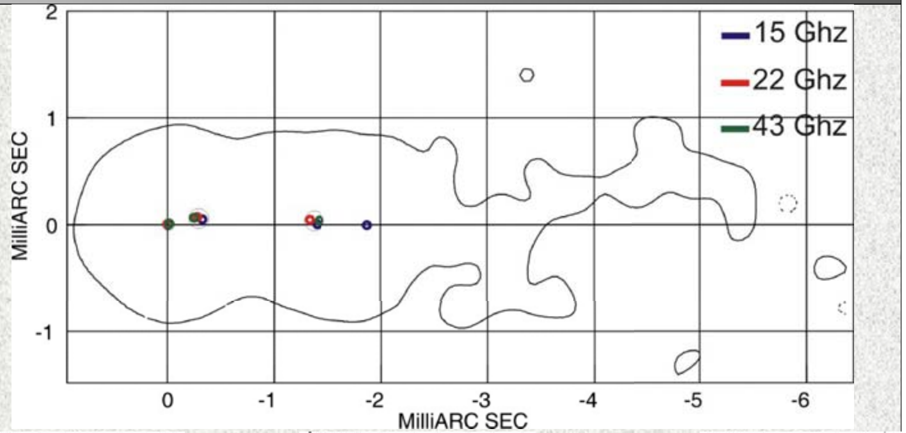

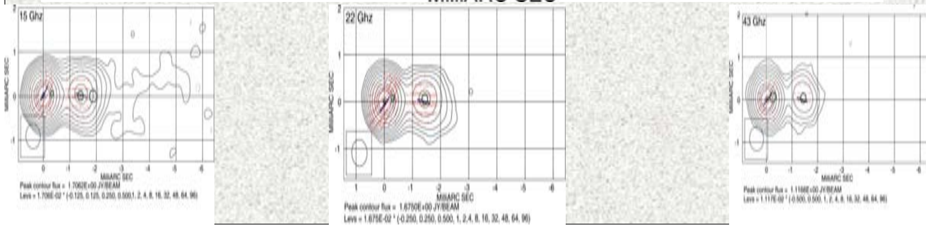

1803+784. May 2002 Epoch compare with MOJAVE data.

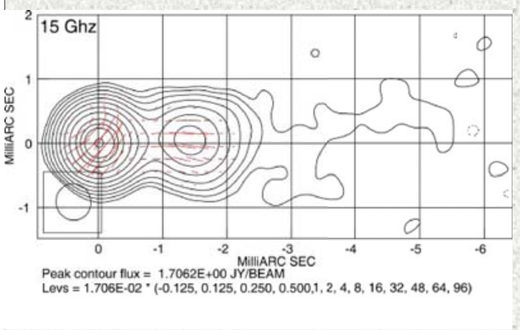

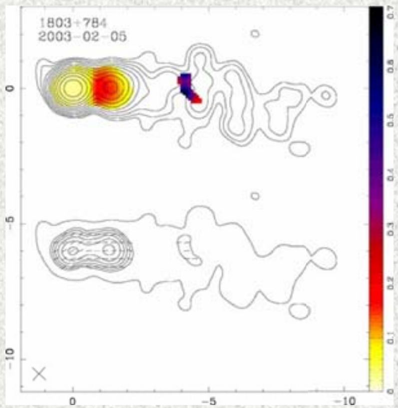

1803+784. Rotation measure.

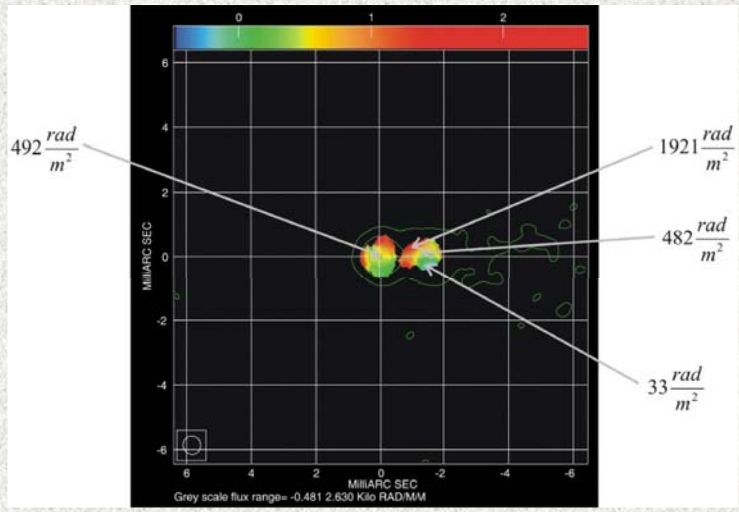

1803+784. Rotation measure..

RM gradient change direction !!!

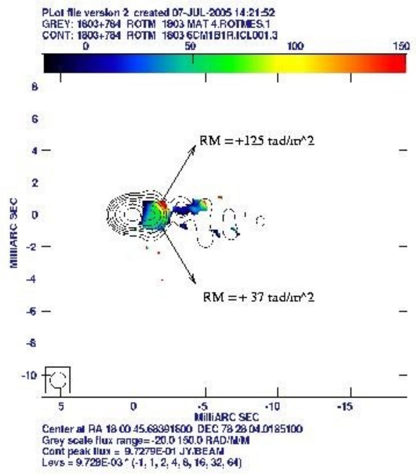

Mehreen Mahmud image

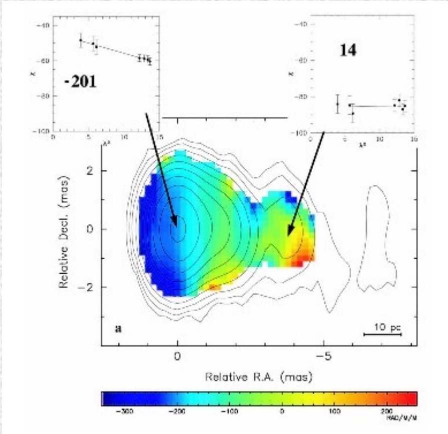

Zavala and Taylor et. el.

Summary.

- Possibility of Helical magnetic field in these sources
  - 1308+326 : asymmetric total intensity distribution across the jet;
  - 0828+493 : polarization rotates by 90 degrees across the jet;
  - 1803+784 : asymmetric RM distribution across the jet;
- 1308+326 core changes from optically thick in 15 and 22 GHZ to optically thin between 22 and 43 GHz which gives rise to polarization degree rotation to 90 in 43 GHz.
- Found asymmetric RM distribution in 1803+784;
  Asymmetry found to be opposite to previous observations made by Zavala and Taylor;
- Finished analysis for entire set of sources: 17 sources in 3 frequencies;
- Produced and tested version of VISFIT program in Linux (intensity and polarization model fitting);

Acknowledgements to

Dr. Denise Gabuzda,

PhD Mehreen Mahmud,

Radio Astronomy Lab at UCC,

Enigma, Irish Group

La Palma telescopes

NOT, WHT, ING, TNG, LT, Mercator

Tapio Pursimo

tpursimo@not.iac.es

Nordic Optical Telescope

Background

La Palma the west most island of the Canary Islands
Observatory Roque de Los Muchacos run by the IAC

- Altitude about 2400 m, above the inversion layer

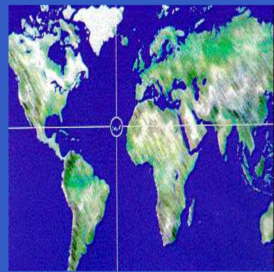

ORM

telescopes: INT, LT, Mercator, WHT, NOT, TNG, GTC,
SuperWASP, KVA,
MAGIC I & II, solar towers: Swedish solar tower, DOT

Meteorology

- One of the best astronomical sites in the world.
- The length of night between 7 to 11 hours
- on average; the effective length of night constant

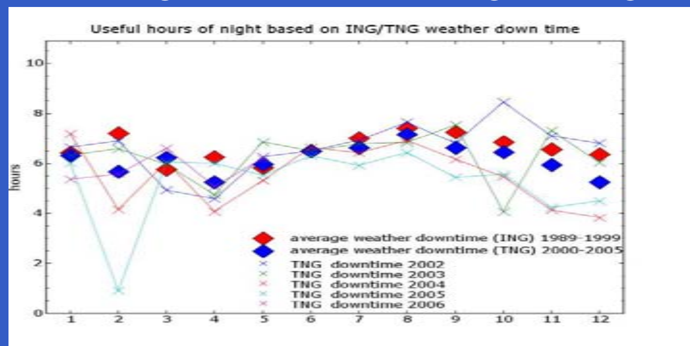

NOT (Nordic Optical Telescope)

2.56 meter alt-az mount telescope

- instruments: ALFOSC, MOSCA, NOTCam, FIES, SOFIN, StanCam, TurPol, LuckyCam(?)

NOT: ALFOSC science example

- Time resolved spectroscopy, resolution 43 sec
- low-spectral resolution (3Å) 3500-5050Å, dispersion 0.77Å/pixel (about 54 kms^{-1}/pixel)(grism #16) (Telting & Ostensen A&A 450, 1149, (2006))

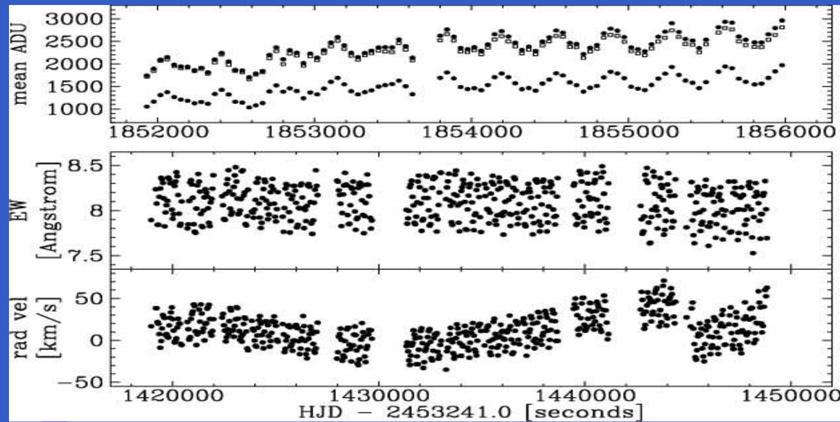

NOT: NOTCam +StaCam science example

- broad band SED using NOTCam & StanCam
3C454.3 during the 2005 outburst
A&A 453 cover illustration by Villata et al p821

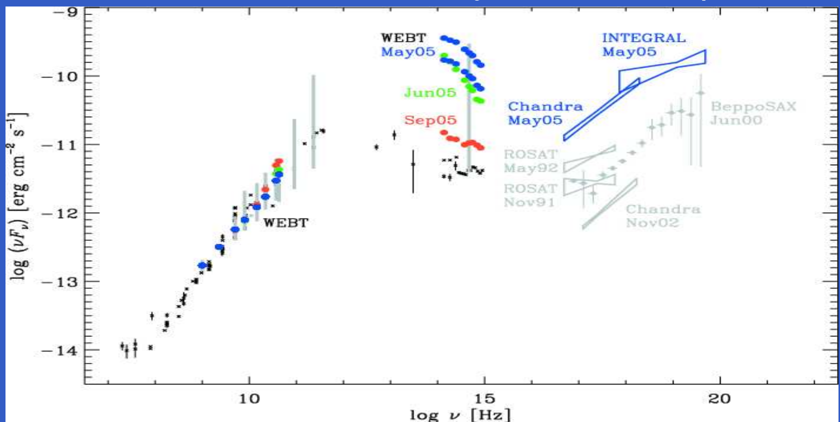

NOT: Own instrument

- Mounted at the Cassegrain focus
- Weight less than about 250 kgs
- focal plane 200mm below the adapter flange
- Contact staff (staff@not.iac.es)

TNG (Telescopio Nazionale Galileo)

- 2 Nasmyth foci hosts 5 instruments
  - imaging: OIG (2×2k×4k EEV CCD, 4.9′ square), Dolores (9.4′ field)
  - spectroscopy: SARG (echelle), Dolores (low res.)
  - NIR: NICS, 1k Hawaii array, AdOpt (Adaptive Optics module for NIR imaging, tip-tilt)

3.58m Alt-Az telescope

ING:INT (Isaac Newton Telescope)

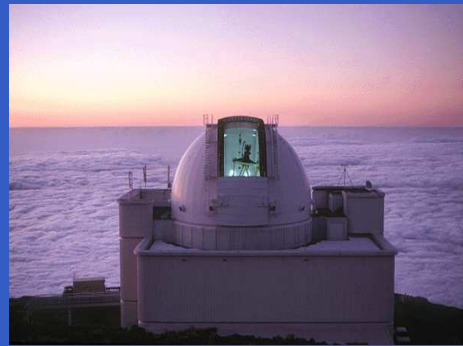

2.5 meter equatorial mount

- Wide Field Camera (WFC), 34 ′ square
- Intermediate Dispersion Spectrograph (IDS)

ING: WHT (William Herschel Telescope)

4.2 meter altazimuth mount

- imaging: PFIP (16′ square)
- spectroscopy ISIS (two arm, longslit), AF2/WYFFOS (MOS), NAOMI/OASIS (IFS,17″ field)
- NIR: LIRIS (imager/spectrograph), NAOMI/INGRID (high resolution)
- GLAS:Rayleigh laser

Mercator

- 1.2 meter altazimuth mount
- instruments:
  - P7: photometer with Geneva-filters
  - MEROPE CCD camera: 6.5 ′ field
  - HERMES: Echelle Spectrograph R=40000 and 90000

Liverpool

2 meter robotic telescope

- RATCAM: CCD 4.6 $'$ field
- SupIRCam: NIR camera 1.7$'$ field
- Meaburn Spectrograph: 49 x 1.7$''$ fibre bundle

SuperWasp

- Wide Angle Search for Planets (WASP)
  eight Canon 200mm f/1.8 lenses + Andor E2V 2k CCD
  non-standard broad band filter
  limiting magnitude 15.5 (1% photometry at 12)
- observing strategy: eight, 500 sq deg fields in succession, with 30 sec integration
  the cadence per field is therefore 8 minutes
  The whole sky once per night (takes about 30 minutes)

Comparing the ORM instruments

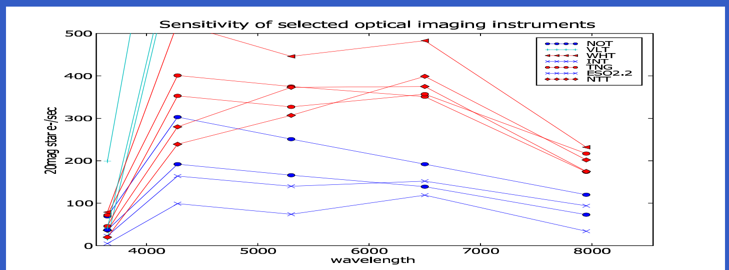

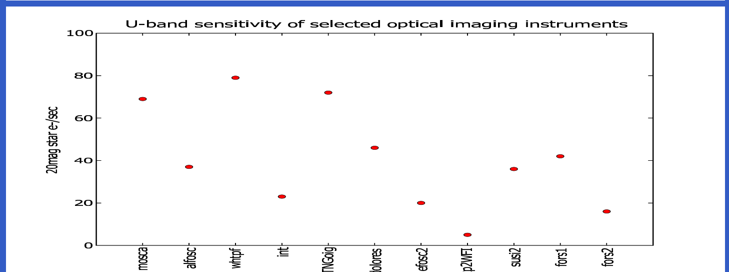

Comparing the ORM instruments

- Polarimetry: NOT
- U-band imaging: NOT
- NIR-optical SED: TNG NOT
- NIR imaging/spectrocopy: TNG WHT
- imaging survey: INT
- lowresolution spectroscopy bright objects: NOT INT
- lowresolution spectroscopy faint objects: WHT TNG
- Deep imaging (B-band and redder): TNG WHT
- high resolution spectroscopy: TNG NOT Mercator
- monitoring: Liverpool

Who can get time?

- NOT-OPC,CAT,PATT,TNG-TAC,NFRA PC, Dr Hans Van Winckel (hans.vanwinckel@ster.kuleuven.be)
- SuperWASP private telescope (so far???)
- Opticon: WHT, INT, TNG, LT, NOT
- CCI: WHT, INT, TNG, LT, Mercator, NOT

THANKS!

NOT: ALFOSC

Andalucia Faint Object Spectrograph and Camera the workhorse at NOT

- imaging, lowresolution spectrograph, polarimetry (linear/circluar imaging/spctrophotometry), multi object spectroscopy, fast photometry (on-line analysis)
- three filter wheels (14 slots available), aperture wheel (five slots), grism wheel (six slots)
- CCD E2V 2k$\times$2k one pixel 13.5 μ, 0.19$''$

NOT: NOTCam +StaCam science example

NIR imaging spectrograph

- two modes: Wide Field / high resolution camera
- imaging 22 filters, polaroids, one grism, two slits
- Spectroscopy: intermediate resolution (2-pixel R=2500, with dispersion 2.5-4.1 Angstrom/pixel) in J (5th and 6th order), H (4th order) and K (3rd order) when used with the WFC.
  HR Camera the resolution will be about 3 times higher, but the sampled wavelength range will be about 3 times less.

NOT: MOSCA

- Mosaic of four Loral 2k CCDs, with FOV of 7.7′ square
- Very sensitive in U band

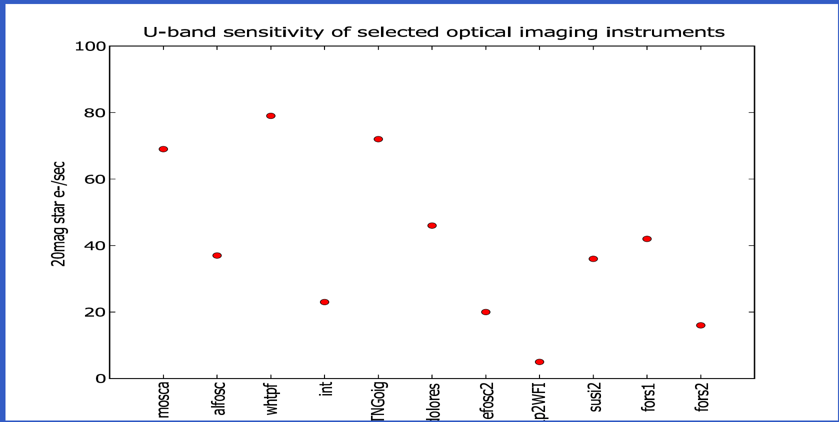

NOT: SOFIN (SOviet FINish spectrograph)

- High resolution sopectrograph
  also spectorpolarimetry limited use: contcat Ilya Ilyin (ilyin@aip.de)

NOT: TurPol

- photo polarimeter, simultaneous UBVRI
  for bright objects

NOT: StanCam

- Stand by optical imager (folded cassegrain)
  SITe 1k CCD with UBVRIzHαfilters
- Imaging instrument when ALFOSC/MOSCA is not mounted
  FIES fiber viewer
- longterm monitoring, (almost) simultaneous
  UBVRIJHK photometry with NOTCam

NOT: FIES (high-resolution FIbre-fed Echelle Spectrograph)

- Stand by instrument
- 4000-8300 Å with R=25k,45k,65k, depending on the fibre
- The “sky” fibre about 40 arcsec away
- high degree of mechanical and thermal stability

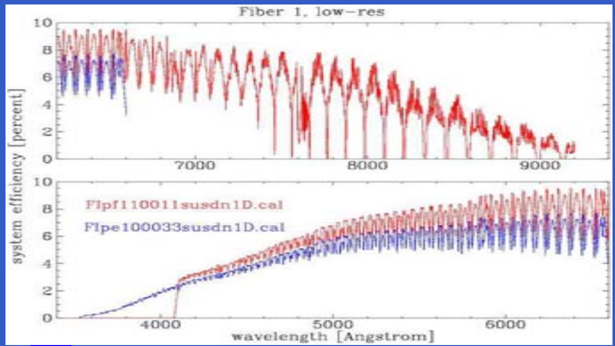

NOT: LuckyCam

- L3CCD: Hα and redder for high resolution imaging
  idea: shift & add the best images
- Diffraction limited I-band images can be achieved in good (< 0.6") seeing. Under poorer conditions the seeing resolution can be improved by as much as a factor of four
- Could be used for high time resolution photometry as well

TNG

- 2 Nasmyth foci hosts 5 instruments
  - SARG: cross dispersed echelle spectrograph
    3700Å- 1μ R=29k - 164k
  - NICS: NIR Camera Spectrometer 1024x1024 HgCdTe Hawaii array FOV 4.2$'$ $\times$ 4.2$'$
    Zero point K 21.8mag per 1ADU/sec H 22.3 J 22.1
    (1 ADU about 8 e^-)

TNG

- Adopt:The Adaptive Optics module for NIR imaging corrections tip-tilt and higher orders (future?)
  guide star with V/R$<$ 13 within 30$''$ improves the NIR FWHM by a factor of 2 if seeing 1 $''$ or better (K seeing limit 1.3 $''$)
- OIG (Optical Imager Galileo) 2$\times$2k$\times$4k EEV CCD, 4.9$'$ square
- DOLORES (Device Optimized for the LOw RESolution)
  low resolution (1.25 - 11.0 Å/pix), 2k Loral CCD
  Imaging FOV: 9.38 x 9.38 arcmin with a 0.275 arcsec/pix scale.

ING:INT

- two instruments Wide Field Camera (WFC) and Intermediate Dispersion Spectrograph (IDS)
- WFC: 4$\times$ 2k $\times$4k E2V CCD resulting 34 $'$ square reading out time 42 seconds ; 22 filters available
- IDS: resolution: from 0.5 Å to 7.5 ÅFWHM corresonding dispersion from 0.24 to 3.7 Å per pixel

ING:WHT

- ISIS:long-slit (4$'$) double-armed (blue: EEV12, red: Marconi2) spectrograph, medium-resolution (8 - 120 Å/mm) R < 10000
- AF2/WYFFOS: multi-object fibre-fed spectroscopy, 40$'$ field; 150 1.6$''$ science fibres, and 10 fiducial bundles for acquisition and guiding R $<$ 3000
- LIRIS (Long-slit Intermediate Resolution Infrared Spectrograph) imaging 4$'$ field spectroscopy, R $<$ 4000
- prime-focus - optical imaging, 16$'$ field

ING:WHT

- NAOMI/OASIS: - integral-field spectroscopy with or without adaptive optics (AO), R $<$ 4000, 17$''$ field
- NAOMI/INGRID - IR imaging with or without AO, 40$''$ field 1k Hawaii array
- GLAS: Ground-layer Laser Adaptive optics System Rayleigh laser system
  A 25W pulsed laser will be projected to 15km altitude plus a natural guide star

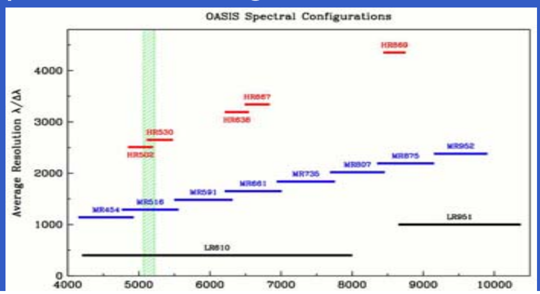

Mercator

- 1.2 m University of Leuven
- P7 : photometer with Geneva-filters
- MEROPE CCD camera: 6.5 $'$ field (0.19$''$/pixel) with Geneva-filters
- HERMES (High Efficiency and Resolution Mercator Echelle Spectrograph) 3800 Å-8750 Å R=40000 and 90000

Liverpool

- RATCAM: CCD camer with SDSS and Bessell BV filters, 4.6 $'$ field
- SupIRCam: NIR camera with JH(K$'$) filters, 1.7$'$, 0.4$''$/pixel
- Meaburn Spectrograph:prototype low dispersion spectrograph fibre bundle with 49 x 1.7$''$ fibres.
- FRODOSpec: integral-field spectrograph (not yet available)
- RINGO: optical polarimeter permanent VR filters, limiting magnitude: about 16

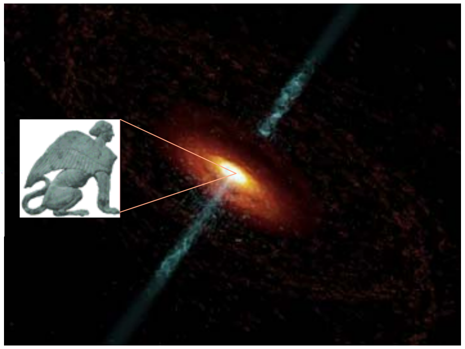

Progress (?) in Our Understanding of Blazars

Alan Marscher
Boston University
External Advisor of ENIGMA

Research Web Page: www.bu.edu/blazars

We have a ~reliable cartoon picture of an AGN

Less reliable closer to black hole

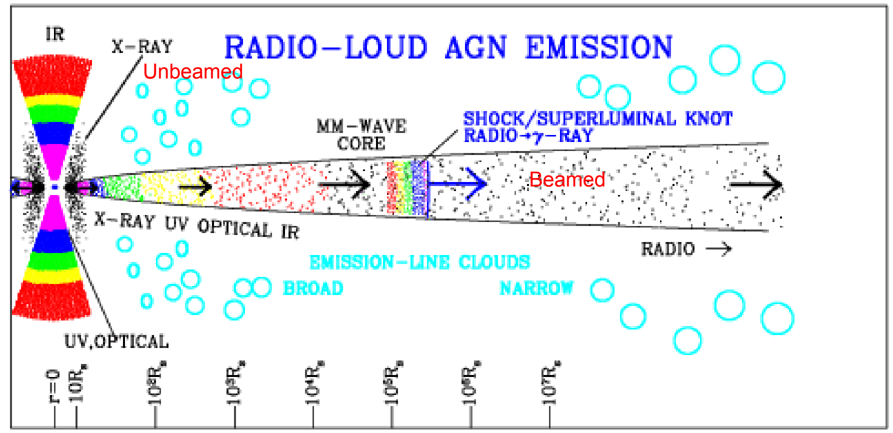

New method determines Lorentz factor & Doppler factor (→ viewing angle) separately

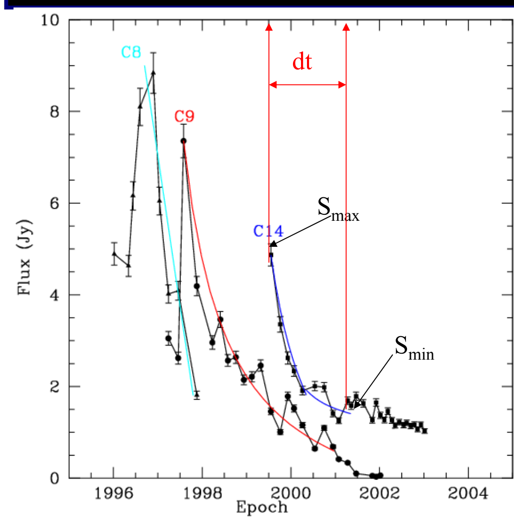

Time Scale of Variability
Burbidge, Jones, & O'Dell 1974, ApJ , 193, 43
$\Delta t_{var} = dt/\ln(S_{max}/S_{min})$

Variability Doppler factor
$\delta_{var} = aD/[c\ \Delta t_{var}\ (1+z)]$
D - luminosity distance
a - VLBI size of component
c - speed of light
z - redshift

Standard jet model agrees well with basic observations

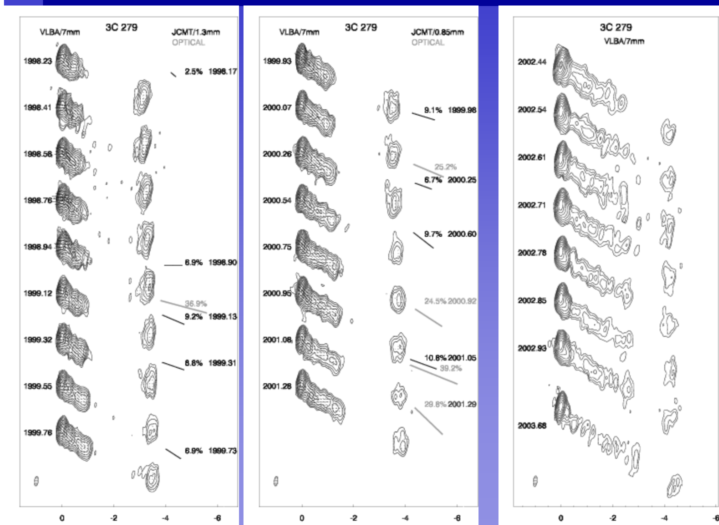

3C 279: Superluminal motion up to ~ 20*c*, bulk Lorentz factor up to ~25, Doppler factor up to ~50 → explains why it is a super blazar

Changes in apparent speed may be due solely to change in direction of jet by about ±2º

Fastest apparent speed consistent with highest variability Doppler factors

Apparent speeds up to 45c (fastest known blazar containing well-defined superluminal knots) → bulk Lorentz factor of at least 45 in jet

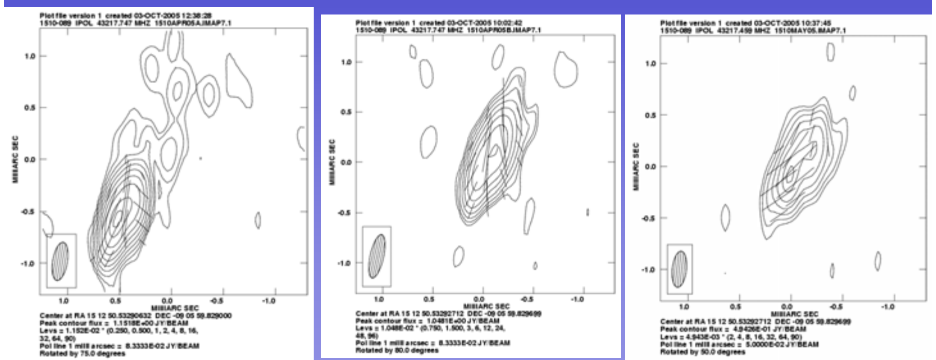

Statistics of radio-loud AGN population makes sense

Relativistic beaming causes strong selection effect in flux-limited radio surveys → Bias toward high-Γ jets pointing almost directly along line-of-sight

Population simulation (Lister & Marscher 1997): observed apparent-motion & redshift distribution reproduced if:

1. **Radio-galaxy luminosity function measured at low *z* is valid at higher *z***
2. **Lorentz factor distribution is a power law, $N(\Gamma) \propto \Gamma^{-a}$, *a* = 1.5-1.75, with a high-Γ cutoff of 45 (highest observed β_{app})**

→ 12-17% of jets in population have Γ = 10-45
5-7% have Γ = 20-45, 2-3% have Γ = 30-45, 0.5-0.9% have Γ = 40-45

Intrinsic half opening angle of jet is inversely proportional to Lorentz factor

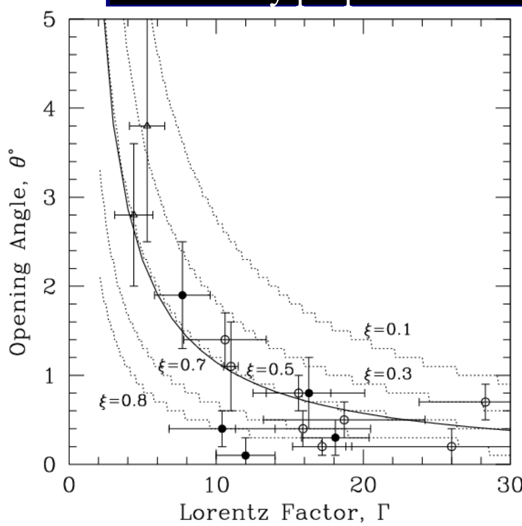

Side-on radio galaxies:
Opening angles typically 1-4°

$\theta \propto 1/\Gamma$ for blazars

Agrees with models in which jet is focused as it is accelerated over an extended region.(HD: Marscher 1980; MHD: Vlahakis & Königl 2004)

Explains why apparent opening angle is uncorrelated with apparent speed

Internal shock model for moving knots in jets seems to work well

Best-liked model: Shocks propagating down turbulent jet
Magnetic field compressed at shock front
Electrons accelerated at shock front

Polarization indicates that in general such shocks must be oblique, especially after correcting for aberration

Need supersonic relative motion to get shock waves → strong shocks are difficult for high-Γ flows with relativistic equation of state
- But don't need very strong shocks for substantial enhancement of radiation & polarization – 10-20% compression is usually enough

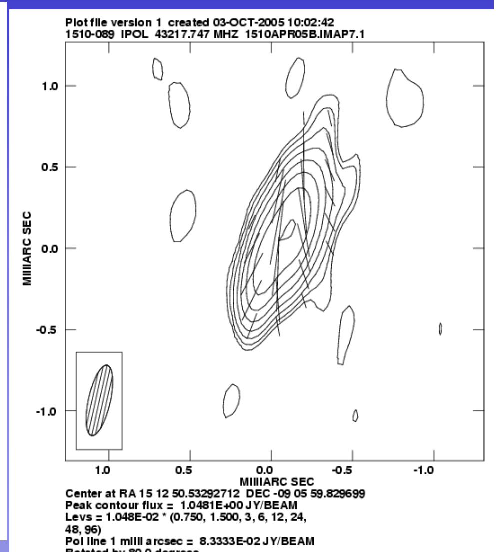

Velocity shear is present in 3C 273 where **B** is parallel to jet axis

Polarization: Most quasars have oblique or nearly perpendicular $\chi \rightarrow$ B nearly parallel to jet (after aberration taken into account)

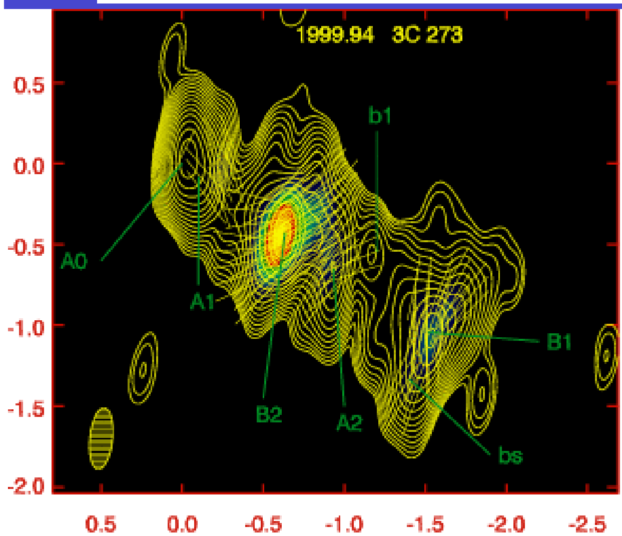

Southern knots: $\Gamma \sim 14$
Northern knots: $\Gamma \sim 8$

The core of blazar jets might be getting clearer

Frequencies below ~ 200±100 GHz:
- $\tau \sim 1$ surface if no bright, stationary features in jet a bit farther downstream
- conical standing shock (Daly & Marscher 1988) (e.g., 1803+784 shown below)

In favor: reproduces polarization pattern if randomly oriented B field is compressed by conical shock; in some sources core position not function of wavelength

At higher frequencies:
- End of zone of accelerating flow, where Doppler factor reaches asymptotic value

But in non-blazars, beaming not important
- Where high-E electrons first appear in jet

1803+784

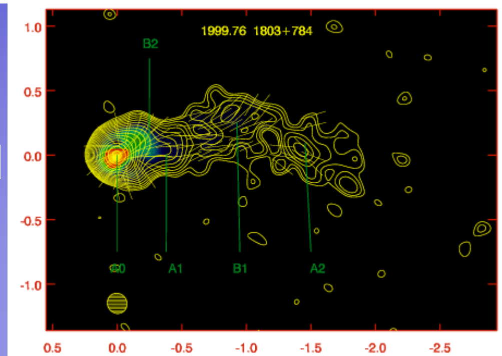

Jet Acceleration over Extended Region

Theory: A jet with $\Gamma >$ ~10 cannot propagate out of nuclear region (Phinney 1987)

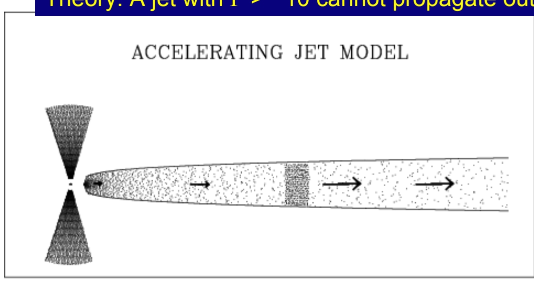

MHD: Models under development
Vlahakis & Königl (2004, ApJ)
Jet accelerated over large distance
Γ decreases away from jet axis
No distinct boundary

Predicts toroidal field in acceleration zone

Maybe we see this at 1 mm (Jorstad et al.2007)

Energy density at base of jet must exceed ~ $2\Gamma\rho c^2$

Might require a magnetosphere (pulsar or ergosphere of spinning BH)

Sketch of Physical Structure of Jet, AGN

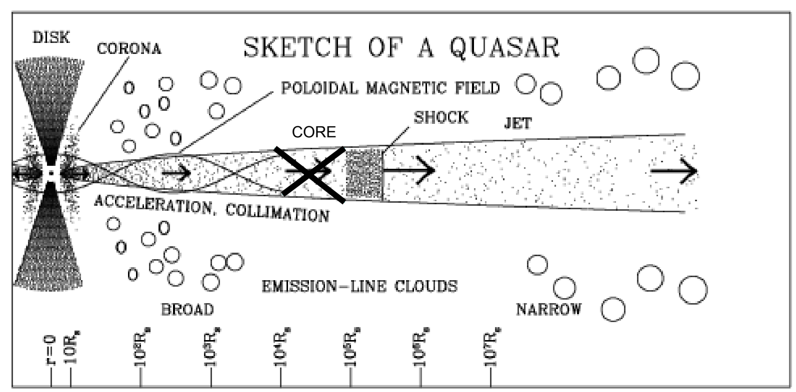

Cygnus A (Bach et al. 2004, 2005)
FR II radio galaxy, jet at large angle to l.o.s.

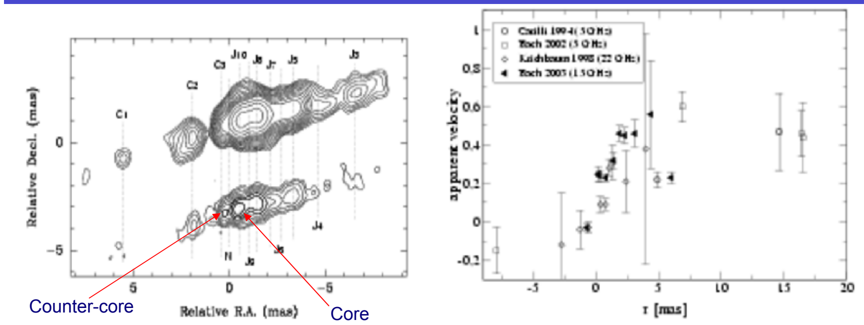

Gap between core & counterjet < 0.2 mas
Apparent speed increases with distance from core

Radio galaxies show a connection between X-rays from central engine region & activity in jet, ~ as in microquasars

The FR I Radio Galaxy 3C 120 (z=0.033)

HST image (Harris & Cheung)

Sequence of VLBA images (Marscher et al. 2002)

Scale: 1 mas = 0.64 pc = 2.1 lt-yr (Ho=70)

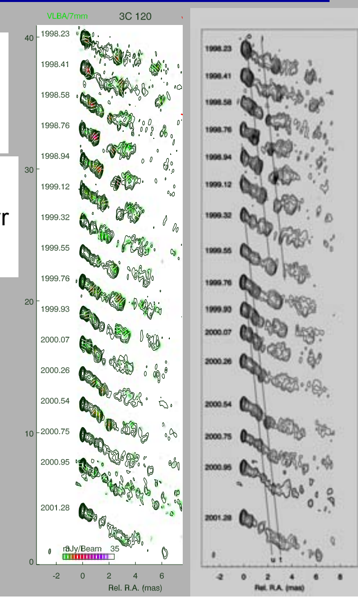

- Superluminal apparent motion, ~5c (1.8-2.8 milliarcsec/yr)
- X-ray spectrum similar to Seyferts
- Mass of central black hole ~ $3x10^7$ solar masses (Marshall, Miller, & Marscher 2004; Wandel et al. 1999)

X-Ray Dips in 3C 120

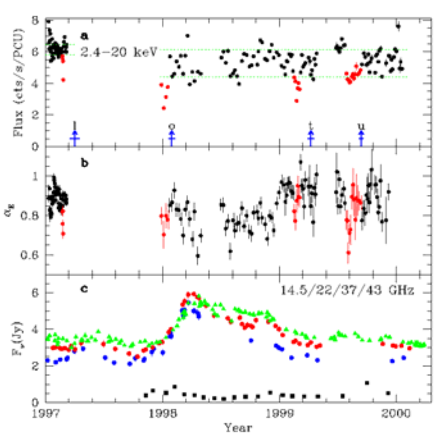

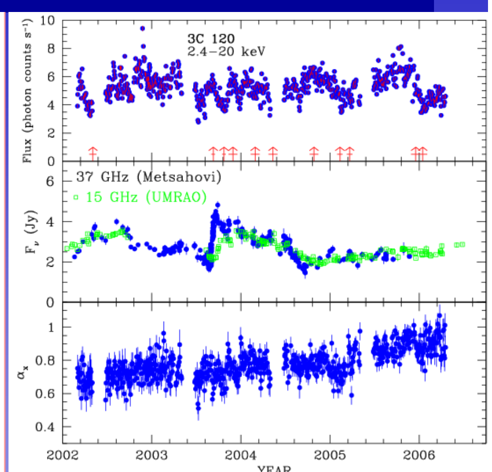

Superluminal ejections follow X-ray dips
→ Similar to microquasar GRS 1915+105

λ3mm core must lie at least 0.4 pc from black hole to produce the observed X-ray dip/superluminal ejection delay of ~ 60 days

Comparison of GRS1915+105 with 3C 120 Light Curves

- BH mass of 3C 120 ~$2x10^6$ times that of GRS 1915+105, so timescales of hours to months in the former are similar to the scaled-up quasi-periods (0.15 to 10 s) & duration of short X-ray dips in the latter.
- Typical fractional amplitude of dips is also similar
- Long, deep dips not yet seen in 3C 120

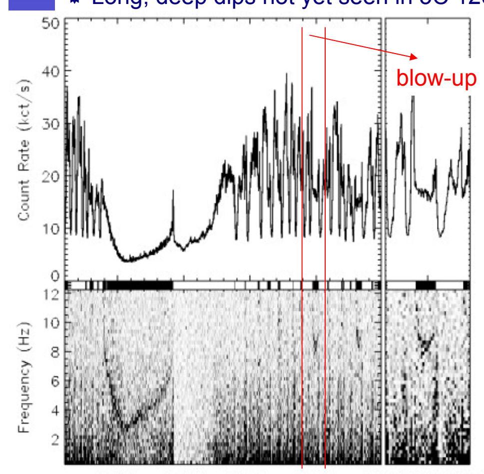

150 s of blow-up should scale up to ~10 yr in 3C 120 if timescales ∝ M_{bh}

Below: X-ray light curve of 3C 120 over 2.2 yr

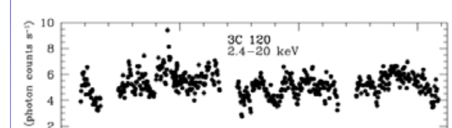

← GRS 1915+105 over 3000 s on 9/9/97
Light curve (top) & PSD (bottom)
(Taken from Markwardt et al. 1999 ApJL)

FR II Radio Galaxy 3C 111 (z=0.0485) Seems to Do the Same

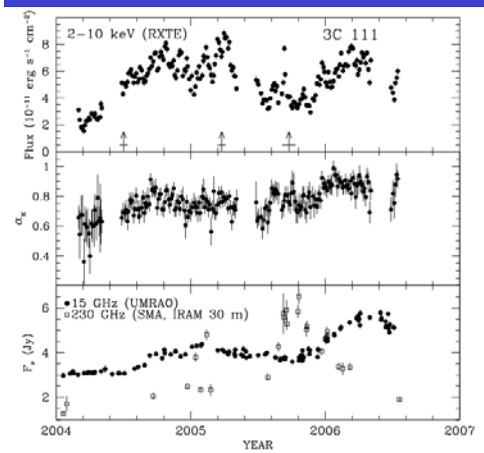

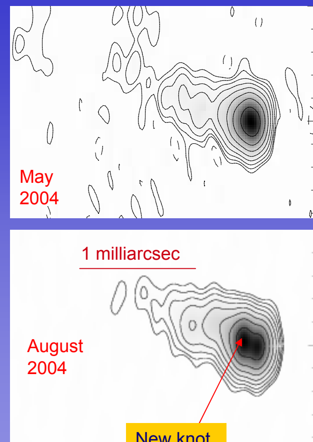

Superluminal ejection follows minimum of deep X-ray by 0.3 yr

λ3mm core must lie at least 0.4 pc from black hole to produce the observed X-ray dip/superluminal ejection delay

It appears that there are flares in the core

Example: Enormous outburst in 3C 454.3 in 2005-06

within ~ 6 months

r very slow or

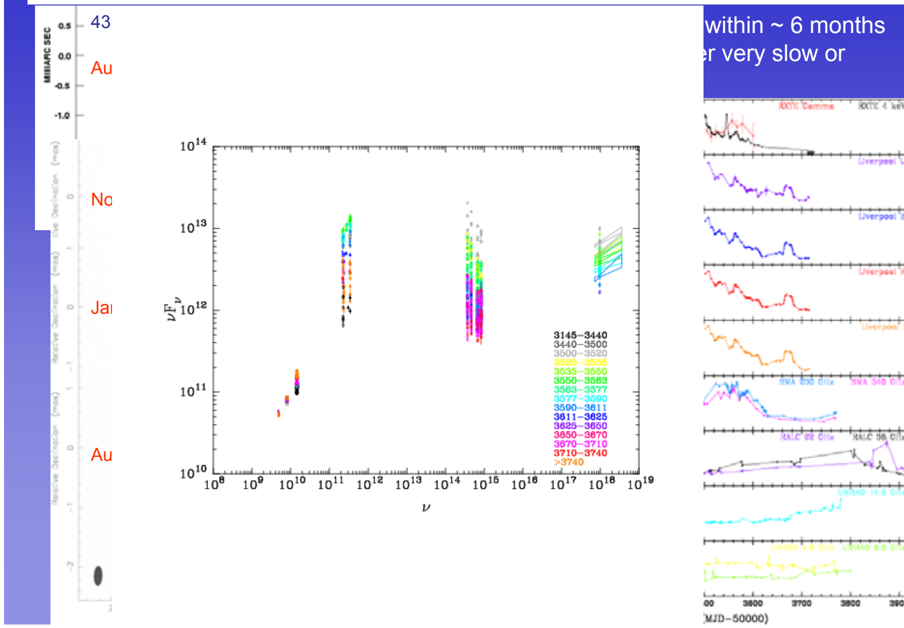

Changes in Direction

Change in apparent speed can be due solely to change in direction

Nonthermal luminosity seems to be related to direction of jet

Changes amplified greatly by projection effects

Velocity seems ballistic in some jets but seems to follow twisting jet in many others

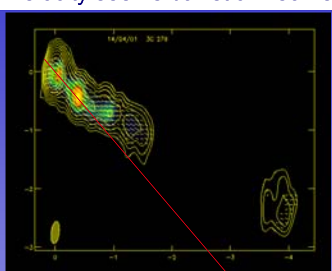

Changes in direction appear to be abrupt, unlike precession (more like an unstable firehose)

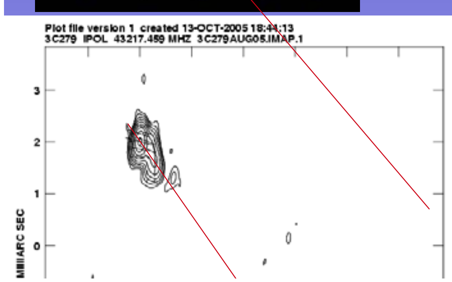

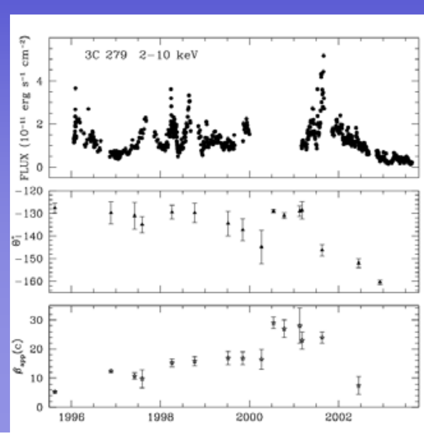

Changes in Direction: OJ 287

What has our darling blazar's jet been doing lately?

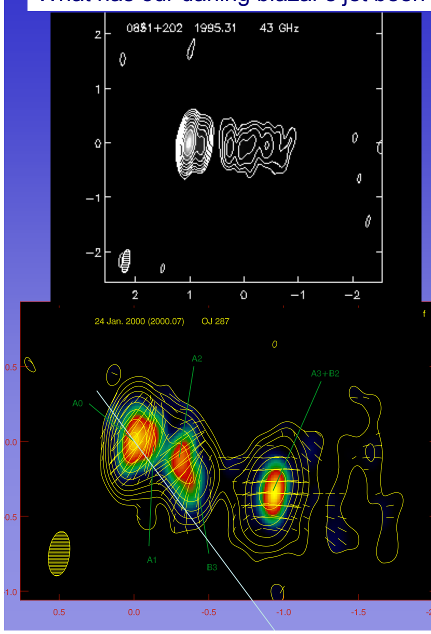

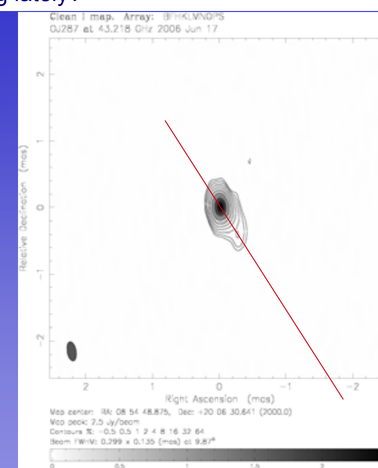

Dramatic change in direction (~ 50° over 11 yr), might be precession

Scandals

From the Lapland Winter School (April 2004)

- No good model for core despite its prominence □
- TeV BL Lac objects: slow apparent speeds, weak radio variability but need high Doppler factors □
- Shock model for flares: no description of rising flux ☹
- Flare profiles sharply peaked; in models they are rounded or flat ☹
- Particle acceleration models only partially developed: how can most particles be relativistic? How can we get energies ~10-100 TeV?
- PKS 0405-385: $T_{b,min}$ ~ 2×10^{14} K: can δ ~200? □?
- Some deprojected opening angles <0.2^{o} □

Scandals

[continued]

- Many prominent blazars have magnetic fields that lie parallel to the jet axis □
- Models for very high γ-ray luminosities: inverse Compton scattering of photons external to jet; but mm-wave flare often precedes γ flare so outside BLR

From 2004 multiwaveband meeting in Bonn:

- We have no complete samples of quasars
- Nature keeps jets together that 3D HD simulations destroy
- Single-zone models widely applied to rapid variations

More Scandals

- No model for abrupt transition from toroidal to turbulent magnetic field in jet
- Jets contain mostly relativistic plasma; we are ignorant of physics
- Jets change direction, usually non-periodically; we don't know why ☹
- Core-sheath model gives us extra free parameters but not tested against existing statistics
- 0716+714 refuses to give us its redshift
- Enigma's external advisor is a crazy professor from the land of Bush (George II) who is even older (by several months) & crazier than Prof. Valtaoja